Preparation and Characterization of Starch based Bionanocomposite Films for Food Packaging Applications

Thesis

Submitted in Partial

Fulfillment of the Requirements for the Degree of

DOCTOR OF PHILOSOPHY

by

Pankaj Jha

Department of Chemical Engineering

Indian Institute of Technology Guwahati

January 2020

CERTIFICATE

This is to certify that the thesis entitled **"Preparation and Characterization of Starch based Bionanocomposite Films for Food Packaging Applications"**, *being submitted by* ***Mr. Pankaj Jha****, to the Indian Institute of Technology Guwahati, India, for the award of Doctor of Philosophy, is a record of bonafide research work carried out by him under my guidance and supervision. The work embodied in this thesis has not been submitted for any other degree or diploma. In my opinion, the thesis is up to the standard of fulfilling the requirements of the doctoral degree as prescribed by the regulations of this Institute.*

Date:

Dr. R. Anandalakshmi
Associate Professor
Department of Chemical Engineering
Indian Institute of Technology Guwahati

Dedicated

To

My Family Members for their Supports and Encouragement Throughout My Research Work

ACKNOWLEDGEMENT

It is my great pleasure to thank each and everyone who helped directly or indirectly to complete my research work and made this thesis possible. I owe my deepest gratitude to all of them.

The first and foremost gratitude goes to my supervisor **Dr. R. Anandalakshmi** for her valuable guidance throughout the research work. I thank her for encouragement, patience towards research and support, which enabled me to develop a better understanding of the subject leading to present this thesis. I would like to thank her for precious time taken to discuss thoroughly on the topic and make me what I am today. I would also like to acknowledge my sincere gratitude to my doctoral committee members, **Dr. Chandan Das, Dr. Prasanna Venkatesh** and **Prof. K. Pakshirajan,** for their advices and suggestions throughout my research work.

I would like to extend my sincere gratitude to **Prof. Takahisa Nishizu, GIFU University, Japan** for giving me a golden opportunity along with necessary resources and guidance.

My sincere thanks go to the faculty members of Department of Chemical Engineering, I.I.T. Guwahati, for their continuous suggestions and inspirations. I would also like to express my thanks to the staff members for making a homely atmosphere. The analytical facilities from Central Instruments Facility (CIF) of Indian Institute of Technology Guwahati are also acknowledged.

I am grateful to my lab members and my friends, **Mr. K. Dharmalingam, Mr. Aditya, Mr. Arul Manikandan, Mr. Randeep Singh, Mr. Venkat, Mr. Ardhedhu, Mr. Wang and Mr. Jia** for the suggestions in performing experiments and lovely support in making my stay at IIT Guwahati and Gifu University.

After all I would like to thank all departmental and office staffs for helping me in many ways for my research work.

Deep heartedly, I thank my parents and my family members for their encouragement, blessings and motivation at each and every step.

Last, but not least, I thank the Almighty God for giving me strength to overcome difficulty, which crossed my way to be a pole star.

Pankaj Jha

ABSTRACT

Modification of starch with ionic gum using microwave heating method is a useful technique to alter the thermal and rheological properties of starch, which finds potential applications in food and pharmaceutical industries. First two and third chapters discuss about introduction and state of the art in food packaging materials. In the fourth chapter, normal potato starch (PS) was modified with xanthan gum (X) using microwave assisted dry heating (MADH) method at different times such as 0, 4, 8 and 12 min designated as PSX-0, PSX-4, PSX-8 and PSX-12, respectively. The modified potato starches by MADH were compared with conventional dry heating at 130°C for 240 min (PSX-240 min). The impact of conventional and microwave dry heating on gelatinization and flow properties was investigated. The results exhibited that modified potato starch with xanthan (PSX-8 min) via MADH showed high peak viscosity, increased apparent viscosity with shear rate, high water holding capacity than other modified potato starches. PSX-8 min showed a sharp absorption peak of ester bond between starch and xanthan in Fourier transform infrared spectroscopy (FTIR). X-ray diffraction pattern revealed that peak intensity of normal potato starch increased for PSX-8 min. Morphology of modified potato starch with xanthan was investigated using Scanning electron microscope (SEM). Modified potato starches with xanthan via MADH can be used in food industries for various applications.

Nowadays, starch based polymeric films gained much attention because of their film forming ability, excellent gas barrier properties, environmental friendliness and biodegradability. The fifth chapter briefly describes about the effect of amylose-amylopectin ratios on physical, mechanical, and thermal properties of starch based bionanocomposite films. Starch sources with different amylose-amylopectin ratios (potato starch, 20:80; wheat starch, 25:75; corn starch, 28:72 and high amylose corn starch, 70:30) are blended with carboxyl methylcellulose (CMC) and nanoclay (Na-MMT) to produce bionanocomposite films. Experimental results revealed that corn starch/CMC/nanoclay bionanocomposite films possessed higher tensile strength, lower film solubility, lower water vapour permeability and higher glass transition temperature due to molecular structure of amylose-amylopectin and their molecular space in corn starch, which helped in strong interaction with CMC and extensive intercalation of nanoclay. The highest degree of crystallinity and strong interaction of corn starch with CMC (–OH, –COOH) and nanoclay (Si-O-Si, Al-OH) were confirmed by XRD and

FTIR results, respectively. Furthermore, the corn starch/CMC/nanoclay bionanocomposite films showed antifungal property for at least 15 days when bread samples were packed at 25°C and 59% RH.

Sixth chapter explains about the influence on physical properties of different bionanocomposite films prepared with starch sources containing various proportions of amylose and amylopectin (potato starch, 20:80; wheat starch, 25:75; corn starch, 28:72 and high amylose corn starch, 70:30) incorporated with chitosan (CH) and nanoclay (Na-MMT). Amylose and amylopectin ratio regulates the orientation of molecular structure in the starch-based film. It was observed that the prepared bionanocomposite films of corn starch showed highest tensile strength, lowest film solubility, lowest water vapor permeability and highest glass transition temperature due to molecular space present in corn starch. This allows strong interaction with chitosan and promotes intercalation in to *nanoclay* galleries. The higher crystallinity and molecular miscibility of corn starch with chitosan (–NH, –COOH) and nanoclay (Si-O-Si, Al-OH) were confirmed by XRD. Fourier transform infrared spectroscopy (FTIR) confirmed the shift of amine peak to a higher wavenumber indicating a stronger hydrogen bond between starch and chitosan. Finally, the best bionanocomposite films were tested for food packaging applications. Low density polyethylene (LDPE) exhibited fungal growth on 5^{th} day when packed with bread slices at 25°C and 59% RH whereas corn starch-CH-nanoclay bionanocomposite films did not show the same for at least 20 days when bread samples at 25°C and 59% RH were packed.

Seventh chapter focuses on effect of plasticizers (glycerol (GLY)/sorbitol (SOR)) and antifungal agents (potassium sorbate (KS)/grapefruit seed extract (GFSE)) on water barrier, mechanical and thermal properties of corn starch (CS)-chitosan (CH)-nanoclay (Na-MMT) bionanocomposite films. Results showed that CS/CH/nanoclay/SOR/GFSE films exhibit a higher crystallinity than any other bionanocomposite films. Molecular miscibility among corn starch, chitosan (–NH, –COOH) and nanoclay (Si-O-Si, Al-OH) was confirmed by XRD. Films plasticized with SOR showed the highest tensile strength, lowest film solubility, lowest water vapor permeability, highest glass transition temperature and thermal stability. Fourier transform infrared spectroscopy (FTIR) confirmed that the main interactions among the components in a bionanocomposite film are due to hydrogen bonding. Bionanocomposite films containing GFSE showed a maximum zone of inhibition

against *Aspergillus niger***.** Synthetic plastic films exhibited fungal growth on 6th day whereas CS/CH/nanoclay/SOR/GFSE films did not show the same up to 20 days when bread samples were packed at 25°C and 59% RH.

Further, the eighth chapter dealt with the effect of different ratios of grapefruit seed extract (GFSE) on crystallinity, mechanical, water barrier, and thermal properties of bionanocomposite films of corn starch (CS) incorporated with chitosan (CH) and nanoclay (Na-MMT) prepared via solution casting technique. Experimental results showed that GFSE was properly dispersed with corn starch incorporated with chitosan (CH) and nanoclay (Na-MMT) bionanocomposite films. The presence of GFSE up to 1.5% v/v showed higher crystallinity, tensile strength, lower elongation at break, film solubility and water vapor permeability. Furthermore, an addition of GFSE above 2% v/v decreases physical properties of the bio nanocomposite films. Fourier transform infrared spectroscopy (FTIR) analysis revealed that strong hydrogen bonding exists in bionanocomposite films, which is the main reason for interaction among CS, CH, nanoclay and GFSE. Synthetic plastic exhibited fungal growth in 6th days whereas CS/CH/nanoclay/GFSE bionanocomposite films did not reveal the same for at least 20 days when bread samples were packed at 25°C and 59% RH. The prepared bionanocomposite films could potentially be used for active packaging in order to extend the shelf life, maintain the quality and safety of food products and thus could substitute synthetic plastic packaging materials.

Keywords:

Starch, Xanthan gum, Microwave heating, Gelatinization temperature, Carboxymethyl cellulose, Chitosan, Amylose-amylopectin ratios, Potassium sorbate, Grapefruit seed extract, Nanoclay, Mechanical properties, Barrier properties, Thermal properties, Anti-fungal activity.

TABLE OF CONTENTS

LIST OF FIGURES

LIST OF TABLES

Chapter 1

Introduction

1.1. Plastics

Plastic is a polymer, made up of many small units of molecules (monomer), which join together to form a larger polymeric structure (**Vivaldo and Saldivar, 2013)**. Plastics are mainly originating from the petroleum products. Petroleum products are mainly composed of carbon and hydrogen compounds with traces of sulphur, vanadium, and nickel. Petroleum products are toxic when exposed to environmental life sources such as plants, animals etc. due to the presence of heavy metals and chlorinated hydrocarbons like dichlorodiphenyltrichloroethane (DDT) and polychlorinated biphenyls (PCB). During plastic production processes, several types of poisonous gases, which contain lethal elements like hydrocarbons, particulates, nitrous oxide, carbon monoxide and sulphur dioxide, are released in environment and also remain in the petroleum after the process of fractionation. These harmful gases can cause acidification in ecosystem, which further results in harmful acid rain. Conventional plastics produced from fossil fuels finds a huge market in the world. Synthetic plastics are mostly limited to fossil resources, which increase greenhouse gas emissions. Due to low production cost and adaptability, synthetic plastics are more in demand with their wide range of application like food packing, agriculture, automobiles and infrastructure **(Mekonnen et al., 2013)**. According to Federation of Indian Chambers of Commerce & Industry (FICCI), utilization of plastics are more in food packaging industry than in any other applications **(FICCI, 2014)**. According to recent available survey of FICCI, total plastic consumption (%) in food packaging, infrastructure, automobile, agriculture and others in India are 43, 21, 16, 2 and 18, respectively whereas 35, 25, 17, 8 and 15, respectively in world as shown in **Figure 1.1**. Synthetic plastics remain in the environment for a longer period without degradation and thus results in pollution. In the recent global survey report, the synthetic fossil fuel-based plastics were mostly used as packaging material which is estimated as 8300 million metric tons (Mt). In 2015, production of plastic wastes reached approximately 6300 Mt in

which around 9% recycled, 2% incinerated, and 79% accumulated as waste disposal in landfills or the natural environment. It is predicted that it will reach up to 12000 Mt by 2050 **(Geyer et al., 2017)**.

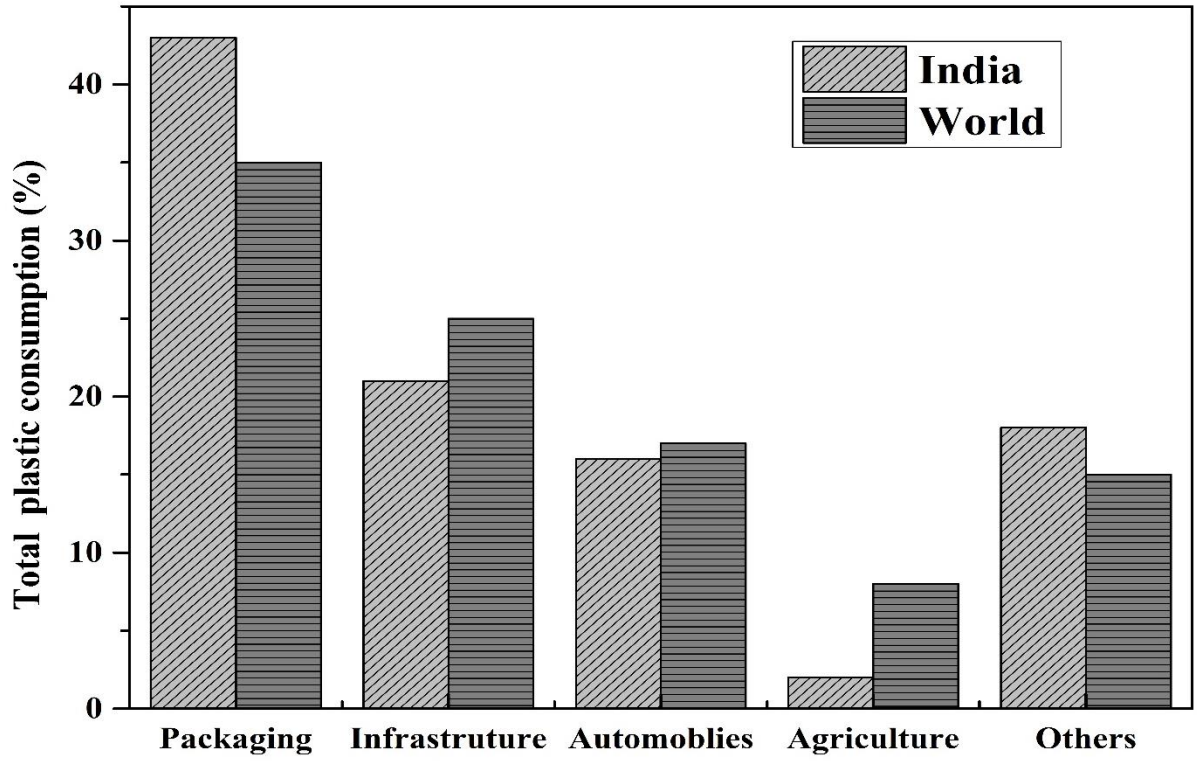

Figure 1.1. Plastic utilization in various sectors in India and in the world **(FICCI, 2014)**

1.2. Plastic wastes in India

India is a largely populated country as well as the third largest in plastic production and generates million tons of plastic wastage every year. Approximately, 4.38 pounds is generated by an individual. It is essential to recycle those plastic wastes instead of incineration, which leads to a higher carbon footprint in the ecological system for million years. Plastic wastage occupied landfill spaces release hazardous chemicals to the environment in the presence of water and spread waterborne diseases like malaria. In India, plastic utilization has increased dramatically and almost 50% of plastic pollution is caused by polyethylene (PE) bags. These PE bags take longer time to degrade. Street animals like cow and bull ingest the improper plastic disposal on the roadsides. In recent available data by Central Pollution Control Board (CPCB), average plastic waste per day in (in tonnes)

Delhi, Chennai, Kolkata and Bengaluru is 690, 429, 426, and 314 in the year 2010-11 **(Seetharaman, 2017)**.

1.3. Environmental impact of plastic wastes

Various routes of plastic pollutant disturb the biological chain. Their harmful effects are shown in **Figure 1.2**. Chemical pollution can be through acidification, bio magnification and eutrophication. Marine pollution is due to micro plastics in water and helps in accelerating the mortality rate which is estimated at around 100,000 aquatic animals and 1-2 million marine birds per year. During burning, poisonous gases are produced and that further leads to climatic change, global warming and greenhouse effect. Plastic wastes are exposed to living being in many ways and produce toxic effects disturbing the natural biological cycle. In the recent past, plastic wastes and litters are the main causes of environmental pollution and increased carbon footprints **(Silva, 2011)**.

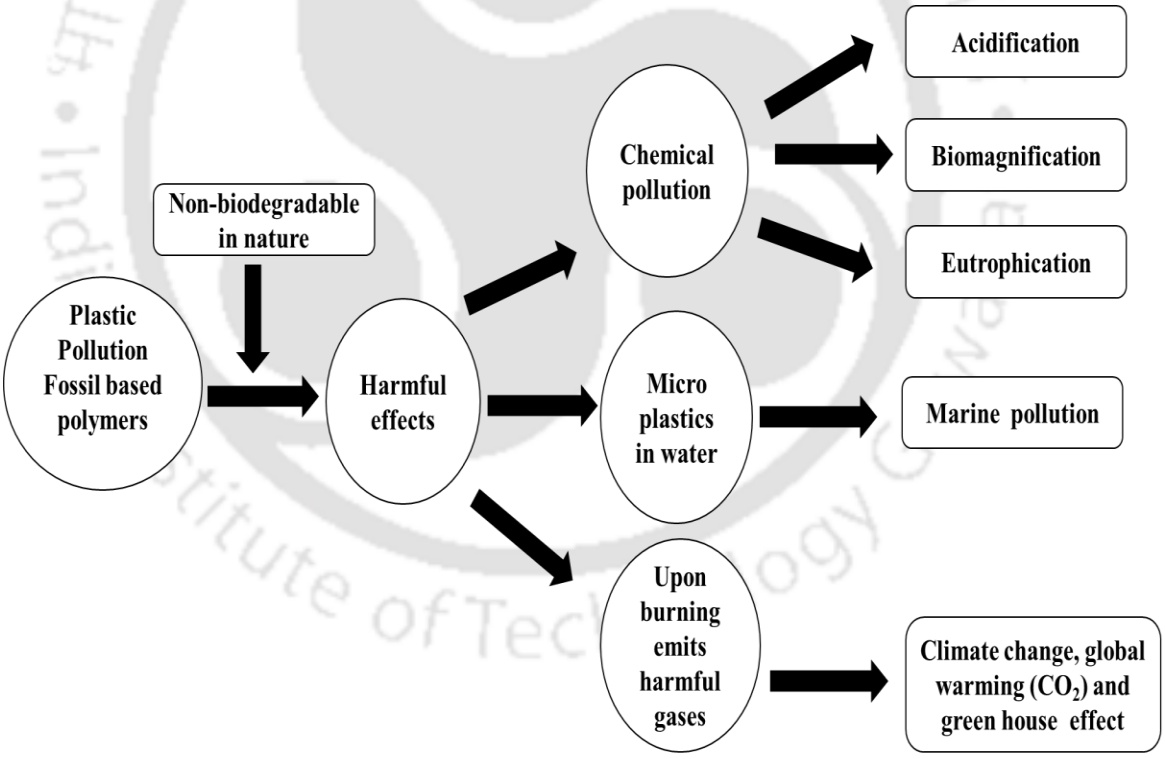

Figure 1.2. Harmful effects of plastic pollution **(Silva, 2011)**

Environmental impact of various traditional plastics and bioplastics is compared in **Table 1.1**. Traditional plastics from non-renewable sources show a higher environmental impact. Production of plastic consumes a lot of energy adversely emitting a large quantity of

greenhouse gases. Bioplastics from renewable raw materials such as PLA, PHA, and TPS offer a great deal of advantages than the traditional plastics. Especially, thermoplastic starch (TPS) shows a very less impact than other bioplastics. On the contrary, they show strong impact on the environment for acidification and eutrophication **(Gironi and Piemonte, 2011)**. Utilization of plant based sources is more advantageous over conventional plastics in order to reduce the dependency on limited fossil resources and greenhouse gas emissions. These plastics were significantly made from renewable materials like biomass and save up to 40% of energy in production as compared to their petrochemical counterparts. They play a crucial role in the further advancement of the plastic industry. The bio-based materials and products were reused or recycled and eventually used for energy recovery (i.e. renewable energy) **(FICCI, 2017)**. Thermoplastic starch blends with natural additive improve barrier, mechanical and thermal properties which can be used as packing material.

Table 1.1. Energy requirement and global warming potential for various synthetic polymers and biopolymers **(Gironi and Piemonte, 2011)**

Source	**Synthetic polymers and biopolymers**	**Energy requirement, MJ/kg**	**Global warming potential, kg CO_2 eq/kg**
From non-renewable sources	High density polyethylene (HDPE)	80.0	4.84
	Low density polyethylene (LDPE)	80.6	5.04
	Polyethylene terephthalate (PET)	77.0	4.93
	Nylon 6	120.0	7.64
	Polystyrene (PS)	87.0	5.98
	Polyvinyl alcohol (PVOH)	102.0	2.70
	Polycaprolactone (PCL)	83.0	3.10
From renewable sources	Thermoplastic starch	25.4	1.14
	Thermoplastic starch+ 15% PVOH	24.9	1.73
	Thermoplastic starch+ 60% PCL	52.3	3.60
	Polylactic acid (PLA)	57.0	3.84
	Polyhydroxyalkanoates (PHA)	57.0	Not available

1.4. Global markets for bioplastics: current and future aspects

A recent European bioplastic survey (**Figure 1.3 (a)**) reported that the total global production of bioplastics is 2.05 million tons. In which, non-biodegradable bioplastics

contribution is 57.1%, which majorly includes polymeric material such as polyethylene terephthalate (PET =26.3%), polyamides (PA =11.9 %), polyethylene (PE =9.7%) and other non-biodegradables (=9.2 %). The total biodegradable production is 42.9%, which majorly includes starch blends (=18.8%), polylactic acid (PLA =10.3%), polybutylene adipate terephthalate (PBAT =5%), polybutylene succinate (PBS =4.9%), polyhydroxyalkanoates (PHA =2.4%) and other biodegradables (=1.5%). The global production capacities of bioplastics will increase significantly from 2.05 million tonnes in 2017 to approximately 2.44 million tonnes in 2022.

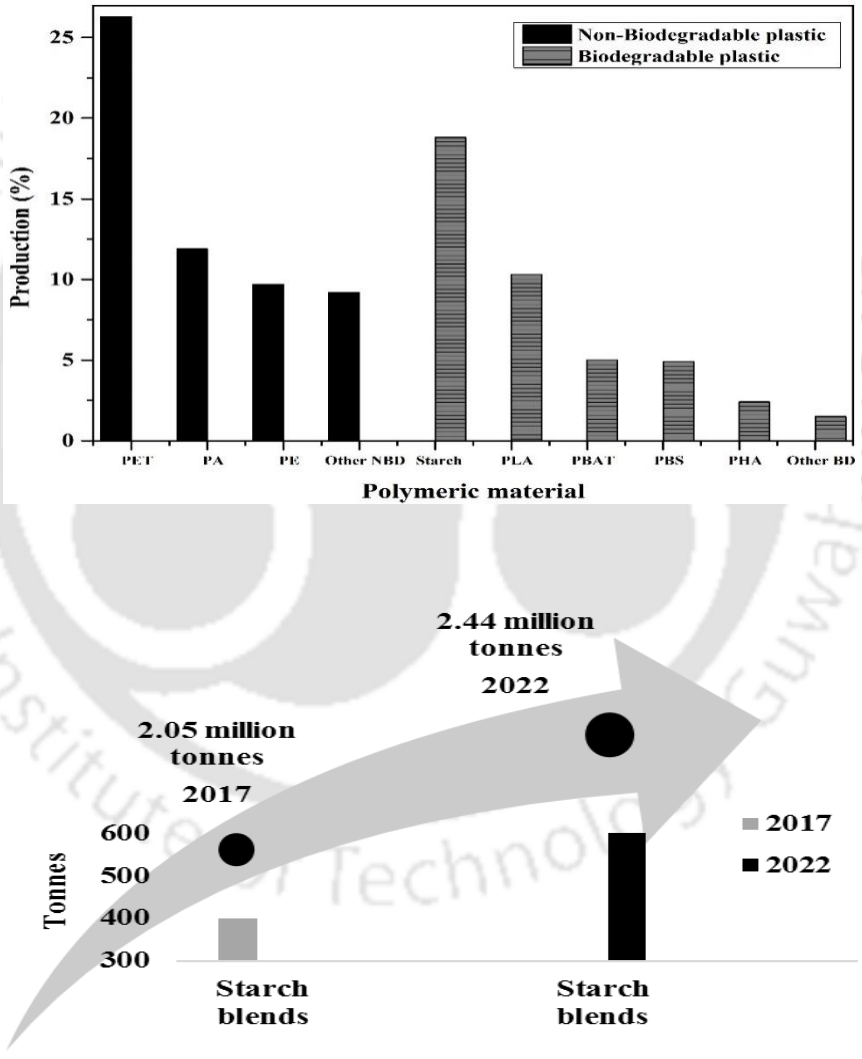

Figure 1.3. (a) Total global production of non-biodegradable and biodegradable bioplastics and (b) Production forecast of starch blends (2017-2022) **(European Bioplastics, 2017)**

Starch blends production forecasted to increase from 400 tonnes in 2017 to 550 tonnes (**Figure 1.3 (b)**). Out of 2.05 million tonnes of bioplastics, the contribution of Asia, North America, Europe, and South America are around 57%, 18%, 16% and 10%, respectively. Bioplastics are more focused on global markets for various applications such as packaging, agriculture/horticulture, textiles, catering products etc. In 2017, around 60% bioplastics were used in the packaging field among total bioplastics market. In packaging, two types of package materials are used such as flexible and rigid. Starch blends are mainly used in the application of flexible packaging (**European Bioplastics, 2017**).

1.5. Commercially available starch polymer-blends

List of companies currently marketing starch-based polymer products are shown in **Table 1.2.** Starch-based commercially available polymers are used in various applications such as packaging (wrapping film, board lamination, film for dry food packaging etc.), food containers, agricultural films and disposable items (plates, cutlery, cup lids etc.). These products have shown a great potential to substitute conventional fossil-based plastics. Presently, starch-based plastic like Bio-P™, Evercorn™ and Ecoform® made by Bioenvelope (Japan), Novamont (Italy) and American Excelsior Company (USA), respectively are available in the market **(García et al., 2009; Robertson, 2008; Vroman and Tighzert, 2009)**. In India, Truegreen Greendiamz Biotech manufactures corn starch based product to be used in the application of packaging and agriculture field **(Das, 2013)**. It is reported that the Cadbury® (United Kingdom) and Coop® (Italy) uses corn starch-based packaging materials for milk chocolates and organic tomato products (**Peelman et al., 2013).** It is also reported that several starch-based plastics are there in the market and the largest producer is Novamont with the manufacturing capacity of 80×10^3 tonnes with their starch-based bioplastic called Mater-Bi®. The second largest producer is Solanyl Biopolymers with a manufacturing capacity of 65×10^3 tonnes with their starch-based bioplastic called Solanyl BP® (**Laycock and Halley, 2014)**. According to FICCI, many companies target towards a bio-based raw material for packaging although the product market is expensive. Researchers, entrepreneurs, and consumers are more focused in green packing. It is expected that more awareness and inclination towards eco-friendly packaging material bring down cost of bioplastics. Also, plant-based raw material provide an additional source of income for the agriculture sector **(FICCI, 2017)**.

Table 1.2. Commercially available starch based polymer blends and its applications

Products	Manufactures	Compositions	Applications	Reference
Bio-P™	Bioenvelope (Japan)	Starch	Packaging materials	**Robertson (2008)**
EverCorn™	Novamont (Italy)	Starch	Packaging materials	**Garcia et al. (2009)**
Ecofoam®	American Excelsior Company (USA)	Starch	Wrapping film	**Vroman and Tighzert (2009)**
Biolice®	Truegreen Greendiamz Biotech. Ltd. (India)	Corn starch	Food packaging and mulch film	**Das (2013)**
Cadbury®	Cadbury Schweppes food group, Marks & Spencer (United Kingdom)	Corn starch-based	Corn based packaging	**Peelman et al. (2013)**
Coop®	Iper supermarkets (Italy), Coop Italia	Corn starch-based	Corn based packaging	
Mater-Bi®	Novamont (Italy)	Starch and polyester	Food containers, agricultural films, disposable items.	**Laycock and Halley (2014)**
Solanyl BP®	Solanyl Biopolymers Inc. (Canada)	Starch based bio-plastic	Packaging	

1.6. Cost comparison between biodegradable and traditional polymers

According to **Mohanty et al. (2000)**, it was estimated that PHA costing 4.00-6.30 US$/lb is around 2.5 times costlier than starch, which costed only 1.60-2.90 US$/lb. Starch and starch blends were approximately equal to PLA. **Muller et al. (2017)** reported that main drawback of PLA was its less oxygen barrier properties compared to starch-based packaging film. Oxygen permeability of PLA is very high (2.4×10^{-15} kg s^{-1} Pa^{-1}). This permeation of oxygen through packaging material leads to oxidative discoloration process along with microbial growth and causes food spoilage and degradation of food quality. Gas (He, O_2, CO_2) barrier capacity of PLA is mainly due to its hydrophobic nature and makes them more brittle. PLA plastics do not break down into elements in natural ways and commercial composting facility is required for compositing, which leads to solid plastic

wastes. Improper disposal of PLA can contribute to contamination during recycling processes **(Biomass Packaging, 2015)**. Due to its slow degradation than starch-based polymers. Starch-based films are more advantageous due to good oxygen barrier properties as well as extensibility. Starch-based films show oxygen permeability of nearly about 0.4 × 10^{-13} to 2.5 × 10^{-13} cm^3 m^{-1} s^{-1} Pa^{-1} based on various film formulations **(Muller et al., 2017)**. Furthermore, starch-based films are described as non-hazardous and sources of income for agricultural farming, which contributes to their growth as a potential packaging alternative. Starch-based polymers occupy a major market in biodegradable plastics till date.

1.7. Biodegradable food packaging

Rhim et al. (2013) studied important functional properties of biodegradable food packaging material as represented in **Figure 1.4**. Antimicrobial activity is one of the important properties for contamination, which can possibly be occurring from light, water, gases, odor and spoilage microorganisms. Antimicrobial agent maintains the quality and safety of food products during storage to extend the shelf life of food products. Mechanical properties would provide strength to safeguard food products from physical damage during transportation, storage and shipping.

Barrier properties are another important parameter to be considered for biodegradable food packaging material. Permeability is mainly considered for water vapor, O_2, CO_2 and other volatile compounds through the packaging materials. Thermal properties are to be considered to maintain proper thermal resistant, which further enhances shelf life, food quality and safety. Eco-friendly, green plant-based packaging materials grow in interest now days in order to protect the environment from fossils based pollution.

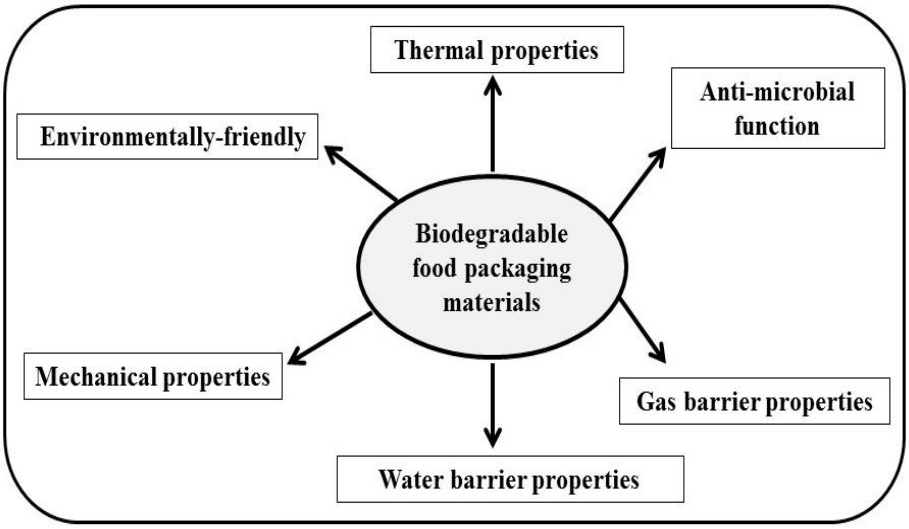

Figure 1.4. Essential properties of biodegradable food packaging materials **(Rhim et al. (2013))**

1.8. Biodegradable polymers

The biodegradable polymer is derived from various renewable sources such as agriculture feedstock, animal, and microbial source. The main property that distinguishes between biopolymers and fossil fuel-derived polymers is their sustainability and biodegradability. Normally, biopolymers require less time to decompose or break down of bigger unit into small unit in presence of microbes and bacteria after being discarded to the environment. In the process of composting, they mix with soil and increase the fertility level of the soil or marine sediment and helps in ecological safety as shown in **Figure 1.5 (Prashanth and Tharanathan, 2007)**.

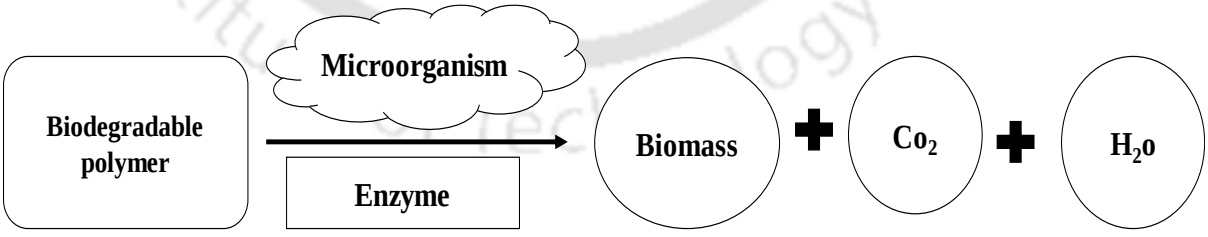

Figure 1.5. The process of biological degradation of biodegradable polymers

Biodegradable polymers can be classified into four categories depending on their synthesis and on their sources (**Figure 1.6).**

(i) Polymers, which are directly extracted from various sources such as agro-polymers (agro-resources), polysaccharides e.g., starches (wheat, potatoes, maize), cellulose, carrageenan, konjac glucomannan, alginate, protein and lipids, e.g., animals (casein, whey, collagen, gelatin), and plants (zein, soy and gluten).

(ii) Polymers, which are obtained by microbial production, e.g., polyhydroxyalkanoates (PHA) such as poly(hydroxybutyrate) (PHB), pullulan, FucoPol.

(iii) Polymers, which are chemically synthesized using renewable bio-based monomers such as polylactic acid (PLA).

(iv) Polymers whose monomers are obtained by chemical synthesis from fossil resources, e.g., polycaprolactones (PCL), polyesteramides (PEA), aliphatic co-polyesters (e.g., PBSA) and aromatic co-polyesters (e.g., PBAT).

Polysaccharides such as starch and cellulose are natural polymers, otherwise called as biopolymers, which are found in nature during the growth cycles of all organisms. Other natural polymers are proteins that can be used to produce biodegradable materials. These polymers are often chemically modified with the goal to modify the degradation rate and to improve the mechanical properties **(Vroman and Tighzert, 2009)**.

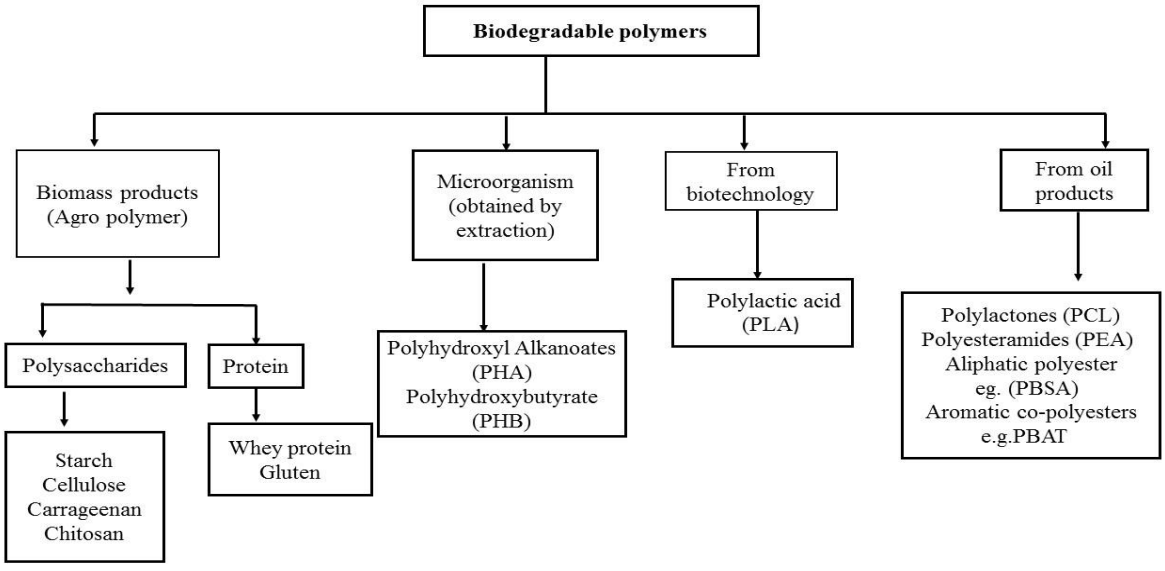

Figure 1.6. Classification of biodegradable polymers **(Vroman and Tighzert, 2009)**

1.8.1. Cellulose

Cellulose, which is found in cell walls of plants is an abundant, natural and renewable source of polymer. Cellulose is the regular linear structure polymer composed of three hydroxyl groups present on anhydroglucose. Cellulose derivatives are cellulose ethers and cellulose esters. Cellulose ethers comprise carboxymethylcellulose (CMC), methylcellulose (MC), hydroxypropyl methylcellulose, ethylcellulose, hydroxyethyl methylcellulose and hydroxyethyl cellulose while cellulose esters include cellulose acetate, cellulose butyrate, and cellulose triacetate (**Figure 1.7)**. Carboxymethylcellulose (CMC), methylcellulose (MC), and cellulose acetate (CA) are cellulosic derivatives that are mainly used in the industry, especially in film formation and packaging. Methylcellulose films with 30% glycerol were developed and tested at 75% RH and 25°C. It was found that tensile strength was around 38.6 MPa, elongation at break was about 4.4 % and water vapor permeability (WVP) was 8.16 $x10^{-11}$ g. Pa^{-1} s^{-1} m^{-1}. Methylcellulose is a cellulosic ether, exhibits thermal gelation, forms excellent films for pharmaceutical and food industries **(Paunonen, 2013**).

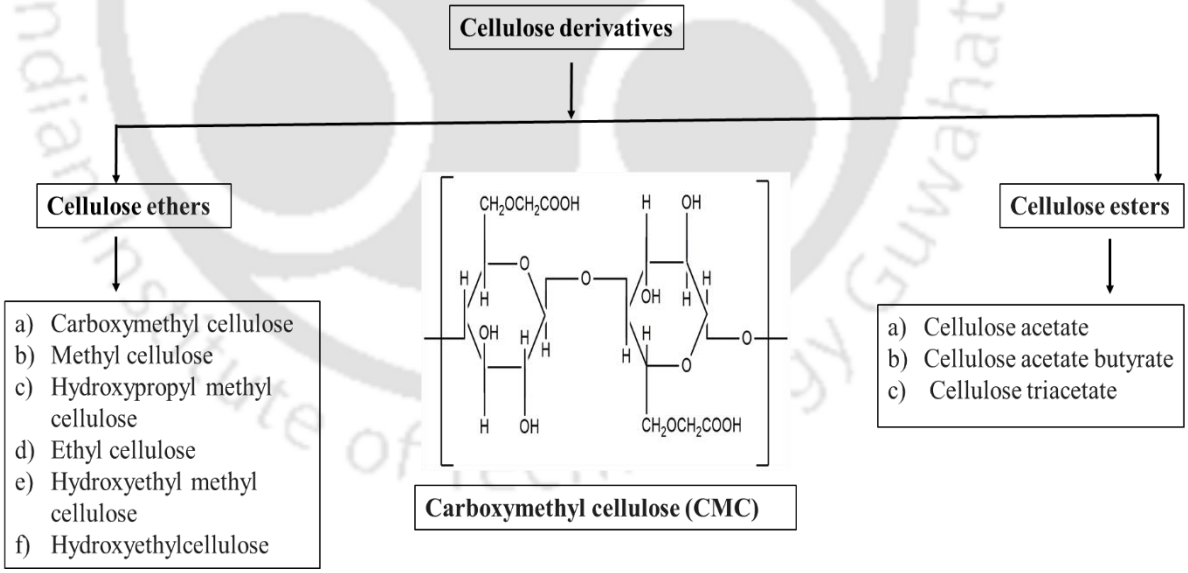

Figure 1.7. Cellulose and its derivatives **(Paunonen, 2013)**

Cellulose acetate (CA) films were prepared with 5% polyethylene glycol and tested at a condition of 100% RH and 25°C. Tensile strength, elongation at break and WVP were

estimated as 7.92 MPa. 7.2% and 7.82 x 10^{-10} g. Pa^{-1} s^{-1} m^{-1}, respectively **(Bai et al., 2012; Varsha et al., 2010)**. Carboxymethyl cellulose films were developed with 40 % glycerol at a test condition of 97 % RH and 25°C. Tensile strength, elongation at break and WVP of carboxymethyl cellulose films were estimated as 17.6 MPa, 6.6 % and 1.37 x 10^{-11} g. Pa^{-1} s^{-1} m^{-1} **(Sayanjali et al., 2011)**. **Soroka (2010)** studied the properties of different cellulosic derivative films, which were prepared by blending them with other biopolymers to enhance their shelf life, mechanical and barrier properties for food packaging applications. Thermoplastic behavior was improved for CMC with starch films due to free hydroxyl groups. Cross-linking in these films reduced the WVP of the composite depends on the type of starch used.

1.8.2. Properties and applications of carboxymethyl cellulose (CMC)

Carboxymethyl cellulose (CMC), which are water-soluble heteropolysaccharides with high molecular weights are often used together with starches to provide appropriate texture, water mobility and moisture control of products. CMC is an anionic linear polysaccharide, which is widely available, easily processed, inexpensive, durable, non-toxic, renewable, biocompatible, biodegradable and with excellent film-forming properties. Several hydroxyl and carboxylic groups in CMC enable water binding and enhance moisture sorption properties. CMC can be used as a filler material in biocomposite films because of its high molecular weight and better interaction with the polymeric matrix. CMC is able to improve mechanical and barrier properties of pea starch-based films. It is an important industrial polymer with the huge range of applications in food, pharma, textile and paper industries as represented in **Figure 1.8**. CMC is used to improve various properties such as viscosity, non-toxicity, non-allergic nature and overall product quality/stability (**Ghanbarzadeh et al., 2010; Tongdeesoontorn et al., 2011)**.

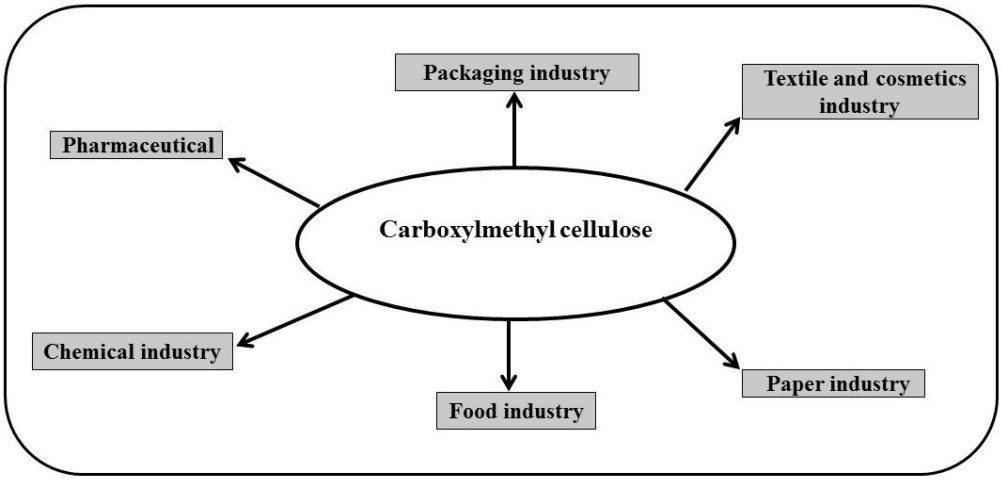

Figure 1.8. Various applications of carboxylmethyl cellulose **(Ghanbarzadeh et al., 2010)**

1.8.3. Chitosan

Chitin or chitosan (CH) is a natural and second most abundant polymeric material. Chitin is a nitrogenous polysaccharide, which is an extract from the core part of the exoskeleton of crustaceans, arthropods and cell walls of fungi (**Figure 1.9 (a)**). The only difference between chitin and cellulose is the presence of acetamide ($-NHCOCH_3$) functional group. Chitosan comprises of two monomers of D-glucosamine units linked by β- (1–4) bonds and N-acetyl-D-glucosamine and can easily be prepared by deacetylation (under alkaline conditions) of chitin (**Figure 1.9 (b)**). The degree of deacetylation (DD) of chitin determines the extraction process of chitosan. Percentage of deacetylation (DD %) depends on the conversion of chitin into chitosan. This conversion of chitosan depends on alkaline concentration, temperature and deacetylation time. Presence of free amine groups in chitin make them more soluble and reactive when compared to chitosan **(Tang et al., 2007)**.

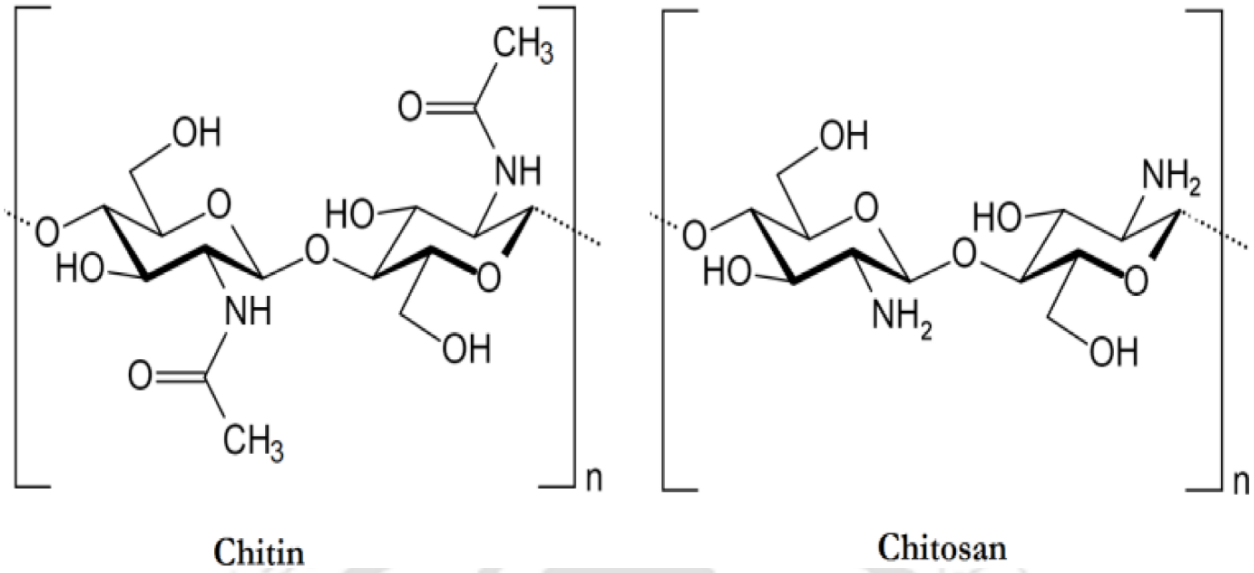

Figure 1.9. Chemical structure of (a) chitin and (b) chitosan **(Tang et al., 2007)**.

1.8.4. Properties and applications of chitosan

Chitosan has properties like bio-renewable, biocompatible, bioactive, bio functional and biodegradable. It is cheap, efficient and approved by FDA. Chitosan is soluble in a low pH (<6) medium due to the presence of free amino groups present in each monomeric unit. It is protonated in acidic media and convert into NH_3^+ (**Prashanth and Tharanathan, 2007)**. It is a hydrophilic material with excellent film-forming ability, adequate water vapor barrier property and low oxygen permeability **(Loredo et al., 2016)**. Chitosan has another important feature of food protection due to its inherent anti-bacterial and anti-fungal properties against spoilage microorganism and several groups of pathogens **(Tan et al., 2015)**. Chitosan is an eco-friendly biopolymer used in several manufacturing and industrial processes such as food packaging, processed food, agriculture, pharmaceutical (filler in tablet and coating material), water waste treatment etc. (**Figure 1.10)**.

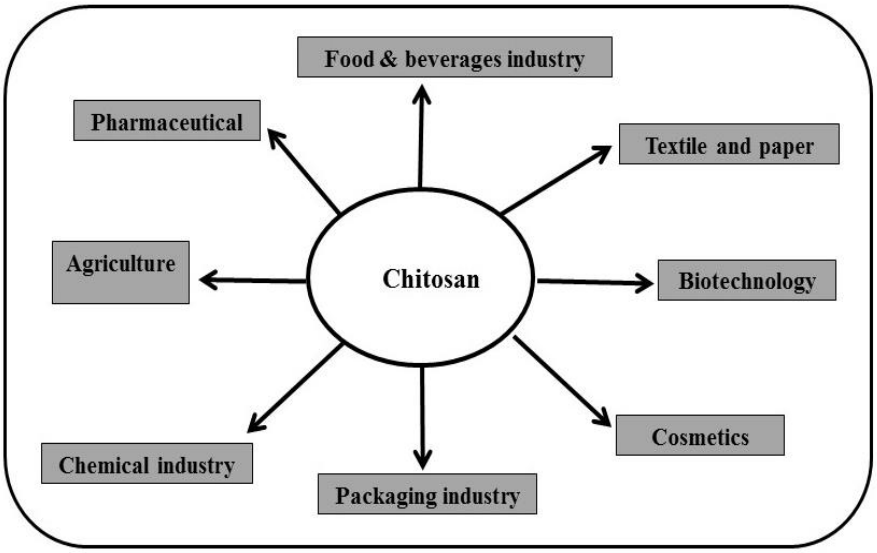

Figure 1.10. Various applications of chitosan **(Prashanth and Tharanathan, 2007)**

1.9. Starch

Starch is the most abundant natural biopolymers on earth along with cellulose and chitosan. Starch can be obtained from plants, for example in the fruits, roots, leaves, shoots, and seeds. It is found mainly in legumes (25–50 % of the dry matter) tubers (60–90%) and cereals (30–70%). Largest natural sources of starch are corn, wheat, tubers (potatoes) and roots (cassava). Starch is a polysaccharide carbohydrate consisting of a large number of monomer glucose units joined by glycosidic bonds. The two main components of starch are amylose, which comprises of linear chain linked by α-D-(1, 4) glycosidic bonds and amylopectin, which consists of branched chain linked by α-D-(1, 4) glycosidic bonds and α-D-(1, 6) glycosidic bonds **(Blanshard, 1987)**. The various sources of starch and chemical structures of amylose and amylopectin are shown in **Figure 1.11**. The molecular weight of branched amylopectin varies between 2-7×10^8 g/mol depends on the sources of the starch. On the other hand, amylose molecular weight is significantly lower than amylopectin and it varies between 0.2-2×10^6 g/mol. The crystallinity of the starch depends on amylopectin component while the amorphous region mainly signifies amylose content **(Alcazar and Meireles, 2015)**.

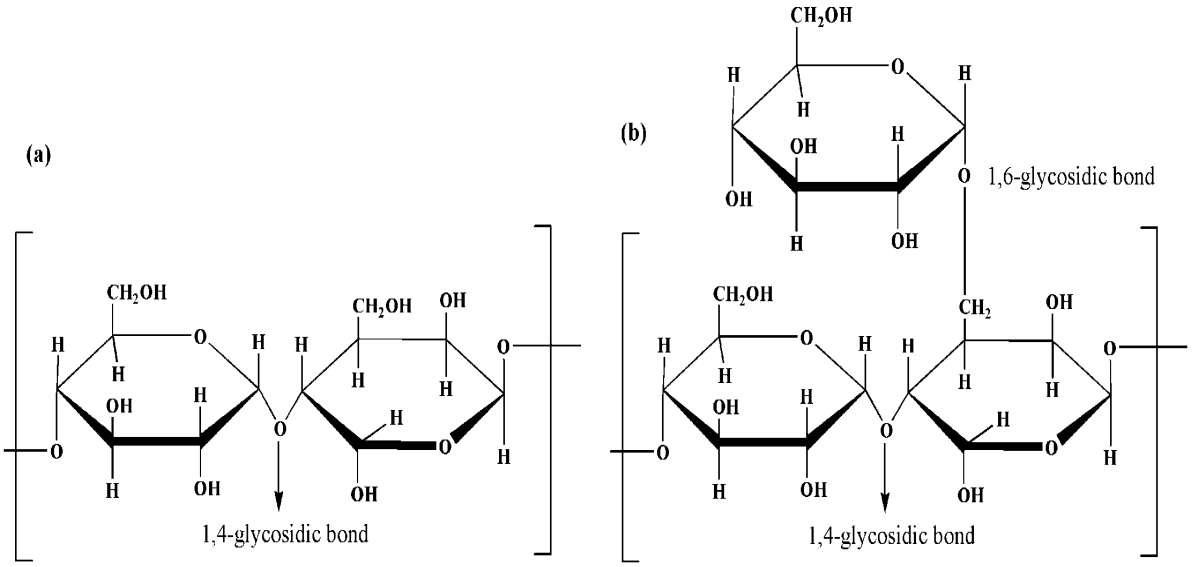

Figure 1.11. Chemical structures of (a) amylose and (b) amylopectin **(Blanshard, 1987)**

1.9.1. Physicochemical properties of starch

1.9.1.1. Composition and structural properties

The most important properties of starch depend on its composition (phosphorylation, moisture, α-glucans, lipids and proteins). The structural arrangement depends on an amylose-amylopectin ratio, length of α-glucan chains, and variation between crystalline and amorphous regions. A higher ratio of amylopectin exhibits larger crystallinity. Depending on the plant origin, starch crystalline structure is distinguished into three types as A, B and C-pattern. A-pattern appears in cereal starches like maize, wheat, rice cassava and waxy maize, B- pattern is a characteristic of certain tubers like potato and other tuber starches and C-pattern is intermediate between A- and B-types which appears in legumes like pea starch. The sharp diffraction patterns in the XRD correspond to a crystalline material while the non-sharp areas refer to amorphous regions **(Alcazar and Meireles, 2015)**.

1.9.1.2. Swelling and solubility properties

Swelling of starch granules starts when water enters into the amylose-amylopectin region, losses its crystallinity and phase separation occurs, which causes amylose to leach out towards inter-granular space. Starch molecules dissolve in excess of water during heating which results in a semi-crystalline structure and separation of amylose and amylopectin molecules. Hydroxyl groups in the outer region of amylose and amylopectin

molecules form a hydrogen bond with water molecules. This leads to swelling, solubility and increase in granule size. The swelling capacity and solubility provide an indication of the magnitude of interaction in starch granules and also defines the crystalline and amorphous regions. This interaction is guided by amylose-amylopectin ratios that depend on molecular weight, polymerization degree, length of chain branching and molecular conformation. In starch, swelling capacity is enhanced by amylopectin content, while amylose acts as a diluent and inhibitant of swelling **(Alcazar and Meireles, 2015)**.

1.9.1.3. Gelatinization and retrogradation properties

In the process of gelatinization, starch granules absorb water and then swell due to disruption in crystallinity and molecular order. Different starches have different gelatinization temperatures ranging from 60-80^{o}C. Amylose content of starch has an inverse relationship with gelatinization temperature. In gelatinization process, disruption of crystalline order causes irreversible changes in starch granules such as breaking of the double helix in the crystalline region, leaching of amylose, granule swelling and pasting **(Atwell et al., 1988; Hoover, 2001; Stevens and Elton, 1971)**. During retrogradation, amylose molecules form double helix associate while amylopectin molecules re-crystallize through its short outer chain. After retrogradation, starch possesses a lower enthalpy and gelatinization temperature than native starch because of weaker starch crystallinity. During cooling, amylose undergoes quick crystallization while amylopectin recrystallizes slowly. Degree of retrogradation depends on the distribution of amylopectin, chain length and storage under freezing. The rate of recrystallization is based on the type of polymer used **(Alcazar and Meireles, 2015)**. The properties and applications of different starches with different amylose ratios are presented in **Table 1.3.**

1.9.2. Limitations of starch

Native starches have a limited number of applications in the industry as they have a few cons like high syneresis, high viscosity, low shear resistance, poor solubility, limited digestibility and susceptibility to retrogradation. For these reasons, most of the starches are modified using physical, chemical or enzymatic processes or a combination thereof to provide desirable functional properties **(Santana and Angela, 2014)**. However, starch-based films are highly hydrophilic due to the water sensitivity and show poor water vapor barrier such as moisture content, solubility and water vapor permeability along with low

mechanical strength **(Ghanbarzadeh et al., 2011)**. Improvement in starch film properties such as tensile, elongation at break and barrier properties can be possible when added with biopolymer additive, the proper ratio of plasticizer agent (glycerol and sorbitol) and reinforced with nanoclay. Starch based bionanocomposite films are able to improve the mechanical, thermal and barrier properties and these bionanocomposite films can be used in food packaging applications.

Table 1.3. Properties and applications of starches from various sources

Starch	Amylose (%)	Type	Properties	Applications	Reference
Potato	20-25	Tuber	Thickener, film forming, bulking ingredient and water binder	Anti-caking ingredient, packaging, frozen food and pharmaceutical	**Kraak (1992)**
Pea	35	Legumes	Good resistance to heat and solvent, film-forming and gelling properties	Bakery and dairy products	**Ratnayake et al. (2002)**
High amylose corn	70	Cereal	Opaque, strong gel, film forming and textural properties	Gum candies, jam and packaging	**Bertuzzi et al. (2012)**
Corn	26-28	Cereal	Film forming, binder, thickener and water retention	Sauces and soups, packaging and medicine	**Wang et al. (2013)**
Tapioca starch	17	Root	Freeze-thaw stability, high viscous paste, clarity, opacity	Confectionary products, dressings, soups and sauces**,** pharmaceutical and cosmetic	**Wongsagonsup et al. (2014)**
Rice starch	17	Cereal	Emulsifying agent, freeze thaw stability, adhesive and film forming	Confectionary products, pharmaceutical, plastic, cosmetic, paper, textile and photographic	**Amagliani et al. (2016)**
Wheat	26-27	Cereal	Solubility, swelling capacity, adhesive, thickener and gel formation	Dairy products, packaging, paper, textile, chemical, fermentation, pharmaceutical and petrochemical industries	**Shevkani et al. (2017)**
Waxy corn	0-5	Cereal	Binder, thickener and stability	Dairy products and confectionery	**Sarka and Dvoracek (2017)**

1.9.3. Applications of starch

Starch is a promising candidate for making bioplastic material due to its abundance, worldwide availability, film-forming properties and low cost. Starch is biodegradable, renewable, biocompatible, bio functional and bioactive. Applications of starch in packaging and food industries are shown in **Figure 1.12**. It can also be utilized in pharmaceutical, textile, paper, cosmetic, and chemical industries **(Bastioli and Magistrali, 2014; Baumberger, 2002; Koch et al., 2014).**

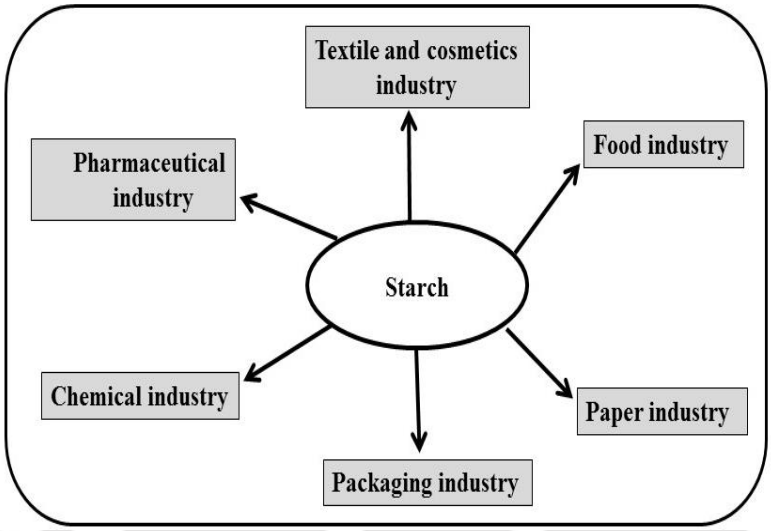

Figure 1.12. Various applications of starch **(Bastioli and Magistrali, 2014)**

1.10. Modification of starch

Native starches are structurally too weak and have limited functionally for an application. Modifications are necessary to create a ranges of functionality. The modification can be done by chemical, physical and enzymatic methods. The starch modification can be introduced by changing the structure or disturbing the structure including hydrogen bonding in a controlled manner to enhance and extend their applications in pharmaceutical, food, and non-food industries (paper industry, textile industry, plastic industry and petroleum industry). Modified starches are used as a thickener, stabilizer, emulsifier and to texturally influence a food product **(Alcazar and Meireles, 2015).** Various types of modification of starches are shown in **Figure 1.13.**

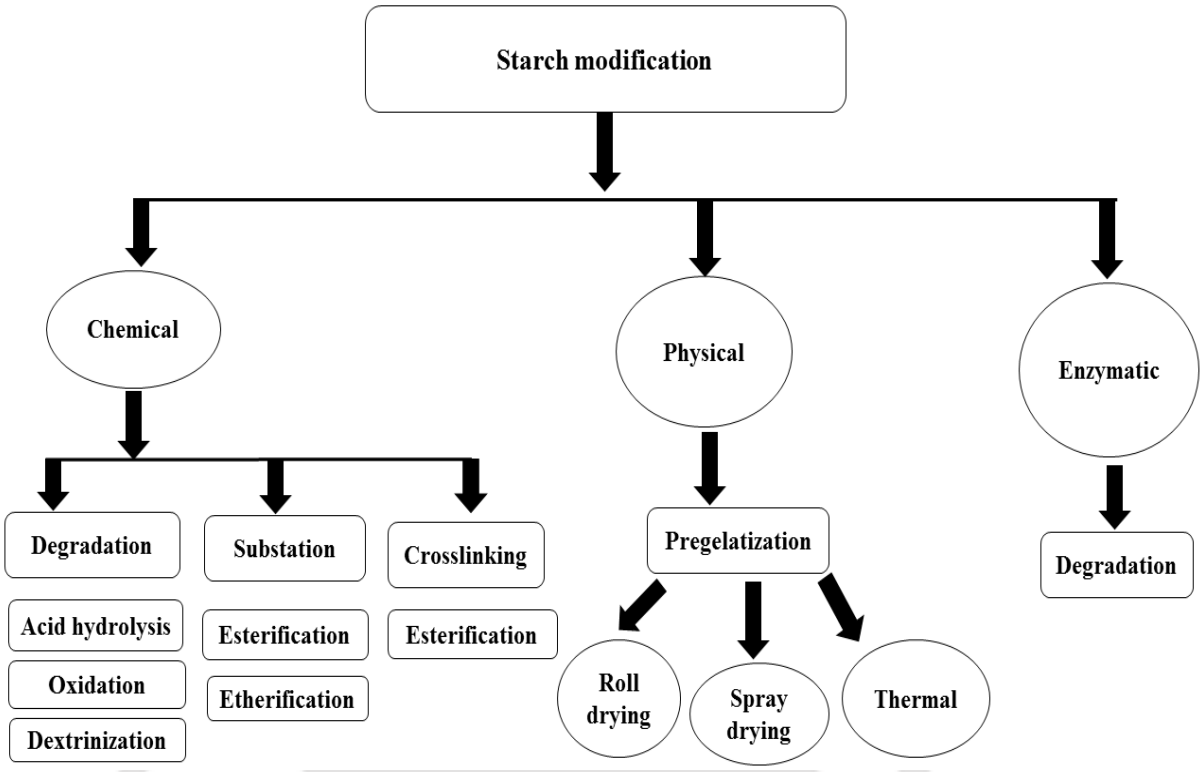

Figure 1.13. Types of starch modifications product **(Alcazar and Meireles, 2015)**

1.10.1 Physical modification of starch

Physical modification techniques are simple, cheap and safe to use such as pre-gelatinization, heat-moisture treatment (HMT), conventional dry heating and non-thermal techniques such as microwave-assisted dry heating (MADH). Heat-moisture treatment is one such technique employed on native starch wherein starch granules with moisture levels (<35%, w/w) are heated at 80–140°C, above the glass transition (T_g). Low gelatinization temperature improves properties such as paste stability and excellent thaw or freeze stability. Effects of HMT on the properties of starches from various sources were reported by **(Zia-ud-Din et al., 2017)**. The conventional dry heating process as an alternative to chemical modification for starches or flours of various origins resulted in low moisture levels (<10%, w/w). Dry heat treatment of starch with ionic gums requires high temperature (> 130°C) heating for a prolonged period (2–3 h) to improve functional properties as well as chemical cross-linking. This impregnated gum-starch by dry heating forms ester bond, which increases the resistance to viscosity breakdown and shortens the paste texture **(Sun**

et al., 2013). On the other hand, industries move toward microwave dry heating (MADH) method for modification of starch in order to avoid energy loss during prolonged heating in dry heating treatment. Among physical modification methods, processing with MADH provides several advantages such as cheap, eco-friendly, fast reaction rate, uniform heating produces, desirable functionality and higher yield. Microwave is non-ionizing energy source of electromagnetic radiations in the frequency ranges between 300 MHz and 300 GHz. Important microwave frequencies allocated for industrial and domestic usages are 896-2450 MHz and 2375 MHz, respectively. Mechanism of microwave heating is based on the heat and mass transference or interactions between microwave energy and individual polar molecules. In the case of polymers, the mechanism involves the dipolar reorientation in the presence of an electric field. It is well known that the movement of isolated single molecules is not responsible for heat generation upon microwave penetration in liquids, but the bulk movement inside the liquid. Electromagnetic heating is mainly due to internal heat generation and is having several advantages over conventional heating such as shorter processing time, uniform heating throughout the whole sample volume, greater penetration depth and quality enhancement of food products **(Cardenas et al., 2008; Chandrasekaran et al., 2013)**. Modification of starch using MADH depends on many factors such as time duration of heating, moisture content, temperature at which dielectric properties of the starch are influenced. MADH treatment on starch changes its properties like swelling capacity, solubility, rheological properties, gelatinization temperature and enthalpies **(Alcazar and Meireles, 2015)**.

1.10.2. Hydrocolloids and its properties

Hydrocolloids or ionic gums are hydrophilic in nature and originate from plant, animal and microbial. Ionic gums are generally added to starch in various food products to modify characteristics of the products. Carboxymethyl cellulose (CMC), xanthan, chitosan, pectin, carrageenan, alginate and agar that are water-soluble heteropolysaccharides with high molecular weights, are often used together with starches to provide thickening, gelling and to control rheological and textural properties. Ionic gums are also used to improve moisture retention, control water mobility and to maintain overall product quality during processing **(Yoon et al., 2016).**

Xanthan gum is a branched polysaccharide produced by bacterial fermentation (**Vania et al., 2013)**. It consists of D-glucose residues linked by α-(1-4) glycosidic bonds and a trisaccharides (β-D-mannose-β-D-glucuronic acid-α-D-mannose) side chain attached to alternate D-glucose units of the main chain. Owing to glucuronic acid and pyruvic acid groups in the side chain of xanthan, it exhibits anionic nature as represented in **Figure 1.14**. Xanthan favors both physical and chemical modifications. Xanthan branched chain heated at 165 °C for seven minutes in the absence of any cross-linking agent forms ester bonding formation between xanthan acid groups (pyruvyl or acetyl) and OH groups**.**

The products prepared by starch blended with xanthan using dry heat treatment increase paste viscosity, which further increases peak viscosity with restricted swelling of granules and shear stability of the paste. The interaction of starch with xanthan during heat treatment is well documented by food science researchers in order to modify the starch as an emulsifier, thickener and stabilizer and to improve its rheological and textural properties **(Sun et al., 2013)**. Modified product used in various food products such as soups, ketchup, dessert, topping, instant beverages and fillings **(Saha and Bhattacharya, 2010)**.

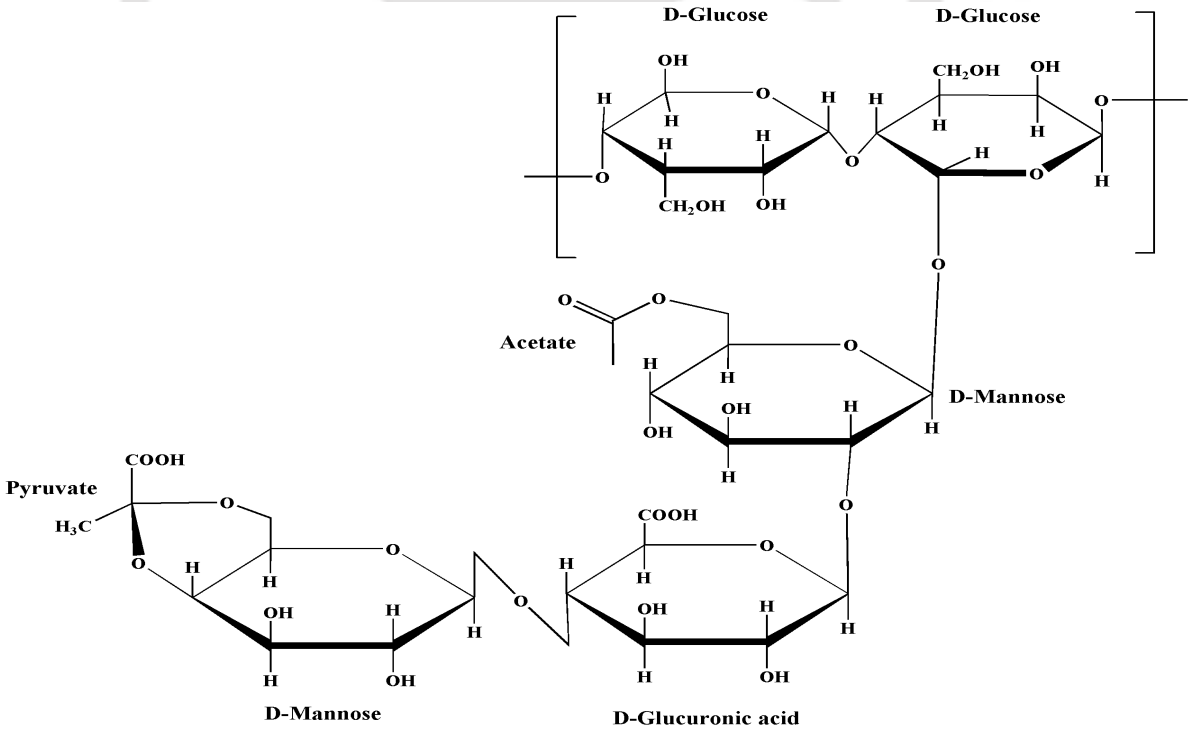

Figure 1.14. Chemical structure of xanthan **(Vania et al., 2013)**

1.11. Plasticizers

Native starches are brittle in nature and are not suitable for processing. Role of plasticizer is to overcome the brittleness of starch and to improve the flexibility, processability and workability of polymers. Some common plasticizers (polyol) used in starch films are glycerol, mannitol, and sorbitol and some monosaccharides (glucose, polyethylene glycol, mannose, and fructose). Plasticizers intersperse between polymer chains, break hydrogen bonding and distribute the mobility of the polymer chains apart, which further enhance flexibility as shown in **Figure 1.15**. Further it lowers glass transition temperature along with more permeation of water vapor and gas **(Kuorwel et al., 2011)**. Starch-based films depend on the concentration of plasticizer and storage relative humidity. Based on plasticizer water vapor permeability, tensile strength and glass transition temperature of bionanocomposite films can be controlled **(Talja et al., 2007)**. Similarly, plasticizer shows direct impact on mechanical properties such as rigidity and deformability of starch films based on the type of plasticizer used **(Lagos et al., 2015)**.

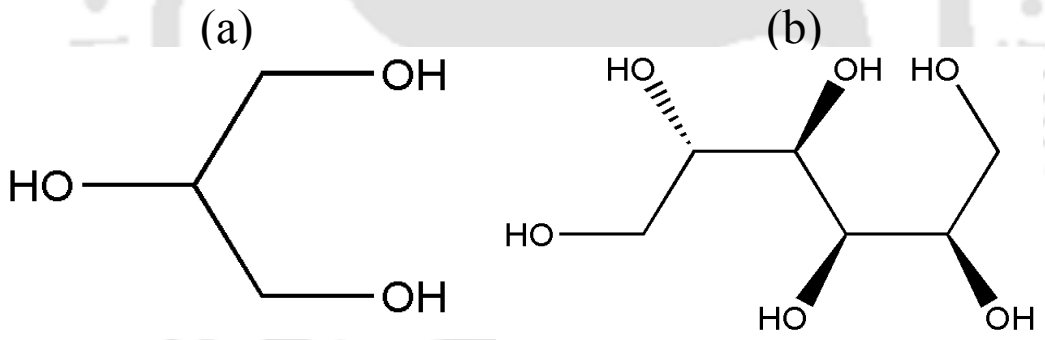

Figure 1.15. Chemical structure of (a) Glycerol and (b) Sorbitol **(Kuorwel et al., 2011)**

1.12. Nanoclay

Recently, nano additives such as nanoclay, nanotubes, nanoparticles, and nanofibers are added into food-packaging material for enhancement in their physical properties. Nanoclays in particular attracted interest with a specific focus on their incorporation into various polymers to produce bionanocomposites. Various forms of nanoclays, including montmorillonite (MMT), Na^+-MMT, Cloisite-Na^+, Cloisite 30B, and Cloisite 20A can be reinforced into packaging films to improve the performance of various biopolymers **(Kumar et al., 2010)**. Most commonly used nanoclay is montmorillonite

(MMT) and is used in various applications such as food packaging, nanoencapsulation of nutrients etc. MMT is a hydrated alumina-silicate layered clay consisting of an edge-shared octahedral sheet of aluminum hydroxide between two silica tetrahedral layer **(Kuorwel et al., 2015)**.

Preparation of nanocomposites using montmorillonite (MMT) has been considered as a promising method to improve barrier properties, mechanical properties and thermal stability without affecting the transparency of biopolymers. MMT is a kind of aluminum silicate classified as phyllosilicates that are environment friendly and readily available in large quantities with relatively low cost (**Ray and Bousmina, 2005)**. MMT is used in packaging materials in the food industry due to its antifungal activity and MMT has no side effects **(Alekseeva et al., 2017; Malachova et al., 2011)**. There are three types of polymer-clay formations, namely conventional, intercalated, and exfoliated as presented in **Figure 1.15**. Conventional structures remain in a polymer when the interlayer space of the clay galleries do not expand like aggregated form, which is due to its poor interaction with the polymer. The intercalation is the state in which polymer chains are present between the clay layers, resulting in a multi-layered structure with an alternating polymer or inorganic layers. This is the result of moderate interaction between clay and polymer. Exfoliation is a process in which the silicate layers are completely separated and dispersed in a continuous polymer matrix. This enhances the properties due to a maximum interaction between clay and polymer **(Bensadoun et al., 2011)**.

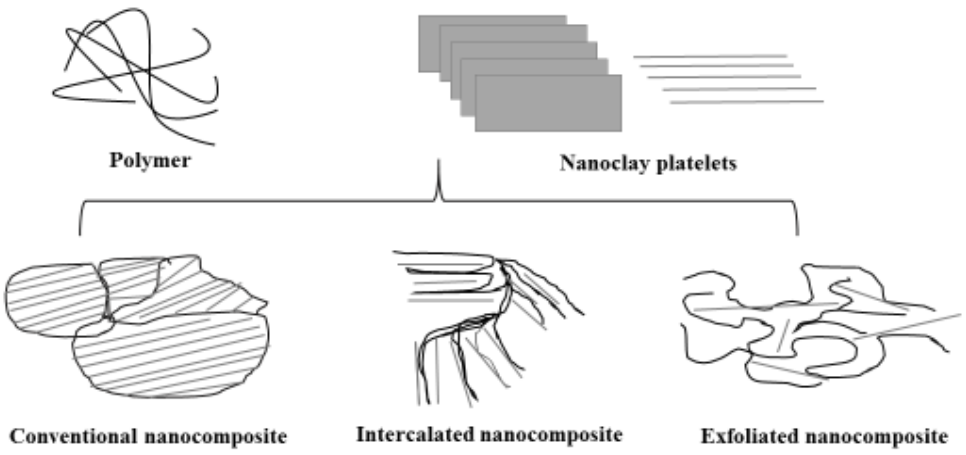

Figure 1.16. Polymer-clay morphologies **(Bensadoun et al., 2011)**

1.13. Antimicrobial activity of starch based materials

Active packaging (AP) is a method in which the packed food product interact with the environment in such a way that to prolong its shelf life, to use as a preservative agent, to improve sensory properties, to prevent from microbial spoilage and to maintain the quality and safety of food products. Active packaging in starch-based films is necessary to prevent microbial growth when packing material is in direct contact with the food product. Active packaging component is also to be considered while designing the films for food packaging applications apart from barrier and mechanical properties of films. Active packaging technique allows a slow release of antimicrobial agents on the food surfaces and preserves a sufficient concentration of the agents for active inhibition of microbial growth during storage of food products. Some commonly used antimicrobial agents in starch-based packaging films are potassium sorbate, chitosan, Dermaseptin S4, Lauric acid, Lysozyme, Lemongrass oil, Oregano Eos and Grape fruit seed extract. Polarity properties of antimicrobial agents should be compatible with the polymer used and should maintain thermal stability during the processing stage **(Kuorwel et al., 2011)**. Potassium salts (sorbates), which are naturally found in plants and some fruits (like the berries of mountain ash) is shown in **Figure 1.16 (a)**. It is categorized as GRAS additive and is more effective against yeast, bacteria and molds. During storage condition, potassium salt is unstable in aqueous solution and hence undergoes an oxidative degradation which can be metabolized by microorganisms. Edible films incorporated with sorbates showed a response against surface contamination of microbes **(Barzegar et al., 2014)**. Biodegradable films incorporated with potassium sorbate as antimicrobial agent inhibited or delayed the growth of microorganisms **(Durango et al., 2006)**. Natural antimicrobial agents such as spice extracts, essential oils and fruit seed extracts (grape, papaya, banana, tamarind, guava, and jackfruit) are also most widely used in the application of food packaging. Among them, grape fruit seed extract (GFSE) was often used due to its better compatibility, anti-microbial and antifungal activity (**Debnath et al., 2011; Kanmani and Rhim, 2014a**).

The GFSE is usually extracted from pulp and seed of grapefruit (*Citrus paradise Macf. Rutaceace*) and contains large quantities of flavonoids (mainly naringin), polyphenolic compounds, ascorbic acid, citric acid, limonoid, and tocopherol (**Figure 1.16 (b))**. Antioxidant activity of citrus flavonoids is an added advantage. GFSE has been used

for the extension of shelf-life of food products such as fruits, fish products and minimally processed vegetables. However, very few works only were reported in the literature on the application of GFSE as an antimicrobial agent in food packaging films **(Kanmani and Rhim, 2014b)**.

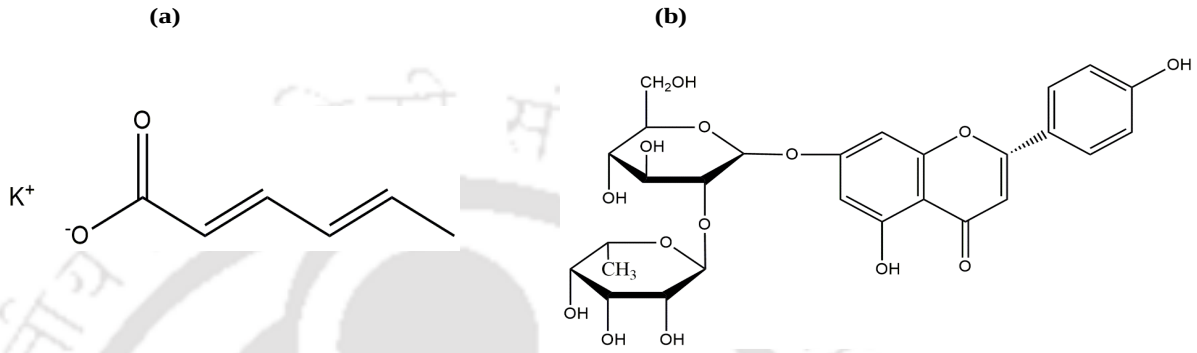

Figure 1.17. Chemical structure of (a) potassium sorbate (KS) and (b) grapefruit seed extract (GFSE) **(Kanmani and Rhim, 2014b)**.

भारतीय प्रौद्योगिकी संस्थान गुवाहाटी
Indian Institute of Technology Guwahati

Chapter 2

Literature Review

2.1. Modification of starch

Lim et al. (2002) studied modification of starches (potato and waxy maize) incorporated with 1% (w/w) ionic gums (xanthan, CMC and sodium alginates) using dry heating method for 2-4 hrs at 130^{o}C. It was observed that addition of ionic gums increases paste viscosity and reduces swelling capacity in native and hydroxypropylated (HP) waxy maize starch whereas opposite conclusions were drawn in the case of potato starch.

Lim et al. (2003) investigated dry heating treatment of sodium alginate, Na-CMC and xanthan with potato and waxy maize starches at pH 6.0 and pH 8.0. Viscosity decreased for the heat-treated starch products due to mild acidity (pH 6.0) whereas alkalinity (pH 8.0) increased the viscosity regardless of the presence of gum.

Lim et al. (2006) examined the effect of dry heating on waxy maize starch in the presence of sodium alginate, sodium carboxymethyl cellulose (CMC) and xanthan. Peak viscosity increased in case of waxy maize-xanthan whereas waxy maize starch incorporated with CMC and sodium alginate exhibited higher peak and final viscosities after the heating treatment.

Sun et al. (2013) reported the effect of dry heating of potato, corn and pea starches impregnated with ionic gums (xanthan, sodium alginate, CMC). Corn and potato starches mixed with xanthan exhibited lower pasting temperature and higher paste viscosity whereas corn and potato starches mixed with sodium alginate showed higher pasting temperature and lower paste viscosity. Potato starch mixed with CMC showed higher paste viscosity whereas corn and pea starches mixed with CMC showed lower paste viscosity.

Xie et al. (2013) investigated physiochemical change in potato starch when treated with microwave heating at 750 W for 5 to 20 s and the treated starch showed shear rate thinning behavior. After microwave modification, storage modulus (G') and loss modulus (G") increased with shear rate up to 15 s and decreased from 15 to 20 s.

Sun et al. (2014b) studied the effect of microwave heat treatment on corn starch blended with xanthan gum. It was found that leaching of amylose granules and granules interspacing decreased with addition of gums. Both peak viscosity and water-holding ability of CS and WCS increased for modified starches.

Gul et al. (2014) modified water chestnuts starch (*Trapa natans*) with carboxymethyl cellulose (CMC) and sodium alginate using dry heating method. Modified starches exhibited reduction in peak viscosity, paste clarity, solubility, swelling capacity and gelatinization temperature. On the other hand, water binding capacity increased.

Pramodrao et al. (2014) used hydrocolloids like carboxymethyl cellulose (CMC) and sodium alginate to modify starches (potato, sweet potato and taro) using dry heating method. Modified starches showed reduction in paste clarity, swelling capacity and solubility.

Vashishta et al. (2017) incorporated sodium alginate in starches from *Dioscorea alata* and *Dioscorea bulbifera* and heat treated at 130°C for 2-4 hrs. Modified starches exhibited reduction in swelling, higher solubility, and improved flow properties.

2.2. Biodegradable polymers

Polymers derived from fossil resources such as aliphatic polyester polycaprolactone (PCL), Polyesteramides (PEA), Poly (butylene succinate-co-adipate) (PBSA) and aromatic co-polyesters Poly (butylene adipate-co-terephthalate) (e.g., PBAT) are included as biodegradable polymers.

Vroman and Tighzert (2009) studied polycaprolactone (PCL) and reported tensile strength of 23 MPa and elongation at break is around 700%. It was reported that the glass transition temperature of PCL was nearly -60°C and melting point was 60 - 65°C. **Zou et al. (2004)** prepared polyesteramides (PEA) and reported tensile strength of 21.2 MPa and elongation to break of 194 %.

Qi et al. (2013) reported glass transition temperature and melting point of poly (butylene succinate-co-adipate) (PBSA), a white crystalline thermoplastic, were about -32.9°C and 73°C, respectively. Tensile strength and elongation at break of PBSE were 30.2 MPa and 261.7%, respectively. It is used in the application of food packaging and medicinal uses.

Hadj-Hamou et al. (2014) reported that poly (butylene adipate-co-terephthalate) (PBAT), an aromatic polyester, showed glass transition temperature of nearly -30°C and melting point of about 125°C. Tensile strength and elongation at break were reported as 18.9 MPa and 436.0%, respectively for PBAT. It is used for medicinal purposes, pharmacy, food packaging and eco-packaging.

Muller et al. (2017) studied polylactic acid (PLA), aliphatic thermoplastic polyester, produced from lactic acid, showed WVP ranging from 1×10^{-14} to 4×10^{-14} kg Pa^{-1} s^{-1}, tensile strength of around 17 to 74 MPa, elongation at break about less than 10%. PLA with 15% glycerol was used as a food packaging material and prepared films showed tensile strength of 2.36 MPa and elongation at break of about 84.10% at 75% RH at 25°C. **Tanada-Palmu and Grosso (2003)** investigated that gluten films showed water vapor permeability (WVP) of about 6.62 $x10^{-11}$ g. Pa^{-1} s^{-1} m^{-1}. It is used for edible packaging.

Carrageenan is a naturally occurring polysaccharide extracted from red seaweeds which possesses an anionic sulphate and exhibits hydrophilicity. Carrageenan films were prepared with addition of 30% glycerol. Tensile strength, elongation at break and WVP of the carrageenan films were found to be 44.63 MPa, 24.22% and 1.22 $x10^{-9}$ g. Pa^{-1} s^{-1} m^{-1}, respectively. Carrageenan films are of particular interest in edible film packaging, pharmaceutical, coating and food industries as gelling, stabilizing and emulsifying agents (**Kanmani and Rhim, 2014b)**.

2.3. Role of amylose in starch based films

Physiochemical properties of starch depend on amount of amylose present in the starch. Amylose content may vary within the same botanical diversity due to alterations in culture conditions and geographic origins. The amount of amylose present signifies the prevention of swelling and solubility in the granules as swelling signifies quick leaching of amylose molecules. Films prepared from amylose are very strong, tasteless, odourless and colourless according to **Alcazar-Alay and Meireles (2015)**.

Lourdin et al. (1995) reported that tensile strength and elongation at break of films increased from 40-70 MPa and 4-6% when amylose content increased from 0-100%. The films were prepared without any plasticizer.

Mali et al. (2006) studied cassava (19% amylose), corn (25% amylose), and yam (29% amylose) starch films for glass transition temperature, crystallinity and mechanical properties prepared under controlled storage (64% relative humidity at 20˚C). It was found that the yam starch films had the lowest glass transition temperature, the highest degree of crystallinity and improved mechanical properties (both initial sample and stored sample). The films with higher amylose content were shown to have better characteristics for being food-packaging films**.**

Tang et al. (2008) reported amylose content beyond 50% in the films did not significantly improve tensile strength, elongation at break and WVP in the presence of plasticizer**.**

2.4. Effect of additives on starch based food-packaging films

Bourtoom and Chinnan (2008) reported the effect of chitosan on mechanical properties and water vapor permeability (WVP) of the prepared rice starch films stored at 60% RH and 25°C. It was found that incorporation of 10-40% (w/w) chitosan increased the tensile strength (TS) from 27 to 38 MPa and deceased the elongation at break from 12.99% to 8.06%. Water vapor permeability (WVP) of the films increased from 4.75 to 9.0×10^{-11} g. Pa^{-1} s^{-1} m^{-1}.

Phan et al. (2009) investigated the effect of arabinoxylan (0-30%) on the WVP and mechanical properties of cassava starch-based films. As the concentration of arabinoxylan increased, WVP decreased from 5.58×10^{-11} to 1.99×10^{-11}g m^{-1} s^{-1} Pa^{-1}. There was a moisture barrier development during the addition of arabinoxylan due to increase in crystallinity of cassava starch-based films. Tensile strength decreased from 35.17 to 20.86 MPa and elongation at break increased from 2.64% to 2.86%.

Muller et al. (2009) prepared cassava starch films incorporated with 50% (w/w) cellulose fibers and stored at 25°C and RH: 64–90%. Tensile strength and elongation at break increased from 2.78 to 23 MPa and 45 to 95% when compared to control films. This could be explained as a result of film rigidity and chemical structure of cellulose and starch. On the other hand, the impregnated cellulose fibers films deceased in its WVP from 2.83 to 1.59×10^{-10} g m^{-1} s^{-1} Pa^{-1}.

Ghanbarzadeh et al. (2010) prepared corn starch films blended with 0-20% (w/w) CMC and stored at 25°C, 97% RH. Tensile strength increased significantly as the concentration of CMC increased from 6.57 to 16.11 MPa. There was a hydrogen-bonding interaction between the filler that presents in the matrix and the starch. Elongation at break and WVP reduced from 55% to 28% and from 7.27 to 6.61 × 10^{-11} g m^{-1} s^{-1} Pa^{-1}, respectively compared to control films.

Tongdeesoontorn et al. (2011) prepared cassava starch films loaded with different concentration of CMC from 0-40% w/w in the film formulation and the films were stored at two different RH 34% and 54% at 25°C for mechanical properties estimation. There was fivefold increment in the tensile strength from 5 to 25 MPa at RH 34% whereas only threefold increment from 3 to 10 MPa at RH 54%. Elongation at break decreased from 42% to 3% and 88% to 18% at RH 34% and 54%, respectively.

Melo et al. (2011) studied 4% (w/w) xanthan gum impregnated into cassava starch films and tested at 25°C and 75% RH. There was a slight improvement in tensile strength from 2.7 to 3.4 MPa and significant increment in elongation at break from 45% to 95% when compared to control films. Also, WVP of the film increased from 1.40 to 1.57 × 10^{-10} g m^{-1} s^{-1} Pa^{-1}.

Abdou and Sorour (2014) investigated the effect of various concentrations (0.50 and 0.75% (w/w)) of carrageenan at 38°C and 98% RH on the WVP, tensile strength and elongation at break. Addition of carrageenan into starch matrixes show less interaction between them and thus rise in WVP was very less (3.6-3.7 x 10^{-10} g m^{-1} s^{-1} Pa^{-1}). Tensile strength and elongation at break were decreased from 25 to 20 MPa and from 55% to 40 %, respectively, when compared to control films.

Ren et al. (2017) studied two different storage conditions of 75% and 95% RH at 25°C on the barrier and mechanical properties of corn starch based films incorporated with 0-40% chitosan. The water vapor permeability (WVP) of the films stored at 75% and 95% RH were increased from 1.5 to 7.8 x 10^{-10} and from 1.8 to 9.2 x 10^{-10} g m^{-1} s^{-1} Pa^{-1}, respectively. Tensile strength of the films kept at 75% and 95% RH were increased from 3.2 to 6.3 MPa and from 1.0 to 3.5 MPa, respectively. Elongation at break at 75% and 95% RH was increased from 58% to 122% and from 25% to 100%, respectively.

Ji et al. (2017) developed chitosan (0-50% (w/w)) incorporated corn starch films reinforced with $CaCO_3$ nanoparticles. Tensile strength and elongation at break lied in the range of 2.24-10.7 MPa and 118.9-78.7%, respectively. The WVP was increased considerably from 1.58 to 7.47 x 10^{-10} g m^{-1} s^{-1} Pa^{-1}**.**

2.5. Effect of plasticizer on properties of starch-based films

Mali et al. (2006) studied important mechanical properties such as tensile strength (TS) and elongation at break (EB) in cassava, corn, and yam starch films contained 20% of glycerol and the films were stored at 64% RH and 20°C. The films were less deformable with storage time. This indicated that crystallinity increased during storage time and thus tensile strength. On the other hand, films become stronger and stiffer but less flexible after several weeks of storage and therefore, water vapor permeability (WVP) decreased in case of stored films.

Dias et al. (2010) developed rice starch films plasticized with different concentrations (20% and 30%) of glycerol and sorbitol and stored at 58% RH and 25°C. There was a reduction in tensile strength and elongation at break (E) of the films when the concentration of plasticizer was increased. Films prepared with glycerol are more flexible and stretchable than sorbitol, thus indicating the greater plasticizing effect of glycerol. This is due to smaller size of glycerol molecules, which easily gain access between the polymer chains through hydrogen bonds, reduce intermolecular interactions, increase intermolecular spacing, and lower the tensile strength of the starch films. The water vapor permeability (WVP) of the films stored at 2-75% RH and 25°C increased with plasticizer concentration. WVP of sorbitol impregnated films are lower than glycerol impregnated films due to higher hydrophilic nature of glycerol compared to sorbitol, which leads to more water molecules absorption.

Bertuzzi et al. (2012) reported high corn starch films plasticized with glycerol at different concentrations from 0-15% and stored at 52% RH and 25°C. When the glycerol content was increased, tensile strength got reduced due to decrease in the rigidity of the films. Elongation at break (EB) of the films increased due to dislocation in polymeric chain, which leads to more flexibility.

Arvanitoyannis and Biliaderis (1999) investigated the effect of plasticizer (glycerol, sorbitol, xylose, and water) concentration on starch blended methylcellulose (MC) films. Tensile strength of the films decreased when the concentration of plasticizer was increased from 5-30% (w/w). In contrast, elongation at break and WVP were increased with plasticizer concentration.

Zhang and Han (2006) studied glucose, fructose and mannose impregnated (1.2% to 3% (w/w)) starch films. There was a decrease in tensile strength and increase in elongation at break. Increase in elasticity of polymeric chain lowers WVP as the concentration of plasticizer (monosaccharides) increases in the films.

Rodriguez et al. (2006) developed starch films with varying concentration (0 to 20% (w/w)) of glycerol and tested for its mechanical and barrier properties. The prepared films exhibited reduction in the tensile strength from 44.1 to 20.3 MPa. This is due to decreasing intermolecular attraction and increasing polymer mobility in the starch packaging films. However, elongation at break increased from 5.9% to 12.1%. The WVP of prepared starch films significantly increased from 4.16×10^{-10}-6.11×10^{-10} g m^{-1} s^{-1} Pa^{-1}.

Da Roz et al. (2006) reported the influence of sorbitol (15% to 30% (w/w)) on casted starch films. There was a significant reduction in the tensile strength from 4.8 to 1.1 MPa. Elongation at break increased from 10% to 28% with sorbitol concentration.

Alves et al. (2007) found the effect of glycerol concentration (20 to 45 (w/w)) on mechanical and barrier properties of starch films. It was observed that tensile strength of the film reduced (21.7 to 5.4 MPa) with increase in glycerol concentration (20% to 45%). However, there was a drastic increase in elongation at break from 5.2% to 153.2%. Furthermore, it was found that the increase in glycerol concentration significantly increased WVP from 2.4×10^{-9} to 4.9×10^{-9} g m^{-1} s^{-1} Pa^{-1}.

2.6. Effect of nanoclay on mechanical and water barrier properties of starch based films

Park et al. (2003) developed potato starch films reinforced with 0-5% (w/w) Cloisite Na^{+} and Cloisite 30B and studied mechanical properties of bionanocomposite films. There was a decrease in tensile strength (TS) for both forms of nanoclay. Elongation at break (EB) increased for the films incorporated with Cloisite-Na^{+} whereas decreased in case of Cloisite 30B impregnated bionanocomposite films.

Tang et al. (2008) studied importance of mechanical and water barrier properties in corn and wheat starch films incorporated with MMT and onium ion modified MMT I30E. Both corn and wheat starch-MMT composite films showed higher tensile strength, lower elongation at break and better WVP with increase in clay content from 0% to 9% (w/w) and this can be explained due to formation of an intercalated nanostructure. But corn starch onium ion modified (MMT) I30E composites films showed lower tensile strength, lower elongation at break and lower WVP properties.

Chung et al. (2010) studied the effect of clay content (0-5 (w/w)) in corn starch and corn starch blended chitosan bionanocomposite films for their mechanical properties. It was reported that tensile strength of the films increased with nanoclay (Na^+-MMT) content. Elongation at break decreased for corn starch films but the opposite result was observed for starch blended with chitosan films. **Almasi et al. (2010)** investigated the effect of MMT (7% (w/w)) in starch blended CMC composite films. Tensile strength increased from 9.83 to 27.55 MPa while elongation at break decreased from 63.52 to 18.25 in comparison to control film.

Melo et al. (2011) developed cassava starch and cassava starch/xanthan films containing 5% (w/w) Na^+-MMT and studied the impact of additives on mechanical and barrier properties of the films. With the addition of Na^+-MMT content tensile strength significantly increased and WVP decreased for both films. Elongation at break decreased from 45% to 37% in cassava starch films while it increased from 45% to 69% for cassava starch/xanthan films.

Piyada et al. (2013) examined the barrier and mechanical properties of rice starch films containing 0-20 % (w/w) starch nanocrystal. Tensile strength of the film increased with starch nanocrystal content whereas elongation at break and WVP reduced compared to control films. Recently, **Sun et al. (2014a)** investigated barrier and mechanical properties of corn starch films blended with $CaCO_3$ nanomaterial. Increase in $CaCO_3$ content from 0-0.5 % (w/w) decreased WVP whereas the tensile strength and elongation at break increased with the concentration of the $CaCO_3$.

2.7. Effect of antimicrobial agent in starch based packaging films

Growth of bacterial and fungal microbes might be possible in food packaging materials. Such growth of microorganisms could be inhibited using natural antimicrobial agent, which is compatible with food packaging materials.

Baron and Sumner (1993) incorporated 0-20% (w/w) potassium sorbate into starch-based films and acidified with lactic acid effectively to inhibit the proliferation of *E. coli* O157: H7 and *S. typhimurium.* Both *E. coli* O157: H7 and *S. typhimurium* reduced by 2 log CFU mL^{-1} after 3.5 h at 37°C and 4 log CFU mL^{-1} after 2 h at 37°C, respectively. Moreover, starch films incorporated with potassium sorbate suppressed the growth of *E. coli* O157 H7 and *S. typhimurium* on poultry products after 12 days of storage at 7°C.

Durango et al. (2006) developed starch films coated with chitosan at different concentrations from 0-5% (w/v). There was an inhibition of *S. enteritidis* in liquid culture medium. **Miltz et al. (2006)** found that peptide derivative dermaseptin S4 incorporated into starch-based films effectively suppressed the growth of aerobic bacteria and molds on cucumbers. **Salleh et al. (2007)** investigated incorporation of lauric acid (1-8% (w/w)) and chitosan (1-9% (w/w)) on starch films. It was found that antibacterial agents showed strong antimicrobial activity against *B. subtilis.* But, no inhibition effect was shown against the proliferation of *E. coli*. **Nam et al. (2007)** found that starch based films with lysozyme effectively inhibited the growth of *B. thermosphaceta B2*.

Maizura et al. (2008) studied starch-alginate films added with lemongrass oil using agar diffusion method. The antibacterial activity of lemongrass oil suppressed the proliferation against *S. enteritidis* and *E. coli O157:H7* but not against *S. aureus*. **Pelissari et al. (2009)** prepared starch films containing oregano essential oil (EO). Suppression of proliferation of *E. Coli O157:H7*, *S. enteritidis* and *B. cereus* were found in the agar diffusion method.

Corrales et al. (2009) studied the activity of grape seed extract in starch films. There was a significant reduction in the proliferation of *B. thermosphaceta B2* by 1.3-log CFU mL^{-1} after 4 days of storage at 4°C compared to the films with no grapefruit seed extract films. **Kuorwel et al. (2011)** reported that sweet potato starch films impregnated with 15% (w/w) potassium sorbate showed suppression of *S. aureus* growth on solid and semi-solid media compared to films with no potassium sorbate**.**

2.8. Research gap in the prior art

Green packaging has received worldwide commercial and industrial usages. The starch based packing films can be used to pack dry solid food products such as bread, snacks, biscuits, cereals, vegetables and fruits products with lower water activity. Higher shelf life and food quality are preferred among consumers. Starch based materials have the potential to be environmental friendly with essential required packaging properties of high water barrier, better mechanical properties and thermal resistance. Also, prepared films exhibited heat sealability properties.

- Native starch has limited usage in food industry due to its poor stability, cohesive structure, insolubility in cold water, loss of viscosity, easy retrograde and syneresis, which contribute to its main challenges in its uses. Despite many conducted studies to modify different starches with xanthan, till now potato starch (PS) with xanthan gum (X) via MADH has not been studied.
- Main challenges in starch based films are their highly hydrophilic property due to water sensitivity and low mechanical strength. There is no existing study available on how amylose: amylopectin ratios of starches affect barrier properties such as moisture content, solubility and water vapor permeability along with their mechanical strength.
- Limited literature are available on the addition of proper plasticizing as well as antimicrobial agents to improve physical properties, anti-bacterial and anti-microbial properties of starch blended films for food packaging applications.

2.9. Objectives of Research

The aim of the current research is to develop starch based food packaging films with highly abundant natural additive such as carboxymethyl cellulose (CMC) and chitosan (CH) in order to improve its water barrier, mechanical, thermal properties. Nanoclay is used as a reinforcing agent to improve water barrier, mechanical, thermal and anti-microbial properties of packaging materials. Addition of antimicrobial agents in the starch based blended films such as chitosan, potassium sorbate and grapefruit seed extract inhibits microbial growth and extends the shelf life and food quality of the products. This novel

starch based food packaging films, which are cost effective will be used to pack perishable foods such as bread slices.

The following objectives are designed to carry out this work

- To study the effect of microwave and conventional heating on modification of potato starch with xanthan gum.
- To investigate the effect of amylose-amylopectin ratios on physical, mechanical and thermal properties of starch based bionanocomposite films incorporated with CMC and nanoclay.
- To study the influence of amylose-amylopectin ratios on barrier, mechanical and thermal properties of starch bionanocomposite films blended with chitosan and nanoclay.
- To analyze the effect of plasticizers and antifungal agents in corn starch-nanoclay bionanocomposite films blended with chitosan.
- To study the effect of grape fruit seed extract ratios on physical and functional properties of corn starch-chitosan-nanoclay bionanocomposite films for food packaging applications.

Chapter 3

Experimental Details

3.1. Materials and Methodology

3.1.1. Materials and Reagents

Potato starch (PS), wheat starch (WH) and corn starch (CS) containing amylose: amylopectin ratios and moisture content of 20:80, 25:75 and 28:72 and 18.62%, 14.24% and 13.83%, respectively were purchased from *Nacalai* Tesque Inc. (Kyoto, Japan). High amylose corn starch (HACS) containing amylose: amylopectin ratio of 70:30 and 14.18% moisture content was supplied by Sanwa Starch Co., Ltd. (Nara, Japan). Carboxymethyl cellulose (CMC) was procured from *Nippon Paper Industries Co., Ltd.* (Tokyo, Japan). Chitosan from shrimp shells with <75 % deacetylation degree was supplied by Sigma Chemical Co (St. Louis, MO, USA). Glycerol $C_3H_8O_3$ (MW= 92 g/mol) and sorbitol $C_6H_{14}O_6$ (182 g/mol) as plasticizers were purchased from *Nacalai* Tesque (Kyoto, Japan). Xanthan (food grade) was purchased from Tokyo Chemical Industries, Tokyo, Japan. Calcium chloride, sodium bromide and sodium chloride were obtained from *Nacalai* Tesque Inc. (Kyoto, Japan). Sodium montmorillonite (Na-MMT) nanoclay was procured from Sigma-Aldrich (St. Louis, MO, USA). Potassium bromide (KBr) and Tween 80 solutions were supplied from Merck, Mumbai (India). Potato dextrose agar (PDA) and modified mineral salt basal (MMSB) media used in this study was obtained from Himedia (India). Deionized (DI) water (conductivity 0.055 μS cm^{-1}) of Millipore Filtration Unit (Elix-3, USA) was used to prepare all the reagents and solutions.

3.1.2. Antimicrobial Agents

Potassium sorbate (KS) was purchased from *Nacalai* Tesque (Kyoto, Japan). Grapefruit seed extract (GFSE) was purchased from ABC Techno Inc. (Tokyo, Japan). Ampicillin B used in this study was obtained from Himedia (India).

3.1.3. Microorganisms

The microorganism for bacterial strain *Rhodococcus opacus* DSM 43205 and fungal strain *Aspergillus niger* at MTCC 1785 used in this study was collected from Microbial Type Cell Culture (MTCC, Chandigarh, India).

3.1.4. Other Materials

Ethanol was used as solvent (absolute, AR grade) and was supplied by Merck India. Hydrochloric acid (HCl) and acetic acid were purchased from *Nacalai* Tesque (Kyoto, Japan). Commercially available bread samples were purchased from local confectionery shop. Synthetic plastic was obtained from the local market. Black soil was collected from the bank of Brahmaputra River, Indian Institute of Technology Guwahati.

3.2. Methodology

3.2.1. Starch modification using MADH treatment

Starch was modified with xanthan gum using dry heating method based on the procedure mentioned by **Lim et al. (2002)** with certain modifications. Briefly, 0.5 g of xanthan gum was steadily mixed in 100 mL of deionized water. The solution was vigorously mixed to dissolve the gum completely. Starch (45.5 g, dry basis) was distributed into gum solution by stirring for 30 min at normal temperature. The slurry was then shifted to a petri dish and conventionally heated at 45^{o}C. The powder mixture was grounded by mortar and pestle after moisture content reached < 10%. The finely grounded mixture of starch-gum was passed through the 75-mesh sieve. The starch-xanthan sample was kept in petri dish and packed with plastic cover with small holes to allow steam to escape. The samples were microwave irradiated in the microwave oven (Panasonic, 1E96250824) at 600 W for 4, 8 and 12 mins. In order to compare both the heating methods, the starch-xanthan sample was heated in the convection oven at 130^{o}C for 4 h. The sample starch xanthan without heating was used as standard. All the dried starch samples were stored in a desiccator at 25^{o}C for further testing. Experimental procedure for modification of potato starch with xanthan gum using MADH treatment are presented in **Figure 3.1.**

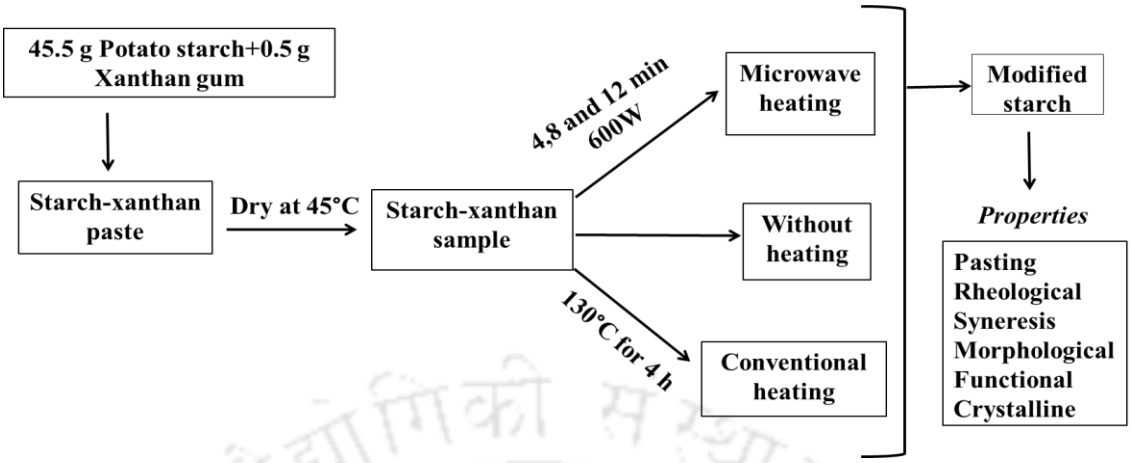

Figure 3.1. Experimental procedure for modification of starch with xanthan gum using MADH.

3.2.2. Film preparation

3.2.3. Preparation of starch-carboxymethyl cellulose biocomposite films

The films were prepared using solution-casting technique. First, an amount of 5 g of different starch sources and 2 g of CMC were added into 100 ml of distilled water under constant magnetic stirring condition (700 rpm) at room temperature for 1 h. Then, the above film forming solutions were heated until gelatinization. Finally, 40% (w/w) of glycerol as the plasticizing agent was added under constant magnetic stirring condition.

3.2.4. Preparation of starch-carboxymethyl cellulose-nanoclay bionanocomposite films

An amount of 0.01 g of nanoclay was dispersed into 50 ml of distilled water by the ultrasonic mixer (Ultrasonic cleaner, Mainland, China) for 5 h. After complete dispersion, 5 ml of nanoclay was added into the mixture of different starch sources blended with CMC. After mixing the solution for 15 min, 10 ml of the sample was poured into 12 cm diameter petri dishes. Petri dishes, which contain samples, were kept at 55°C for 3 h for film formation. The films were peeled off and kept at 25°C and 75% RH for further examination. The film samples were designated as PS/CMC/nanoclay, WH/CMC/nanoclay, CS/CMC/nanoclay and HACS/CMC/nanoclay. The control film sample was also prepared using similar procedure without any starch source and it was

named as CMC/nanoclay. Experimental procedure for preparation of starch-carboxymethyl cellulose-nanoclay bionanocomposite films are shown in **Figure 3.2.**

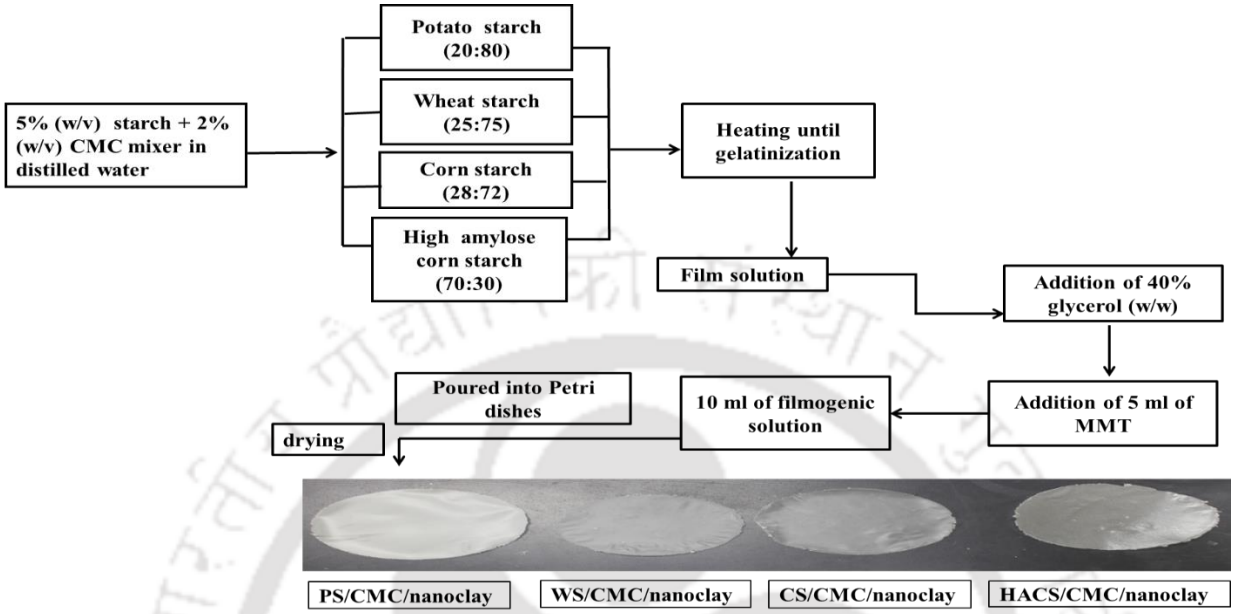

Figure 3.2. Experimental procedure for preparation of starch-carboxymethyl cellulose-nanoclay bionanocomposite films

3.2.5. Preparation of starch-chitosan biocomposite films

Chitosan powder (1g) in 1% (v/v) acetic acid solution was prepared. 5g starch was mixed in 100 mL deionized water and the suspension was agitated under constant magnetic stirring (700 rpm) at room temperature for 60 min followed by heating until complete gelatinization. The two solutions obtained above were mixed under constant agitation (700 rpm) and later 40 % (w/w) of glycerol was dissolved in solution under constant magnetic stirring.

3.2.6. Preparation of starch-chitosan-nanoclay bionanocomposites films

Clay nanoparticles (0.01 g) were suspended into distilled water (50 mL) by ultrasonic mixer (Ultrasonic cleaner, Mainland, China) for 5h. 5 mL of this solution was added to mixture of starch-chitosan film solution and stirred for 15 min. 10 mL of film-forming suspension was poured into petri dishes (12 cm in diameter). The films were formed by drying at 55°C for 3 hours of conventional heating. The films were prepared using the solution-casting method. The samples were denoted as PS/CH/nanoclay,

WH/CH/nanoclay, CS/CH/nanoclay, HACS/CH/nanoclay and the control sample was denoted as CH/nanoclay. The peeled films were kept in a chamber at room temperature and 75% RH for 72 h prior to further characterization. The procedure for preparation of CH/nanoclay film is same as that of other films with the absence of the starch solution. Experimental procedure for preparation of starch-chitosan-nanoclay bionanocomposite films are shown in **Figure 3.3**.

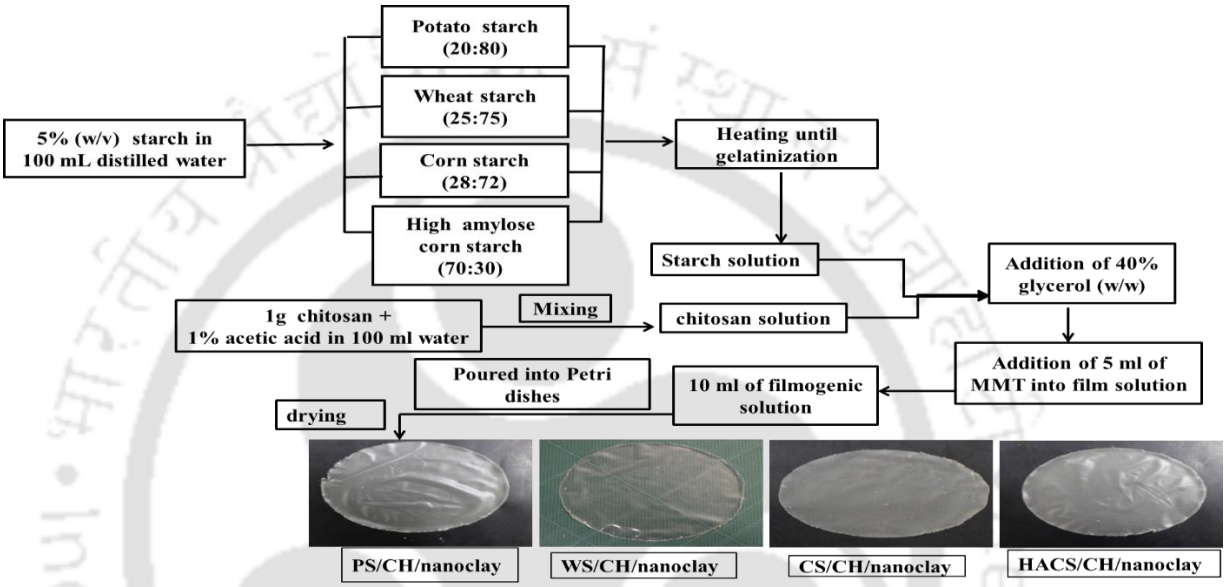

Figure 3.3. Experimental procedure for preparation of starch-chitosan-nanoclay bionanocomposite films.

3.2.7. Preparation of corn starch-chitosan biocomposite films

Initially, 1g of chitosan powder in 1% (v/v) acetic acid solution was prepared and 5 g of corn starch was added into 100 ml distilled water under constant magnetic stirring (700 rpm) at room temperature for 1 h. Then, the above film-forming solutions were heated until gelatinization. The two solutions obtained above were mixed under constant stirring (700 rpm) and later 30 % (w/w) of glycerol and sorbitol was dissolved in film forming solution under constant magnetic stirring condition for 2h. Antimicrobial agent, 0.2 g of potassium sorbate (KS) was dissolved in 15 mL distilled water and the solution was mixed in film forming solution. The pH of the film forming solution was maintained at 4.5 by adding 2 M HCl. Another antimicrobial agent grapefruit seed extract (GFSE) (0.5 g) was added during mixing.

3.2.8. Preparation of corn starch-chitosan-nanoclay bionanocomposite films

An amount of 0.01 g of nanoclay was dispersed into 50 ml of distilled water by the ultrasonic mixer (Ultrasonic cleaner, Mainland, China) for 5 h. After complete dispersing, 5 ml of nanoclay was added into the mixture of corn starch blended with CH. After completely solubilization and well dispersion, 10 ml of the film-forming solution was cast on 12 cm diameter petri dishes. All films sample were allowed to dry at room temperature 25°C for 2 days. All dried bionanocomposite films were peeled off and kept at 25ºC and 75% RH prior to further characterization. The samples were designated as CS/CH/nanoclay/GLY/KS, CS/CH/nanoclay/SOR/KS, CS/CH/nanoclay/GLY/GFSE and CS/CH/nanoclay/SOR/GFSE. Starch-chitosan films without addition of plasticizer and antimicrobial agents were used as a control (CS/CH/nanoclay). The remaining procedures were same for CS/CH/nanoclay film preparation. Experimental procedure for preparation of corn starch-chitosan- nanoclay bionanocomposite films with different plasticizing and antimicrobial agents are shown in **Figure 3.4**

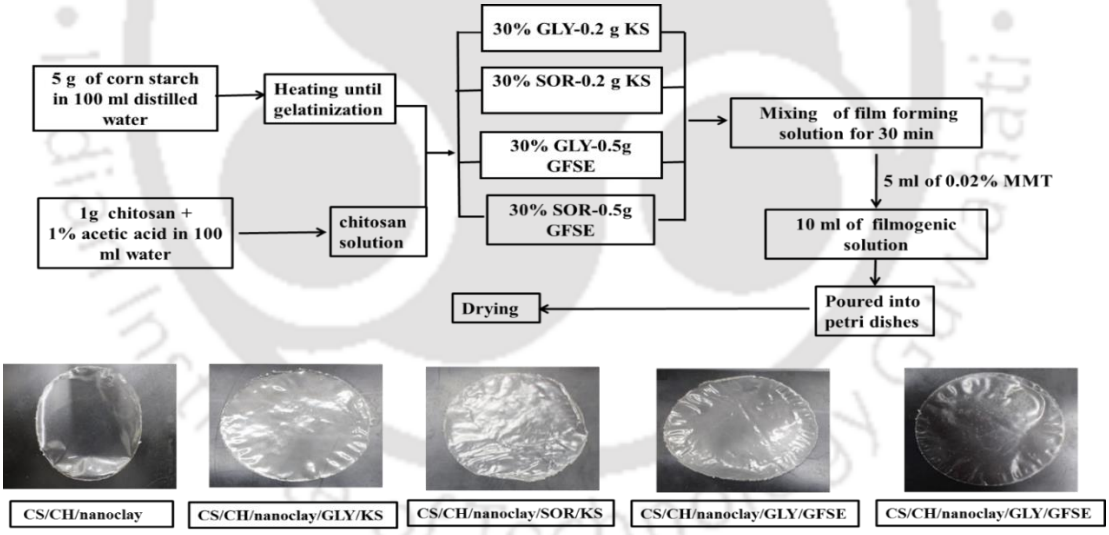

Figure 3.4. Experimental procedure for preparation of corn starch-chitosan-nanoclay bionanocomposite films with different plasticizers and antimicrobial agents.

3.2.9. Preparation of corn starch-chitosan-nanoclay-grapefruit seed extract bionanocomposite films

Initially, 5 g of corn starch was added to 100 ml of distilled water under a constant magnetic stirring condition (700 rpm) at room temperature for 1 h. Then, the above film forming

solution was heated until gelatinization. Chitosan powder (0.75 g) was mixed with 1% (v/v) acetic acid solution along with gelatinized starch solution. Sorbitol as the plasticizing agent (30% (w/w)) was added under constant magnetic stirring for 2h. Finally, antimicrobial agent grapefruit seed extract (GFSE) was added at concentrations 0.5, 1.0, 1.5 and 2.0% (v/v) during the mixing period of 1h. An amount of 0.01 g of nanoclay was dispersed into 50 ml of distilled water by the ultrasonic mixer (Ultrasonic cleaner, Mainland, China) for 5 h. After complete dispersion, 5 ml of nanoclay was added to the mixture of film forming solution. After mixing the solution for 15 min, 10 ml of the sample was poured into 12 cm diameter petri dishes using a solution-casting technique. Films were formed by keeping all the samples at 55ºC for 3 h. The films were peeled off and kept at 25°C and 75% RH prior to further examination. The prepared samples were designated as CS/CH/nanoclay/0.5% GFSE, CS/CH/nanoclay/1% GFSE, CS/CH/nanoclay/1.5% GFSE and CS/CH/nanoclay/2% GFSE bionanocomposite films. The control sample (CS/CH/nanoclay) was also prepared without addition of GFSE. The remaining procedures were same for CS/CH/nanoclay bionanocomposite films preparation. Experimental procedure for preparation of corn starch-chitosan-nanoclay bionanocomposite films with different amount of antimicrobial agents are shown in **Figure 3.5.**

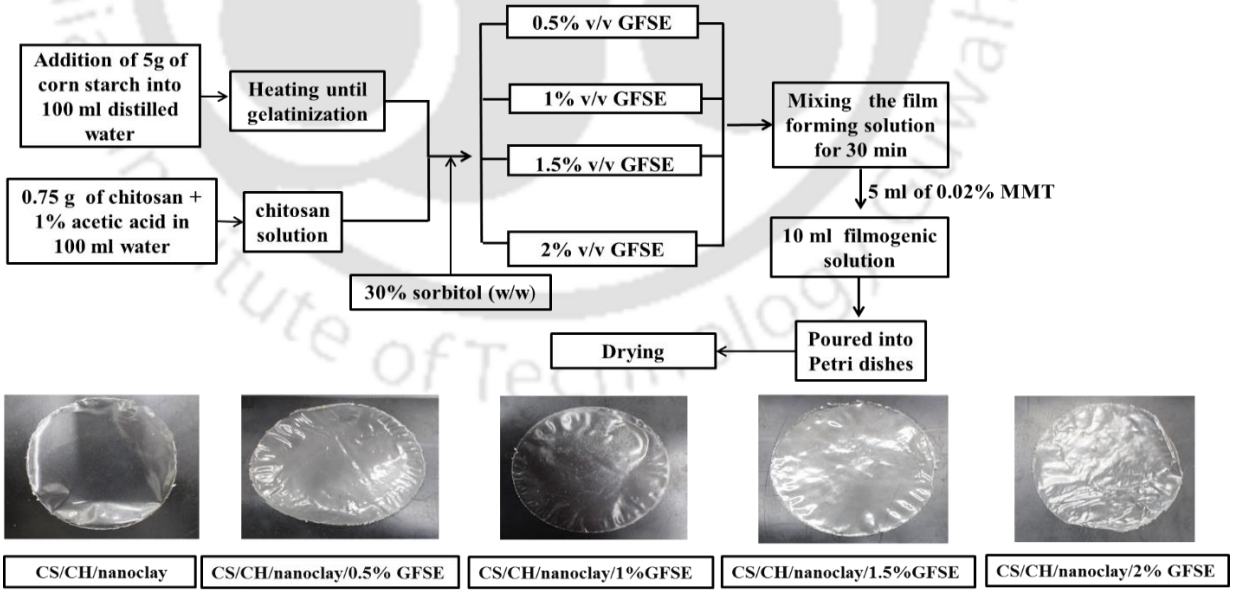

Figure 3.5 Experimental procedure for preparation of corn starch-chitosan-nanoclay bionanocomposite films with different amount of antimicrobial agents (GFSE).

3.3. Analytical instrumentation and characterizations

3.3.1. Measurement of amylose content in starch

Amylose:amylopectin ratios mentioned in starch sources were determined using Megazyme starch determination kit **(Megazyme, 2016)**.

3.3.2. Pasting properties

Paste viscosity of the starches was measured using Rapid Visco-Analyzer (RVA), (RVA Super 3 Newport scientific Pvt. Ltd., Australia). Samples slurry (12.5 %) was weighed and added into deionized water in the RVA container to attain a total weight of 28 g. A programmed set of 13 min was used for constant heating and cooling cycle where it was heated from 50 to 95^{o}C in 5 min, equilibrated at 95^{o}C for 2 min and cooling from 95 to 50^{o}C in 4 min and equilibrated at 50^{o}C for 2 min 30 s. Parameters measured recorded were pasting temperature (PT), peak viscosity (PV), trough viscosity (TV i.e. minimum viscosity at 95^{o}C), final viscosity (FV i.e viscosity at 50^{o}C), breakdown viscosity (BV = PV-TV) and setback viscosity (SV = FV-TV).

3.3.3. Flow and dynamic rheological properties

The rheological properties of starches were measured using rheometer (AR2000, G2KG, TA Instruments, New Castle, DE, USA). The parallel plate system of diameter was 40 mm and a gap of 1 mm was selected. Modified starch of 5g (w/w) was added with 95 g of distilled water. Sample was kept on plate at 25°C. Shear rate was varied from 0 to 1000 s^{-1} and apparent viscosity value was recorded according to the procedure mentioned by **Xie et al. (2013)**. Dynamic shear data was obtained by operating at varying frequency (0.1-10 Hz) and constant strain (3%) to obtain elastic modulus (G′) and loss modulus (G″).

3.3.4. Syneresis properties (freeze-thaw stability)

Syneresis was obtained according to the procedure mentioned in **Alamri et al. (2012)** with minor modifications. Briefly, 6 g starch slurry obtained by RVA was transferred into centrifuge tubes and allowed to be frozen at -20^{o}C. After storage for four days the suspension slurry was shifted into water bath at 50^{o}C for 30 min and centrifuged at 3000 × *g* for 15 min. The clear water was decanted, remaining gel was weighted, and this residual were kept in freezer for next four days of cycle. Aforementioned procedure

was continued for eight days. The percentage of syneresis value (SV) was estimated. W_E is the weight of the exudate from paste and W_P is the initial weight of the paste and syneresis value (SV) was calculated using Eq. (3.1).

$$SV = \left(\frac{W_E}{W_P} \right) \times 100 \qquad (3.1)$$

3.3.5. Diff erential scanning calorimeter

Thermal properties were estimated using diff erential scanning calorimeter (SII EXSTAR 6200, DSC, Japan) according to **Chanvrier et al. (2007)** with minor modifications. Briefly, samples (4.0 mg, dry basis) were weighed in an aluminum pan and mixed with 8μL of distilled water. The pan was hermetically sealed and equilibrated at room temperature for at least 2 h. Each sample was heated under nitrogen atmosphere from 30^{o}C to 120^{o}C at 5^{o}C/min with an empty sealed pan as a reference to analyze the gelatinization enthalpy.

3.3.6. Thickness measurement

The film thickness was measured using digital micrometre (Mitutoyo, Japan) with an accuracy of 0.001 mm. The thickness of the film was measured at three different places.

3.3.7. X-ray diffraction analysis

The crystalline structure of the starch-based material was analyzed using an X-ray diffractometer (Bruker D8 Advance, Karlsruhe, Germany). The instrument was employed with Ni-filtered Cu Kα radiation (λ = 0.15406 nm, 40 kV, 20 mA). The diffractograms were recorded over an angular range (2θ) of 5–50°, with a step size of 0.02° and a scan rate of 2 s per step**.**

3.3.8. Water barrier properties

3.3.8.1. Moisture content

The moisture content of films was determined using a drying oven method (**Rhim et al., 2013)**. The rectangular films were cut into sizes of 40 mm × 15 mm and subsequently dried at 105^{o}C for 24 h. The moisture content was estimated from film weight loss and expressed as percentage moisture content.

3.3.8.2. Film solubility

The method described by **Farahnaky et al. (2013)** was adopted with minor modifications for the determination of film solubility. In a typical experiment, the films were cut into sizes of 40 mm × 15 mm and heated at 105°C for the determination of initial dry matter. Then, the dried films were placed in 50 ml of distilled water for 24 h at 25°C under constant stirring condition (100 rpm) using an incubator shaker. After this period, the samples were removed and dried at 105°C for the determination of final dry matter that was not dissolved. The percentage solubility was calculated as follows in Eq. 3.2.

$$\text{Percentage solubility} = \frac{\text{Initial dry weight - final dry weight}}{\text{Initial dry weight}} \times 100 \qquad (3.2)$$

3.3.8.3. Water vapour permeability (WVP)

The water vapor permeability (WVP) of films was determined according to the standard method JIS Z0208 known as "cup method **JIS (1976)**. Films were prepared and sealed over the circular opening of 0.00287 m^2 of a permeation cell, which was stored at 25°C in a desiccator. The cell was completely filled with calcium chloride anhydrous ($CaCl_2$ – 0% RH), and the system was placed in a desiccator containing saturated sodium chloride solution (NaCl – 75% RH). Water vapor transport was determined by the weight gain of the permeation cell. The changes in the weight of the cell were recorded as a function of time. The water vapor transmission rate (WVTR) was defined as the ratio of slope (g/s) to the transfer area (m^2). The weight of cups was recorded four times at 12 h interval for 2 days. The water vapor permeability (WVP) was calculated from the water vapor transmission rate (WVTR) as followed by Eq. 3.3 and 3.4.

$$\text{WVTR } (g/m^2 s) = \frac{\text{Change in weight}}{\text{Mesursement time} \times \text{Composite film sample area}} \qquad (3.3)$$

$$\text{WVP} = \frac{\text{WVRT} \times \text{L}}{\Delta \text{P}} = (g/msPa) \qquad (3.4)$$

where, W = increase in cup weight (g), L = thickness of film (m), t = measurement time (s), A= composite film sample area (m^2), and ΔP = pressure difference between outside and inside the cup (Pa).

3.3.9. Mechanical properties

Tensile strength and elongation at break of films were determined at 25±1°C using a tensile tester (EZ-L, Shimadzu, Japan) according to D882-91 method **ASTM (1996)**. All films to be tested were cut into strips of 80 mm × 5 mm and fixed in between grips with a set distance of 50 mm and a cross-head speed of 5 mm/min. Tensile strength was recorded by dividing the maximum force on the sample by the initial cross-sectional area of the film while elongation at break (E) was expressed as a percentage of the ability of film to deform before final breaking.

3.3.10. Dynamic mechanical thermal analysis (DMTA)

The dynamic mechanical thermal analysis (DMTA) was carried out by Q800 DMA (TA Instruments, New Castle, USA) with a liquid nitrogen cooling system using a clamp tension. The test strips were cut into small strips (50 x 10 mm) and clamped in the instrument with an initial grip separation of 20 mm. A sinusoidal strain is applied in the films to determine viscoelastic properties. The testing parameters were frequency = 1 Hz ; strain = 0.05% ; temperature range= -75 to 150°C and heating rate = 5°C/min. Dynamic mechanical spectroscopy was used to calculate Tg value within the linear viscoelastic regime. The storage modulus (E') and loss tangent (tan $\delta = \Delta E'/E''$) were recorded as a function of temperature from selected heating or cooling rate and with constant frequency.

3.3.11. Thermal stability analysis

A thermo-gravimetric analyzer (SII EXSTAR 6300 TG/DTA, Japan) evaluated mass loss in film with rise in temperature. Each film which weighs approximately 5 mg was placed in an aluminum crucible. The sample was then from 40°C to 400°C at 5°C/min in an inert atmosphere with a nitrogen flow rate of 20 mL/min.

3.3.12. Electron microscopic analyses

The morphology of the film was observed using a scanning electron microscopy SEM (S-4800, Hitachi., Japan) at an accelerating voltage of 5 kV. The films that were frozen in liquid nitrogen and freeze-dried for 12 h were sputtered with *oxinium* before the analysis. Normal potato starch and modified potato starch slurry was gelatinized with RVA. Starch pastes were frozen in liquid nitrogen and then freeze-dried for 48 h. All dry

finely ground sample was placed on a carbon tape attached to holder coated with *oxinium* before the analysis. The morphology of the films after microbial and soil degradation was observed using field emission scanning electron microscopy (FESEM) (Zeiss, model-Sigma). All the films were gold sputtered before the analysis.

3.3.13. Fourier transform infrared (FTIR) spectroscopic analysis

The FTIR-ATR spectra of the film was recorded using FTIR spectrometer (Spectrum 100, Perkin Elmer, USA). The films were investigated in between 4000–600 cm^{-1} wavenumbers with a resolution of 4 cm^{-1}. The presence of different functional groups between starch and gum was confirmed from the FTIR spectra using KBr pellet method. KBr salt was dried in a hot air oven (Model: N-101, Navyug, India) at 105°C. KBr to sample ratio of 99:1 (w/w) was grounded in a clean mortar and pestle for homogenization. It was then transferred to the pellet-casting die. The pressure of 5 to 7 tons was imposed to create a thin pellet. The background correction was done using a pure KBr in between 400 to 4000 cm^{-1} wavenumbers with a resolution of 4 cm^{-1}. To ensure noise reduction 40 scans were carried out for each specimen. An FTIR spectrometer (Model: IR affinity 1 Make: Shimadzu, Japan) was employed for this work.

3.3.14. Microbial degradation

Starch-based bionanocomposite films were checked for microbial degradation according to **Mehta et al. (2014)**. The films were cut into a dimension of 30 mm x 10 mm for microbial degradation by *Rhodococcus opacus*. The samples were kept at 30°C and 120 rpm for 3 days. The culture was inoculated into modified mineral salt basal (MMSB) medium contains K_2HPO_4 (3.7 g), 0.1 M $MgSO_4$ (10ml), $(NH_4)_2HPO_4$ (1.1g) and 1.0 ml of microelement solution containing $MnCl_2.4H_2O$ (1.989), $COSO_4.7H_2O$ (2.819), $FeSO_4.7H_2O$ (2.789), $CaCl_2.2H_2O$ (0.179), $ZnSO_4.7H_2O$ (0.299) in 1 L of 1N HCl. The percentage degradation was calculated using the following Eq. 3.5.

$$\text{Weight loss} = \frac{W_1 - W_2}{W_1} \times 100\% \qquad (3.5)$$

where, W_1 is the initial mass and W_2 is the mass of the specimen after 3 days of degradation.

Similarly, LDPE was also checked for its microbial degradation by *Rhodococcus opacus*. All the values are an average of three replicates. After 3 days of microbial degradation, all the film samples were investigated for their surface morphology by FESEM.

3.3.15. Soil burial degradation test

Soil burial degradation was carried out according to the method developed by **Yoon et al. (2012)** with a minor modification. Briefly, 1200 g of agricultural soil was filled in pots. All the films were cut into a size of 30 mm×10 mm and were buried in the soil at the depth of 10 cm. The pots were kept in an open place at room temperature. Soil humidity was maintained around 20-40% by a pinch of water at a regular time interval. Films were carefully taken from the soil and washed gently with distilled water to remove soil. The films dried in an oven till a constant weight was observed. The process was carried out for a regular interval of 15 days from 0 to 60 days as a part of degradation test. The similar method has been used to test the degradation of synthetic plastic. The film degradation was tested by percentage weight loss in the medium using the formula calculated by Eq. 3.6.

$$\text{Weight loss} = \frac{W_1 - W_2}{W_1} \times 100\% \tag{3.6}$$

where, W_1 is the initial mass and W_2 is the mass of the specimen after soil burial degradation. All the results are an average of three replicates. Soil degraded films of 30 and 60 days were examined for their surface morphology by FESEM.

3.3.16. Antifungal activity evaluation

The antifungal activity of films was evaluated by a direct contact with bread samples. The bread samples had a moisture content around 40%. Bread samples were cut in to a uniform size and sealed with synthesized bionanocomposite films. In order to compare the antifungal activity of bionanocomposite films with conventional polymeric packaging materials, same sizes of bread samples were also packed with low-density polyethylene (LDPE). All packed bread samples were stored at 25°C and 59% RH for 15-20 days.

3.3.17 Antifungal assay

3.3.17.1. Culture preparation

Potato dextrose agar (PDA) slant media was used for cultivation of *Aspergillus niger*. The fungal cultures were cultivated on potato dextrose agar slants for 10 days at 25°C. The spores were harvested using 10 ml of Tween 80 solution. Finally, the spore suspension was adjusted to a final spore concentration of 10^5–10^6 spore/ml.

3.3.17.2. Agar diffusion test for antifungal activity

The antifungal activity of prepared films was also carried out using the disc diffusion method according to **Barzegar et al. (2014)**. Briefly, potato dextrose broth (2.4 g) and agar (2 g) are dispersed in 100 mL distilled water and autoclaved at 120ºC and 15 kg cm^{-2} pressure for 20 min. After addition of 0.1 ml spore suspension, a diameter of 12 mm film sample was placed on the PDA. All the petri dishes were kept at 25°C for 72 h. Finally, the zone of inhibition was calculated around the film. Ampicillin B was used as a control.

3.3.18. Statistical analysis

All the experiments were carried out at least in triplicates and mean values and standard deviation were calculated using statistics program in (SPSS Inc., Chicago). The data was analyzed using one-way analysis of variance (ANOVA). Tukey's test was used to verify the significant difference ($p < 0.05$) between the values.

Table 3.1 summarizes the details of various instruments used in the present work.

Table 3.1. Details of instruments used in the present work.

Instrument	Model and make	Purpose	Detection/ working/performance range
Analytical balance	Model: BM-252 Make: Shimadzu, Japan	Weight measurement	0 to 250 g Resolution: 0.1 mg
Centrifuge	Model: KN-70	Separation	Maximum speed: 5000 rpm

	Make: Kubota, Japan		
Dynamic mechanical thermal analysis	Model: Q800 Make: TA Instruments, New Castle, USA	Glass temperatures Viscoelastic behavior	Frequency: 1 Hz Strain: 0.05% Temperature : -75 to 150°C, at 5°C/min
Diff erential scanning calorimeter	Model: 6200 DSC Make: SII EXSTAR , Japan	Gelatinization temperature	Temperature: 30 to 130°C, at 5°C/min
Digital micrometre	Model: 193-111 Make: Mitutoyo, Japan	Thickness	Accuracy of 0.001 mm
Field emission scanning electron microscopy	Model: Sigma Make: Zeiss, Germany	Size and surface morphology	
Freeze dried	Model: Scan Vac Make: Coolsafe, Japan	Drying	-20 °C to -110 °C
FTIR spectrometer FTIR-ATR spectra	Model: IR affinity 1 Make: Shimadzu, Japan Model: Spectrum 100Make: Perkin Elmer, USA	Functional group characterization	Frequency: 700 to 4000 cm^{-1} Frequency: 600 to 4000 cm^{-1}
Heat Sealer	Model: SU RE Make: NL-302, Japan	Sealing	100V/660W 50/60HZ, 280°C -
Hot air oven	Model: WFO-451SD Make: Eyela, Japan Model: ISO 9001-2008 Make Navyug, India	Moisture removal	Temperature: 30 to 250 °C

Incubator	Model: LTI-100SD Make: EYELA, Japan	Constant temperature	Temperature: 25 to 200°C
Magnetic stirrer	Model: RS-6AN Make: AS ONE, Japan	Mixing/agitation	Stirrer speed: 100 to 1500 rpm
Micropipette	Model: T100 & T1000 Make: Tarsons products Pvt Ltd., India	µL range liquid dispensing for analytical work	Capacity T100:10 to 100 µL T1000:100 to 1000 µL
Microwave oven	Model: 1E96250824 Make: Panasonic, Japan	Drying	Frequency: 2450 MHz Microwave: 150 to1200 W
Millipore water purification unit	Model: Elix 3 Make: Millipore, USA	Preparation of all reagent and test solutions	TOC: <30 µg L^{-1} Pyrogens (endotoxins):<0.001 EU mL^{-1} Water resistivity (@ 25 °C): >5 MΩ cm
pH meter	Model: pH 510 Make: Eutech Instruments, Singapore	pH measurement	pH: 0 to 14 Resolution: 0.01 pH
Rapid Visco-Analyzer	Model: RVA Super 3 Make: Newport scientific, Australia	Paste viscosity determination	Programmed set for 13 min
Rheometer	Model: AR2000, G2KG Make: TA Instruments, USA	Rheological properties	Shear rate :0 to 1000 s^{-1} Frequency: 2-10Hz

Scanning electron microscopy	Model: S-4800, Make: Hitachi, Japan	Size and surface morphology	
Thermal gravimetric analyses	Model: 6300 TG/DTA Make: SII EXSTAR, Japan	Mass loss determination	Temperature: 30 to 600 °C
Tensile machine	Model: EZ-L Make: Shimadzu, Japan	Tensile strength and elongation at break	Maximum load: 5KN Test speed range 0.001 to 1000 mm/min
Ultrasonic bath	Model: LS150-SK1 Make: Mainland, China	Mixing	Frequency (sound wave): 40 kHz (fixed) Ultrasonic power: 150 W (fixed)
UV-vis spectrophotometer	Model: MPC-3100 Make: Shimadzu, Japan	Absorbance measurement	Wavelength: 190-1100 nm Resolution: 0.05 nm
Water bath	Model: Isotemp 228 Make: Fisher Scientific, USA	Thermostatic heating	Ambient to 100°C
X-ray diffraction	Model: D8 Advance Make: Bruker, Germany	Crystal structure	2θ = 2 to 40°

भारतीय प्रौद्योगिकी संस्थान गुवाहाटी
Indian Institute of Technology Guwahati

Chapter 4

Microwave-assisted synthesis and characterization of modified potato starch-xanthan gum mixtures

Dry heat modification of starch with ionic gum is a useful method to change the thermal and rheological properties, which finds potential application in various fields of food and pharmaceutical industries. In this chapter, normal potato starch (PS) modified with xanthan gum (X) by microwave assisted dry heating (MADH) at different times is presented. Comparison was made by modifying potato starch with xanthan via MADH and conventional dry heating.

4.1. Specific Background

Starch is biodegradable and inexpensive which is abundantly available on earth in its semi-crystalline polysaccharide form. It is made up of two polysaccharides namely amylose (a linear) and amylopectin (a branched) linked by glycosidic bonds. Wide range of applications are found in pharmaceutical, food and other industries in the form of binder, encapsulate, thickener, bulking agent, colloidal stabilizer, adhesives, flocculating agents and water-holding agent **(Singh et al., 2010; Staroszczyk, 2009a; Sun et al., 2014b)**. Potato starch contains approximately 800 ppm of phosphate component present in amylopectin which increases the anionic character and viscosity of the paste due to its tendency to form a covalent bond making it unique among the other starches**(Craig et al., 1989)**. Native potato starch has a longer glycan chain, high viscosity and large granular size **(Zhao et al., 2018)**. However, native starch is limited in applications due to its low solubility, shear stress resistance, cohesiveness, thermal decomposition and uncontrolled paste consistency **(Adzahan, 2002).** Therefore, researchers focused on modification of starch to expand its applications. While there are different methods (physical, chemical and enzymatic) available to modify the starch, dry heating is a physical modification method which ensures an undistorted granular structure **(Chiu et al., 1999; Singh et al., 2007; Sun et al., 2014b).** Amongst physical modification techniques like annealing (ANN), microwave-assisted dry heating (MADH), heat-moisture treatment (HMT) **(Staroszczyk**

and Janas, 2010; Zavareze and Dias, 2011; Zhao et al., 2013), MADH is cheap, eco-friendly, faster in reaction rate and produces narrow sized product distribution with a fewer by-products (**Biswas et al., 2008; Kappe and Dallinger, 2009; Shogren and Biswas, 2006)**.

Xanthan is a high molecular weight anionic food gum used to modify starch during heat treatment. It consists of D-glucose residues linked by α-(1-4) glycosidic bonds with a trisaccharide (β-D-mannose-β-D-glucuronic acid-α-D-mannose) side chain attached to alternate D-glucose units of the main chain. Owing to the glucuronic acid and pyruvic acid group in the side chain of xanthan is the anionic nature **(Katzbauer, 1998; Shalviri et al., 2010**). Since xanthan acts as a chemical crosslinking agent, the idea of modifying starch with xanthan in pharmaceutical, food and other industries is not new **(Cheng and Wintersdorff, 1981)**. The modified product with xanthan shows an increase in thermal and rheological properties **(Lim et al., 2002**). The products prepared by xanthan treated with dry heat yield an increased shear stability of the paste and restricted granular swelling **(Sun et al., 2013)**. The interaction of starch with xanthan is well documented by several food science researchers **(Christianson et al., 1981; Ferrero et al., 1994; Mandala et al., 2002; Shalviri et al., 2010)**. Heat treatment of starch with ionic gums require heating at high temperatures (> 130°C) for a prolonged period (2–3 h) to ensure the changes in functional properties as well as cross-linking due to the formation of an ester bond **(Sun et al., 2014b, 2013)**. The schematic representation of cross-linking reaction between starch and xanthan gum during heating is shown in **Figure 4.1.** In addition, there may be energy losses due to prolonged heating **(Shogren and Biswas, 2006)**. On the other hand, microwave assisted heating provides fast, uniform heating thus producing desirable starch functionality. It has reported that conventional heat treatment of starch with xanthan increases the peak viscosity (**Lim et al., 2003)**. Waxy rice starch was modified with a combination of xanthan and phosphate salts to increase the viscosity of paste by dry heating **(Chung et al., 2013)**. Potato starch powder impregnated with carboxymethyl cellulose (CMC) was modified by dry heating to obtain compact gel structure **(Sun et al., 2013)**. It has been found that dry heating of waxy rice starch with xanthan improves the pasting properties, rheological properties and gel-forming ability **(Li et al., 2013)**. Microwave-

assisted dry heating (MADH) of corn starch mixed with xanthan increases the peak viscosity **(Sun et al., 2014b)**.

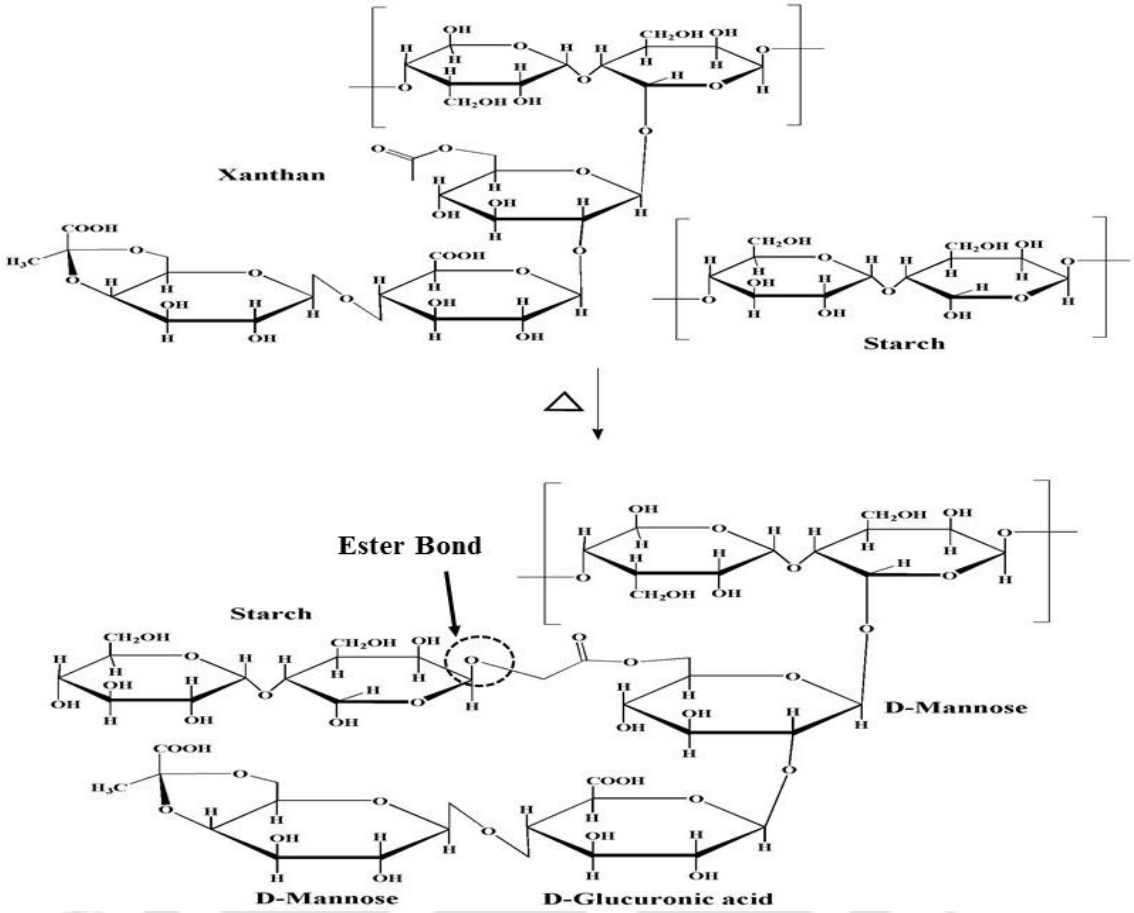

Figure 4.1. Schematic representation of cross-linking reaction between starch and xanthan gum during heating.

In this work, modified starch was prepared to improve the properties of native state starch for various applications by dry heating. The modified starch-xanthan materials were monitored by rapid visco analyzer (RVA) for pasting properties while the flow and rheological properties were observed through a rheometer. Furthermore, the synthesized products were characterized by DSC, SEM, FTIR spectroscopy, and XRD. Potato starch (PS) with xanthan gum (X) via MADH has not been not studied despite many studies being conducted for different starches with xanthan by dry heating. In the present research work, the characteristics like pasting, rheological behaviour, thermal, structural and

morphological properties of synthesized products via MADH were evaluated in comparison with conventional dry heating.

4.2. Effect of microwave and conventional heating on modification of potato starch with xanthan gum

The preparation of modified starch with xanthan gum was through dry heating. The samples were exposed to microwave radiation in the microwave oven at 600 W for 4, 8 and 12 min. To observe the advantage of microwave heating, starch-xanthan sample was heated in a conventional oven at 130^{o}C for 4 h. The sample starch xanthan without heating was used as a control sample. All the dried starch samples were stored in a desiccator at 25^{o}C for before testing methodology explored in **(Chapter 3, Section 3.2.1)**.

4.3. Results and Discussion

4.3.1. Pasting properties

The samples of native starch, unheated starch with 1% xanthan, starch with 1% xanthan processed through conventional heating and microwave dry heating were introduced into the rapid visco analyser (RVA) and paste viscograph to obtain the viscogram data as presented in **Figure 4.2** and **Table 4.1**.

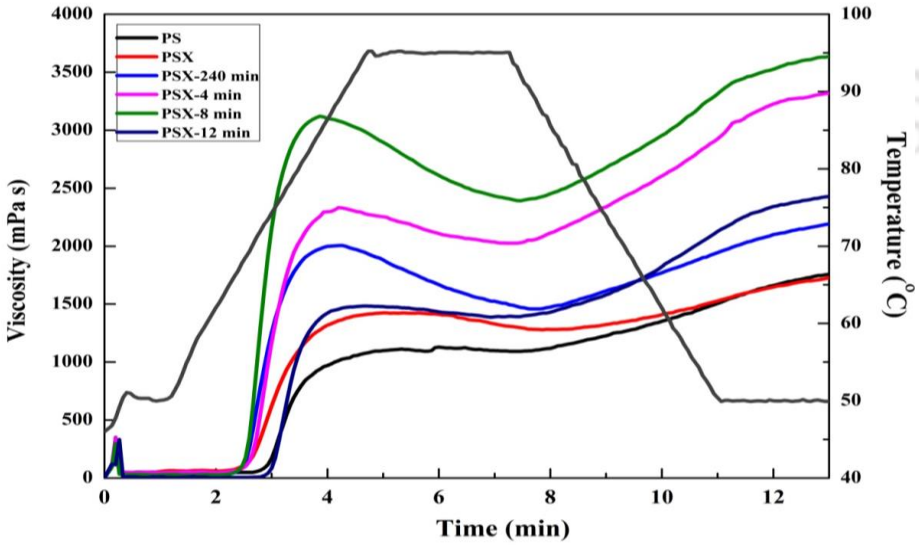

Figure 4.2 RVA-viscogram of normal potato starch (PS) modified with xanthan (X), PSX-0 min (control), PSX-240 min, convention dry heating at 130^{o}C for 240 min, PSX-4, PSX-8 and PSX-12 min, microwave dry heating (MADH).

The peak viscosity increases and pasting temperature decreases in the order of PS, PSX and heat-treated PSX-240 min as shown in **Table 4.1**.

Table 4.1. Pasting properties of normal and modified potato starch with xanthan using conventional heating and microwave dry heating**.**

Sample	PT (^oC)	PV (mPa s)	TV (mPa s)	FV (mPa s)	BV (mPa s)	SV (mPa s)
PS	70.30±014^a	1114±5.03^a	1069±3.00^b	1749±5.50^a	45±4.04^a	680±3.60^a
PSX	68.20±0.20^a	1363±2.64^b	1281±3.60^b	1726±6.55^a	82±5.56^a	445±5.29^b
PSX-240 min	64.45±0.30^a	1984±4.04^b	1555±4.58^a	2187±7.09^a	429±5.00^a	632±5.68^b
PSX-4 min	63.65±0.23^a	2386±3.05^a	1929±3.05^b	3098±7.57^a	457±5.29^a	1169±5.50^b
PSX-8 min	62.55±0.24^a	3102±3.60^b	2414±1.52^b	3616±6.02^b	688±6.02^b	1202±6.80^a
PSX-12 min	64.93±0.23^b	1455±2.54^b	1402±4.04^a	2408±5.03^b	53±2.05^b	1006±4.72^a

$^{a-b}$Different letters represent a significant difference using Tukey test ($p < 0.05$).

Parameters such as pasting temperature (PT), peak viscosity (PV), trough viscosity (TV i.e. minimum viscosity at 95^{o}C), final viscosity (FV i.e. viscosity at 50^{o}C) were measured through which the breakdown viscosity (BV = PV-TV) and setback viscosity (SV = FV-TV) were calculated.

During conventional heating, the granular structure of starch might be disrupted. This leads to disruption of hydrogen bonds in starch granules increasing the absorption of water by starch molecules thereby forming an ester bond while an unheated sample swells rapidly resulting in low peak viscosity. Similar results have been obtained by **(Sun et al., 2013)**. Under MADH conditions, PSX-4 and PSX-8 min showed an increase in peak and final viscosity. This may be due to swelling of starch granule and strong interaction with xanthan that lowers the hindrance effect because of carboxylate groups of xanthan and phosphate groups of potato starch resulting in decrease of pasting temperature. For PSX-8, min increase of the peak viscosities is from 1114 to 3102 mPa s, which is an increase by 18% in comparison to native PS. The pasting temperature was slightly lower while the viscosities were higher in the modified starch pastes (PSX-8 min). The trough viscosity of PSX-8 min is 2414 mPa s reflecting a different susceptibility of modified starch breakdown upon shearing and heating.

In the case of PSX-8 min, restructuring and retro gradation occur resulting in higher viscosities (3616 mPa s) portraying the ability of modified starch to form viscous paste after cooking and cooling. This is suitable as a thickening agent in food application. The breakdown and setback of the PSX-8 min sample significantly raised after being exposed to microwave irradiation which revealed an enhanced interactive bond formation between starch and xanthan resulting in an increase of its hydration as well as swelling power. In the case of PSX-12 min, due to prolonged heating of the modified starch, pasting temperature increases and peak viscosity decreases which result in higher resistance to swelling in water. The same conclusion was inferred by **Sun et al. (2014b).**

4.3.2. Flow and dynamic rheological properties

The modified paste properties can be affected by many factors such as amylose to amylopectin ratio, granular size of starch, molecular characteristics of the starch and the type of heating conditions employed. These rheological properties of starch paste play an important role in various industries as binders, gelling agents and thickeners.

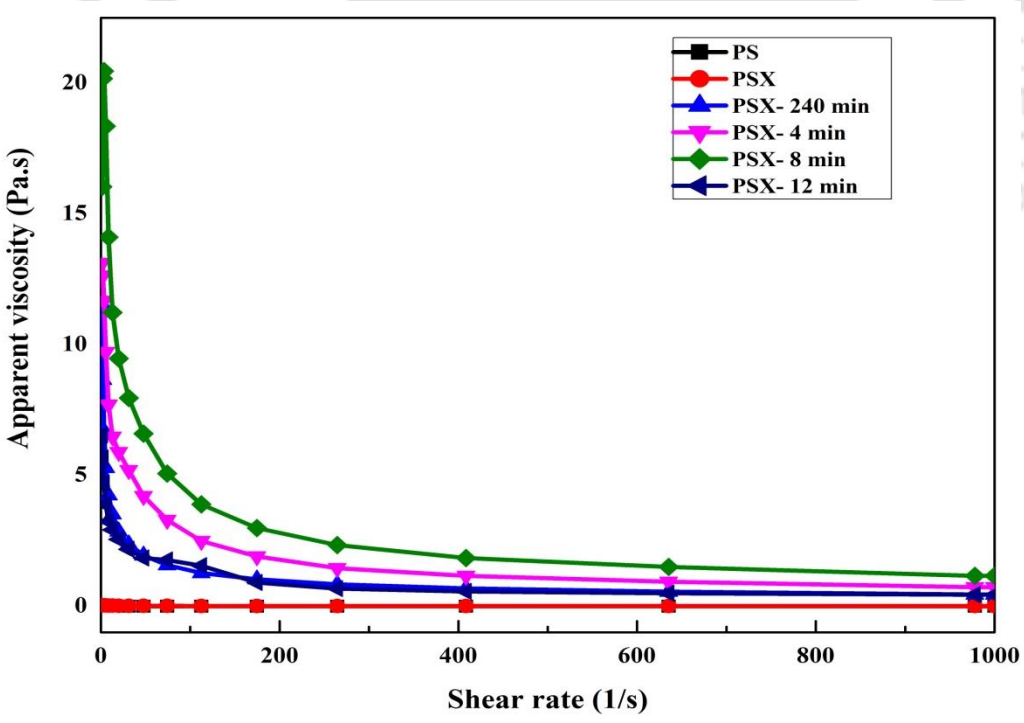

Figure 4.3 Flow properties of normal potato starch (PS) with xanthan (X). Normal potato starch (PS), PSX-0 min (control); PSX-240 min, PSX-4, PSX-8 and PSX-12 min.

The effect of PS, PSX-0, PSX-240, PSX-4, PSX-8 and PSX-12 min starch pastes on apparent viscosity is shown in **Figure 4. 3.** The apparent viscosity of starch paste decreased as shear rate increased revealing the shear thinning behaviour of the material classifying it to be a non-Newtonian fluid. As the shear rate is increased, modified starch granules start to deform and rearrange. Consequently, the progressive orientation of molecules in the direction of flow lower, resulting in a lower viscosity and splitting of the bond formed between amylose-amylopectin-xanthan. **Figure 4.3** exhibits all starches samples under a shear results in a temporary break down of internal structure showing the thixotropic trend where the viscosity decreases with increases in time. Due to the hydrogen bonding between hydroxyl group of starch and acetyl group of xanthan gum, the modified potato starch with xanthan (unheated, PSX-0 min) shows a higher apparent viscosity than unmodified potato starch (PS). During dry heat treatment of PSX- 240 min (130°C for 240 min), starch granules swelled up leading to an increase in absorption of water eventually reducing the availability of free water in the system thereby raising the bar of apparent viscosity in comparison to PS and PSX-0 min. Furthermore, the viscosity of modified starch processed with microwave heating for a period of 4 and 8 min show a significant difference in their values due to rupture in granular structure and gelatinization occurs as a result of vibrational motion of polar molecules during microwave heating. There is no rupture in case of unheated sample. The apparent viscosity of the modified potato starch with xanthan prepared by 8 min microwave heating (PSX-8 min) is higher than the samples of PS, PSX-0, PSX-240, and PSX-4 and PSX-12 min. It could be due to the ester bond formed between the hydroxyl group of starch and acetyl group of xanthan gum. In PSX-12 min, longer microwave heating durations promoted degradation of amylose-amylopectin-xanthan bond resulting in lower gelatinization temperatures and low crystallinity thereby exhibiting lower apparent viscosity. This result was similar to the one reported by **Xie et al. (2013**) where higher reaction and longer duration of microwave heating treatment promoted degradation of starches granules (i.e. rice, corn, potato, waxy corn and barley).

The viscoelastic properties of native and modified starches were examined using dynamic storage modulus (G') which reflect the solid properties and loss modulus (G") portrays the liquid properties of a material as presented in **Figures 4.4 and 4.5.** In the present study, as the frequency range increases G' and G" increase. Elastic property is

superior to viscous property as G' is higher than G". G' and G" for PS and PSX (control) exhibit lower swelling but in the case of heat-treated PSX-240 min G and G" is higher which might be due to disruption granular structure of starch.

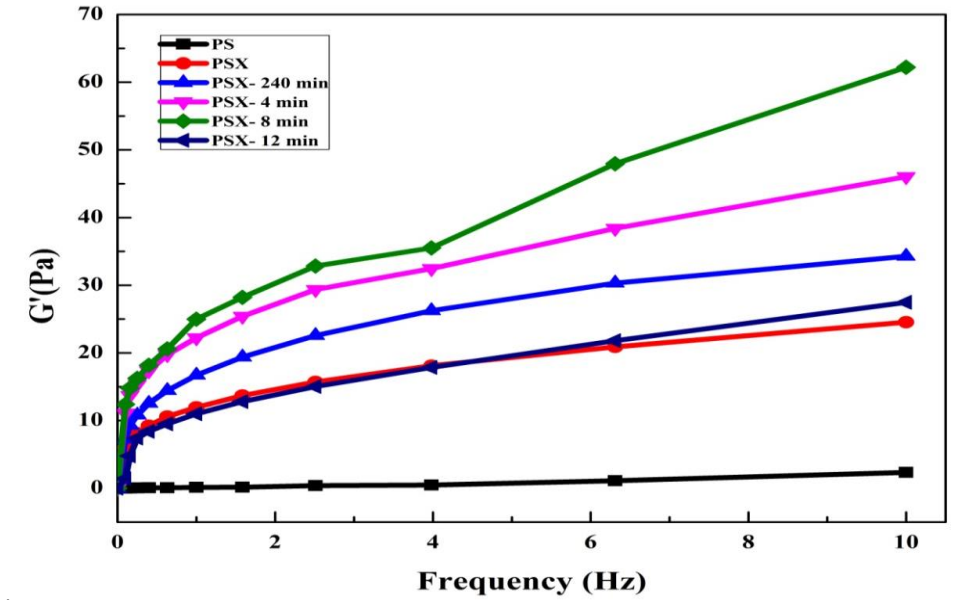

Figure 4.4 Storage modulus (G') versus frequency (Hz) of normal potato starch (PS) with xanthan (X) conventional and MADH.

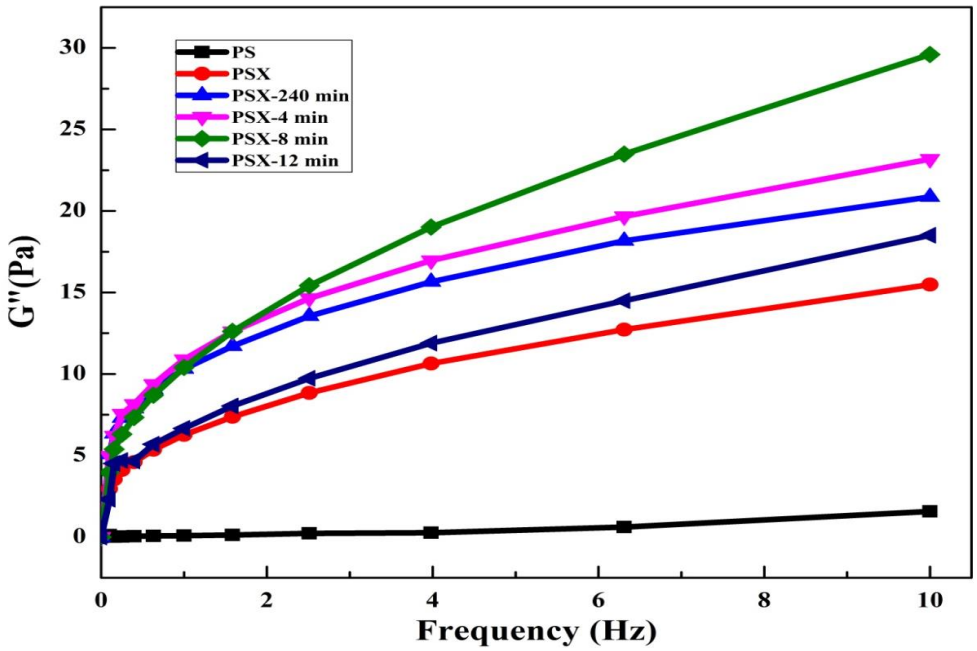

Figure 4.5 Loss modulus (G") versus frequency (Hz) of normal potato starch (PS) with xanthan (X) conventional and MADH.

Under microwave heating conditions for PSX-4 and PSX-8 min increase in the magnitude of G' and G" indicate starch granules swell slowly. This leads to opening of the chain of starch granules thus forming a strong bond with xanthan in the process of forming a cross-linking network. In the case of PSX-12 min, strong vibrational motion of the polar molecules due to prolonged heating lead to the degradation of the modified starch forming a network for gel formation. The storage modulus (G') and loss modulus (G") decreased in accordance with the results of pasting and flow properties as shown in **Figures 4.2 and 4.3.**

4.3.3. Syneresis properties

The syneresis properties of the samples of native starch, unheated starch with 1% xanthan, potato starch with 1% xanthan processed through control, conventional and microwave dry heating are presented in **Table 4.2.**

Table 4.2. Syneresis of potato starch with xanthan through conventional and microwave dry heating.

Sample	1st cycle of 4 days (%)	2nd cycle of 4 days (%)	3rd cycle of 4 days (%)
PS	40.14±3.27^{b}	54.53±0.35^{c}	52.39± 0.36^{c}
PSX	24.20±3.78^{b}	28.11± 2.51^{b}	40.91±0.37^{c}
PSX-240 min	22.36±1.51^{b}	23.87± 1.37^{b}	30.16± 0.55^{c}
PSX-4min	11.21±1.36^{b}	20.56±0.17c	22.64± 0.83^{c}
PSX-8min	5.63±1.88^{a}	9.64±0.25^{c}	12.71± 0.15^{c}
PSX-12 min	13.63±1.32^{b}	23.80±1.72^{b}	25.44± 2.40^{b}

$^{a\text{-}c}$Different letters represent a significant difference using Tukey test ($p < 0.05$).

In the first cycle of freeze-thawing, the syneresis rate of PS was as higher as 40.14% but in case of PSX it exhibited 24.20% which is lower due to the addition of xanthan. It then further decreased to 22.20% on conventional heating (PSX-240 min) and to 11.21% in the case of MADH conditions (PSX-4 min). In case of PSX-8 min lower syneresis rate was observed due to the strength of starch–xanthan as it forms a stronger composite structures. PSX-12 min sample syneresis value is more due to week bonding between

starch and xanthan during prolonged microwave heating. Similarly, in the second cycle, increase in syneresis value shows the decrease in ability to hold water as more gel exudates more water. Finally, third freeze-thaw cycle, PSX-8 min displayed a lower syneresis rate showing an improved ability to hold water in comparison to PS, PSX-240 min, PSX-4 and PSX-12 min.

4.3.4. Thermal properties

The gelatinization temperature (T_o onset temperature, T_p peak temperature, T_c conclusion temperature) and ΔH gelatinization enthalpy are shown in **Figure 4.6 and Table 4.3.** The gelatinization temperature and enthalpy were higher in case of PS and PSX than in heat-treated modified starch as presented in **Table 4.3**.

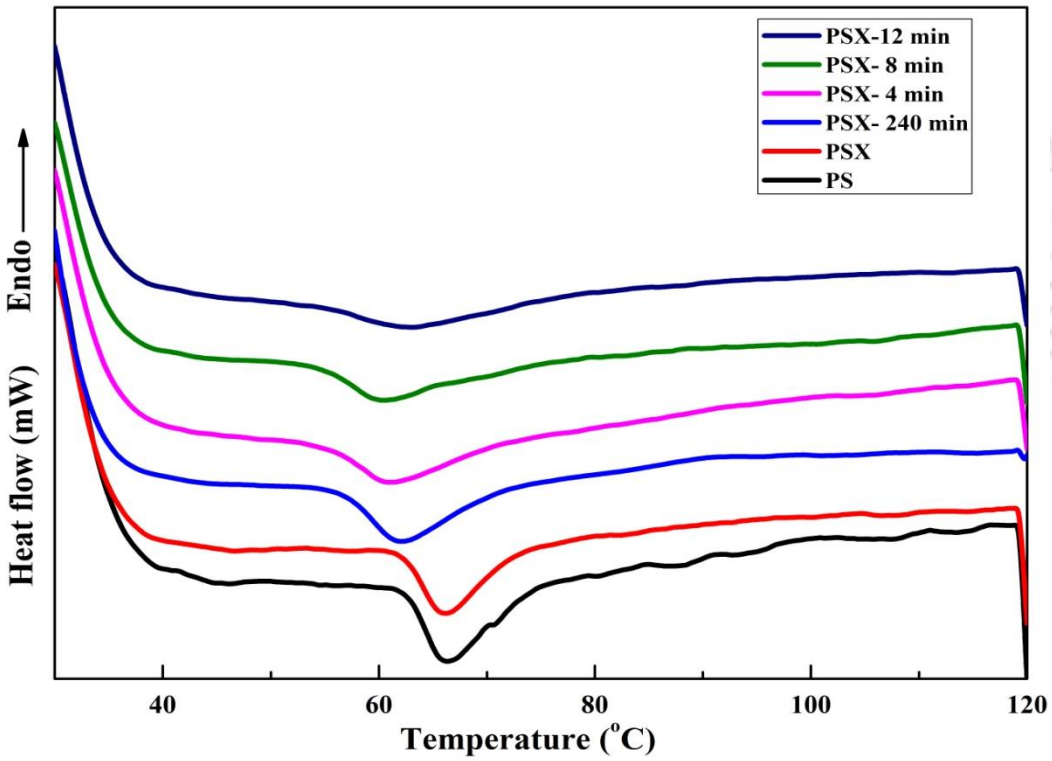

Figure 4.6. Thermal properties of potato starch modified with xanthan (X), PS, PSX-0 min (control); PSX-240 min, PSX-4, PSX-8 and PSX-12 min.

On comparing the native starch and PSX-240 min, the decrease in values of T_o, T_p, T_c and ΔH is respectively 3.45, 3.99, 2.74°C and 0.64 J/g. The decrease in values is due to heating which enhances bonding between hydroxyl groups of starch and acetyl group of

xanthan gum. Similarly comparing and PSX-240 and PSX-4 (MADH), the decrease in the values of T_o, T_p, T_c and ΔH is 0.96, 0.89, 1.52°C and 0.23 J/g while with PSX-8 min the decrease in the values is observed to be 1.05, 0.86, 3.24°C and 0.61 J/g which signify the bonding between starch–xanthan interactions that enhances the compactness of mixture during microwave heating. In case of PSX-12 min gelatinization temperature (T_o, T_p, and T_c) increases by 2.63, 2.37 and 6.24°C and gelatinization enthalpy (ΔH) is also increased by 1.30 J/g. It can explain that prolonged heating breaks the imperfect crystal during MADH.

Table 4.3. Thermal properties of potato starch modified with xanthan (X), PSX-0 min (control); PSX-240 min, PSX-4, PSX- 8 and PSX-12 min.

Sample (min)	T_o (°C)	T_p (°C)	T_c (°C)	ΔH (J/g)
PS	61.59±0.34^{a}	66.33±0.25^{c}	74.46±0.73^{b}	3.94±0.02^{b}
PSX-0 (present work)	60.79±0.49^{c}	66.08±0.33^{b}	72.71±0.29^{a}	3.85±0.05^{a}
PSX-0 **Sun et.al. (2013)**	56.80±0.28^{c}	63.35±0.21^{c}	71.50±0.28^{c}	15.17±0.47^{b}
PSX- 240 (present work)	57.34±0.11^{b}	62.09±0.18^{a}	69.97±0.41^{c}	3.21±0.11^{a}
PSX-240 **Sun et.al. (2013)**	55.90±0^{d}	61.60±0.14^{d}	68.90±0.42^{d}	14.54±0.86^{b}
PSX-4	56.38±0.57^{a}	61.20±0.12^{c}	68.45±0.24^{a}	2.98±0.07^{b}
PSX-8	55.33±0.14^{c}	60.34±0.23^{b}	65.21±0.47^{b}	2.37±0.03^{a}
PSX-12	57.96±0.22^{b}	62.71±0.27^{a}	71.45±0.56^{b}	3.67±0.08^{c}

$^{a\text{-}c}$Different letters represent a significant difference using Tukey test ($p < 0.05$).

In the present work, both gelatinization temperature (T_o, T_p, T_c) and gelatinization enthalpy (ΔH) decrease in conventional heating (PSX-0 (without heating) to PSX-240 min) and microwave heating (PSX-0 (without heating) to PSX-8 min). In conventional dry heating (PSX-0 and PSX-240 min), the values of gelatinization temperature (T_o, T_p, T_c) and gelatinization enthalpy (ΔH) approximately reduce by 3.45°C, 3.99°C, 2.74°C and 0.64 J/g while in microwave dry heating (PSX-0 and PSX-8 min), the values approximately reduce by 5.46°C, 5.74°C, 7.50°C and 1.48 J/g (**Table 4.3**). The present experimental values of gelatinization temperature (T_o, T_p, T_c) and gelatinization enthalpy (ΔH) are compared with the literature (**Sun et.al., 2013)** for conventional heating method .

4.3.5. Scanning electron micrographs

The SEM images of starch with xanthan before pasting with conventional heat treatment and MADH treatment are shown in **Figures 4.7 (a-d).** SEM showed that potato starch incorporated with xanthan was rough **(Figure 4.7 (a))**. This is due to surface interaction of the starch granules with Xanthan. After conventional heat treatment, starch granules particles attach with xanthan even more and thus a big lump under dry heat treatment than in unheated samples **(Figure 4.7 (b))**. After MADH treatment, modified starch formed came even closer and formed into many bigger lumps than conventional heating which confirm the interaction with xanthan **(Figure 4.7 (c))**. A prolonged MADH treatment revealed that potato starch-xanthan formed bigger lumps but the distribution was non-uniform **(Figure 4.7 (d))**.

The gelatinized starch-xanthan both unheated and heated (conventional and MADH) was examined under SEM which revealed that starch granules were disturbed forming a net-like structure similar to honeycombs or holes as shown in **(Figure 4.7 (e-h))**. In unheated sample PSX, many holes were formed due to surface interaction **(Figure 4.7 (e))**. In the case of conventional heating, the gel structure of the PSX 240 min formed a lamellar structure with cracks **(Figure 4.7 (f))**. After MADH treatment, modified starch formed dense net structure and a smooth lamellar structure better than the structure in conventional heating. This indicates that potato starch interacted with xanthan gel in an orderly manner **(Figure 4.7 (g))**.

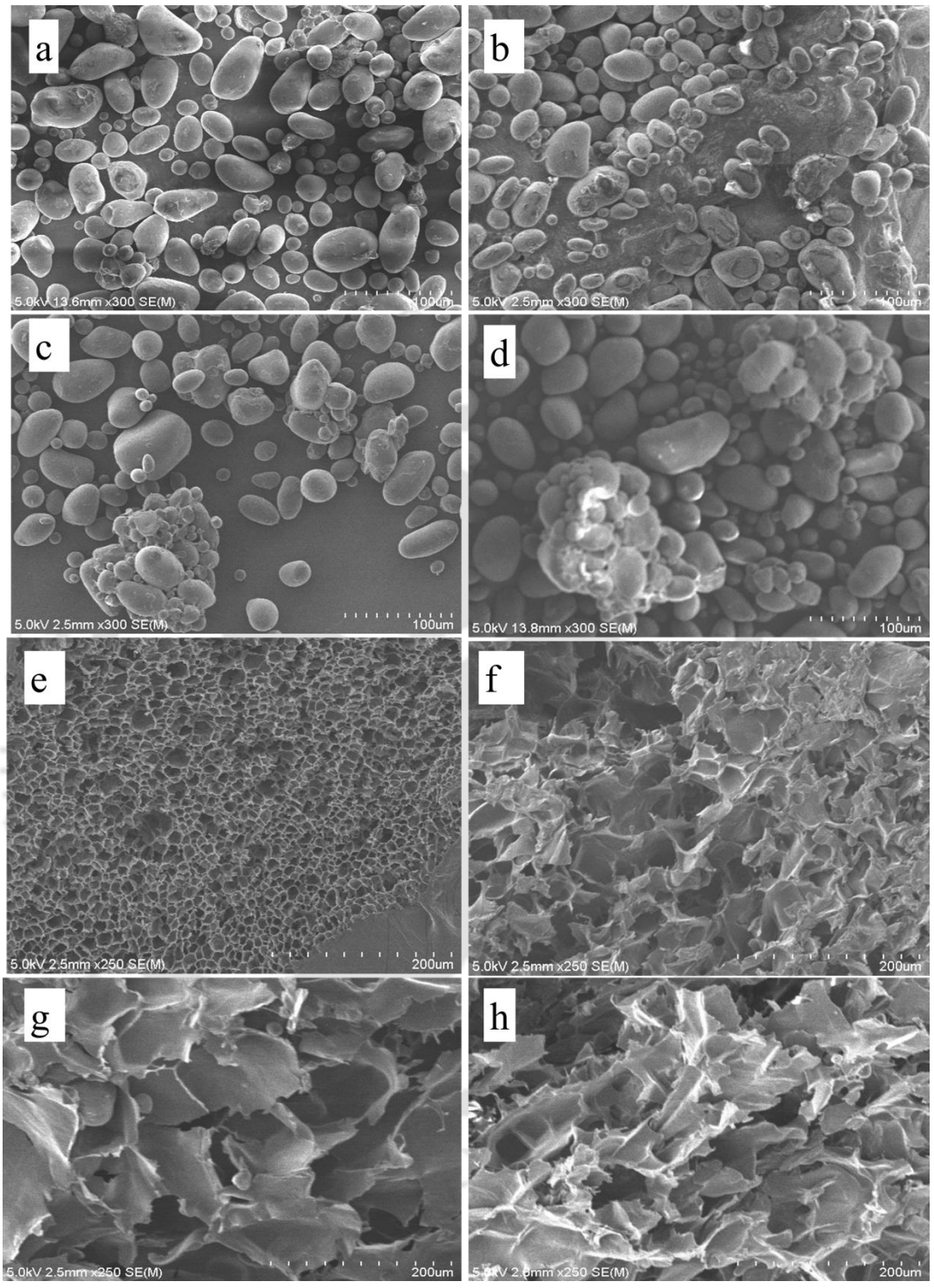

Figure 4.7 Scanning electron micrographs of potato starch modified with xanthan (X). Before pasting: (a) PSX-0 min (b) PSX-240 min (c) PSX-8 min (d) PSX-12 min; After pasting: (e) PSX-0 min (f) PSX-240 min (g) PSX-8 min (h) PSX-12 min.

In the case of prolonged MADH treatment, potato starch with xanthan formed a loosely pored structure with many cracks as shown in **(Figure 4.7 (h))**.

4.3.6. Fourier transform infrared (FT-IR) spectroscopy

FTIR spectra for the samples of native starch, unheated starch with 1% xanthan, starch with 1% xanthan processed through conventional heating and microwave assisted dry heating in the range of 500–4000 cm^{-1} are presented in **Figure 4.8**.

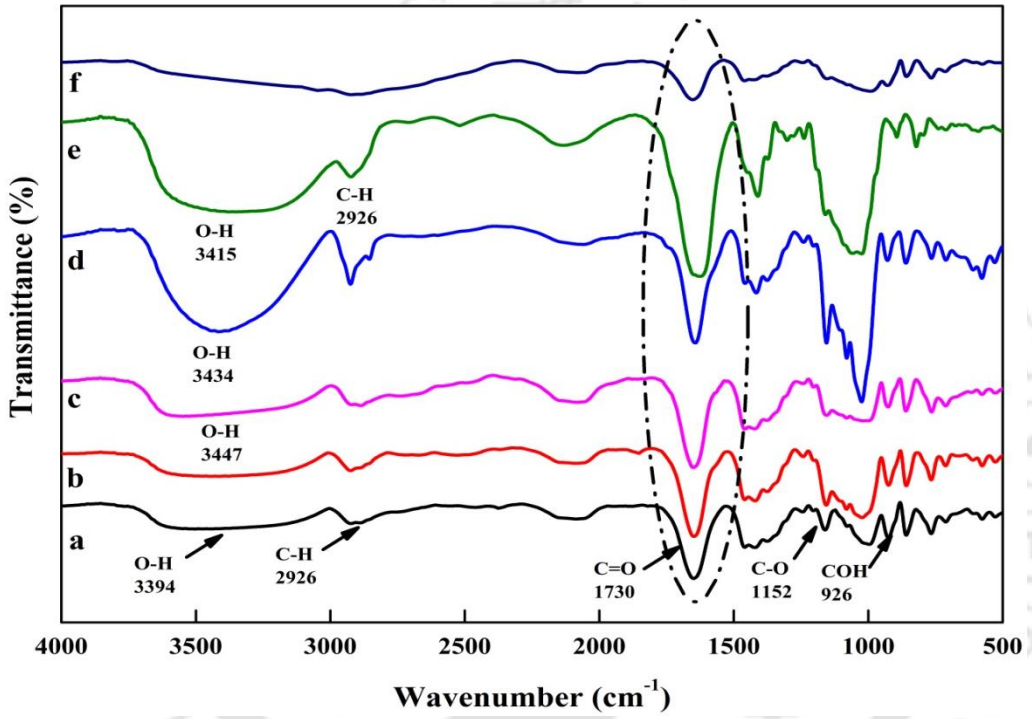

Figure 4.8. Fourier transform infrared spectroscopy (FT-IR) of potato starch modified with xanthan (X). (a) PS (b) PSX-0 min (control), (c) PSX-240 min, (d) PSX-4, (e) PSX-8 and (f) PSX-12 min.

The spectral profile shows the existence of a lot of chemical compounds in the (700–1750 cm^{-1}) fingerprinting region. The characteristic bands of amylose C–O–C skeletal mode of α-glycosidic linkage (926 cm^{-1}) and amylopectin (1052 cm^{-1}) was observed in all spectra excluding PSX-12 min. A sharp absorption band was observed at 1655 cm^{-1} which belongs to C=O functional group in xanthan. A broad band was observed at 3394 cm^{-1} as a result of –OH group and a band at 2926 cm^{-1} attributed to C–H group stretching vibration in PS **(Staroszczyk, 2009b)**. A weak peak of C=O group was found at

1730 cm^{-1} which confirmed the bond formation between hydroxyl groups of starch and acetyl group of xanthan gum resulting in ester bond formation (PSX-0). In case of PSX-240 min, the intensity of C=O band is smaller suggesting the existence of cross-linkage between the starch and xanthan as a result of heat treatment. A strong peak of C=O group was found at 1730 cm^{-1} which confirmed the bond formation between the hydroxyl group of starch and acetyl group of xanthan gum resulting in ester bond formation. The broad peak observed at 3415 cm^{-1} attributes to hydrogen bonding between starch and xanthan due to microwave heating. The intensity of ester bond is 1730 cm^{-1} which is higher in MADH PSX-8 min than PSX-4 and PSX-12 min. The ester bond and other characteristic bands disappeared in PSX-12 min suggesting that prolonged microwave-heating time distorted the entire structure of starch and xanthan. Moreover, it could be noted that the band of –OH group shifted to lower wavenumber in PSX-8 min than in PSX-240 min (conventional drying), PSX-0 (control), PSX-4 and PSX-12 min (microwave drying). It can be described that the xanthan gum enhanced both inter and intra molecular hydrogen bonding between starch granules in the case of MADH PSX-8 min. The present study is well accord with **Sun et al. (2014b)**.

4.3.7. X-ray diffraction

The X-ray diffraction patterns of native starch, unheated starch with 1% xanthan, starch with 1% xanthan processed through conventional heating and microwave assisted dry heating are shown in **Figure 4.9.** The diffractions patterns displayed for native potato starch at $2\theta = 5.6^{o}$, 17.15^{o}, 14.72^{o}, 19.69^{o}, 21.99^{o} and 23.91^{o} are characteristic of B-type crystalline structure **(Lewandowicz et al., 1997)**. Modified potato starch (PSX-0 min) processed without heating displayed a similar diffraction peaks proving significant indifference in crystallinity when compared to native potato starch. It was observed for conventional drying, PSX-240 min, the diffraction peak at $2\theta = 5.6^{o}$ was weaker and also the intensity of the peak at $2\theta = 19.69^{o}$, 21.99^{o} and 23.91^{o} was low relative to normal potato starch (PS). However, PSX-4 min mixing of xanthan occurs mostly in amorphous regions and without a change in its crystalline structure weaker than unheated samples (PS and PSX). The PSX-8 min samples displayed high intensity of crystalline diffraction peaks at 5°, 17°, 14°, 19°, 21° and 23° with no new peaks in the diffractogram. The product PSX-8 min crystalline pattern remained B-type. It can be seen that the strong ester bond which

was confirmed from FTIR spectra increased the intensity of the crystalline peak in case of MADH PSX-8 min when compared to PSX-240 min and PSX-4 min. The intensity and width of the peak (PSX-12) decreased sharply and also shifted to lower 2θ around 17° as the duration of microwave irradiation was increased to 12 min. The crystal lattice structure of B-type potato starch was distorted due to the double helical movement of starch granules during microwave irradiation. Both the results of XRD pattern and FTIR spectra matched for MADH PSX-8 min. The results of present study is in agreement with previous literatures **(Sun et al., 2014b; Zavareze and Dias, 2011)**.

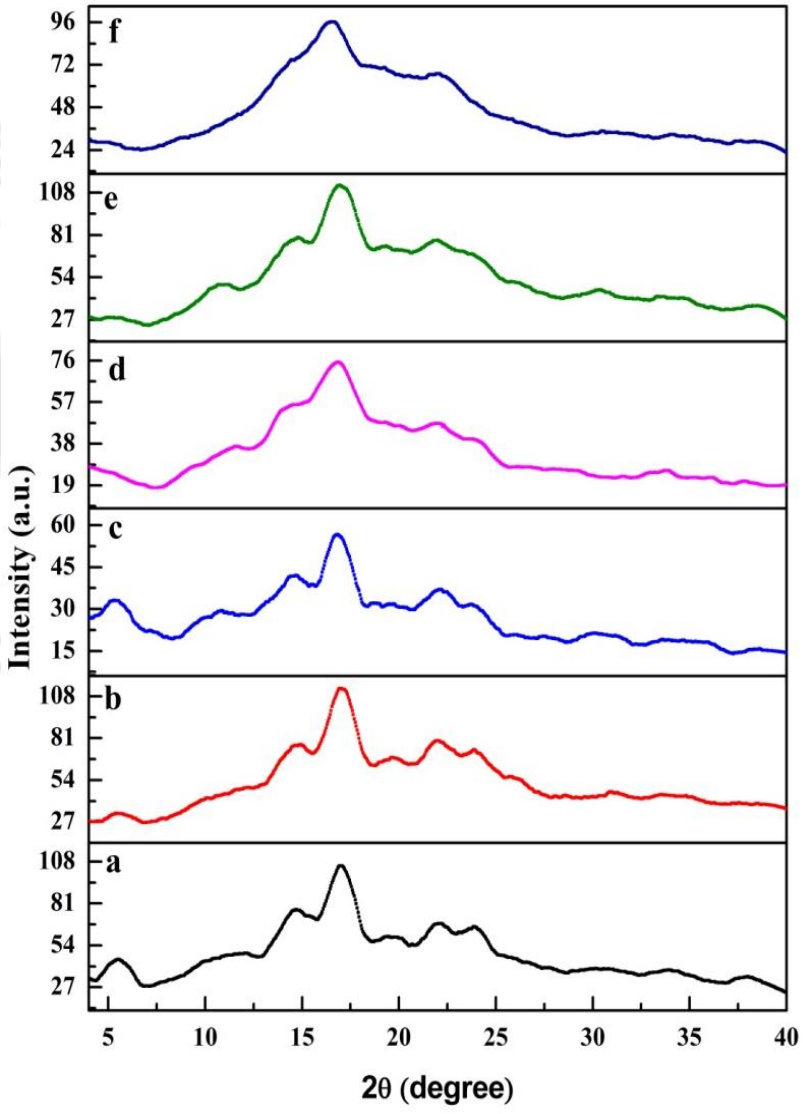

Figure 4.9. X-ray diffraction patterns (XRD) of potato starch modified with xanthan (X). (a) PS (b) PSX-0 min (c) PSX-240 min (d) PSX-4 (e) PSX-8 and (f) PSX-12 min.

4.4. Summary

The microwave heating is quick, uniform and energy efficient. Microwave heating can improve the starch functionality compared to conventional heating. Modified potato starch with xanthan via microwave-assisted dry heating treatment (MADH) was prepared successfully at 600 W for 8 min (PSX-8 min). The results exhibit that modified potato starch with xanthan (PSX-8 min) via MADH has a higher viscosity peak. The apparent viscosity increased with increasing shear rate and also demonstrated an increase in water holding ability than other modified potato starches. In comparison to the native potato starch, the modified starches possess significantly superior properties due to decrease in gelatinization temperatures with decrease in crystalline intensity. PSX-8 min showed a sharp absorption peak of an ester bond between starch and xanthan according to FTIR analysis. X-ray diffraction pattern revealed that peak intensity of normal potato starch increased for PSX-8 min. The modified starch can be used in different applications of food and pharmaceutical industries.

Chapter 5

Effect of amylose-amylopectin ratios on physical, mechanical and thermal properties of starch-CMC-nanoclay bionanocomposite films

This chapter is to examine the effect of amylose-amylopectin ratios on physical, mechanical, and thermal properties of starch based bionanocomposite films. Starch sources with different amylose-amylopectin ratios (potato starch, 20:80; wheat starch, 25:75; corn starch, 28:72 and high amylose corn starch, 70:30) were blended with carboxylmethyl cellulose (CMC) and nanoclay (Na-MMT) to produce bionanocomposite films.

5.1 Specific Background

In recent years, more attention has been given to the development of biodegradable food packaging materials derived from different biodegradable polymeric sources such as starch, protein, lipids and their composites **(Nair et al., 2017)**. One of the major contributors to the present scenario is petrochemical-based plastics as packaging materials, which lead to serious environmental problems due to its decomposition period ranging from hundreds to sometimes thousands of years **(Aider, 2010)**. Consumers' behaviour shows an increase in inclination towards biodegradability and environmental friendly packaging materials with prolonged shelf life during food preservation **(Tan et al., 2015)**. Hence, the demand for biodegradable food packaging is getting larger and it drives the growth of food packaging industry into worldwide market. Also, biodegradable polymeric sources enhance the income for agricultural sector **(Souza et al., 2012)**.

Starch is one of the most common agricultural raw materials used to develop films because of its abundant availability in nature as a reserve carbohydrate in most of the plants, renewable nature, biocompatibility, film forming ability and low cost **(De Oliveira Faria et al., 2012; Toral et al., 2002)**. Starch materials have one of the major disadvantages such as strong hydrophilic behaviour, which imparts poor water barrier, lower mechanical

properties and brittleness compared to petrochemical plastic films **(Souza et al., 2012)**. The newer approach to overcome these drawbacks is to incorporate other natural biopolymers into thermoplastic starch (TPS) matrix. Starch is one of the most abundant natural polymers studied for packaging applications (**Ren et al., 2017)**. Carboxymethyl cellulose (CMC) is water-soluble heteropolysaccharides with high molecular weights, which is often used together with starches to exalt its texture, water mobility and moisture control of products (**Ghanbarzadeh et al., 2010; Tongdeesoontorn et al., 2011)**. Typically, MMT clay is most widely used nanoclay due to its natural occurrence and better properties. Preparation of nanocomposites using montmorillonite (MMT) has been considered as a promising method. Uniform distribution of filler in the polymer matrix enhances interfacial area between filler and matrix. This improves barrier, mechanical and thermal properties **(Bratovcic et al., 2015).**

In this work, synthesis of starch-based packaging material was performed using solution casting technique. The prepared starch-based materials were characterized for moisture barrier properties such as water vapour permeability (WVP), film solubility and moisture content. Prepared bionanocomposite films were also characterized using dynamic mechanical thermal analyser (DMTA), mechanical properties (tensile strength and elongation at break), Fourier transform infrared (FTIR) spectroscopy, X-ray diffraction (XRD), scanning electron microscopy (SEM), thermo gravimetric analysis (TGA) and antifungal activity. Furthermore, no comprehensive study has been reported on the role of amylose/amylopectin ratios on properties of starch-based food packaging films incorporated with CMC reinforced with nanoclay. The objective of this work is to investigate the effect of amylose-amylopectin ratios on mechanical, water barrier, thermal, functional properties and morphological characteristic of starch-CMC-nanoclay bionanocomposite films for eco-friendly food packaging applications.

5.2. Preparation of amylose-amylopectin ratios on physical, mechanical and thermal properties of starch-CMC-nanoclay bionanocomposite films

The preparation of different starch sources (potato starch, 20:80; wheat starch, 25:75; corn starch, 28:72 and high amylose corn starch, 70:30) with carboxymethyl cellulose (CMC) and nanoclay (Na-MMT) to produce bionanocomposite films was given

elsewhere (**Chapter 3, Section 3.3.3 and 3.3.4)**. The prepared bionanocomposite films have uniform thickness of 0.05 mm.

5.3. Results and Discussion

5.3.1. X-ray diffractograms of starch-CMC-nanoclay bionanocomposite films

The XRD patterns of PS/CMC/nanoclay, WH/CMC/nanoclay, CS/CMC/nanoclay and HACS/CMC/nanoclay are shown in **Figure. 5.1.** It was reported that native PS and native HACS showed B-type diffraction patterns (2θ =17°, 22° and 23°) (**Gernat et al., 1993; Manek et al., 2012)** whereas native WH and native CS showed A-type diffraction peaks around 15°, 17°, 18° and 23° (**Sun et al., 2014b; Yu et al., 2016**). CMC/nanoclay showed a broad amorphous peak at 2θ = 21.13° **(Figure 5. 1a)**.

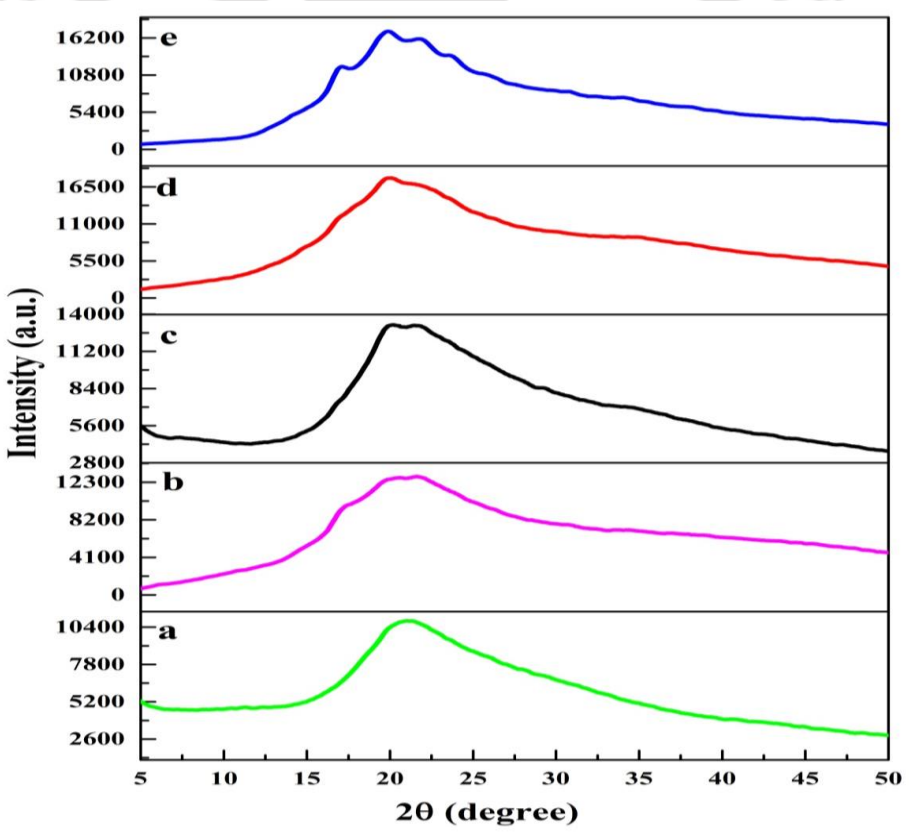

Figure 5.1. XRD patterns of starch-CMC-nanoclay bionanocomposite films: (a) CMC/nanoclay (control), (b) PS/CMC/nanoclay, (c) WH/CMC/nanoclay, (d) CS/CMC/nanoclay and (e) HACS/CMC/nanoclay.

The diffraction pattern has disappeared in all bionanocomposite films due to gelatinization process, which destructs the crystalline granules of starch **(Zhang et al., 2007)** (**Figure 5.1a-e**). It is indicated that the blend of all different starch sources was completely miscible with CMC. It is noted that the broad peak intensity increases in the order of CS/CMC/nanoclay > HACS/CMC/nanoclay > WH/CMC/nanoclay > PS/CMC/nanoclay > CMC/nanoclay (**Figure 5.1a-e**). It may be due to the fact that nanoclay (MMT) intercalates with either CMC or starch polymer chains or both CMC and starch polymer chains via silicate layers and thus forming starch-CMC-nanoclay bionanocomposite films. The ratio of amylose: amylopectin, which guide the molecular structure and molecular space of starches and polar group interaction between the polymer chains and nanoclay, influences the intercalation. No peak around 7.21° (2θ) was observed for Na-MMT **(Hoidy et al., 2009)** in all bionanocomposite films as seen by XRD pattern (**Figure 5.1a-e**). It may be due to extensive intercalation of polymer chains inside the Na-MMT galleries.

5.3.2. Water barrier properties of starch-CMC-nanoclay bionanocomposite films

Water barrier properties of films such as moisture content, solubility and water vapour permeability are shown from **Figure 5.2-4.4. Figure 5.2** shows moisture content of PS/CMC/nanoclay, WH/CMC/nanoclay, CS/CMC/nanoclay and HACS/CMC/nanoclay films. High moisture content (18.06%) was observed for PS/CMC/nanoclay films whereas CS/CMC/nanoclay films showed low moisture content (15.09%) (**Figure 5.2**). It is known that crystallinity is related to moisture content present in the film **(Nair et al., 2017)**. It is also evident that branching point guides the molecular architecture of starch granules, size and ratio of amylose-amylopectin contents, which further affects the functionality of starch **(Bertoft and Blennow, 2009; Mua and Jackson, 1997)**.

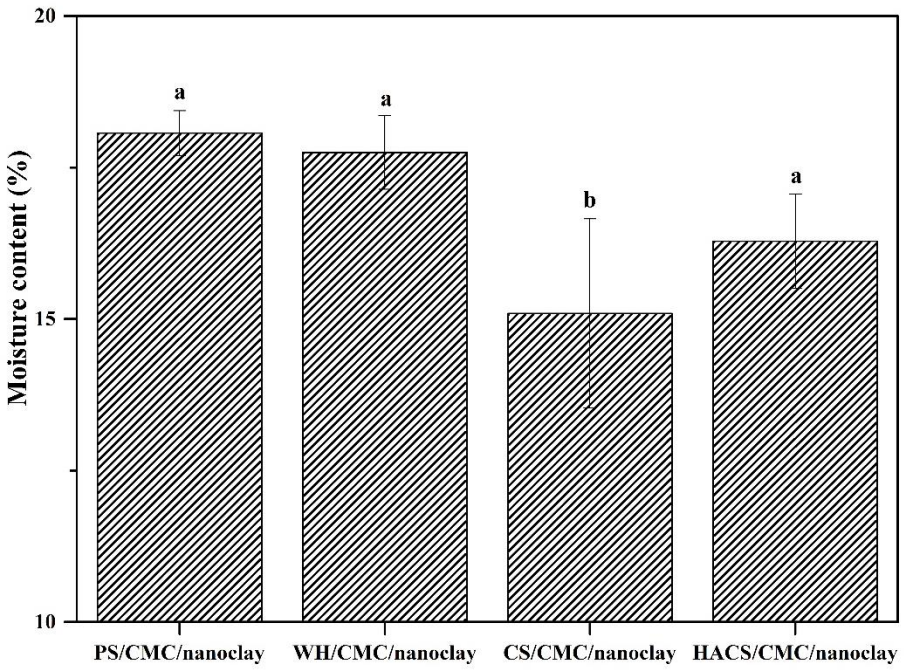

Figure 5.2. Effect of amylose-amylopectin ratios on moisture content of starch-CMC-nanoclay bionanocomposite films. [a-b]Different letters represent a significant difference using Tukey test ($p < 0.05$).

Among the three types of starch like PS, WH and CS, CS has a higher amylose content, which determines its chemical structure and molecular space. The lesser hydrophilicity of CS/CMC/nanoclay films may be due to strong interaction between –OH group of CS and COO^- group of CMC. Hence, absence of free –OH groups in CS/CMC/nanoclay films impedes the water molecule to interact. On the other hand, drastic reduction in amylopectin content (i.e. polymer branching) increases hydrophilic properties of HACS/CMC/nanoclay films by exposing the free -OH groups of amylose (**Figure 5.2**).

The solubility of film plays a vital role in improving the product integrity, shelf life and water resistance for food packaging applications **(Nair et al., 2017).** It was observed that PS/CMC/nanoclay films exhibited higher solubility (28.13%) in water (**Figure 5.3**). Generally, higher solubility indicates lower water resistance. Due to high moisture content, crosslinking between starch and CMC is reduced and that resulted in higher solubility and higher swelling for PS/CMC/nanoclay films (**Figure 5.2**) **(Kurt and Kahyaoglu, 2014)**.

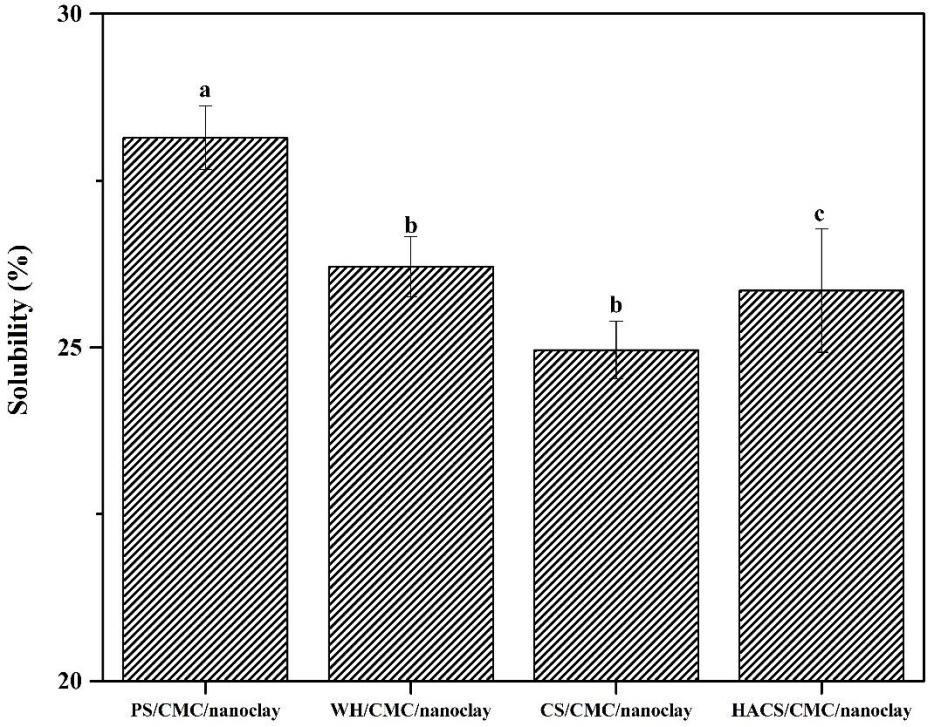

Figure 5.3. Effect of amylose-amylopectin ratios on film solubility of starch-CMC-nanoclay bionanocomposite films. [a-c]Different letters represent a significant difference using Tukey test ($p < 0.05$).

On the other hand, CS/CMC/nanoclay films showed lower solubility (24.9%) in water **(Figure 5.3)** which is due to less moisture content. Also, strong intermolecular interaction between polymers resulted in enhanced cohesiveness and lower swelling of CS/CMC/nanoclay films.

The water vapor permeability (WVP) of films is an important property to be considered for food packaging applications. The moisture transfer between atmosphere and food should be as low as possible to prevent any food spoilage. Water vapor permeability mainly depends on the film structure, filler material, plasticizer, relative humidity and temperature of the surroundings. Moreover, the WVP plays a crucial role in determining the shelf-life of the products. It was observed that the WVP values were in the order of PS/CMC/nanoclay >WH/CMC/nanoclay >CS/CMC/nanoclay films (**Figure 5.4**).

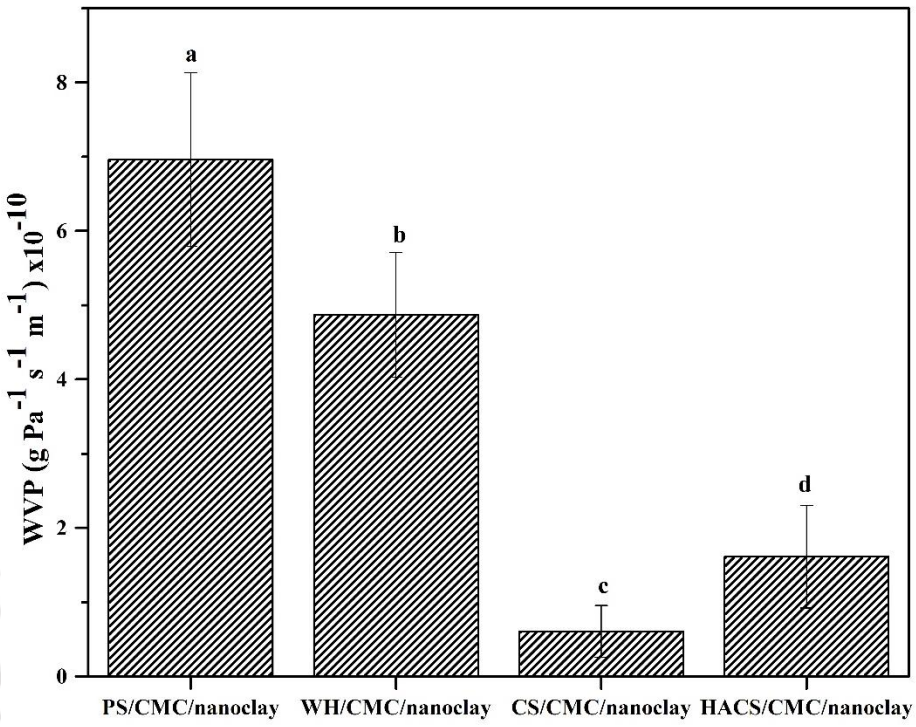

Figure 5.4 Effect of amylose-amylopectin ratios on water vapour permeability of starch-CMC-nanoclay bionanocomposite films. [a-d]Different letters represent a significant difference using Tukey test ($p < 0.05$).

Lower WVP was found to be 6.05×10^{-11}g Pa^{-1} s^{-1} m^{-1} for CS/CMC/nanoclay films. PS/CMC/nanoclay and WH/CMC/nanoclay films showed WVP of about 6.9×10^{-10}g Pa^{-1} s^{-1} m^{-1} and 4.87×10^{-10} g Pa^{-1} s^{-1} m^{-1}, respectively (**Figure 5.4**). Lower WVP of CS/CMC/nanoclay films may be attributed to lesser number of amylopectin branches and higher intermolecular hydrogen interactions with CMC which reduces the molecular space for water that tries to enter the network. Though amylopectin branches are very less in number, HACS/CMC/nanoclay films show higher WVP (1.61×10^{-10}g Pa^{-1} s^{-1} m^{-1}) than CS/CMC/nanoclay (**Figure 5.4**). Generally, water permeation occurs through amorphous zones of films **(Mali et al., 2006)**. The higher WVP of HACS/CMC/nanoclay films is due to large number of amylose linear chains (amorphous zones) and lower amylopectin branches. Also, the chemical structure of HACS exhibited more hydrophilicity (higher moisture content) and less cohesiveness between amylopectin branches of HACS and CMC, which further resulted in higher water permeability. The WVP of CS/CMC/nanoclay

films (**Figure 5.4**) was in accordance with its higher crystallinity and lower moisture content as shown in **Figures 5.1 and 5.2.**

5.3.3. Mechanical properties of starch-CMC-nanoclay bionanocomposite films

Mechanical properties such as tensile strength and elongation at break should be optimum to maintain film's integrity and barrier properties during shipping and handling. The tensile strength of starch blended with CMC and nanoclay films was affected by amylose-amylopectin ratios as shown in **Figure 5.5**.

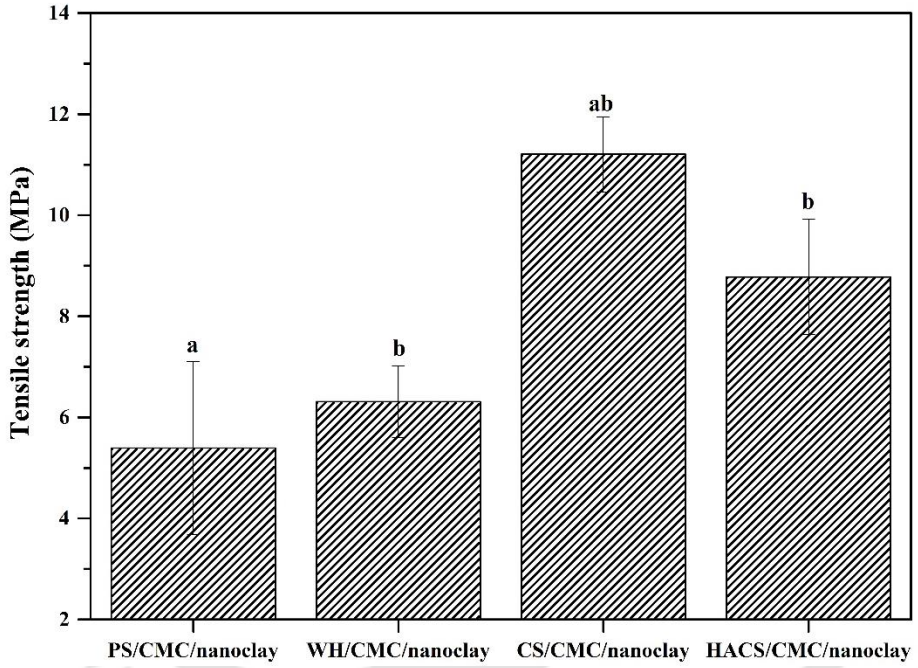

Figure 5.5. Effect of amylose-amylopectin ratios on tensile strength of starch-CMC-nanoclay bionanocomposite films. [a-b]Different letters represent a significant difference using Tukey test ($p < 0.05$).

The tensile strength (TS) of PS/CMC/nanoclay, WH/CMC/nanoclay, CS/CMC/nanoclay and HACS/CMC/nanoclay films was found to be 5.39 MPa, 6.3 MPa, 11.2 MPa and 8.7 MPa, respectively **(Figure 5.5)**. High tensile strength of CS/CMC/nanoclay films may be attributed to strong intermolecular interactions between –OH group of starch and –COOH/–OH group of CMC in the presence of reinforced nanoclay within the film matrix during gelatinization process. Moreover, CS/CMC/nanoclay films showed high degree of

crystallinity **(Figure 5.1)** and low moisture content **(Figure 5.2)**, which further enhanced its tensile strength **(Figure 5.5).**

Elongation at break (EB) describes films' flexibility and stretchability. **Figure 5.5** shows the effect of amylose-amylopectin ratios on elongation at break for different starch films blended with CMC and nanoclay. It is known that elongation at break is inversely proportional to tensile strength. Accordingly, CS/CMC/nanoclay films showed lower EB value (65.54%) due to its higher tensile strength in **Figure 5.5.**

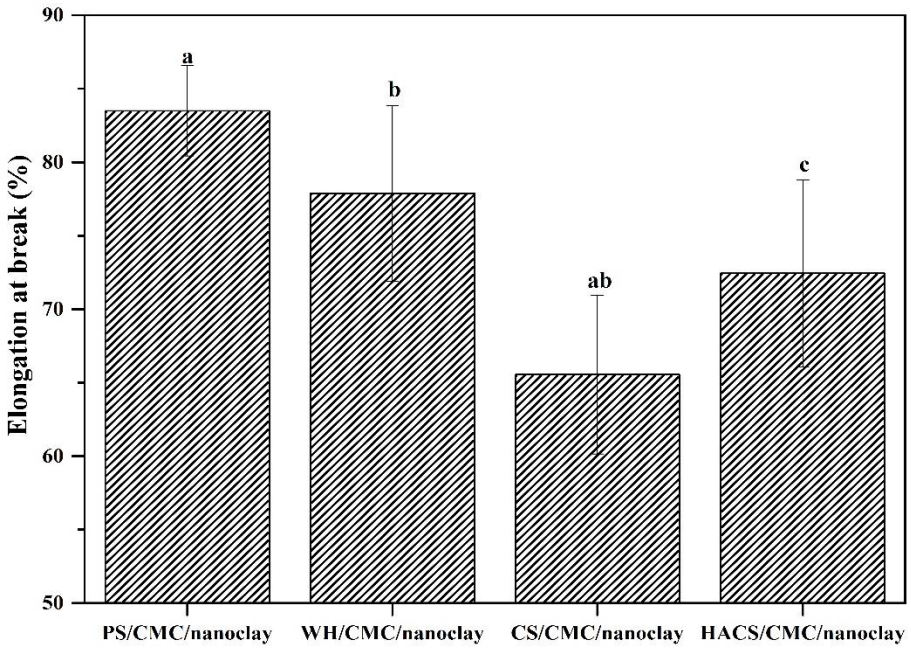

Figure 5.6. Effect of amylose-amylopectin ratios on elongation at break of starch-CMC-nanoclay bionanocomposite films. [a-c]Different letters represent a significant difference using Tukey test ($p < 0.05$).

Higher EB value (83.49%) was observed for PS/CMC/nanoclay films due to its low tensile strength and also due to its high moisture content, lower crystallinity is observed and weaker intermolecular hydrogen interactions between polymers is observed in the presence of nanoclay (**Figures 5.1, 5.2 and 5.5).** The flexibility and chain mobility of polymers were enhanced due to high moisture content in the case of PS/CMC/nanoclay films. High tensile strength and low elongation at break of CS/CMC/nanoclay films were

in accordance with its high crystallinity, low moisture content and low water vapour permeability (**Figures 5.1, 5.2 and 5.4).**

5.3.4. Dynamic mechanical thermal properties of starch-CMC-nanoclay bionanocomposite films

The films were cut into 50 × 10 × 0.05 mm dimension for studying dynamic mechanical properties such as storage modulus and tan delta and are shown in **Figures 5.7 and 5.8**.

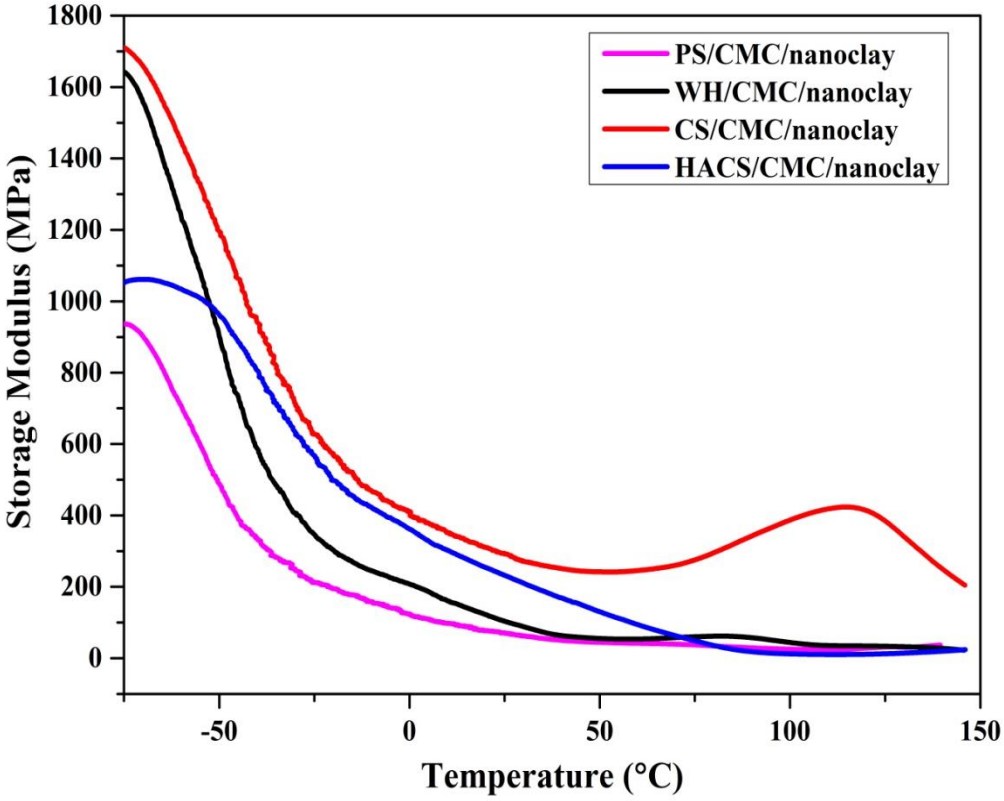

Figure 5.7. Effect of amylose-amylopectin ratios on storage modulus of starch-CMC-nanoclay bionanocomposite films.

As shown in **Figure 5.7**, the storage modulus was higher for CS/CMC/nanoclay films when compared to PS/CMC/nanoclay, WH/CMC/nanoclay and HACS/CMC/nanoclay films. The higher storage modulus is due to better interaction between CS and CMC in the presence of nanoclay. Also, it can be attributed to reduced mobility of polymer chains in CS/CMC/nanoclay films. It is known that storage modulus

increases with stiffness. Accordingly, stiffness was higher for CS/CMC/nanoclay films due to its higher storage modulus.

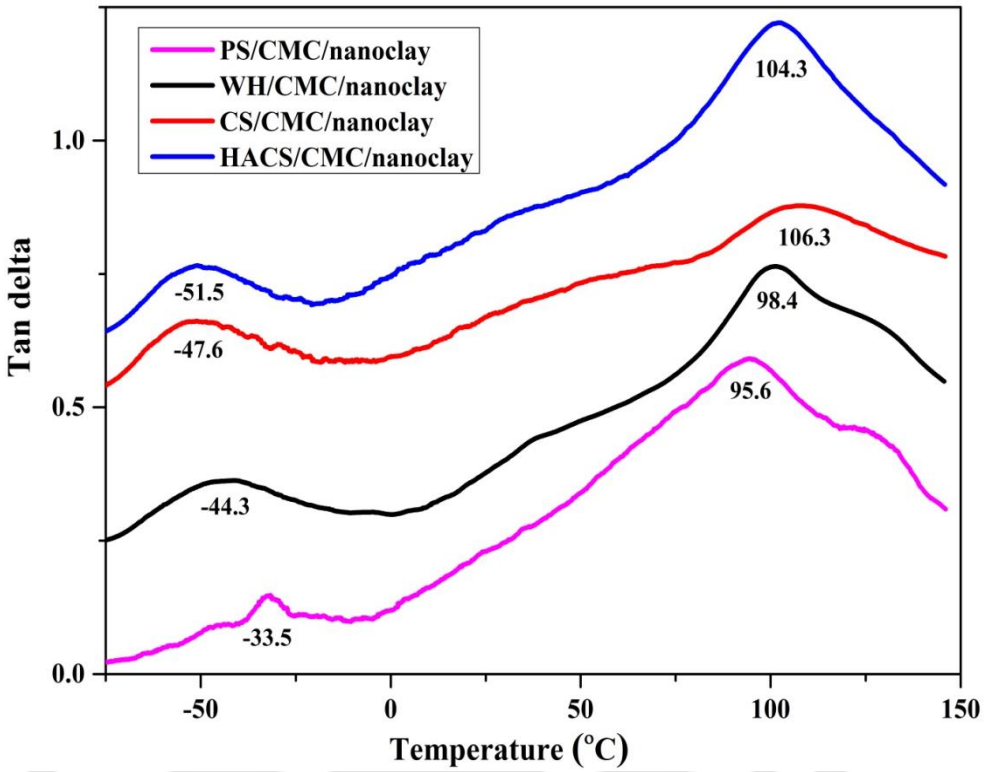

Figure 5.8. Effect of amylose-amylopectin ratios on loss factor (tan delta) of starch-CMC-nanoclay bionanocomposite films.

The loss factor (tan delta) is the ratio of loss modulus to storage modulus and is expressed as a dimensionless number. The curve of loss factor (tan delta) as a function of temperature is shown in (**Figure 5.8)** for different starch based films. The loss factor was sensitive to molecular motions and its peak values were related to T_g. The curve of thermoplastic starch (TPS) revealed two thermal transitions (T_g) due to their two separate phases namely, starch-rich phase (upper) and starch-poor phase (lower). The upper thermal transitions were clearly observed at 95°C, 98°C, 104°C, and 106°C for PS/CMC/nanoclay, WH/CMC/nanoclay, HACS/CMC/nanoclay and CS/CMC/nanoclay films, respectively. They are generally regarded as glass transition temperatures (T_g) of TPS materials because of starch-rich phase. In the case of CS/CMC/nanoclay films, higher T_g was observed due to restraining molecular motion within the polymer chains in the presence of nanoclay. The presence of larger crystal domain of CS with CMC and nanoclay reduces the chain mobility

and free volume, resulting in higher T_g. On the other hand, increase in moisture content increases free volume and thus chain mobility increases, which further lowers the glass transition. Therefore, glass transition temperature (T_g) was lower for PS/CMC/nanoclay, WH/CMC/nanoclay and HACS/CMC/nanoclay films when compared to CS/CMC/nanoclay films (**Figure 5.2**).

5.3.5. Fourier transform infrared (FTIR) spectra of starch-CMC-nanoclay bionanocomposite films

FTIR spectroscopy was investigated to determine the interactions among starch-CMC-nanoclay bionanocomposite films **(Figure 5.9)**.

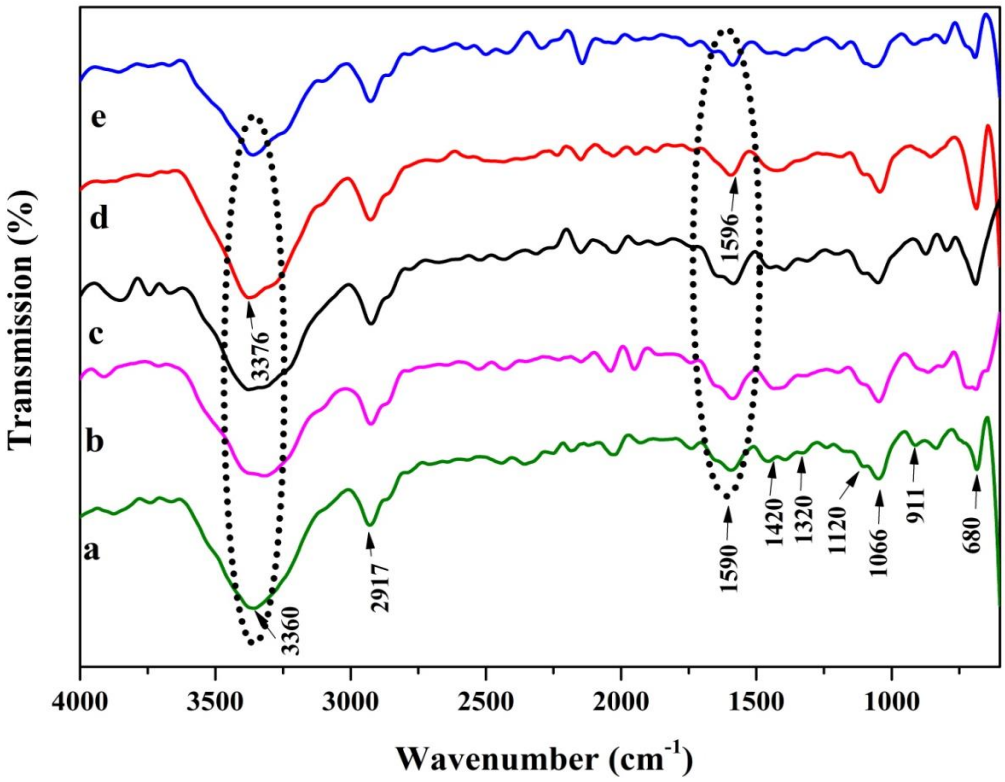

Figure 5.9. FTIR spectra of starch-CMC-nanoclay bionanocomposite films: (a) CMC/nanoclay (control), (b) PS/CMC/nanoclay, (c) WH/CMC/nanoclay, (d) CS/CMC/nanoclay and (e) HACS/CMC/nanoclay.

The broad band at 3360 cm^{-1} refers to O–H stretching from CMC **(Figure 5.9 (a))**. The peak at 2917 cm^{-1} corresponds to C–H stretching occurring in CMC **(Figure 5.9 (a))**. The broad peaks at 1590 cm^{-1}, 1420 cm^{-1} and 1320 cm^{-1} were due to COO^- stretching

vibrations, $–CH_2$ scissoring and –OH bending vibrations of neat CMC, respectively **(Figure 5.9 (a))**. The stretching vibration of C–O–C of polysaccharide skeleton at 1040–1066 cm^{-1} was also observed **(Chai and Isa, 2013; Pinotti et al., 2007; Raucci et al., 2015).**

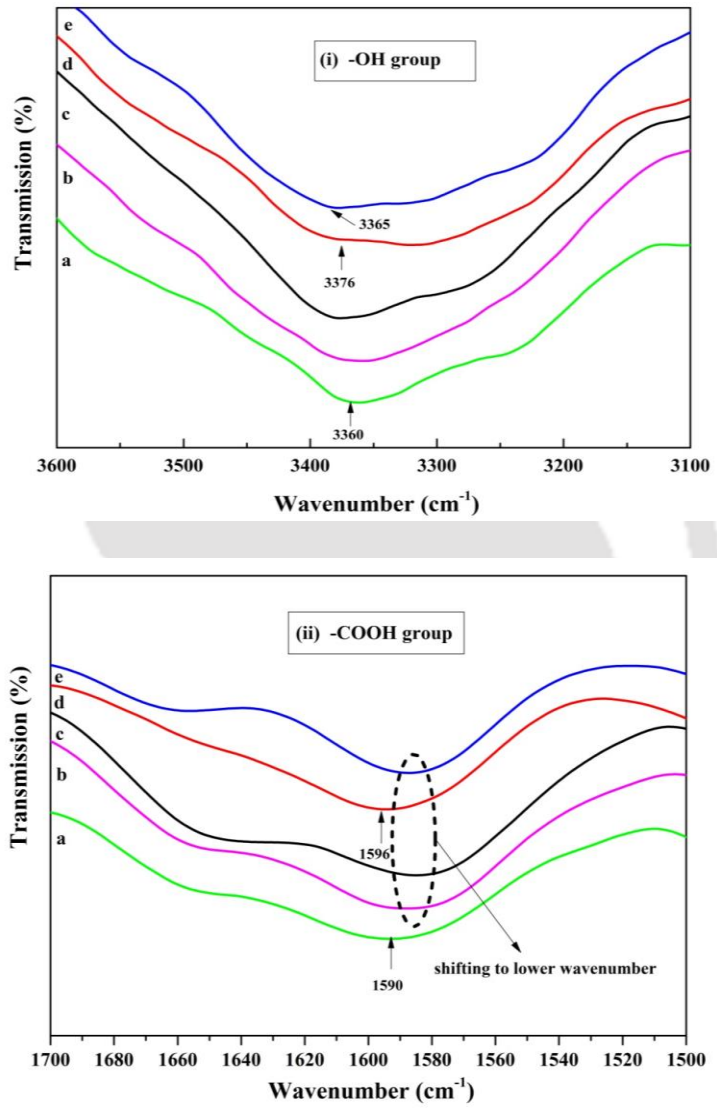

Figure 5.10. FTIR spectra (enlarged view) of selected peaks of (i) –OH group and (ii) –COOH group in starch-CMC-nanoclay bionanocomposite films: (a) CMC/nanoclay (control), (b) PS/CMC/nanoclay, (c) WH/CMC/nanoclay, (d) CS/CMC/nanoclay and (e) HACS/CMC/nanoclay.

The Si-O stretching vibrations at 1120 cm^{-1} and Al-OH stretching vibrations at 911 cm^{-1} and 680 cm^{-1} were also found for CMC/nanoclay films **(Figure 5.9 (a))**. It is possible that –OH and –COOH groups of CMC can be bonded with starch (-OH groups) and Si-O-Si/Al-OH layers of nanoclay through intermolecular hydrogen bonding. It is known that strong hydrogen bond shifts the band to higher wavenumber. Accordingly, the band at 3360 cm^{-1} was shifted to 3376 cm^{-1} and 3365 cm^{-1} with high intensity and large peak area for CS/CMC/nanoclay films and HACS/CMC/nanoclay films, respectively **(Figure 5.9 (d-e))**. On the other hand, -OH band was shifted to lower wave numbers, indicating weak intermolecular interactions between starch and CMC for PS/CMC/nanoclay and WH/CMC/nanoclay films **(Figure 5.9 (b-c))**. The peak at 1590 cm^{-1} was shifted to higher wavenumber (1596 cm^{-1}) with higher intensity for CS/CMC/nanoclay films when compared to other films **(Figure 5.9 (b-e))**. This is due to strong intermolecular hydrogen bonding between –COOH group of CMC and –OH group of CS. Peak intensity and area of silicate and aluminate layers of nanoclay (1120 cm^{-1}, 911 cm^{-1} and 680 cm^{-1}) was higher for CS/CMC/nanoclay films when compared to other films **(Figure 5.9 (b-e)).** It may be due to more intermolecular hydrogen bonding of nanoclay with either CMC or CS starch polymer chains or both, resulting in an extensive intercalation. This is in accordance with increased crystalline intensity of CS/CMC/nanoclay films in XRD pattern (**Figure 5.1**). The enlarged view of selected peaks of –OH and –COOH were presented in **Figure 5.10**.

5.3.6. Thermal stability of starch-CMC-nanoclay bionanocomposite films (TGA)

Thermogravimetric analysis (TGA) curve of different starch-CMC-nanoclay bionanocomposite films is shown in **Figure 5.11.** Three stages of weight loss were observed in all films. In the first stage, desorption of water was observed between 50°C and 100°C. Removal of bound water and evaporation of glycerol was observed in the second stage between 100°C and 200°C. In the third stage, polymers were decomposed from 250°C to 400°C. The residual mass was found to be 0%, 4%, 22%, and 24% for PS/CMC/nanoclay, WH/CMC/nanoclay, HACS/CMC/nanoclay and CS/CMC/nanoclay films, respectively. These results indicate that CS/CMC/nanoclay films are more thermally stable than other films.

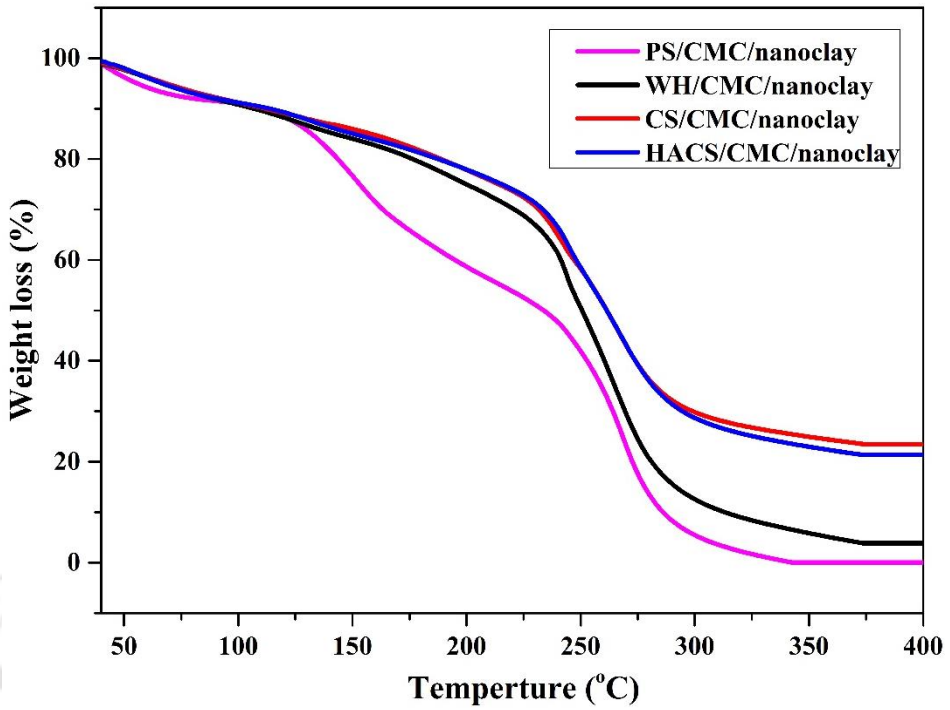

Figure 5.11. TGA curve of starch-CMC-nanoclay bionanocomposite films.

The higher thermal stability can be attributed to strong hydrogen bond between two polymers and higher crystallinity of CS/CMC/nanoclay films. Because of weak intermolecular hydrogen bonding and low crystallinity, PS/CMC/nanoclay films were completely decomposed.

5.3.7. Scanning electron microscopy (SEM) of starch-CMC-nanoclay bionanocomposite films

The SEM images of starch-CMC-nanoclay bionanocomposite films are shown in **Figure 5.12 (a-d).** All the films showed rough surface without any phase separation **(Figure 5.12 (a-d)).** The roughness of CS/CMC/nanoclay films was comparatively lesser than other films. These images revelaed that nanoclay improved the polymeric interactions in CS/CMC films than PS/CMC, WH/CMC and HACS/CMC films, resulting in more uniform surfaces and good compatibility. This extensive diffusion of nanoclay and higher intercalation into polymer chains is due to strong intermolecular interaction of CS/CMC/nanoclay films which are in accordance with XRD (**Figure 5.1(d))** and FTIR pattern **(Figure 5.9 (d))**. Bionanocomposite films PS/CMC, WH/CMC and HACS/CMC were observed to be coated with nanoclay material as compared to CS/CMC. This nanoclay

coating exhibits an increase in roughness of the surface due to lesser interactions with polymers **(Figure 5.9 (b,c and e))**.

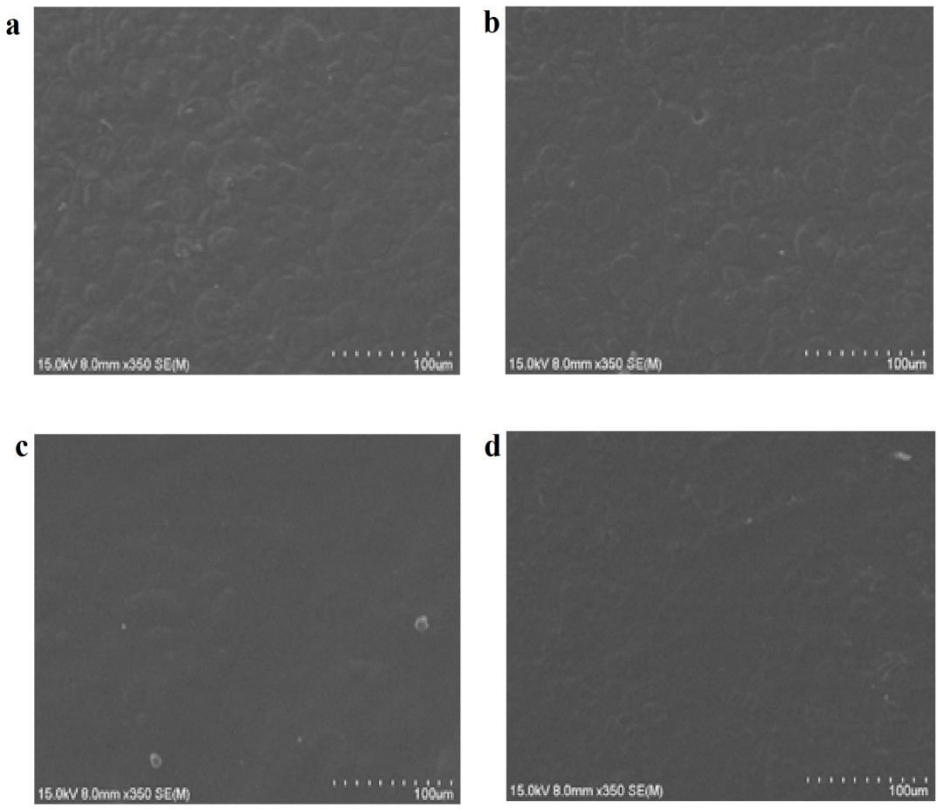

Figure 5.12. SEM images of starch-CMC-nanoclay bionanocomposite films: (a) PS/CMC/nanoclay, (b) WH/CMC/nanoclay, (c) CS/CMC/nanoclay and (d) HACS/CMC/nanoclay.

5.3.8. Antifungal activity of starch-CMC-nanoclay bionanocomposite films

Bread samples of different sizes (3.5 × 4 cm (L1) and 2 × 2 cm (S1)) were sealed with bionanocomposite films. In order to compare the antifungal activity of bionanocomposite films with conventional polymeric packaging materials, same sizes (3.5 × 4 cm (L2) and 2 × 2 cm (S2)) of bread samples were also packed with low-density polyethylene (LDPE). All packed bread samples were stored at 25°C and 59% RH for 15 days. Comparative study of bread samples packed by CS/CMC/nanoclay bionanocomposite films and low density polyethylene (LDPE) films is shown in **Figure 5.13.** Because of low moisture content, low water vapor permeability, low solubility and

high tensile strength, CS/CMC/nanoclay bionanocomposite films were chosen for bread packaging. The LDPE films were served as control.

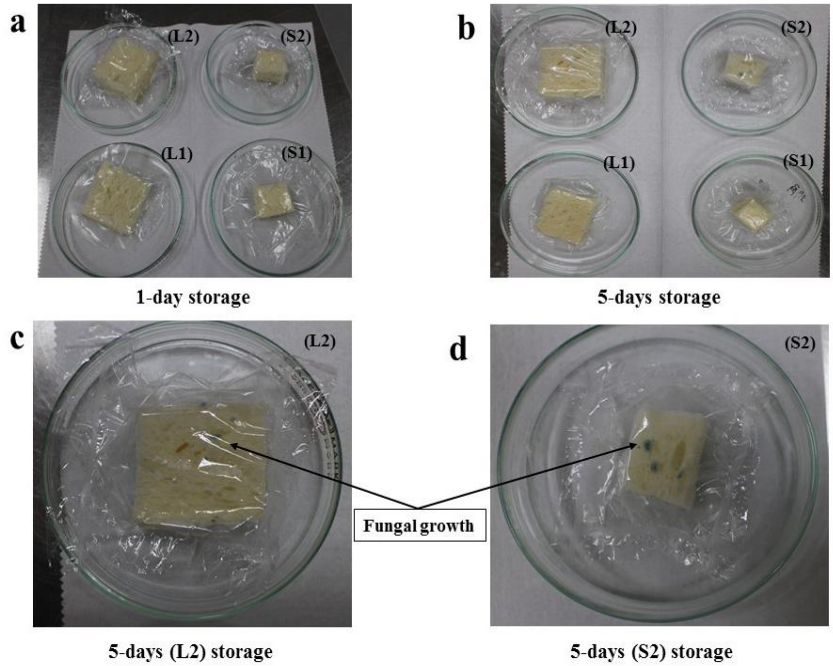

Figure 5.13. Comparative study on bread quality (spoilage) packed with CS/CMC/nanoclay bionanocomposite films and low density polyethylene films (control). The quality of bread samples on (a) 1st day, (b) 5th day, (c) enlarged view of L2 on 5th day and (d) enlarged view of S2 on 5th day.

The fungal growth was observed on 5th day in L2 and S2 control samples, which were packed by LDPE films. But, the fungal growth was retarded by 15 days in the case of L1 and S1 samples packed by CS/CMC/nanoclay films. The antifungal acitivity of nanoclay can be explained as an effect of metal ion release during its interactions with fungi **(Malachova et al., 2011)**. Also, the proliferation of fungal growth was delayed by CS/CMC/nanoclay films due to its property to act as a barrier to water. Hence, the prepared bionanocomposite films can be a potential candidate for food packaging applications to extend the shelf life of products and food safety.

5.3.9. Comparative study of various starches with CMC films selected natural and synthetic polymeric films

The tensile strength, elongation at break and WVP of various starches blended with CMC were compared with selected natural and synthetic polymeric films are summarized in **Table 5.1**.

Table 5.1. Tensile strength, elongation at break and water vapour permeability of various starches with CMC and synthetic films.

Film type	Test condition	TS (MPa)	EB (%)	WVP (g/m s Pa)	Reference
HACS/CMC/nanoclay CS/CMC/nanoclay WH/CMC/nanoclay PS/CMC/nanoclay	25°C, 75% RH	8.77 11.20 6.30 5.39	72.44 65.54 77.88 83.49	1.61×10^{-10} 6.05×10^{-11} 4.87×10^{-10} 6.96×10^{-10}	**Present study**
CS	25°C, 75% RH	3.8-4.3	4.0-10.0	-	**Mali et al. (2006)**
CS/CMC	21°C, 55% RH	9.83	63.52	-	**Almasi et al. (2010)**
Cassava/30% CMC	25°C, 54% RH	5.5	30.5	-	**Tongdeesoontorn et al. (2011)**
CS/10% Citric acid-15% CMC	25°C, 97% RH	11.0	63	6.5×10^{-11}	**Ghanbarzadeh et al. (2010)**
Low density polyethylene (LDPE)	38°C, 90% RH	7.6-17.3	500.0	9.25×10^{-11}	**Bourtoom and Chinnan (2008)**
High density polyethylene (HDPE)	38°C, 90% RH	17.3-34.6	300.0	2.31×10^{-13}	
Polyester	38°C, 90% RH	178.0	70.0-100.0	-	
Cellophane	38°C, 90% RH	-	-	8.41×10^{-11}	

In this present study, high tensile strength (11.20 MPa) and low WVP (6.05×10^{-11} g/m s Pa) was observed for CS/CMC/nanoclay. Elongation at break (less deformable) was slightly lower for CS/CMC/nanoclay films compared with other films. The tensile strength of CS/CMC/nanoclay film was higher than CS, CS/CMC, cassava starch/CMC films and CS/CMC films crosslinked by citric acid **(Almasi et al., 2010; Ghanbarzadeh et al., 2010; Mali et al., 2006; Tongdeesoontorn et al., 2011)**. The WVP of CS/CMC/nanoclay films was lower than CS/CMC films crosslinked by citric acid and

synthetic polymer cellophane films **(Bourtoom and Chinnan, 2008)**. The low WVP of CS/CMC/nanoclay films compared with LDPE and HDPE can be explained by the inherent hydrophilicity of CS and CMC.

5.4. Summary

Effect of amylose-amylopectin ratios in starch on mechanical properties (tensile strength and elongation at break), water barrier properties, thermal properties and glass transition temperature was studied. Among the chosen amylose-amylopectin ratios, CS (28:72) based films were found to be showing higher tensile strength, lower WVP, higher T_g and higher thermal stability. XRD study revealed that the crystallinity was higher for CS/CMC/nanoclay bionanocomposite films due to formation of strong intermolecular hydrogen bond among CS, CMC and nanoclay as confirmed by FTIR results. The SEM study exhibited that the bionanocomposite films containing CS showed more uniform surfaces than other films. The prepared CS/CMC/nanoclay bionanocomposite films showed heat sealing properties and also antifungal activity was observed against *A. niger* in bread samples at 25°C, 59% RH for 15 days. All these results confirmed that the produced films have potential applications in the field of packaging to extend the shelf-life of perishable food products.

Chapter 6

Effect of amylose-amylopectin ratios on physical, mechanical and thermal properties of starch-CH-nanoclay bionanocomposite films

In this chapter, aim of this study was to evaluate the influence of amylose-amylopectin ratios (potato starch, 20:80; wheat starch, 25:75; corn starch, 28:72 and high amylose corn starch, 70:30) on physical, mechanical and thermal properties of starch-CH-nanoclay bionanocomposite films.

6.1 Specific Background

In the past few decades, the issue of environmental pollution intensified and it is a matter of global concern. Mainly, the petrochemical-based plastics employed in packaging pose a serious threat to the environment problems as it has a long decomposition period ranging from hundreds to thousands of years (**Aider, 2010)**. Biopolymer-based packaging material is a possible alternative to substitute for non-biodegradable petrochemical-based plastics. Biodegradable polymer has made an immense contribution in the development of food packaging industry (**Nair et al., 2017**). Biodegradable polymers are gaining much attention in the application of food packaging as they contribute in terms of food safety, food storage, minimization of chemical preservatives and greener environment (**Ozcalik and Tihminlioglu, 2013).**

Starch is the most common agricultural raw material used to develop biodegradable films as it is abundantly available, renewable, biocompatible, cheap and above all it possesses the ability to form films (**Faria et al., 2012; Toral et al., 2002**). Starch based biodegradable films in comparison to petrochemical plastic films exhibit a stronger hydrophilic behaviour which makes them poor in mechanical properties and water resistance **(Souza et al., 2012)**. The chemical, physical and functional properties of amylose present in starch determines the ability to gel and form films in starch based

biodegradable polymers (**Young, 1984**). Amylose is a linear homo polymer chain of α-(1 → 4) glucose units. Amylopectin is a highly branched molecule with α-(1 → 6) glycosidic linkage at branch points as well as linear regions of α-(1 → 4)-linked glucose units (**Murphy, 2000**). The branch points of amylopectin occur after every 24 to 30 glucose residues which guides the molecular structure and effects physical and biological properties (**Perez and Bertoft, 2010**). Different ratios of amylose and amylopectin signify a distinct molecular weight which is due to the nature of chain branching as well as chain lengths and structure characteristics in the starch based products (**Mua and Jackson, 1997**). This is also responsible for starch crystallization which changes the mechanical strength of starch based product (**Cano et al., 2014**).

Chitosan is found to be biodegradable, bioactive, adequate water vapour barrier, low oxygen permeable and demonstrates excellent film forming abilities **(Aguirre-Loredo et al., 2016; Jahit et al., 2016).** Chitosan has unique property of food protection due to its inherent anti-bacterial and anti-fungal properties against spoilage microorganism and several groups of pathogens (**Tan et al., 2015).** The advantage of adding chitosan into starch is that it makes the film more hydrophobic which improves water resistance as well as mechanical properties **(Ren et al., 2017)**. Corn starch impregnated with chitosan and calcium carbonate nanoparticles showed an improvement in tensile properties **(Ji et al., 2017).**

Recently the preparation of nanocomposites using montmorillonite (MMT) is a persuading method to improve the barrier, mechanical, functional and thermal properties without affecting biodegradability of the biopolymers (**Siqueira et al., 2010**). Chitosan-nanoclay bionanocomposite with antioxidant potential are used for active packaging materials **(Ghelejlu et al., 2016).**

Good quality seal is required in order to assure package integrity in the food package, films heat-sealable ability. Sealing of packet bag depends on a thermo-sealing conditions such as temperature, pressure and time. Food package should maintain package integrity and prevent microorganism from entering and thus extending the life of the product **(Lopez et al., 2015).**

Furthermore, there is no study on different biodegradable films prepared from starch sources containing various proportion of amylose and amylopectin incorporated with chitosan and nanoclay based packaging film for food applications. The present work investigates the effect of various amylose-amylopectin ratios on water barrier, mechanical, thermal, functional properties and morphological characteristics that make bionanocomposite an eco-friendly food packaging material.

6.2. Preparation of amylose-amylopectin ratios on physical, mechanical and thermal properties of starch-CH-nanoclay bionanocomposite films

The preparation of different types of starch synthesised using different amylose-amylopectin ratios (potato starch, 20:80; wheat starch, 25:75; corn starch, 28:72 and high amylose corn starch, 70:30) are incorporated with chitosan (CH) reinforced with nanoclay (Na-MMT) to produce bionanocomposite films using the methodology mentioned in elsewhere **(Chapter 3, Section 3.2.5 and 3.2.6).** The prepared bionanocomposite films have uniform thickness of 0.06 mm.

6.3. Results and Discussion

6.3.1. X-ray diffractograms of starch-CH-nanoclay bionanocomposite films

In order to investigate the role of amylose-amylopectin in the polymer matrix, samples related to CH/nanoclay, PS/CH/nanoclay, WH/CH/nanoclay, CS/CH/nanoclay and HACS/CH/nanoclay bionanocomposite films were characterized using XRD and the results are presented in **Figure 6.1.**

The diffraction patterns of native PS and HASC exhibit B-type which show main peaks around 2θ =17°, 22° and 23° **(Gernat et al., 1993; Manek et al., 2012)**. Whereas the diffraction patterns of native WH and CS showed A-type whose main peak is at 15°, 17°, 18° and 23° **(Sun et al., 2014a; Yu et al., 2016)**. The chitosan film showed diffraction peaks at around 8.08°, 11.6°, 17.84° and 22.38° **(Ren et al., 2017).** The peaks found in the diffraction spectra of starch-based films were not seen in case of bionanocomposite films which may be associated with the destruction of crystalline granules of starch during the process of gelatinization. Peak broadening and decreases in intensity can also be seen in the above case **(Zhang et al., 2007)**.

Intercalation refers to the process in which the polymer chain is inserted into the silicate layer without much affecting the clay stacks. CH blended with nanoclay showed a low-intensity crystalline peak at 19.70° (2θ) which depicts low crystallinity as illustrated in **Figure 6.1 (a)**. When starch is completely solubilized with chitosan and reinforced by nanoclay, it depicts a film with three film-forming components (starch-chitosan-nanoclay) which show a main diffraction peak at (2θ =20°) (**Figure 6.1(b-d)**).

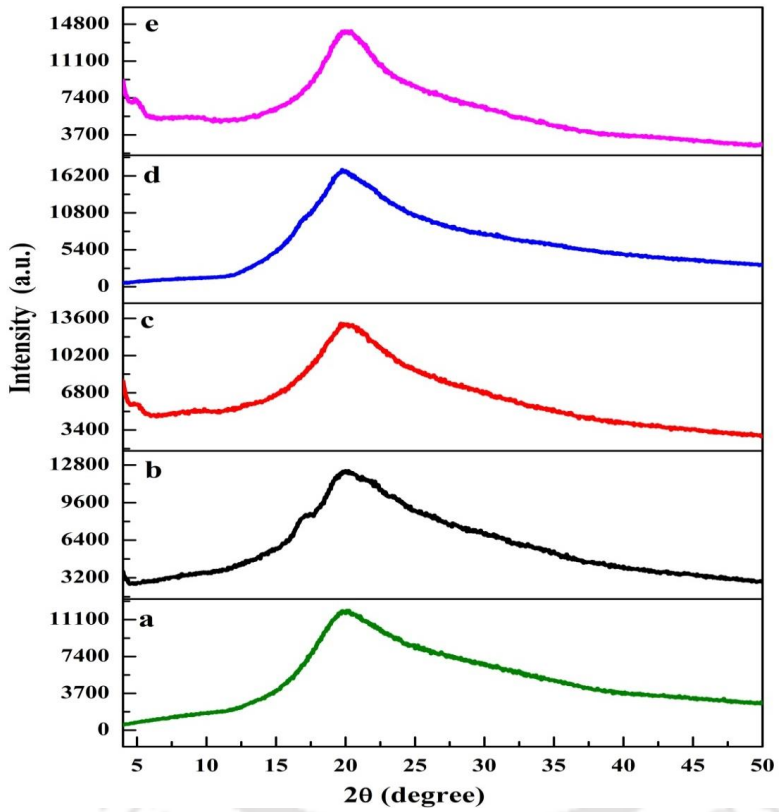

Figure 6.1. XRD pattern of different amylose-amylopectin ratios of starch-CH-nanoclay bionanocomposite films: (a) CH/nanoclay (control), (b) PS/CH/nanoclay, (c) WH/ CH/nanoclay, (d) CS/CH/nanoclay and (e) HACS/CH/nanoclay.

The shifting in diffraction peak was probably due to change in the chain orientation caused by an interaction of hydrogen-bond between chitosan and starch molecules **(Bangyekan et al., 2006)**. The broad peak intensity increases in the order of CS/CH/nanoclay > HACS/CH/nanoclay > WH/CH/nanoclay > PS/CH/nanoclay > CH//nanoclay **(Figure 6.1 (a-e))**. These results revealed that nanoclay (MMT) intercalates

with either CH or starch polymer chains or both via silicate layers and thus forming starch/CH/nanoclay bionanocomposite film. The intercalation is affected by the ratio of amylose-amylopectin and polar group interaction between the polymer chains and nanoclay. The peak of Na-MMT around 7.21° (2θ) is not observed for all the bionanocomposite films which confirms proper intercalation of host polymer chain between nanoclay stacks. The intensity of the crystalline peak in case of CS/CH/nanoclay is higher due to its chemical structure and compatibility, hydrogen bonding between CS and CH reveals a higher intercalation of polymer chains inside the Na-MMT galleries.

6.3.2. Water barrier properties of starch-CH-nanoclay bionanocomposite films

The water barrier properties of the films such as moisture content, solubility and water vapor permeability are shown in **Figures 6.2-6.4.**

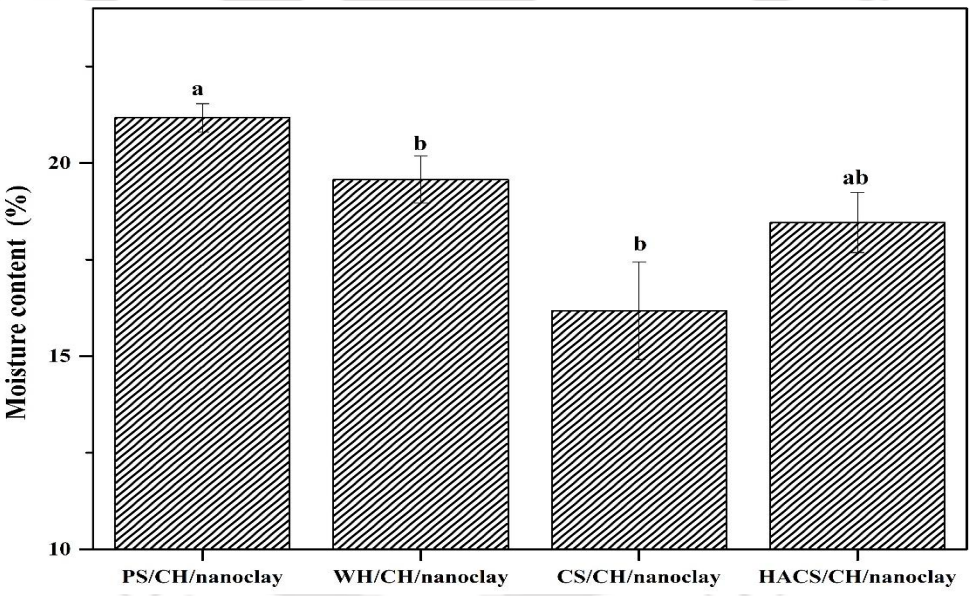

Figure 6.2. Influence of amylose-amylopectin ratio on moisture content of starch-CH-nanoclay bionanocomposite films. [a-b]Different letters represent a significant difference using Tukey test ($p < 0.05$).

The moisture content of PS/CH/nanoclay, WH/CH/nanoclay, CS/CH/nanoclay and HACS/CH/nanoclay is presented in **Figure 6.2.** The values are 21.17, 19.57, 16.18, 18.46% respectively. It was observed PS/CH/nanoclay had highest moisture content while the lowest was found in case of CS/CH/nanoclay. Moisture content of starch-based films does not depend only on relative humidity of environment but also on nature and chemical

structure such as ratio of amylose-amylopectin content, size of branching point, which further guides the molecular architecture of starch granule **(Bertoft and Blennow, 2009; Mua and Jackson, 1997).** The lesser hydrophilicity of CS/CH/nanoclay films might be due to high amylose content which modifies its chemical structure and molecular space resulting in reduction of free water absorption site thus decreasing the percentage of moisture content. This may be associated with a strong interaction between –OH group of CS and NH_2 group of CH. The presence of free –OH groups in case of PS/CH/nanoclay and WH/CH/nanoclay increase the interaction with water molecule. Though HACS/CH/nanoclay has the highest amylose content its moisture content is higher than CS/CH/nanoclay which may be due to the drastic reduction in amylopectin content. Thus, an increase in the amylose content to an optimum value results in very stable molecular orientation forming dense and stronger films enhancing the ability of its linear chains to interact with hydrogen bonds. The difference in moisture content is observed due to their difference in chemical structures and hygroscopic nature **(Kurt and Kahyaoglu, 2014)**. The results shown in XRD spectrum and moisture content together confirm the lower hydrophilic property of CS/CH/nanoclay. The same conclusion has been inferred **(Nair et al., 2017)**.

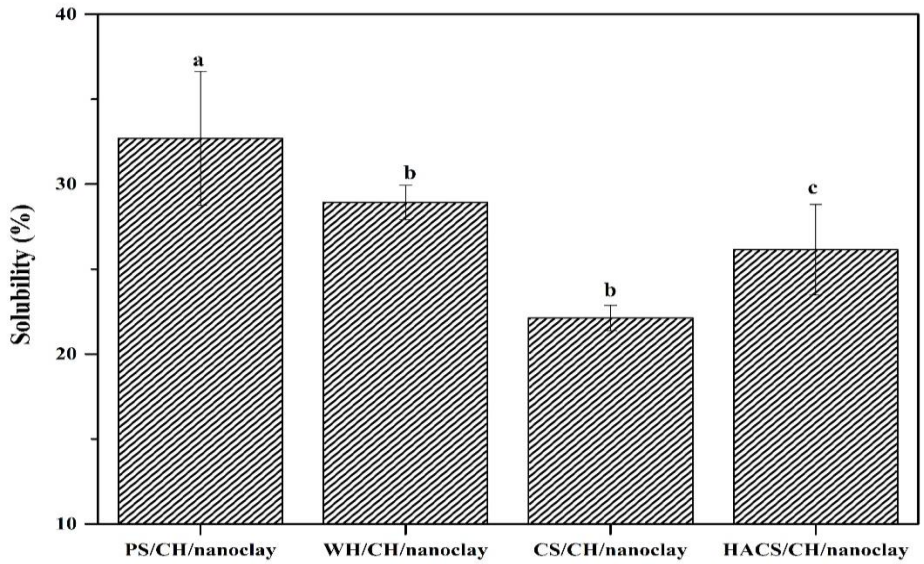

Figure 6.3. Influence of amylose-amylopectin ratios on film solubility of starch-CH-nanoclay bionanocomposite films. [a-c]Different letters represent a significant difference using Tukey test ($p < 0.05$).

Film solubility is one of the important parameters that determine the product reliability, shelf life and moisture resistance in food packaging. Generally water resistance and film solubility are inversely related as in **(Nair et al., 2017)**. As shown in **Figure 6.3,** the film solubility of PS/CH/nanoclay, WH/CH/nanoclay, CS/CH/nanoclay and HACS/CH/nanoclay was found to be 32.70%, 28.92%, 22.12% and 26.14% respectively. It was observed PS/CH had the highest film solubility while the lowest was found in case of CS/CH/nanoclay. PS/CH/nanoclay which had higher moisture content due to which the crosslinking of starch and water is increased resulting in the lesser degree of interaction with CH thus forming swollen film structure. This increases the solubility of the film that was in accordance with **(Kurt and Kahyaoglu, 2014).** In addition to this, CS/CH/nanoclay showed a lower solubility in water due to lower water sensitivity and strong intermolecular interaction between polymers that resulted from the improved cohesiveness of the biopolymer matrix. These result in lower swelling of the films that maintain a stronger product integrity.

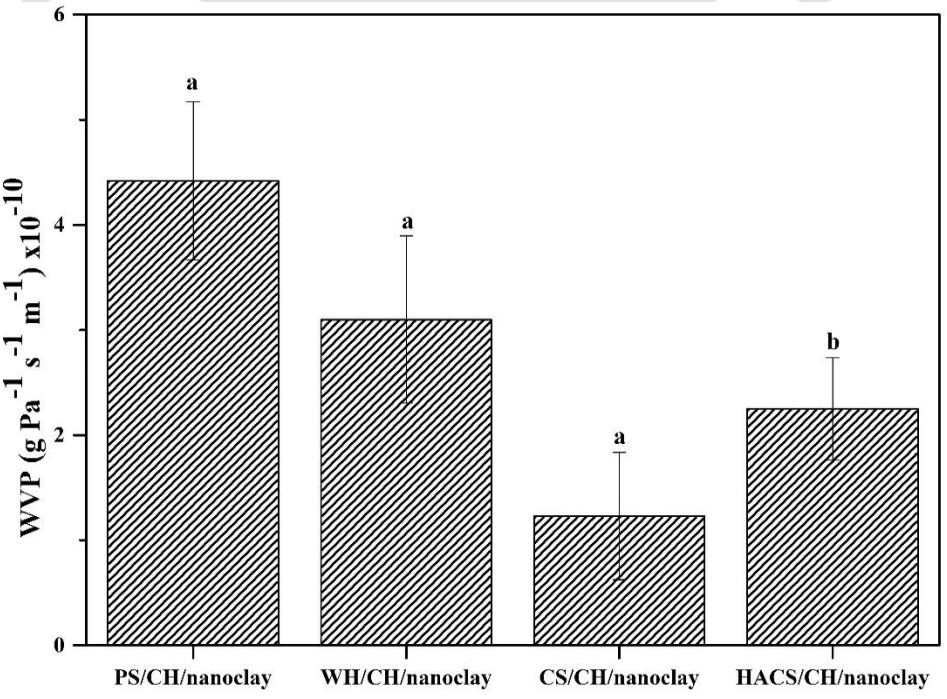

Figure 6.4. Influence of amylose-amylopectin ratios on water vapor permeability of starch-CH-nanoclay bionanocomposite films. [a-b]Different letters represent a significant difference using Tukey test ($p < 0.05$).

The water vapor permeability (WVP) of biopolymer films is yet another important property to considered for food packaging applications. Food spoilage is more when there is large transfer of moisture between the food and atmosphere. Generally, water permeation occurs through amorphous zones of films **(Mali et al., 2006)**. Water vapor permeability is a proportionality constant which is assumed to be independent of the difference in pressure applied to the films specimen. However, water sensitive biomaterials such as starch-based films contain polar functional groups in the film structure through which water molecules permeate **(Hagenmaier and Shaw, 1990)**. This WVP depends on the film structure, plasticizer, relative humidity and temperature of the surrounding atmosphere. Moreover, WVP plays a crucial role in determining the shelf life of a packaged product. It was observed that the WVP was in the order PS/CH/nanoclay > WH/CH/nanoclay > CS/CH/nanoclay **(Figure 6.4)**. The results exhibit that WVP of the biopolymer films decrease as amylose ratio increases as seen in the order of PS/CH/nanoclay (4.42×10^{-10}g Pa^{-1} s^{-1} m^{-1}), WH/CH/nanoclay (3.10×10^{-10}g Pa^{-1} s^{-1} m^{-1}) and CS/CH/nanoclay (1.23×10^{-10}g Pa^{-1} s^{-1} m^{-1}) bionanocomposite films. Low WVP of CS/CH/nanoclay may be attributed to higher amylose content due to which there is a higher intermolecular hydrogen interaction between CS and CH, thus reducing the molecular space for water to enter into the network. In case of HASC/CH/nanoclay (2.25×10^{-10} g Pa^{-1} s^{-1} m^{-1}) film, lower amylopectin results in increase of the free volume of the film matrix which showed higher hydrophilicity. This leads to higher diffusivity and increased WVP. WVP obtained is in accordance with the results of crystallinity and moisture content as shown in **Figure 6.1 and 6.2.**

6.3.3. Mechanical properties starch-CH-nanoclay bionanocomposite films

Mechanical properties such as tensile strength and elongation at break determine the properties like film's integrity and barrier properties that in turn decide the application of packaging material like in handling, shipping and preserving the packed foods during storage. The tensile strength of starch blended with CH and a nanoclay films was affected by amylose-amylopectin ratios as shown in **Figure 6.5.**

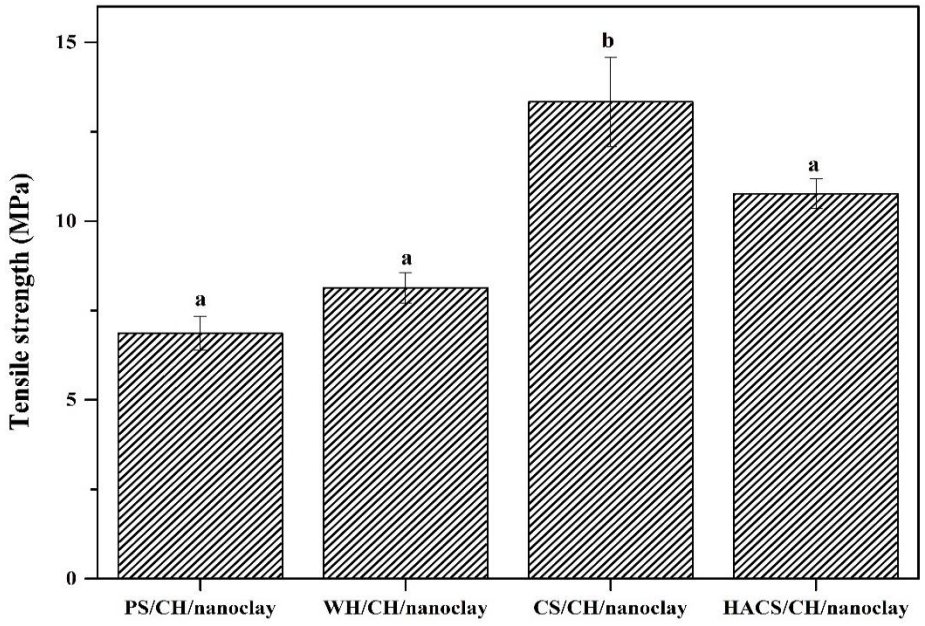

Figure 6.5. Influence of amylose-amylopectin ratios on tensile strength of starch-CH-nanoclay bionanocomposite films. [a-b]Different letters represent a significant difference using Tukey test ($p < 0.05$).

Tensile strength (TS) shows the capacity to accept load or maximum force applied on bionanocomposite before breaking and it depends on the chemical structure of starch matrix binder with CH and the reinforcement nanoclay in composite materials. Tensile values determine both stretch ability and strength that is a significant requirement for food-packing material **(Arvanitoyannis et al., 1998)**. Mechanical properties are related to moisture content and glycerol concentration (plasticizing agent) within a hydrophilic material film **(Loredo RA Yaneli et al., 2016)**. The results confirmed that PS/CH/nanoclay with 20% amylose has an average tensile strength of 6.86 MPa, WH/CH/nanoclay film containing 25% amylose shows close to 8.13 MPa, CS/CH/ nanoclay film containing 28% amylose is near 13.33 MPa and the tensile strength of HACS/CS/ nanoclay with 70% amylose is 10.76 MPa. The amino (NH_2) functional groups in the backbone of chitosan are protonated and converted into NH_3^+ in the acetic acid solution. Nanoclay is a potential filler that enhances the ordered crystallinity structures of starch/CH molecules. CS/CH/nanoclay (28% amylose) showed the highest tensile strength which might be due to a highly linearized structure formed during gelatinization as a result of the formation of a stronger

intermolecular hydrogen bonding between OH^- of the starch and NH_3^+ in the backbone of chitosan which resulted in a denser packing of polymer network compared to PS/CH/nanoclay and WH/CH/nanoclay. Despite having 70% amylose content in HACS/CH/nanoclay had a lower tensile strength as compared to CS/CH/nanoclay. The reason attributed to this is the drastic increase in amylose content that lead to the weakening of intra-molecular attraction between the polymer chains due to more exposure of unbound free-OH groups. These results support that CS/CH/nanoclay has a higher degree of crystallinity as shown in XRD (**Figure 6.1)** and lower moisture content (**Figure 6.2).**

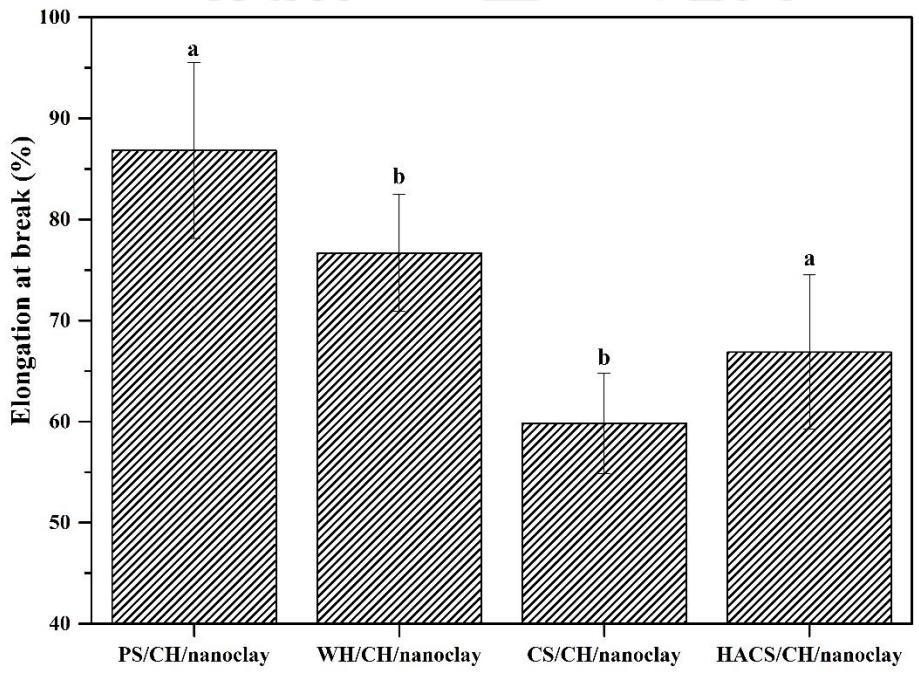

Figure 6.6. Influence of amylose-amylopectin ratio on elongation at break of starch-CH-nanoclay bionanocomposite films. [a-b]Different letters represent a significant difference using Tukey test ($p < 0.05$).

Elongation at the break (EB) describes the extensibility and flexibility in packaging films. **Figure 6.6** presents the effect of amylose-amylopectin ratios on elongation at break for starch incorporated with chitosan and reinforce with nanoclay. The average EB values of the biodegradable blend film behaved inversely to the tensile strength value decreasing from 86.81% (PS/CH/nanoclay) to 79.69% (WH/CH/nanoclay) to 66.87% (HACS/CH/nanoclay) to a minimum of 59.82% (CS/CH/nanoclay). It is interesting to note

that on increasing amylose content (from 20% to 28%), EB as well as moisture content (plasticizing effect of water) decreased which was probably due to -OH groups of amylose bound with NH_3^+ of chitosan with strong intermolecular hydrogen interactions in the presence of nanoclay. In case of higher moisture content, the effect of reinforcement is weak which is due to interaction of water with polymer matrix. Aforementioned, the increase in amylose improves the film strength along with decrease in its flexibility. In case of 70% amylose content (HACS/CH/ nanoclay) which shows more flexibility and chain mobility of polymers than CS/CH/nanoclay, the behaviour could be explained by the presence of high moisture content and exposure to free –OH groups of starch which interact with water leading to decrease in the rigidity of the polymer network. According to the result of high tensile strength and low elongation at break, CS/CH/nanoclay with 28% amylose content was optimum with its high crystallinity and less water vapor permeability properties.

6.3.4. Dynamic mechanical thermal properties of starch-CH-nanoclay bionanocomposite films

The dynamic mechanical properties such as storage modulus and tan delta of starch-CH-nanoclay bionanocomposite films are shown in **Figures 6.7 and 6.8.**

The storage modulus of CS/CH/nanoclay film was found to be higher than PS/CH/nanoclay, WH/CH/nanoclay, and HACS/CH/nanoclay films as shown in **Figure 6.7.** The storage modulus is related to the stiffness of composite film. The stiffness of CS/CH/nanoclay is higher due to a strong inter-chain bond between CS and CH in the presence of nanoclay. This implies that stiffness of the polymer material in CS/CH/nanoclay is high as it restrains the chain mobility leading to a higher value of storage modulus of the films.

The loss factor (tan delta) is a dimensionless number and is expressed as the ratio of loss modulus to storage modulus. The curve of loss factor (tan delta) as a function of temperature is presented in **Figure 6.8.** Glass transition temperature (T_g) depend upon presence of water molecule in the polymer which have significant role in the molecular structure that show hydrophilic nature as well as arrangement of inter-and intra-molecular forces in the polymer matrix. The value of T_g increases with polymer-polymer interaction

while the value decreases with an increase in moisture content because of polymer-water-polymer interactions resulting in more flexible polymeric chains **(Loredo RA Yaneli et al., 2016).**

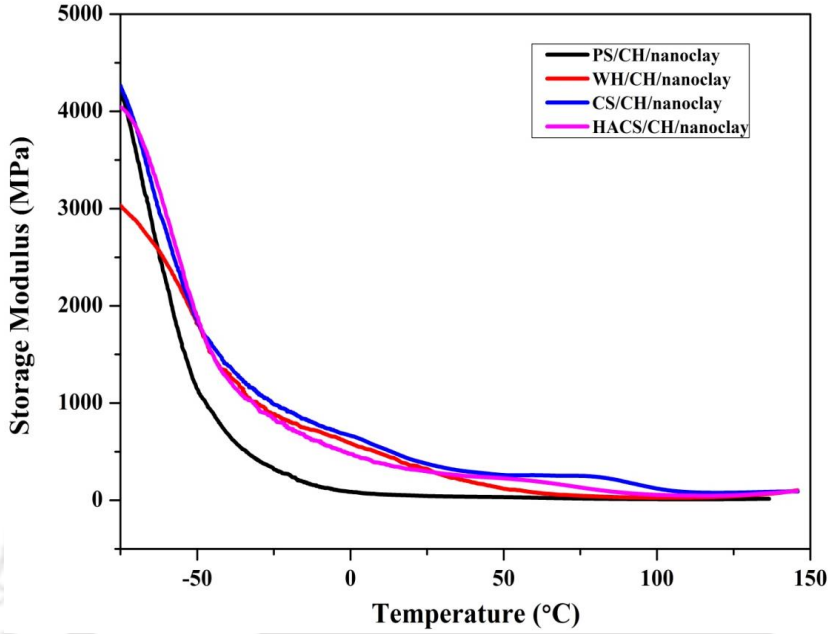

Figure 6.7. Influence of amylose-amylopectin ratios on storage modulus of starch-CH-nanoclay bionanocomposite films.

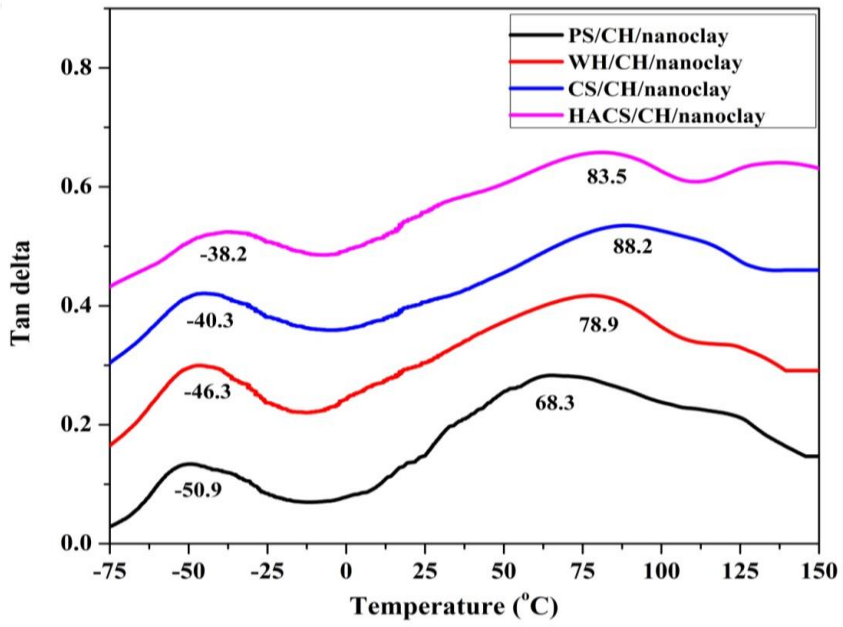

Figure 6.8. Influence of amylose-amylopectin ratios on tan delta of starch-CH-nanoclay bionanocomposite films.

The loss factor was sensitive to the molecular motions and its peak was related to the glass transition temperature. The curve of thermoplastic starch (TPS) revealed two thermal transitions (T_g) due to their two separate phases namely starch-poor phase (lower) and starch-rich phase (upper). The upper phase is generally regarded as glass transition temperature (T_g) of TPS materials. The upper transition for PS/CH/nanoclay, WH/CH/nanoclay, CS/CH/nanoclay and HACS/CH/nanoclay is 68.3°C, 78.9°C, 88.2°C and 83.5°C respectively in the order (PS/CH/nanoclay < WH/CH/nanoclay < HACS/CH/nanoclay < CS/CH/nanoclay). In case of CS/CH/nanoclay reinforced with nanoclay particles that attribute to highest T_g because of the restricted rotational motion in polymer matrix leads to decrease in distance between adjacent chains of polymer thereby reducing the free volume. Larger crystal domain with stronger strength is thus formed. On the other hand, lower glass transition temperature (T_g) of PS/CH/nanoclay, WH/CH/nanoclay and HACS/CH/nanoclay than CS/CH/nanoclay is due to their higher free volume resulting in higher molecular mobility. This is in conformity with the result obtained in case of moisture content as shown in **Figure 6.2.**

6.3.5. Fourier transform infrared (FTIR) spectra of starch-CH-nanoclay bionanocomposite films

ATR-FTIR spectroscopy is a very powerful tool for examining the interaction of the three components of starch, chitosan and nanoclay in composite films are shown in **Figure 6.9**. The broad peak in between 3600-3000 cm^{-1} is the stretching vibration of O–H and –NH due to the presence of chitosan (CH) film. The peak at 2919 cm^{-1} corresponds to the C–H stretching. The broad three characteristic peaks observed at 1640 cm^{-1} and 1580 cm^{-1} in pure chitosan film are due to the presence of a carbonyl group, C=O stretching vibrations (amide I) and NH bending (amide II) of pure chitosan film, respectively **Figure 6.9(a).** The peak located at 1408 and 1340 cm^{-1} was attributed to C-H in plane bending. The stretching vibration of C-O-C of polysaccharide skeleton at 1040-1066 cm^{-1} was observed **(Chai and Isa, 2013; Pinotti et al., 2007; Raucci et al., 2015)**. The Si-O and Al-OH stretching vibrations in CH/nanoclay were found at 1112 cm^{-1}, 911 cm^{-1} and 680 cm^{-1}, respectively **Figure 6.9(a).**

It is possible that starch mixed CH-nanoclay in composite films -NH_2, C=O and -OH groups of CH can be bonded to starch (-OH groups) and Si-O-Si from silicate and Al-OH deformation of aluminates present on the surface of nanoclay bounded through intermolecular hydrogen bonding. The band at 3345 cm^{-1} was shifted to 3365 cm^{-1} and 3350 cm^{-1} showing higher wavelength in turn proving the formation of intermolecular hydrogen bonding with chitosan. The peak for CS/CH/nanoclay and HACS/CH/nanoclay with high intensity and increased peak area improved its compatibility (**Figure 6.9 (d-e)).** However, -OH band was shifted to lower wavenumbers for PS/CH/nanoclay and WH/CH/nanoclay indicating weaker intermolecular interactions between starch and CH films **Figure 6.9 (b-c)**

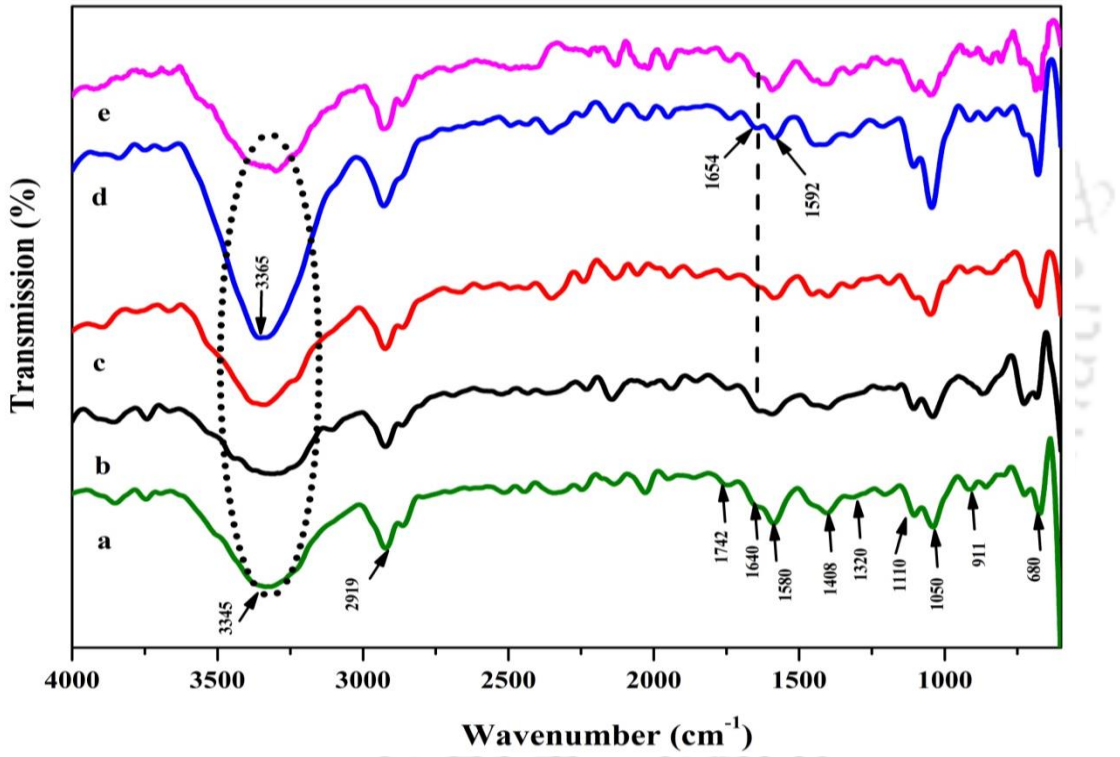

Figure 6.9. FTIR pattern of different amylose-amylopectin ratios of starch-CH-nanoclay bionanocomposite films: (a) CH/nanoclay (control), (b) PS/CH/nanoclay, (c) WH/CH/nanoclay, (d) CS/CH/nanoclay and (e) HACS/CH/nanoclay.

In the spectrum of bionanocomposite films, main peak related to the amino N-H bending peak of chitosan shifted from 1580 to 1592 cm^{-1} with the addition of (28% amylose) corn starch. The peak at 1580 cm^{-1} was shifted to higher wavenumber (1592 cm^{-}

^{1}). The small peak shifted from 1640 cm^{-1} to 1654 cm^{-1} is associated with C=O stretching (amide II) with high intensity for CS/CH/nanoclay among all other bionanocomposite films, suggesting strong intermolecular hydrogen bonding between -NH_2, C=O group of CH, and -OH group of CS **(Figure 6.9(d)).**

The enlarged view of selected peaks of –OH and -NH_2 –COOH were presented in **Figure 6.10.**

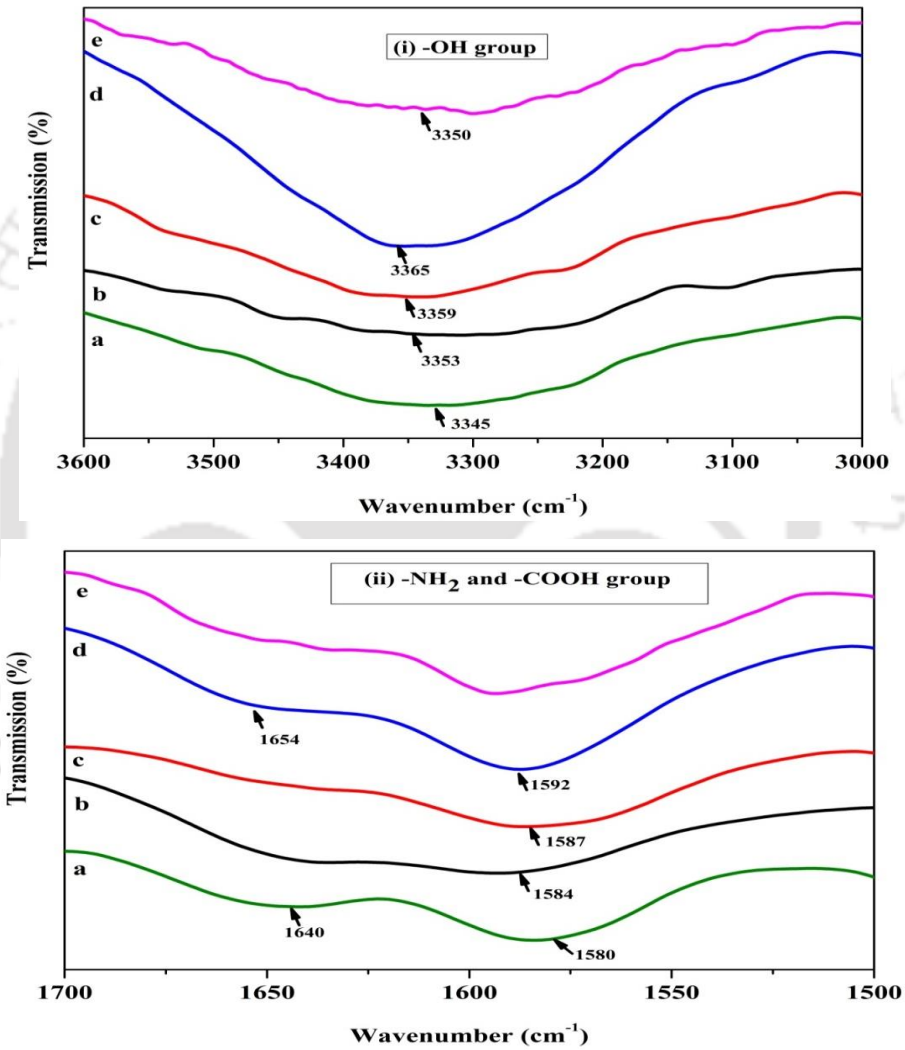

Figure 6.10. FTIR spectra (enlarged view) of selected peaks of (i) –OH group and (ii) –NH_2 and –COOH group in starch-CH-nanoclay bionanocomposite films: (a) CH/nanoclay (control), (b) PS/CH/nanoclay, (c) WH/CH/nanoclay, (d) CS/CH/nanoclay and (e) HACS/CH/nanoclay.

Peak intensity and area was increased in CS/CH/nanoclay related to silicate and aluminate layers of nanoclay (1110 cm^{-1}, 911 cm^{-1} and 680 cm^{-1}) compared with PS/CH/nanoclay, WH/CH/nanoclay and HACS/CH/nanoclay as shown in **Figure 6.9 (b-e).** It is due to a stronger intermolecular hydrogen bonding between CH and starch polymer chains it results in higher intercalation with nanoclay. This is confirmed with increased crystalline intensity in XRD pattern of CS/CH/nanoclay **Figure 6.1**. Similar hydrogen bonding was reported by **Ji et al. (2017)** between hydroxyl group of corn starch and amino group of chitosan in bionanocomposite films.

6.3.6. Thermal stability of starch-CH-nanoclay bionanocomposite films

TGA curve of different amylose-amylopectin ratio of starch-CH-nanoclay bionanocomposite films are show in **Figure 6.11.**

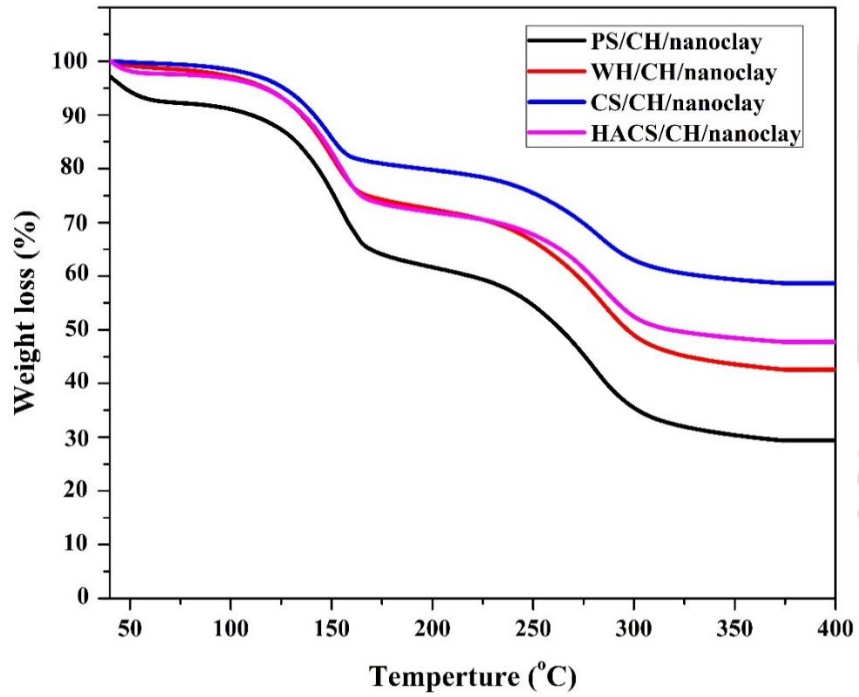

Figure 6.11. TGA curve of different amylose-amylopectin ratios of starch-CH-nanoclay bionanocomposite films.

TGA thermograms of the three stages exhibited a weight loss in all the films. The initial decomposition of film was observed around less than 100°C. The weight loss in the first stage was due to the evaporation or dehydration of free water and low molecular

weight in the films. The weight loss in the second stage (120–175°C) was due to evaporation of bound water and glycerol. Further weight loss in the third stage was observed around 300°C, which was due to the decomposition of complex polymer; depolymerisation and breaking of the functional group associated chain in polymeric films. After the final thermal degradation, the residual percentages at 400°C of the bionanocomposite films with different amylose PS/CH/nanoclay, CH/nanoclay, WH/CH/nanoclay, HACS/CH and CS/CH/nanoclay bionanocomposite film were 35, 45, 55, and 65%, respectively. These results indicate that among all the different films, CS/CH/nanoclay bionanocomposite film is thermally much stable while other films exhibit lower thermal resistance which could be ascribed to a weaker intermolecular hydrogen bonding.

6.3.7. Scanning electron microscopy (SEM) of starch-CH-nanoclay bionanocomposite films

Microstructure of the starch-CH-nanoclay bionanocomposite films was examined using SEM as shown in **Figure. 6.12 (a-d)**.

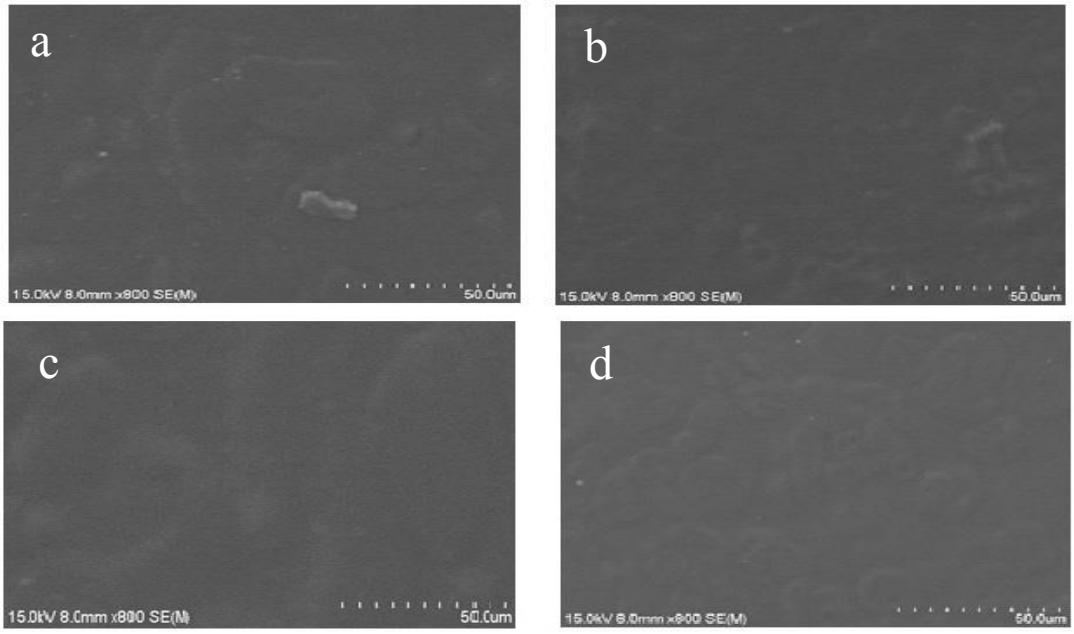

Figure 6.12. SEM images of starch-CH-nanoclay bionanocomposite films: (a) PS/CH/nanoclay, (b) WH/CH/nanoclay, (c) CS/CH/nanoclay and (d) HACS/CH/nanoclay.

Results exhibit that all the bionanocomposite film showed a slight rough surface without any phase separation **(Figure. 6.12 (a-d)).** These images revealed that the introduction of nanoclay improved the biopolymeric interaction in CS/CH/nanoclay than in PS/CH/nanoclay, WH/CH/nanoclay and HACS/CH/nanoclay. The micrograph of CS/CH films exhibit a homogenous surface due to its better miscibility as a result of interfacial adhesion between amylose of corn starch and CH which is due to extensive dispersion of nanoclay leading to strong intermolecular interactions in the polymer chain. Resulting CS/CH/nanoclay seems to be relatively more smooth (plain without any pores or cracks), continuous, compact and maintain good structural integrity due to its greater compatibility which is in accordance with XRD **Figure 6.1(d)** and FTIR pattern **Figure 6.9 (d)**. While in the case of PS/CH/nanoclay, WH/CH/nanoclay and HACS/CH/nanoclay impregranted with nanoclay bionanocomposite film absense of large agglomerates and smooth surfaces are observed as a result of lesser chance interactions thus forming a weak interaction and adhesion on the interface with filler and matrix **(Figure 6.12 (b,c and e)).**

6.3.8. Antifungal activity of starch-CH-nanoclay bionanocomposite films

CS/CH/nanoclay film was evaluated for antifungal activity by direct contact with bread slice sample. Uniform bread slice samples of size 2×2 cm were sealed in direct contact with CS/CH/nanoclay bionanocomposite films. Sample packed in low-density polyethylene (LDPE) serve as the control. All of the samples were stored at 25°C at 59% RH. Comparative study of bread sample packed by CS/CH/nanoclay bionanocomposite films and low density polyethylene (LDPE) films is shown in **Figure. 6.14**.

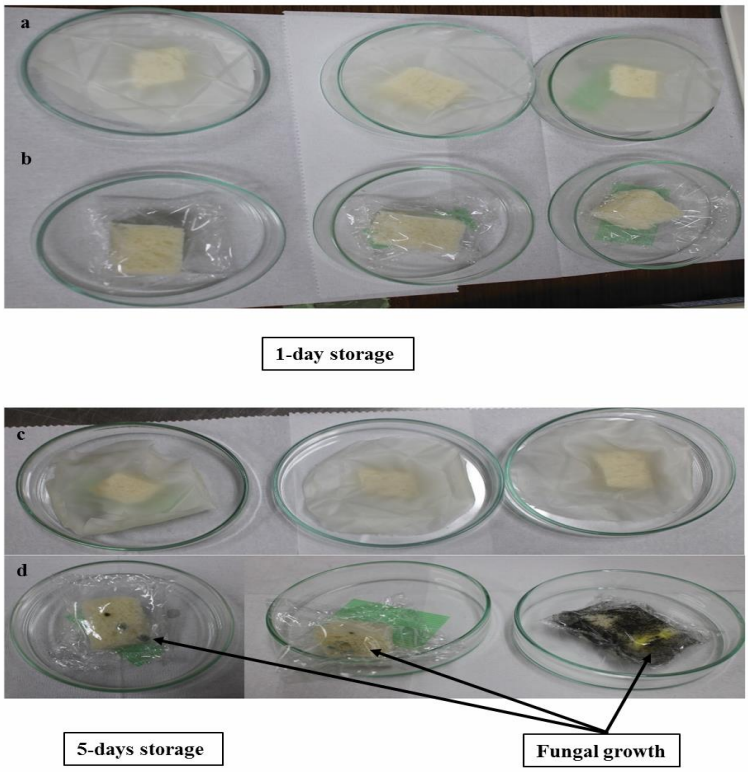

Figure 6.13 Comparison of bread quality (spoilage) sample packed in CS/CH/nanoclay bionanocomposite films with low density polyethylene films (control): (a) CS/CH/nanoclay on 1st day, (b) LDPE on 1st day, (c) CS/CH/nanoclay on 5th day and (d) LDPE on 5th day.

Because of impoved water barrier and better mechanical properties, the CS/CH/nanoclay bionanocomposite film was considered for bread packaging. The LDPE film served as control.The fungal growth was observed on the 5th day in samples **(Figure 6.13 (d))** that were packed with LDPE films. But, in the case of samples packed with CS/CH/nanoclay films, the fungal growth was inhibited until 20 days **(Figure 6.13 (c))**. The addition of nanoclay releases metal ions during its interaction with fungi and retards its growth exhibiting antifungal activity (**Malachova et al., 2011)**. Investigation showed that the presence of chitosan disrupt the membrane leading to the leak of cellular protein by binding its positively charged amino ($-NH_3^+$) group to negatively charged carboxylate (-COO-) group on the surface of microbial cell wall **(Ji et al., 2017).**

Also, it may be due to that the CS/CH/nanoclay films structure impove water barrier properties and thus delayed the proliferation of fungal growth. Thus, this bionanocomposite

film can find potential applications in active food packaging to impove the quality of food during storage therby extending the shelf life of products ensuring food safety.

6.3.9. Comparative study of starch blended with CH films with selected natural and synthetic films polymers

Properties like tensile strength, elongation at break and WVP of CS/CH/nanoclay bionanocomposite films were compared with selected natural and synthetic polymeric films **(Table 6.1)**.

Table 6.1. Tensile strength, elongation at break and water vapour permeability of various starches with CH and synthetic films.

Film type	Test condition	TS (MPa)	EB (%)	WVP (g/m s Pa)	Reference
HACS/CH/nanoclay CS/CH/nanoclay WH/CH/nanoclay PS/CH/nanoclay	25°C, 75% RH	10.76 13.33 8.13 6.86	66.87 59.82 79.69 86.8	2.25×10^{-10} 1.23×10^{-10} 3.10×10^{-10} 4.42×10^{-10}	**Present study**
CS	25°C, 75% RH	3.8-4.3	4.0-10.0	-	**Mali et al. (2006)**
CS/CH	25°C,75 % RH 25°C,95 % RH	3.2-6.3 1.0-3.5	58.0-122 25.0-100	$1.5\text{-}7.8\times10^{-10}$ $1.8\text{-}9.2\times10^{-10}$	**Ren et al. (2017)**
$CS/CH/CaCO_3$	25°C,75 % RH	2.04-10.7	78.7-134.3	$1.58\text{-}7.47\times10^{-10}$	**Ji et al. (2017)**
Low density polyethylene (LDPE)	38°C, 90% RH	7.6-17.3	500.0	9.25×10^{-11}	**Bourtoom and Chinnan (2008)**
High density polyethylene (HDPE)	38°C, 90% RH	17.3-34.6	300.0	2.31×10^{-13}	
Polyester	38°C, 90% RH	178.0	70.0-100.0	-	
Cellophane	38°C, 90% RH	-	-	8.41×10^{-11}	

The study involving CS/CH/nanoclay film revealed a higher tensile strength (13.3 MPa), lower elongation at break (less deformable) and a low WVP (1.23×10^{-10}) when compared to PS/CH/nanoclay, WH/CH/nanoclay and HACS/CH/nanoclay. The tensile strength of CS/CH/nanoclay film was higher than CS, CS/CH and CS/CH/$CaCO_3$. Elongation at break was higher for CS/CH/nanoclay film than CS and CS/CH while it was lower than CS/CH/$CaCO_3$**(Ji et al., 2017; Mali et al., 2006; Ren et al., 2017).** The WVP of CS/CH/nanoclay films was lower than CS, CS/CH, CS/CH/$CaCO_3$ which is slightly lower than synthetic polymer cellophane films **(Bourtoom and Chinnan, 2008)**. The high WVP of CS/CH/nanoclay films compared with LDPE and HDPE is explained by the inherent hydrophilicity of CS, and CH.

6.4. Summary

Effect of varying amylose-amylopectin ratios on mechanical properties (tensile strength and elongation at break), water barrier properties, thermal properties and glass transition temperature was studied. The present study revealed that amylose-amylopectin ratio of CS (28:72) based films demonstrated a higher tensile strength, lower WVP, higher T_g and higher thermal stability. XRD study revealed the crystallinity to be higher for CS/CH/nanoclay bionanocomposite films due to the formation of strong intermolecular hydrogen bond between CS and CH reinforced with nanoclay which was confirmed by FTIR results. The SEM study revealed that the bionanocomposite films containing CS had uniform surfaces than other films. The prepared starch based bionanocomposite films showed heat-sealing properties. The prepared CS/CH/nanoclay bionanocomposite films exhibit antifungal activity in a stored bread sample at 25°C, 59% RH for 20 days. These results show that the prepared films could potentially be used in food packaging industry to extend the shelf life; maintain its quality and ensure safety to perishable food products providing an alternative option for conventional plastic.

भारतीय प्रौद्योगिकी संस्थान गुवाहाटी
Indian Institute of Technology Guwahati

Chapter 7

Preparation and characterization of corn starch-chitosan-nanoclay bionanocomposite films with different plasticizers and antifungal agents

This chapter was aimed to examine the influence of plasticizer (glycerol (GLY)/ sorbitol (SOR)) and antifungal (potassium sorbate (KS)/grapefruit seed extract (GFSE)) agent on water barrier, mechanical and thermal properties of prepared corn starch (CS)-chitosan (CH)-nanoclay (Na-MMT) bionanocomposite films.

7.1. Specific Background

Nowadays, petrochemical-based plastic utilization is increasing rapidly in the food industry. The increased usage of petrochemical-based plastic as a packaging material leads to serious environmental problems **(Aider, 2010; Ezeoha and Ezenwanne, 2013)**. The substitute for this problem is to increase the usage of biodegradable based packaging material that decomposes or breaks down in a short period during compositing. Biodegradable materials mixed with the soil is degraded by microbes and bacteria adding up to soil fertility. Nowadays, utilization of active packaging is increasing rapidly in the food industry. Active packaging is used to increase the shelf life or sensory properties of food and improves safety while maintaining the quality of food through active compounds in packaging materials. The active packaging materials have received more attention in recent years due to its capability to prevent food spoilage by inhibiting the growth of pathogenic microorganism in the food (**Ren et al., 2017**). Hence, the demand for active packaging is increased and it drives the growth of food industry into the worldwide market.

Starch is the most promising biodegradable as well as biocompatible material than any other natural polymers that have received attention due to its wide availability, renewability, film-forming ability, non-toxic, low cost and lastly it acts as a source of income for the agricultural sector. However, the applications of starch films are limited due

to its strong hydrophilic behaviour, which makes the film to absorb high moisture and lowers the mechanical properties **(Abreu et al., 2015; Borges et al., 2015; Souza et al., 2012)**.

Chitosan has an unique property in food protection due to its inherent anti-bacterial and anti-fungal properties against food spoilage microorganisms **(Tan et al., 2015)**.

The native starches are brittle thereby posing a problem for the processing sector. Plasticizer can be used to overcome the brittleness of starch, improve the flexibility and workability of polymers. Plasticizers are normally small size of molecules like glycerol and sorbitol that intersperse between polymer chains, break hydrogen bonding and increase the mobility of the polymer chains while enhancing the flexibility (**Kuorwel et al., 2011)**. The characteristics of starch-based films depend upon the concentration of plasticizer and its acceptable relative humidity for storage. When concentration of plasticizer increases, the water vapor permeability increases and tensile strength and glass transition temperature of films decreases **(Talja et al., 2007)**. Similarly, the type of plasticizer also affects the mechanical properties of starch based films (**Lagos et al., 2015**).

Potassium sorbates (KS) and sorbic acid are categorized in as a GRAS additive and are more effective against yeast, most of the bacterial and mold species. During storage conditions, potassium salts are unstable in aqueous solution and undergo an oxidative degradation or can be metabolized by microorganisms. Edible films incorporated with sorbates reduce the surface contamination of microbes by inhibiting or delaying the growth of microorganisms (**Barzegar et al., 2014; Durango et al., 2006)**.

Grapefruit seed extract (GFSE) is a natural active agent used in food packaging materials due to its powerful anti-microbial and antifungal activity **(Choi et al., 2014)**.

In this chapter, the effect of different types of plasticizers (glycerol (GLY) and sorbitol (SOR)) and antifungal agents (potassium sorbate (KS) and grapefruit seed extract (GFSE)) is studied by adding them into corn starch (CS) blended with chitosan (CH) and nanoclay (Na-MMT) bionanocomposite films. The prepared films estimate its crystallinity, water barrier, mechanical, thermal and morphological properties. The films were also studied for its biodegradability in soil as well as by microbial degradation.

7.2. Preparation of plasticizers and antifungal agents in corn starch-chitosan-nanoclay bionanocomposite films

The film forming solution containing corn starch with chitosan was added with glycerol/sorbitol and potassium sorbate/grapefruit seed extract. Finally, the nanoclay (Na-MMT) was added into the film forming solution to produce bionanocomposite films **(Chapter 3, Section 3.2.7 and 3.2.8)**. The uniform thickness of 0.07 mm bionanocomposite films was prepared.

7.3. Results and Discussion

7.3.1. X-ray diffractogram of bionanocomposite films

The XRD patterns of CS/CH/nanoclay (control), CS/CH/nanoclay/GLY/KS, CS/CH/nanoclay/SOR/KS, CS/CH/nanoclay/GLY/GFSE and CS/CH/nanoclay /SOR/GFSE bionanocomposite films are shown in **Figure. 7.1**.

Native CS showed A-type diffraction peaks around 15°, 17°, 18° and 23° **(Sun et al., 2014b)**. CH film sample without plasticizer showed broad amorphous peak at 2θ = 20.3º. Furthermore, the main peak was observed around 20º in all films due to formation of van der Waals forces in polymers **(Aytunga et al., 2014)**. The diffraction pattern of starch disappeared in all the films due to the gelatinization process which is capable of destructing the crystalline starch granule **(Zhang et al., 2007)**. It indicates that the blend of all CS/CH/nanoclay was completely miscible among them. The CS/CH/nanoclay (control film) without plasticizer and antimicrobial agents showed a peak at 2θ = 19.5º **(Figure 7.1a)**. In the case of GLY blended film, highest peak was observed at 2θ = 19.5º, which is similar to control film **(Figure 7.1b,d)**. But, the peak is slightly shifted by 20º for sorbitol incorporated starch-chitosan-nanoclay films **(Figure 7.1c,e)** compared with control and glycerol blend films. This slight peak shifting is due to glycerol which creates more free space in polymeric chains.

The broad peak intensity increases in the order of CS/CH/nanoclay/SOR/GFSE > CS/CH/nanoclay/SOR/KS > CS/CH/nanoclay/GLY/GFSE > CS/CH/nanoclay/GLY/KS > CS/CH/nanoclay. The CS/CH/nanoclay/SOR incorporated with KS or GFSE showed a higher degree of crystallinity **(Figure 7.1c,e)**. This could be attributed to higher

intermolecular hydrogen bonding of KS or GFSE with CS/CH/nanoclay as confirmed in FTIR analysis.

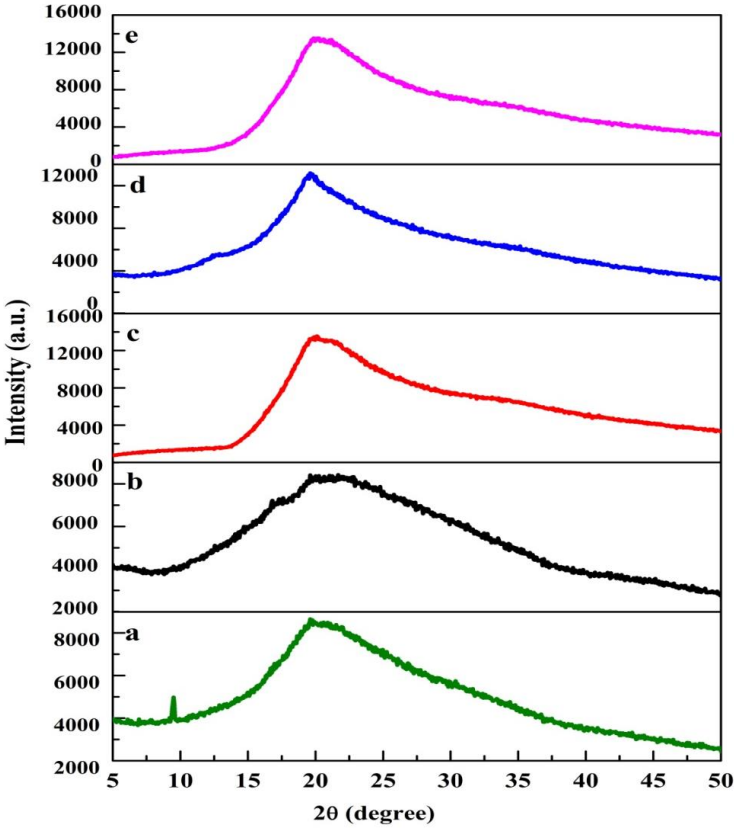

Figure 7.1. XRD patterns of starch-chitosan-nanoclay bionanocomposite film: (a) CS/CH/nanoclay (control), (b) CS/CH/nanoclay/GLY/KS, (c) CS/CH/nanoclay/SOR/KS, (d) CS/CH/nanoclay/GLY/GFSE and (e) CS/CH/nanoclay/SOR/GFSE.

CS/CH/nanoclay/SOR/GFSE bionanocomposite film's XRD portrayed the highest peak intensity due to intercalation of GFSE with either CH or starch polymer chains or both CH and starch polymer chains via silicate layers. In XRD patterns, no peak around 7.21° (2θ) was observed for Na-MMT **(Hoidy et al., 2009)** for all bionanocomposite films. It may be due to extensive intercalation of polymer chains inside the Na-MMT galleries. It is known that crystallinity is related to moisture content present in the film **(Nair et al., 2017**). Mechanical properties such as tensile strength, toughness and the resistance against moisture adsorption are directly related to crystallinity **(Aytunga et al., 2014**). Similar

trend in variation of crystalline intensity was also observed for two different types of plasticizer incorporated in the starch films **(Edhirej et al., 2017)**.

7.3.2. Water barrier properties of films

The water barrier properties of the films such as moisture content, solubility and water vapor permeability (WVP) are shown in **Figures 7.2, 7.3 and 7.4.** The moisture content of CS/CH/nanoclay, CS/CH/nanoclay/GLY/KS, CS/CH/nanoclay/SOR/KS, CS/CH/nanoclay/GLY/GFSE and CS/CH/nanoclay/SOR/GFSE is presented in **Figure 7.2**.

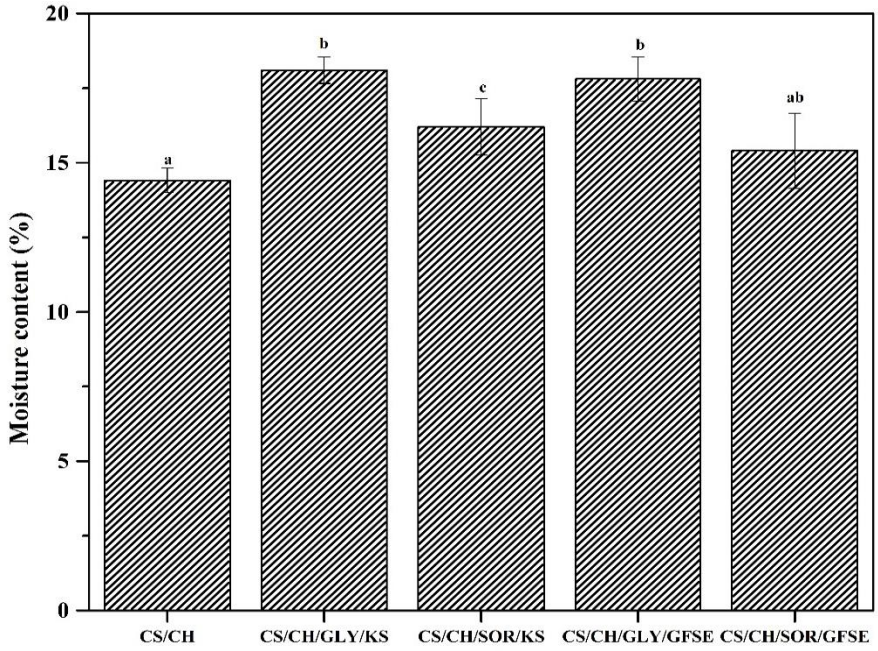

Figure 7.2. Influence of different types of plasticizer and antimicrobial agents on moisture content of starch-chitosan-nanoclay bionanocomposite films. $^{a-c}$Different letters represent a significant difference using Tukey test ($p < 0.05$).

The moisture content of starch-based films does not depend only on the relative humidity of environment, but also on the chemical structure such as ratio of amylose-amylopectin and branching point which further guides the molecular architecture of starch granule **(Bertoft and Blennow, 2009; Mua and Jackson, 1997).** It was observed that control films CS/CH/nanoclay showed lowest moisture content (14.44%) due to the absence of plasticizer. Whereas higher moisture content was observed for CS/CH/nanoclay/GLY/KS (18.1%) and CS/CH/nanoclay/GLY/GFSE (17.8%) due to

glycerol which is more hydrophilic as well as smaller in size compared to sorbitol. CS/CH/nanoclay/SOR/KS (16.2%) and CS/CH/nanoclay/SOR/GFSE (15.4%) films showed lower moisture content. It may be attributed to high molecular structure of glucose units in sorbitol, causing stronger intermolecular interactions among polymer chains. The strong intermolecular interaction affects the chemical structure and molecular space in the network resulting in reduction of moisture adsorption. The lower hydrophilic property of CS/CH/nanoclay/SOR/GFSE bionanocomposite film is matched with XRD pattern and moisture content.

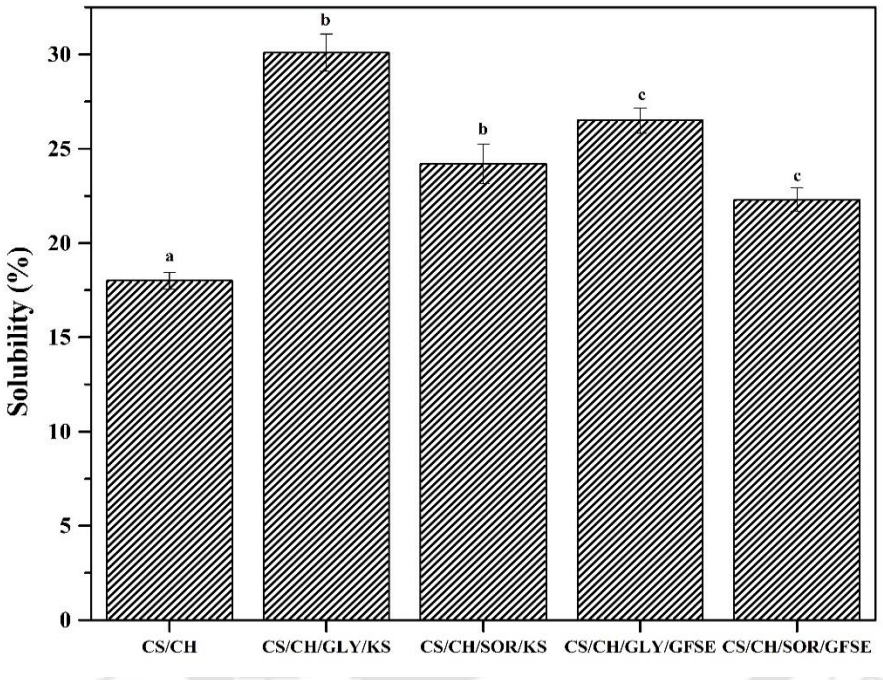

Figure 7.3. Influence of different types of plasticizer and antimicrobial agents on solubility of starch-chitosan-nanoclay bionanocomposite films. [a-c]Different letters represent a significant difference using Tukey test ($p < 0.05$).

The solubility of biodegradable films plays a vital role in food packaging applications. Lower solubility maintains the product integrity and shelf life of food **(Nair et al., 2017)**. Generally, higher solubility indicates lower water resistance. Films prepared with glycerol and sorbitol exhibited a higher solubility in water than unplasticized (CS/CH/nanoclay) films. As shown in **Figure 7.3**, it was observed that the solubility of CS/CH/nanoclay/GLY/KS (30.1%) and CS/CH/ nanoclay/GLY/GFSE (26.5%) was higher

than CS/CH/nanoclay (18.1%) in water. Glycerol showed a higher solubility than sorbitol, because it is more hygroscopic and thus increases the solubility. The solubility of CS/CH/nanoclay/SOR/KS (24.2%) and CS/CH/nanoclay/SOR/GFSE (22.3%) was lower than CS/CH/nanoclay/GLY/KS (30.1%) and CS/CH/nanoclay/GLY/GFSE (26.5%) in water. The strong intermolecular interaction between polymers resulted in enhanced cohesiveness and lowers swelling of the films. This is in accordance with results observed in moisture content and FTIR analysis.

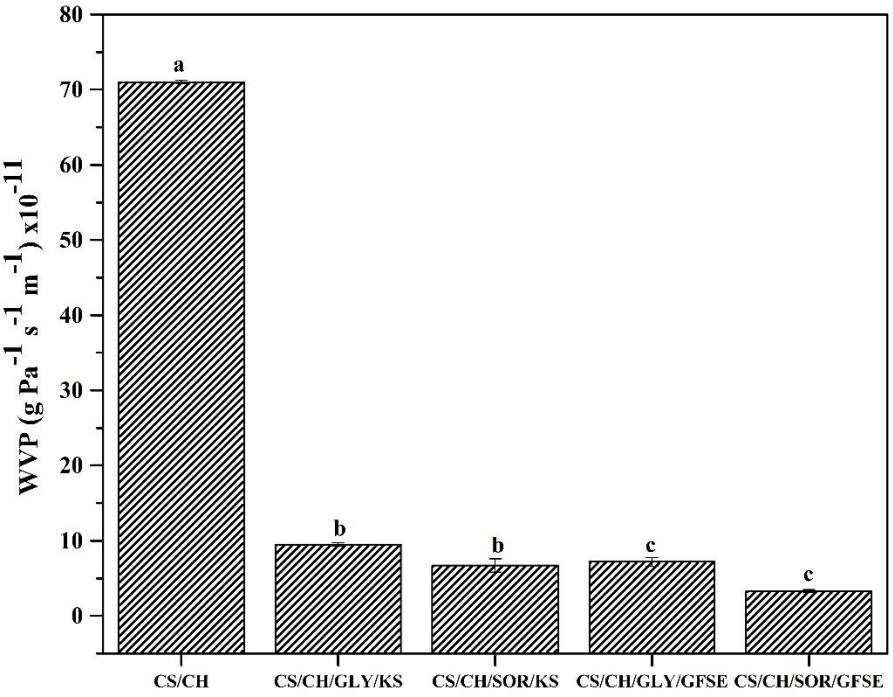

Figure 7.4. Influence of different types of plasticizer and antimicrobial agents on water vapor permeability of starch-chitosan-nanoclay bionanocomposite films. [a-c]Different letters represent a significant difference using Tukey test ($p < 0.05$).

The water vapor permeability (WVP) of films is an essential property for food packaging applications. The WVP plays a crucial role to determine the shelf-life of the products. The water is important in deteriorative reactions in foods and moisture transfer from surrounding atmosphere to food should be low as possible to prevent food spoilage. This WVP property depends on the film structure, type of plasticizer, relative humidity and temperature of the surrounding atmosphere. In the case of starch based films, WVP property also depends on hydrophilic-hydrophobic ratio, crystalline to amorphous ratio and

mobility of polymeric chains. Our results revealed that the WVP is in the order of CS/CH/nanoclay (control) > CS/CH/nanoclay/GLY/KS > CS/CH/nanoclay/GLY/GFSE > CS/CH/nanoclay/SOR/KS > CS/CH/nanoclay/SOR/GFSE **(Figure 7.4)**. The highest WVP was found for CS/CH/nanoclay (71×10^{-11} g Pa^{-1} s^{-1} m^{-1}). It may be due to the absence of plasticizer that made the film to be more brittle with a high porous nature.

The WVP for GLY bionanocomposite films of CS/CH/nanoclay/GLY/KS and CS/CH/nanoclay/GLY/GFSE was 9.5×10^{-11} and 7.2×10^{-11} g Pa^{-1} s^{-1} m^{-1}, respectively. The WVP for SOR bionanocomposite films of CS/CH/nanoclay/SOR/GFSE and CS/CH/nanoclay/SOR/KS was 3.3×10^{-11}g Pa^{-1} s^{-1} m^{-1} and 6.2×10^{-11} g Pa^{-1} s^{-1} m^{-1}, respectively **(Figure 7.4)**. It was observed that the WVP of GLY bionanocomposite films was higher than SOR based films. This is due to the hydrophilic nature of glycerol that induces favourable sorption of water molecules. The lowest WVP of CS/CH/nanoclay/SOR/GFSE films might be attributed due to strong interaction of intermolecular hydrogen bonding between SOR and GFSE results in more compact structure. This strong interaction reduces the molecular space for water to enter the networks. The similar observation was found in previous literature that the water barrier property of sorbitol blend starch films was lower than glycerol-based films (**Sanyang et al., 2015)**. The WVP results are in accordance with higher crystallinity of CS/CH/SOR/GFSE than other bionanocomposite films as shown in **Figure 7.1**.

7.3.3. Mechanical properties

Mechanical properties such as tensile strength (TS) and elongation at break (EB) should be optimum to maintain the film's integrity and barrier property during shipping, handling and storage of the food products. The tensile strength of starch-chitosan-nanoclay bionanocomposite films was affected by different types of plasticizer and antimicrobial agents as shown in **Figure 7.5**. The tensile strength of CS/CH/nanoclay, CS/CH/nanoclay/GLY/KS, CS/CH/nanoclay/SOR/KS, CS/CH/nanoclay/GLY/GFSE and CS/CH/nanoclay/SOR/GFSE were found to be 28.5, 12.7, 18.7, 16.3 and 19.2 MPa, respectively **(Figure 7.5)**.

Sorbitol based films showed more resistant to breakage than glycerol based films. It is due to the large molar mass of sorbitol (182 g/mol) that makes stronger intermolecular

hydrogen bond storage during gelatinization process between –OH group of CS and –OH and amino ($–NH_2$) functional groups at the backbone of CH in the presence of reinforced nanoclay.

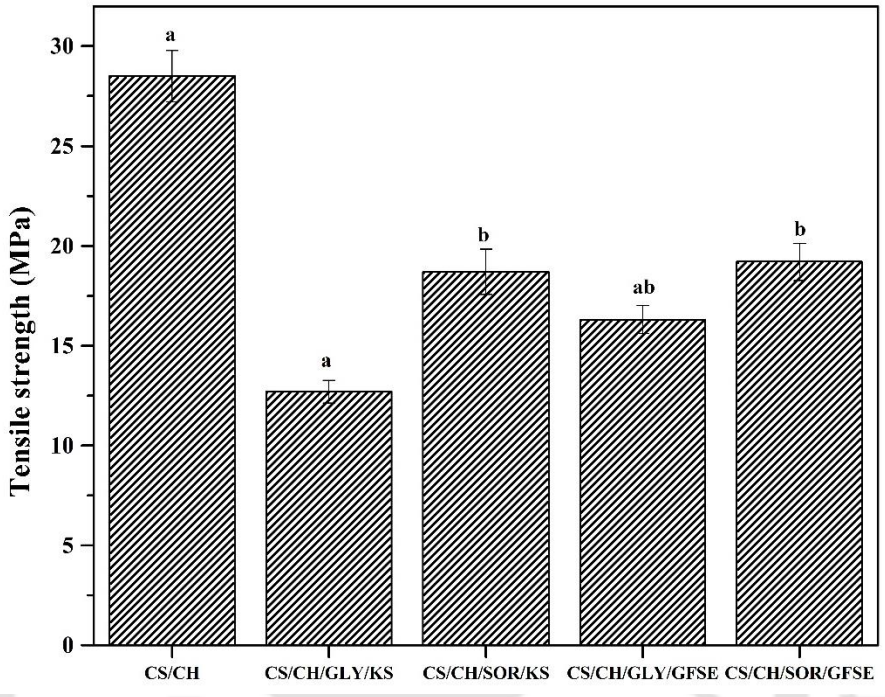

Figure 7.5. Tensile strength of starch-chitosan-nanoclay bionanocomposite films with different types of plasticizer and antimicrobial agents. [a-b]Different letters represent a significant difference using Tukey test ($p < 0.05$).

According to XRD results, SOR incorporated bionanocomposite films exhibited higher degree of crystallinity (**Figure 7.1 c,e)** and higher water barrier properties (**Figure 7.4)** than GLY based films. The influence of plasticizers such as sorbitol and glycerol on the tensile strength of the sugar palm starch/soy-based blend films was studied and found that sorbitol-plasticized films showed a higher tensile strength than glycerol-plasticized films **(Sanyang et al., 2015; Tummala et al., 2006)**.

Figure 7.6 shows the effect of different types of plasticizer and antimicrobial agents on elongation at break (EB) of starch-chitosan-nanoclay bionanocomposite films. The parameter EB (%) is used to determine the flexibility and stretchability of films. The EB of control film (CS/CH/nanoclay) was found to be 8.6%. The control film exhibited poor EB (%) due to the absence of plasticizing agent.

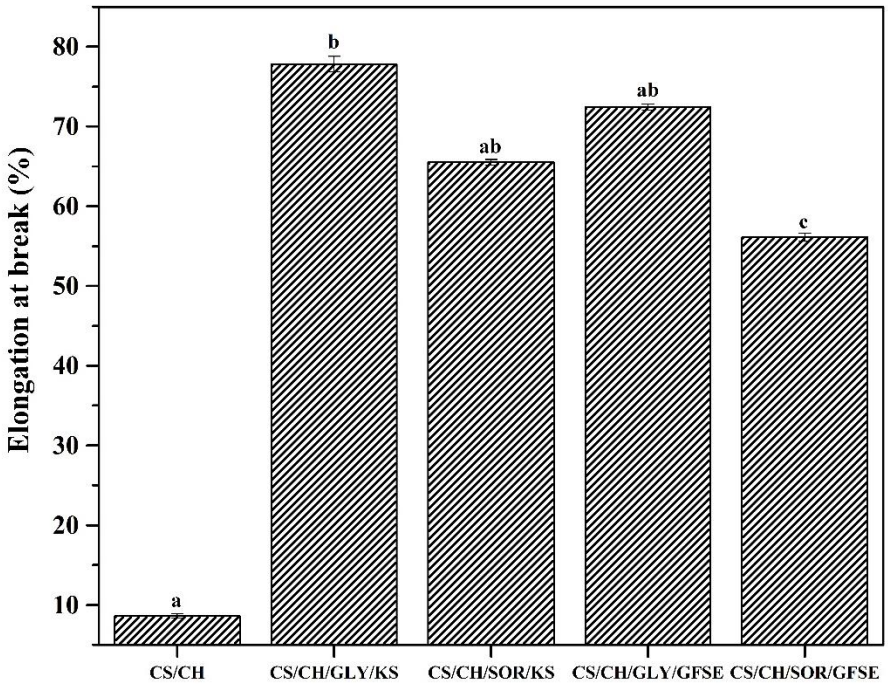

Figure 7.6. Elongation at break of starch-chitosan-nanoclay bionanocomposite films with different types of plasticizer and antimicrobial agents. [a-c]Different letters represent a significant difference using Tukey test ($p < 0.05$).

In general, tensile strength and elongation at break were inversely correlated. The SOR based bionanocomposite films such as CS/CH/nanoclay/SOR/GFSE and CS/CH/nanoclay/SOR/KS showed low EB compared with GLY based films. The EB of CS/CH/nanoclay/GLY/KS and CS/CH/nanoclay/GLY/GFSE bionanocomposite films was found to be 77.8% and 72.4%. A higher EB (%) was observed for GLY based films because of its high moisture content, less crystallinity and tensile strength. It was found that the EB (%) of bionanocomposite films is inversely correlated to the tensile strength. The high tensile strength and low EB (%) of CS/CH/nanoclay/SOR/GFSE is in accordance with its high crystallinity, low moisture content and high water barrier properties.

7.3.4. Dynamic mechanical thermal properties

The dynamic mechanical thermal properties of bionanocomposite films such as storage modulus and tan delta are shown in **Figures 7. 7 and 7.8**.

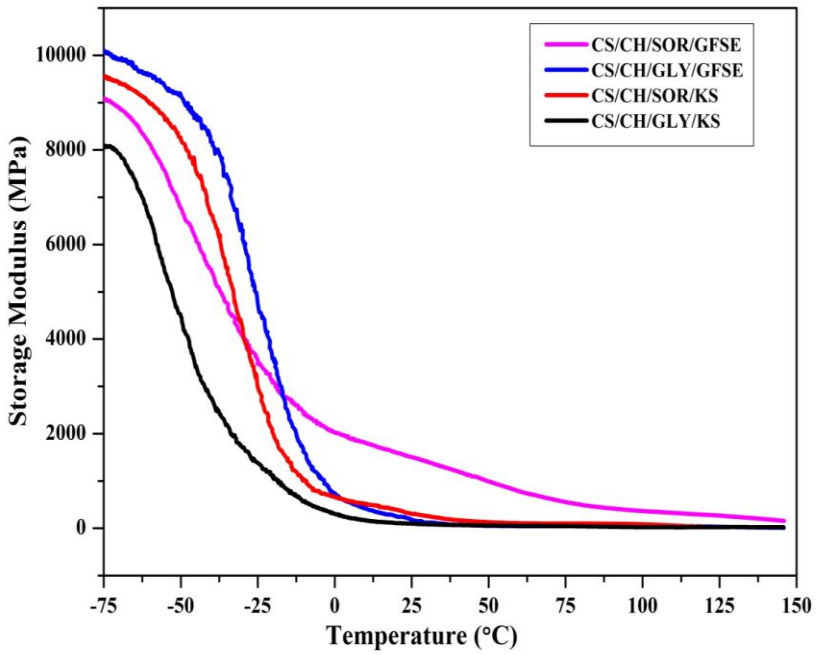

Figure 7.7. Influence of different types of plasticizer and antimicrobial agents on storage modulus of starch-chitosan-nanoclay bionanocomposite films.

The storage modulus of CS/CH/nanoclay/SOR/GFSE bionanocomposite film was higher compared to CS/CH/nanoclay/GLY/KS, CS/CH/nanoclay/SOR/KS and CS/CH/nanoclay/GLY/GFSE bionanocomposite films **(Figure 7.8)**. The higher storage modulus is due to interaction between CS and CH/GFSE in the presence of nanoclay. Also, it can be attributed to reduced mobility of biopolymer chains in films. It is known that storage modulus is related to the stiffness. The stiffness of a film increases with increase in storage modulus. The enhancement of stiffness in CS/CH/nanoclay/SOR/GFSE was observed due to strong interface of the polymer chains, which increases its storage modulus and resulting in higher glass transition temperature (T_g).

The loss factor (tan delta) is the ratio of loss modulus to storage modulus and expressed as a dimensionless number. The curve of loss factor (tan delta) is as a function of temperature for different plasticizers (GLY/SOR) and antimicrobial agents (KS/GFSE) incorporated in corn starch with CH, and nanoclay films are shown in **Figure 7.8**.

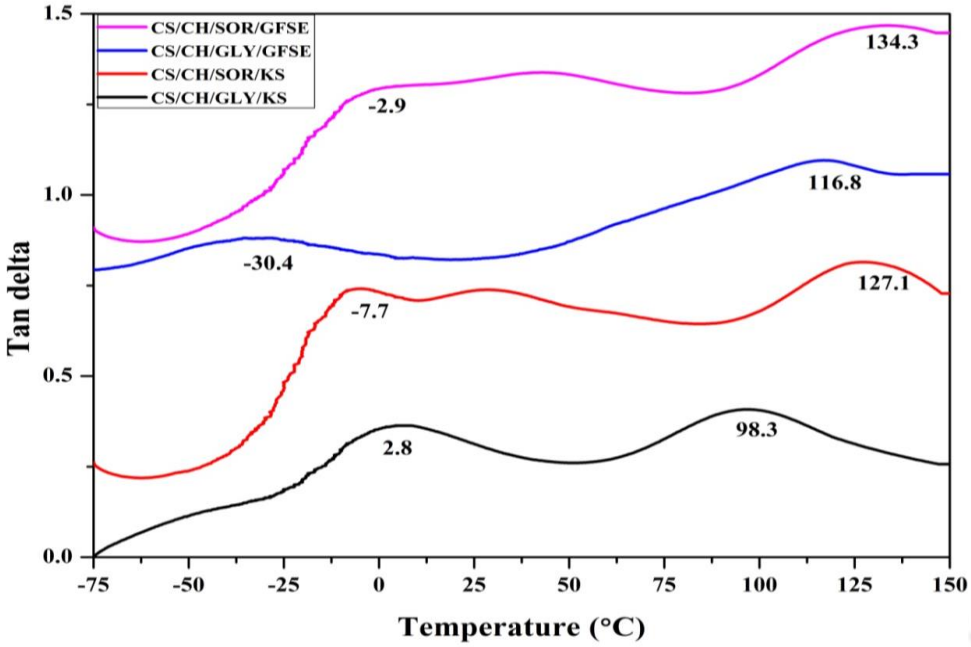

Figure 7.8. Influence of different types of plasticizer and antimicrobial agents on tan delta of starch-chitosan-nanoclay bionanocomposite films.

The loss factor was sensitive to molecular motions and its peak values were related to T_g. Generally, brittleness of starch based films increases when the films have high (T_g). The curve of thermoplastic starch (TPS) revealed two thermal transitions (T_g) for all different starch sources due to two separate phases such as starch-rich phase (upper) and starch-poor phase (lower). Starch-rich phase is generally regarded as T_g of TPS materials. The upper thermal transitions were found to be 98°C, 127°C, 116°C, 134°C for CS/CH/nanoclay/GLY/KS, CS/CH/nanoclay/SOR/KS, CS/CH/nanoclay/GLY/GFSE and CS/CH/nanoclay/SOR/GFSE, respectively. The order of glass transition is CS/CH/nanoclay/GLY/KS < CS/CH/nanoclay/GLY/GFSE < CS/CH/nanoclay/SOR/KS < CS/CH/nanoclay/SOR/GFSE. In the case of CS/CH/SOR/GFSE, highest T_g was observed due to restraining molecular motion within the chain of biopolymers in the presence of nanoclay. The presence of larger crystal domain in CS/CH/nanoclay/SOR/GFSE reduces the chain mobility and free volume, resulting in rising of T_g. The high moisture content increases chain mobility and decreases T_g. The T_g value was lower for CS/CH/nanoclay/GLY/KS, CS/CH/nanoclay/GLY/GFSE and CS/CH/nanoclay/SOR/KS, than CS/CH/SOR/GFSE because of high moisture content. Similar results were found in a

previous study that the higher the moisture content lowers T_g in tapioca starch films (**Chang et al., 2006)**. According to the recent studies by **Chiumarelli and Hubinger (2014) and Sanyang et al. (2015),** sorbitol containing films exhibited higher T_g values compared to glycerol containing films. The present study also reveals that the SOR based films showed higher T_g than GLY based films.

7.3.5. Thermal stability of bionanocomposite films (TGA)

TGA curves of starch-chitosan-nanoclay bionanocomposite films containing different types of plasticizer (GLY/SOR) and antimicrobial agents (KS/GFSE) are shown in **Figure 7.9**. Three stages of weight loss were observed in all the films.

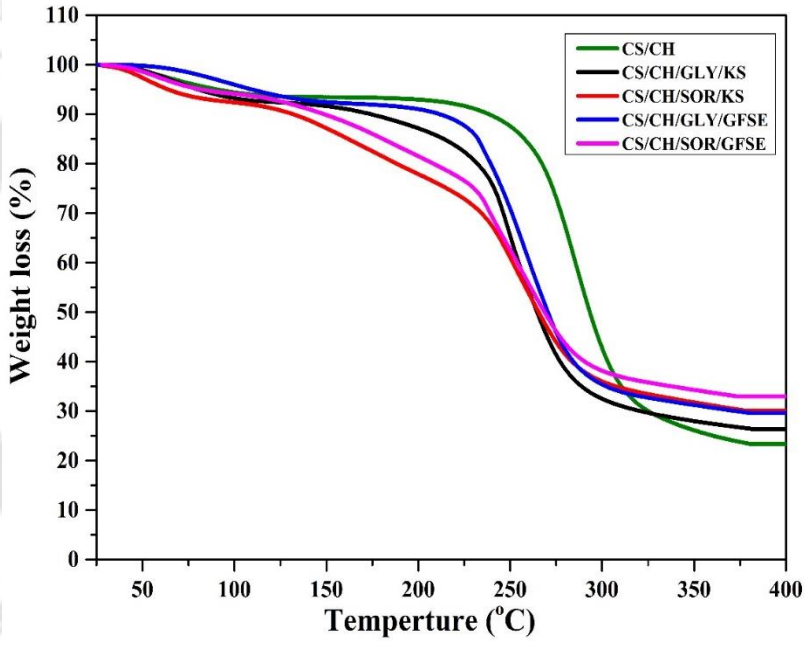

Figure 7.9. TGA curve of starch-chitosan-nanoclay bionanocomposite films with different plasticizers and antimicrobial agents.

In the first stage, desorption of water was observed at less than 100°C. The mass loss at this stage can be associated with the evaporation or dehydration of loosely bound water and low molecular weight compounds in the films. Removal of bound water and glycerol evaporation was observed in the second stage between 200 to 300°C. In the third stage, polymers decomposed in between 350 and 400°C. The residual mass was found to be 23%, 26%, 30%, 29%, and 33% for CS/CH/nanoclay, CS/CH/nanoclay/GLY/KS,

CS/CH/nanoclay/SOR/KS, CS/CH/nanoclay/GLY/GFSE and CS/CH/nanoclay/SOR/GFSE, respectively. These results indicate that CS/CH/nanoclay/SOR/GFSE film is more thermally stable than other films. The higher thermal stability can be attributed to the strong hydrogen bond between two polymers and higher crystallinity of CS/CH/nanoclay/SOR/GFSE films. It was reported that sorbitol mixed with sugar palm starch and soy protein biodegradable film exhibited the highest thermal stability than glycerol blend films **(Sanyang et al., 2015; Tummala et al., 2006)**.

7.3.6. Fourier transform infrared (FTIR) analysis of bionanocomposite films

Figure 7.10 shows the FTIR spectra of starch-chitosan-nanoclay bionanocomposite films containing different types of plasticizer (GLY/SOR) and antimicrobial agents (KS/GFSE).

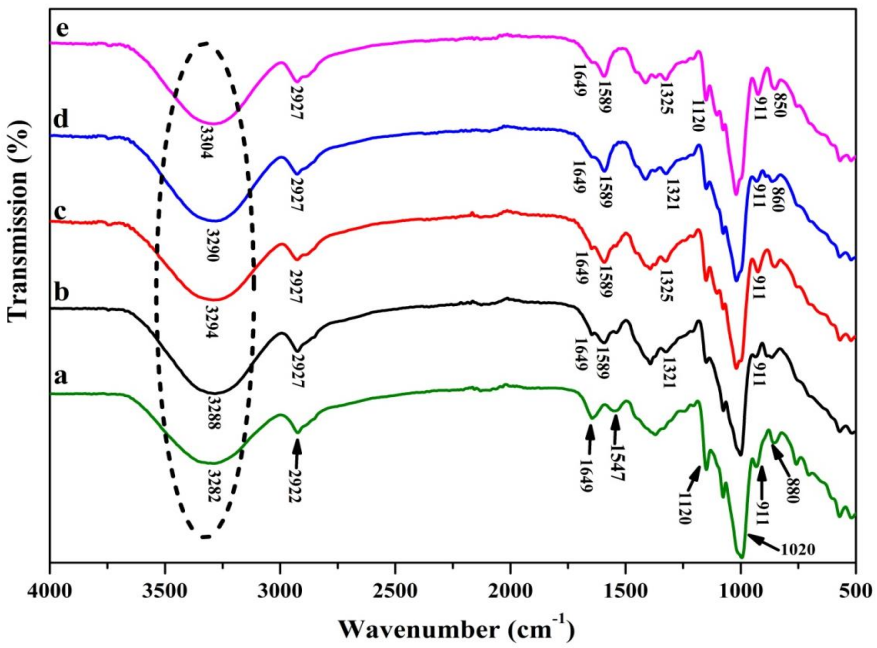

Figure 7.10. FTIR patterns of starch-chitosan-nanoclay bionanocomposite films with various types of plasticizer and antimicrobial agents: (a) CS/CH/nanoclay, (b) CS/CH/nanoclay/GLY/KS, (c) CS/CH/nanoclay/SOR/KS, (d) CS/CH/nanoclay/GLY/GFSE and (e) CS/CH/nanoclay/SOR/GFSE.

The stretching vibrations of Si-O and Al-OH from nanoclay was found at 1120 cm^{-1} and 911 cm^{-1}, respectively. **(Figure 7.10 (a))**. No peak was observed at 1310–1330 cm^{-1}

for CS/CH/nanoclay films because of the absence of plasticizer **(Figure 7.10 (a))**. But, all the CS/CH incorporated with glycerol and sorbitol based films showed a shoulder peak at 1310–1330 cm^{-1} due to stretching of CH_2 group from plasticizers **(Figure 7.10 (b-e))**. It was observed that the peak intensity of CH_2 stretching group was shifted to higher wavenumber in case of sorbitol incorporated films (**Figure 7.10 (c-e))** due to strong interaction. Starch-chitosan-nanoclay films incorporated with KS/GFSE showed a distinct peak at 1587 cm^{-1} due to asymmetrical stretching vibration of –COO **(Flores et al., 2007)**. The intense peak at 1587 cm^{-1} was observed for SOR based films than GLY based films. It may be attributed to strong hydrogen bonding of starch-chitosan and sorbates **(Figure 7.10 (c-e))**. In the pure GFSE spectra, there is a main peak at 890 cm^{-1} corresponding to C–H stretching, which is characteristic of aromatic compounds **(Bof et al., 2016)**. The –OH band and C-H stretching band of CS/CH/nanoclay/SOR/GFSE was shifted to 3304 cm^{-1} and 850 cm^{-1} indicating strong intermolecular interactions among –OH group of aromatic/phenolic compounds of GFSE, —NH_2, C=O group of CH and –OH group of CS compared with CS/CH/GLY/GFSE **(Figure 7.10 (d-e)).** Sharp peak intensity of silicate and aluminate layers of nanoclay at 1120 cm^{-1}, 911 cm^{-1} were higher for CS/CH/nanoclay/SOR/GFSE films when compared to other bionanocomposite films **(Figure 7.10 (b-e)).** This is in accordance with increased crystalline intensity for CS/CH/nanoclay/SOR/GFSE nanoclay films in XRD pattern **(Figure 7.1)**. The strong intermolecular interactions observed for CS/CH/nanoclay/SOR/GFSE matched with results of water barrier properties (**Figure 7.4)**, mechanical properties (**Figures 7.5 and 7.7)** and thermal properties (**Figures 7.8 and 7.9)**.

7.3.7. Microbial degradation of bionanocomposite films

The bionanocomposite film degradation was investigated by microorganisms (**Chapter 3, Section 3.3.14**). The extracellular enzymes of microorganisms play a key role in biodegradation process of polymers **(Pathak and Kumar, 2017**). The biodegradability of bio-based materials is the most important factor that depends on the chemical structure, hydrophilicity, reactivity and swelling behaviour of polymeric chains. Other important factors are physical and physico-mechanical properties such as crystallinity, molecular weight, porosity, elasticity and morphology (**Leja and Lewandowicz, 2010**). Starch-

chitosan-nanoclay bionanocomposite film was incubated in a mineral salts medium with *Rhodococcus opacus* for 3 days. The turbidity in the medium reveals the growth of microbes (**Figure 7.11)**. The weight loss (%) of bionanocomposite films and synthetic films after 3 days of degradation test by *Rhodococcus opacus* is shown in **Table 7. 1**.

CS/CH/nanoclay (control) films showed higher percentages of microbial degradation than other bionanocomposite films because of the absence of antimicrobial agent **(Table 7.1)**. CS/CH/nanoclay/GLY/KS showed higher biodegradability than CS/CH/nanoclay/SOR/GFSE due to low crystallinity **(Figure 7.1b)**, high hydrophilicity **(Figure 7.2),** low water barrier properties (**Figure 7.4)**, low mechanical properties (**Figures 7.5 and 7.7)**. The low biodegradability was found in the case of CS/CH/nanoclay/SOR/GFSE bionanocomposite films due to strong resistance to microbial attack according to antibacterial test **(Figure 7.16)** besides high crystallinity **(Figure 7.1e)**, low hydrophilicity **(Figure 7.2),** high water barrier properties (**Figure 7.4)**, high mechanical properties (**Figures 7.5 and 7.7)**. But, CS/CH/nanoclay/GLY/GFSE and CS/CH/nanoclay/SOR/KS bionanocomposite films did not show significant difference in biodegradation.

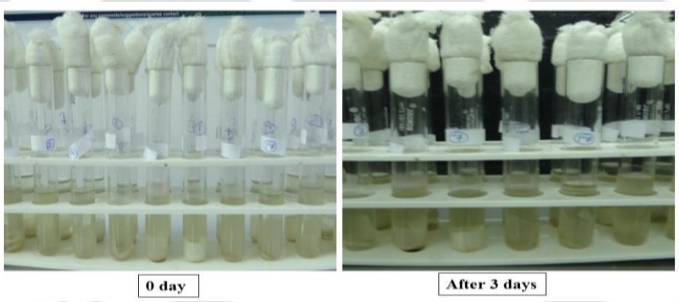

Figure 7.11. Pictorial images showing microbial degradation of different starch-chitosan-nanoclay bionanocomposite films and synthetic plastic films.

In the case of negative control, microbial degradation was lower than other bionanocomposite films. It is due to the absence of *Rhodococcus opacus*. Low density polyethylene (LDPE) consists of long chains of ethylene monomers that made up of only carbon and hydrogen atoms, are generally less susceptible to microbial attack.

Table 7.1. Weight loss in starch-chitosan-nanoclay bionanocomposite films and synthetic plastic films after 3 days of microbial degradation.

S.No.	Films	Weight loss after 3 days (%)
1.	CS/CH/nanoclay (control)	68.1±0.84
2.	CS/CH/nanoclay/GLY/KS	66.7±1.07
3.	CS/CH/nanoclay/SOR/KS	62.4±0.23
4.	CS/CH/nanoclay/GLY/GFSE	61.8±0.66
5.	CS/CH/nanoclay/SOR/GFSE	55.4±0.81
6.	CS/CH (negative control)	10.4±0.80
7.	LDPE	0.1±0.77

Among all films, LDPE showed a little weight loss. The weight loss could be attributed to biodegradation by *Rhodococcus opacus*. It was observed in a previous study that *Rhodococcus ruber* degrades polyethylene via colonizing on them and forms a biofilm (**Basnett et al., 2012**).

FESEM images of bionanocomposite film before and after microbial degradation is shown in **Figure 7.12 (a-k).** All the films showed rough surface without any phase separation on 0^{th} day (**Figure 7.12 (a-e)**). The CS/CH/nanoclay/SOR/GFSE bionanocomposite film showed smooth surface with less number of cracks compared to other bionanocomposite films on 0^{th} day. It is due to strong intermolecular interactions which was confirmed by FTIR analysis **(Figure 7.10 (e)).** The morphological study of bionanocomposite films revealed that CS/CH/nanoclay/SOR/GFSE film was more compact and homogenous structure with good dispersion of nanoclay than CS/CH/nanoclay/GLY/GFSE, CS/CH/nanoclay/SOR/KS, CS/CH/nanoclay/GLY/KS and CS/CH/nanoclay on 0^{th} day. The respective film samples were observed for the morphological study after 3^{rd} day. In general, water enters through amorphous region and finally microbial attack takes place. The order of *Rhodococcus opacus* growth on bionanocomposite film was CS/CH/nanoclay/SOR/GFSE < CS/CH/nanoclay/SOR/KS < CS/CH/nanoclay/GLY/GFSE < CS/CH/nanoclay/GLY/KS < CS/CH/nanoclay (**Figure**

7.12 (f-j)) which is in agreement with decrease in crystallinity **(Figure 7.1 (a-e))** and mechanical properties **(Figures 7.5 and 7.7).** In the case of negative control, *Rhodococcus opacus* growth was not observed **(Figure 7.12 (k))**.

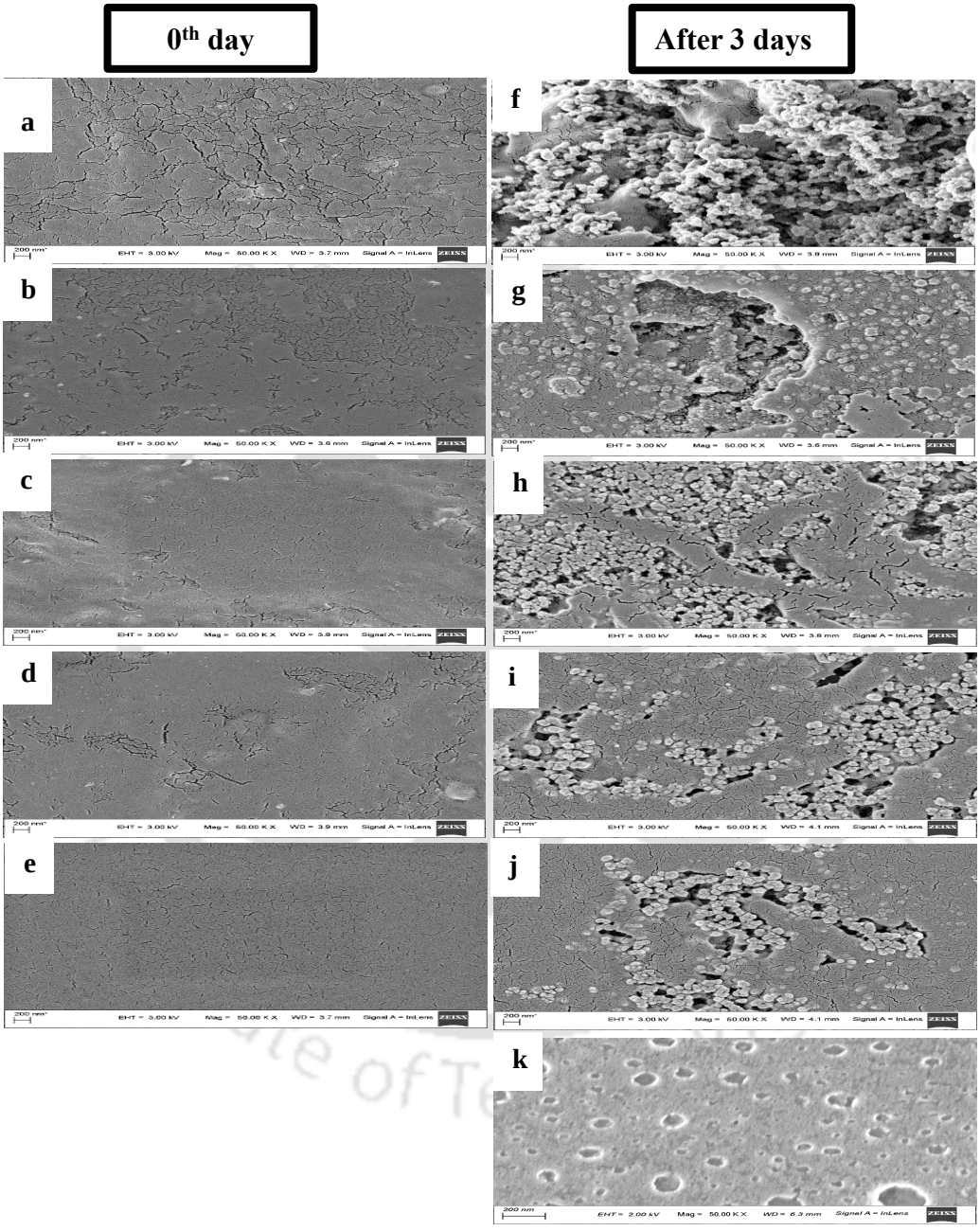

Figure 7.12. FESEM images of CS/CH/nanoclay bionanocomposite films on 0th and after 3rd day. CS/CH/nanoclay (a and f), CS/CH/nanoclay/GLY/KS (b and g), CS/CH/nanoclay/SOR/KS (c and h), CS/CH/nanoclay/GLY/GFSE (d and i), CS/CH/nanoclay/SOR/GFSE (e and j) and CS/CH/nanoclay (negative control) (k).

7.3.8. Soil burial degradation test

Biodegradation of prepared bionanocomposite films was also investigated in soil. The biodegradability in soil depends on temperature, humidity, type of microorganism and composition of films **(Guohua et al., 2006)**. The biodegradability of all bionanocomposite films was studied by evaluating the weight loss of the films up to 60 days, and the results are shown in **Figure 7.13**. As it can be observed, all starch-chitosan-nanocaly bionanocomposite films degrade rapidly during first 15 days, followed by slow and steady degradation until 60 days. The degradation of CS/CH/nanoclay (control) film was faster than other bionanocomposite films because of the absence of antimicrobial agent. The final residual mass of CS/CH/nanoclay bionanocomposite films after 60 days of biodegradation in soil was 45%. The soil degradation of films containing KS and GFSE was lower than control films due to high antibacterial activity against the soil microbes.

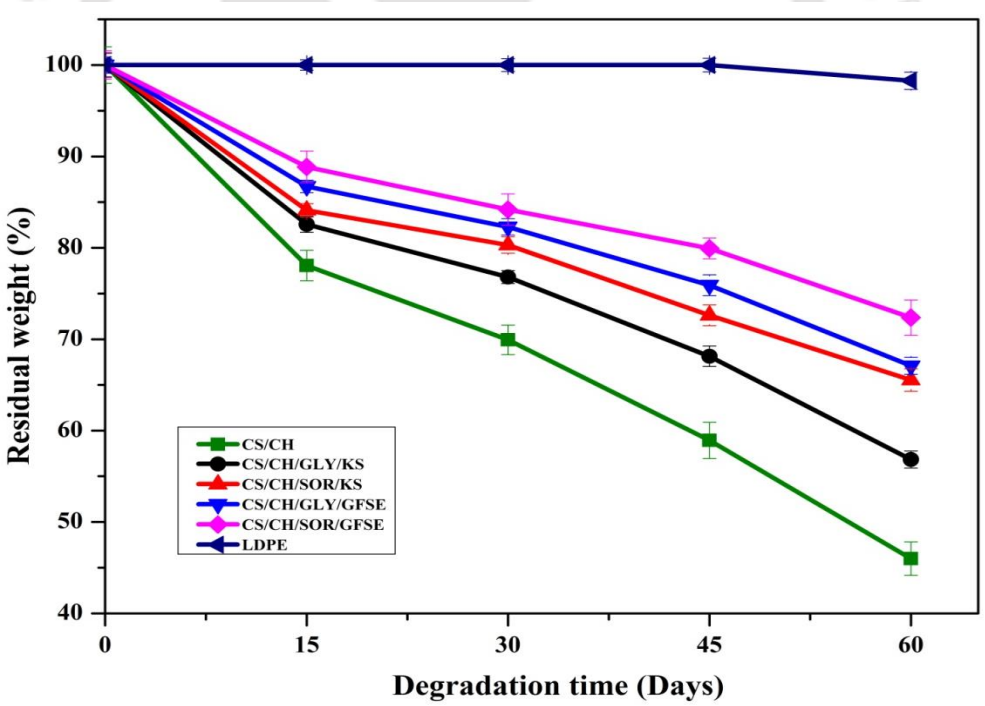

Figure 7.13. Weight loss (%) of starch-chitosan-nanoclay bionanocomposite films and LDPE in soil.

The residual mass of CS/CH/nanoclay/GLY/KS, CS/CH/nanoclay/SOR/KS, CS/CH/nanoclay/GLY/GFSE and CS/CH/nanoclay/SOR/GFSE was 56%, 65%, 67% and 72%, respectively. The soil degradation of CS/CH/nanoclay/SOR/GFSE

bionanocomposite film was lower than CS/CH/nanoclay/GLY/GFSE film. The soil biodegradability result is in accordance with microbial degradation of *Rhodococcus opacus* **(Figure 7. 12)**. No significant weight loss was observed for LDPE in soil. The photographic images of soil biodegradability of prepared bionanocomposite films and LDPE for 0, 30 and 60 days are shown in **Figure 7. 14 (a-c)**.

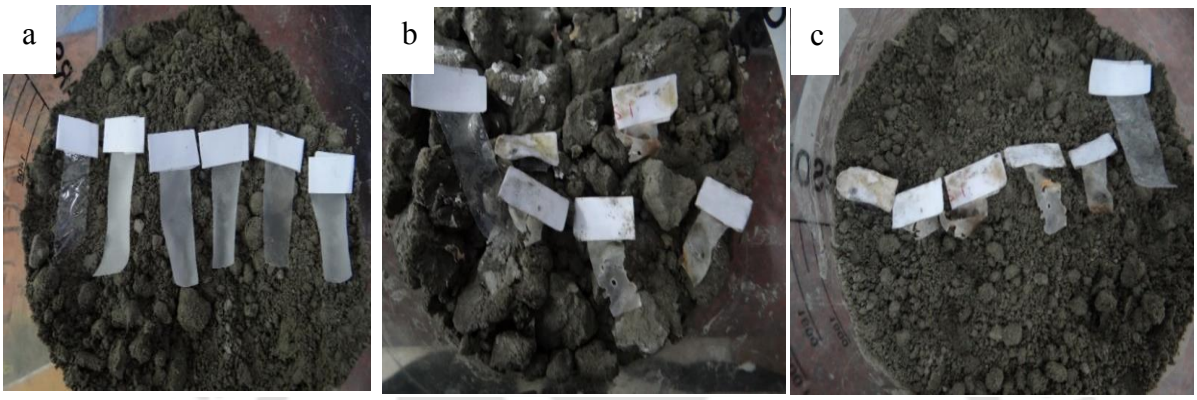

Figure 7.14. Images of soil biodegradability of starch-chitosan-nanoclay bionanocomposite films and LDPE for (a) 0 day, (b) 30 and (c) 60 days.

FESEM morphology of bionanocomposite films after 30 and 60 days of soil degradation is shown in **Figure 7.15 (a-j)**. In the case of CS/CH/nanoclay film, many big cavities, irregular and rough surface was formed after 30 and 60 days of soil degradation **(Figure 7.15 (a-b))**. The bionanocomposite films of CS/CH/nanoclay/GLY/KS, CS/CH/nanoclay/SOR/KS, CS/CH/nanoclay/GLY/GFSE and CS/CH/nanoclay/SOR/GFSE showed smaller holes on the surface compared to control film after 30 days of soil burial due to the presence of plasticizers and antimicrobial agents **(Figure 7.15 (c,e,g and i))**.

After 60 days of degradation, all the holes in the films became more porous compared to 30 days films **(Figure 7.15 (d,f,h and j))**. The high crystallinity and strong intermolecular interactions with high antibacterial activity of CS/CH/nanoclay/SOR/GFSE restricted the degradation by microorganisms in soil, resulted in less porous on the surface of the film **(Figure 7.15 (i and j))** compared to CS/CH/nanoclay/GLY/KS, CS/CH/nanoclay/SOR/KS, CS/CH/nanoclay/GLY/GFSE and CS/CH/nanoclay films.

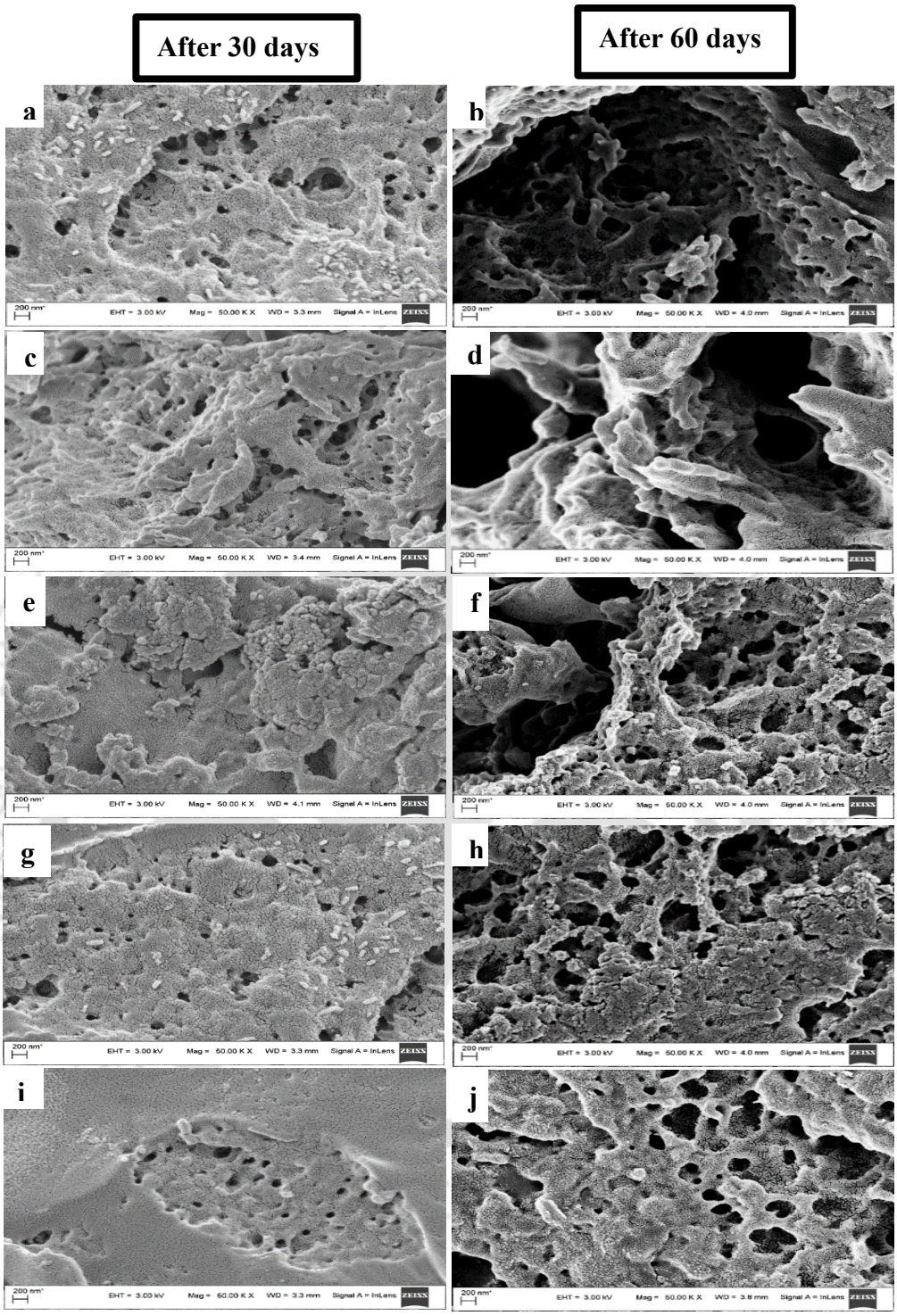

Figure 7.15. FESEM images of (a and b) CS/CH/nanoclay, (c and d) CS/CH/nanoclay/GLY/KS, (e and f) CS/CH/nanoclay/SOR/KS, (g and h) CS/CH/nanoclay/GLY/GFSE and (i and j) CS/CH/nanoclay/SOR/GFSE after 30 and 60 days of soil burial test.

7.3.9. Agar diffusion test for antifungal activity

Antifungal activity of bionanocomposite films incorporated with different plasticizers and antimicrobial agents is shown in **Figure 7.16 (a-g).** The fungi growth inhibitory zone (mm) was observed after 72 h of incubation at 37^{o}C.

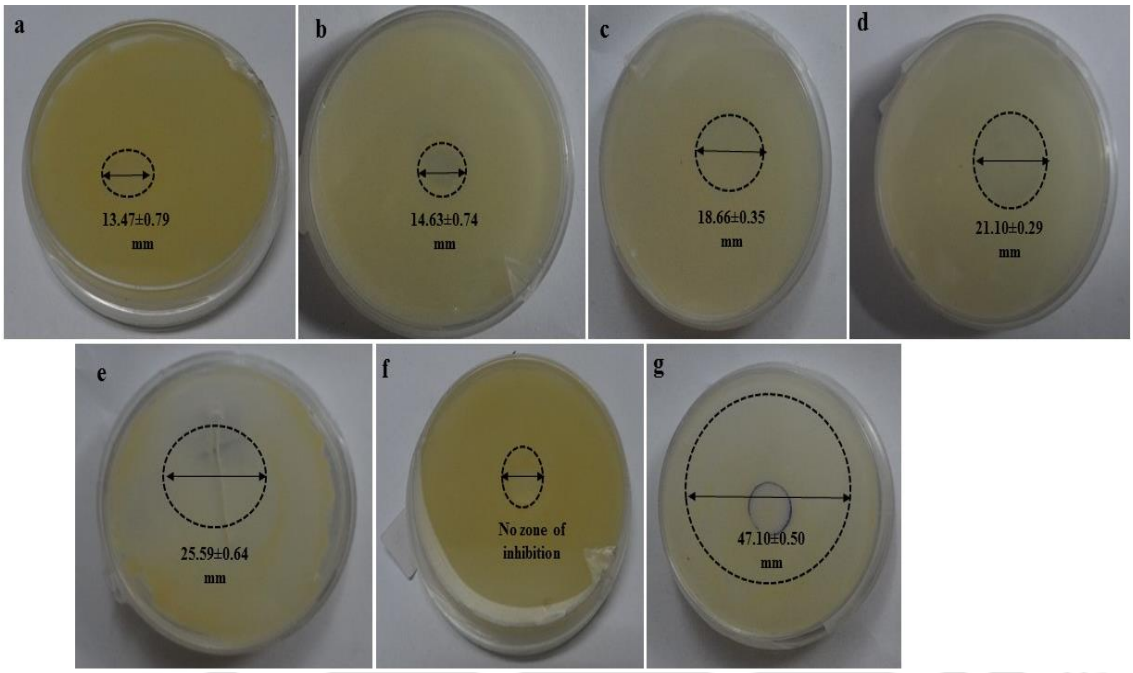

Figure 7.16. Antifungal activity of bionanocomposite films against *Aspergillus niger*: (a) CS/CH/nanoclay, (b) CS/CH/nanoclay/GLY/KS, (c) CS/CH/nanoclay/SOR/KS, (d) CS/CH/nanoclay/GLY/GFSE, (e) CS/CH/nanoclay/SOR/GFSE, (f) LDPE and (g) Ampicillin B.

The CS/CH/nanoclay film showed a small zone of inhibition of 13.47±0.79 mm against *Aspergillus niger* **(Figure 7.16 (a))**. The bionanocomposite film of CS/CH/nanoclay/GLY/KS, CS/CH/nanoclay/SOR/KS, CS/CH/nanoclay/GLY/GFSE and CS/CH/nanoclay/SOR/GFSE exhibited zone of inhibition of 14.63±0.74, 18.66±0.35, 21.10±0.29 and 25.59±0.64 mm, respectively **(Figure 7.16 (b-e))**. The highest zone of inhibition was found for CS/CH/nanoclay/SOR/GFSE among all bionanocomposite films. It was observed that antifungal activity of GFSE containing films was higher than KS films. GFSE contains phenolic compounds and citric acid which can potentially disturb the function of the cell wall in *Aspergillus niger*. No zone of inhibition was observed against

Aspergillus niger for LDPE **(Figure 7.16 (f))**. The positive control of ampicillin showed a zone of inhibition of 47.10±0.50 mm **(Figure 7.16 (g))**. The present study strongly encourages that GFSE (natural) incorporated bionanocomposite films can be used for food packaging applications.

7.3.10. Antifungal activity of bionanocomposite film

Comparative studies of bread sample packed by CS/CH/nanoclay/SOR/GFSE bionanocomposite films and low-density polyethylene (LDPE) films are shown in **Figure 7.17**. CS/CH/SOR/GFSE biocomposite film was chosen for bread packaging because of low moisture content, low water vapor permeability, low solubility, high tensile strength and high antifungal activity. The LDPE film served as control.

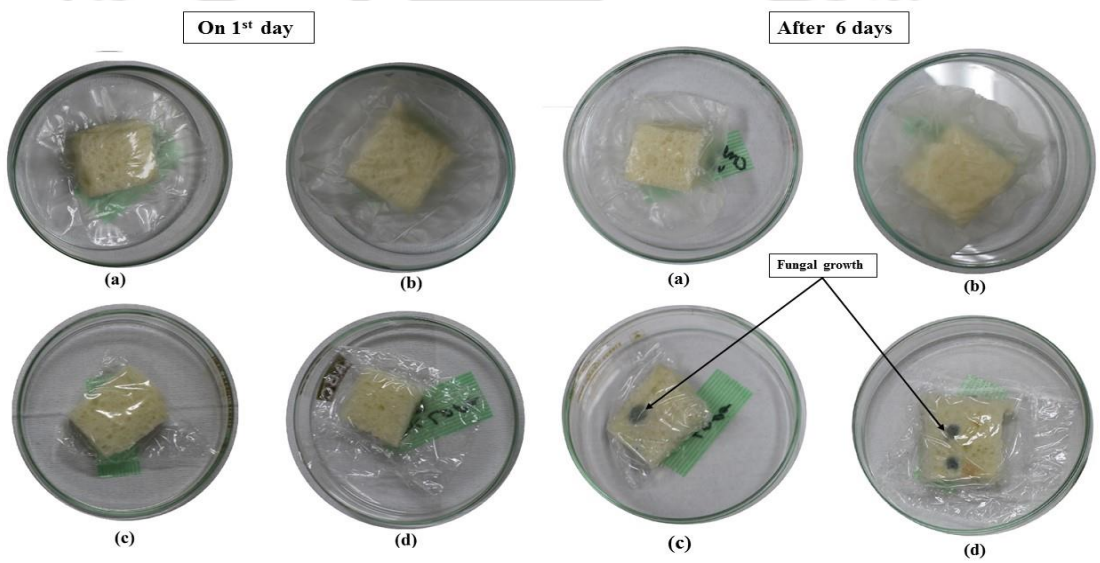

Figure 7.17. Comparative study on bread sample packed with (a and b) CS/CH/nanoclay/SOR/GFSE films (c and d) and low density polyethylene films.

After 6 days, the fungal growth was observed in control samples, which were packed by LDPE films **(Figure 7.17 (c and d))**. But, in the case of samples packed by CS/CH/nanoclay/SOR/GFSE bionanocomposite films, the fungal growth was retarded till 20 days. The presence of CH and GFSE in the bionanocomposite films extended the shelf life of bread samples significantly. Moreover, the antifungal activity of nanoclay can be explained by release of metal ions during its interactions with fungi **(Malachova et al., 2011)**. Hence, the prepared bionanocomposite film can be a potential candidate for food

packaging applications to extend the shelf life of products and food safety. It was reported that a low density polyethylene (LDPE) films incorporated with GFSE can be used to extend shelf life of beef stored under 3°C till 14 days **(Sung et al., 2013)**. According to a recent study, the antifungal activity of chitosan-based composite films significantly increased with addition of GFSE **(Tan et al., 2015)**.

7.3.11. Comparative study of corn starch blended with CH vs. selected natural and synthetic polymeric films

The tensile strength, elongation at break and WVP of CS/CH/nanoclay films were compared with selected natural and synthetic polymeric films **(Table 7.2)**

Table 7.2. Tensile strength, elongation at break and water vapour permeability of various films**.**

Film type	Test condition	TS (MPa)	EB (%)	WVP (g/m s Pa)	Reference
CS/CH/nanoclay CS/CH/nanoclay/GLY/KS CS/CH/nanoclay/SOR/KS CS/CH/nanoclay/GLY/GFSE CS/CH/nanoclay/SOR/GFSE	25°C, 75% RH	28.5 12.7 18.7 16.3 19.2	8.67 77.88 65.54 72.40 56.15	71×10^{-11} 9.5×10^{-11} 6.7×10^{-11} 7.2×10^{-11} 3.3×10^{-11}	**Present study**
CS	25°C, 75% RH	3.8-4.3	4.0-10.0	-	**Mali et al. (2006)**
CS/CH	25°C, 75% RH 25°C, 95% RH	3.2-6.3 1.0-3.5	58.0-122 25.0-100	$1.5\text{-}7.8 \times 10^{-10}$ $1.8\text{-}9.2 \times 10^{-10}$	**Ren et al. (2017)**
CS/CH/$CaCO_3$	25°C, 75% RH	2.04-10.7	78.7-134.3	$1.58\text{-}7.47 \times 10^{-10}$	**Ji et al. (2017)**
CH/0-1.5(% v/v) GFSE	23°C, 50% RH	54.9-8.93	4.72-96.8	-	**Tan et al. (2016)**
CS/CH/0-3% GFSE	23°C, 50% RH	18.3-14.4	57-67	$2.08\text{-}2.08 \times 10^{-9}$	**Bof et al. (2016)**
Low density polyethylene (LDPE)	38°C, 90% RH	7.6-17.3	500.0	9.25×10^{-13}	**Bourtoom and Chinnan (2008)**
High density polyethylene (HDPE)	38°C, 90% RH	17.3-34.6	300.0	2.31×10^{-13}	
Polyester	38°C, 90% RH	178.0	70.0-100.0	-	
Cellophane	38°C, 90% RH	-	-	8.41×10^{-11}	

In the current study, CS/CH/nanoclay/SOR/GFSE film showed lower WVP (3.3×10^{-11}) and higher tensile strength (19.2 MPa) compared with the films prepared by **Mali et al. (2006), Ren et al. (2017), Ji et al. (2017) and Tan et al. (2016).** The WVP of CS/CH/nanoclay/SOR/KS,CS/CH/nanoclay/GLY/GFSE,CS/CH/nanoclay/SOR/GFSE films was lower than cellophane film **(Bourtoom and Chinnan, 2008)** and CS/CH/0-3% v/v GFSE film **(Bof et al., 2016)**.

7.4. Summary

Corn starch-chitosan-nanoclay films were prepared with different plasticizers (GLY and SOR) and antifungal agents (KS and GFSE). The prepared films were studied for their physical, mechanical and thermal properties. Among the prepared films, SOR/GFSE and SOR/KS showed better physical, mechanical and thermal properties than GLY/GFSE and GLY/KS. A comprehensive characterization revealed that SOR/GFSE bionanocomposite film possess high crystallinity, low hydrophilicity, high water barrier and high mechanical properties. Morphological study showed that more uniform surfaces was found in SOR/GFSE films compared to other films. Among all films, SOR/GFSE films showed the highest antifungal activity, which is essential for food packaging applications. The results strongly motivate us to employ SOR/GFSE films as active packaging materials in the food industry.

Chapter 8

Effect of antifungal agent on corn starch-chitosan-nanoclay bionanocomposite films

This chapter was aimed to examine the effect of various ratios of grapefruit seed extract (GFSE) on crystallinity, mechanical, water barrier, and thermal properties of corn starch (CS)-chitosan (CH)-nanoclay (Na-MMT) bionanocomposite films.

8.1. Specific Background

The consumer demand has increased for biodegradable packaging material due to the environmental problems (**Tan et al., 2015)**. Hence, active packaging utilization is adopted in the food industry. Active packaging is used to extend the shelf life of food which improves food safety through active compounds present in the packaging material (**Ren et al., 2017**). The demand for active packaging drives the growth of food industry into the worldwide market.

Starch is a natural as well as the biocompatible polymer compared to other polymers. It has received more attention due to its wide availability from the plant source, renewability, film-forming ability, non-toxic, low cost and a source of income for the agriculture sector. However, the uses of starch film have been limited due to its strong hydrophilic behaviour. Though, starch films have high oxygen barrier properties, they are highly moisture sensitivity which lowers their mechanical properties **(Abreu et al., 2015; Borges et al., 2015; Souza et al., 2012)**.

Chitosan has been investigated for food protection due to its inherent anti-bacterial and anti-fungal properties against food spoilage microorganisms **(Tan et al., 2015)**.

Grapefruit seed extract (GFSE) is a natural antimicrobial agent which can be used in active food packaging. GFSE has been found to be an effective broad-spectrum antimicrobial agent against *Salmonella, Escherichia coli, Candida* and *A. niger* **(Choi et al., 2014).** The GFSE is usually extracted from the pulp and seed of grapefruit (*Citrus*

paradise Macf. Rutaceace). It contains large quantities of vitamins, minerals, hydroxy cinamic acids, trans-reveratol, flavanols, tannins, polyphenolic compounds (epicatechin, catechins, procyanidin), flavonoids (mainly *naringin*), citric acid, ascorbic acid, tocopherol and limonoid. It also shows antioxidant activity due to the presence of citrus flavonoids. Only a few studies have attempted to make use of this natural antimicrobial agent (GFSE) for food packaging films **(Debnath et al., 2011; Kanmani and Rhim, 2014a)**.

The present research work focuses on the effect of GFSE in corn starch (CS) blended with chitosan (CH) and nanoclay (Na-MMT) bionanocomposite films for food packaging applications. The prepared films were studied for its crystallinity, water barrier, mechanical, thermal and morphological properties. Finally, the prepared films were also checked for biodegradation by microbial and soil.

8.2. Film preparation of grapefruit seed extract containing corn starch-chitosan-nanoclay (Na-MMT) bionanocomposite films

The preparation of CS-CH-nanoclay (Na-MMT) with varying amount of grapefruit seed extract (GFSE) from 0.5% to 2% v/v to produce bionanocomposite films was mentioned in detail elsewhere **(Chapter 3, Section 3.2.9).**

8.3. Results and Discussion

8.3.1. X-ray diffraction analysis

The XRD patterns of CS/CH/nanoclay (control), CS/CH/nanoclay/0.5% GFSE, CS/CH/nanoclay/1% GFSE, CS/CH/nanoclay/1.5% GFSE and CS/CH/nanoclay/2% GFSE bionanocomposite films are shown in **Figures 8.1 (a-e).**

Native CS showed A-type diffraction peaks around 15°, 17°, 18° and 23° **(Sun et al., 2014b).** CH film sample exhibited two main broad amorphous peaks at 2θ = 11° and 20° **(Bourtoom and Chinnan, 2008).** The diffraction peaks of starch were not seen in all the films due to gelatinization process, which can disturb the crystalline structure of starch granule. The control film CS/CH/nanoclay showed a maximum diffraction peak at 2θ = 20.2° **(Figure 8.1 (a))**. In the case of GFSE (from 0.5% to 2% v/v) added films, the maximum peak was slightly shifted by 19.4° probably due to interaction of GFSE with CS/CH/nanoclay **(Figure 8.1 (b-e))**. Similarly, slight peak shifting was observed in

carrageenan/GFSE composite films for increasing amounts of GFSE (**Kanmani and Rhim, 2014a**).

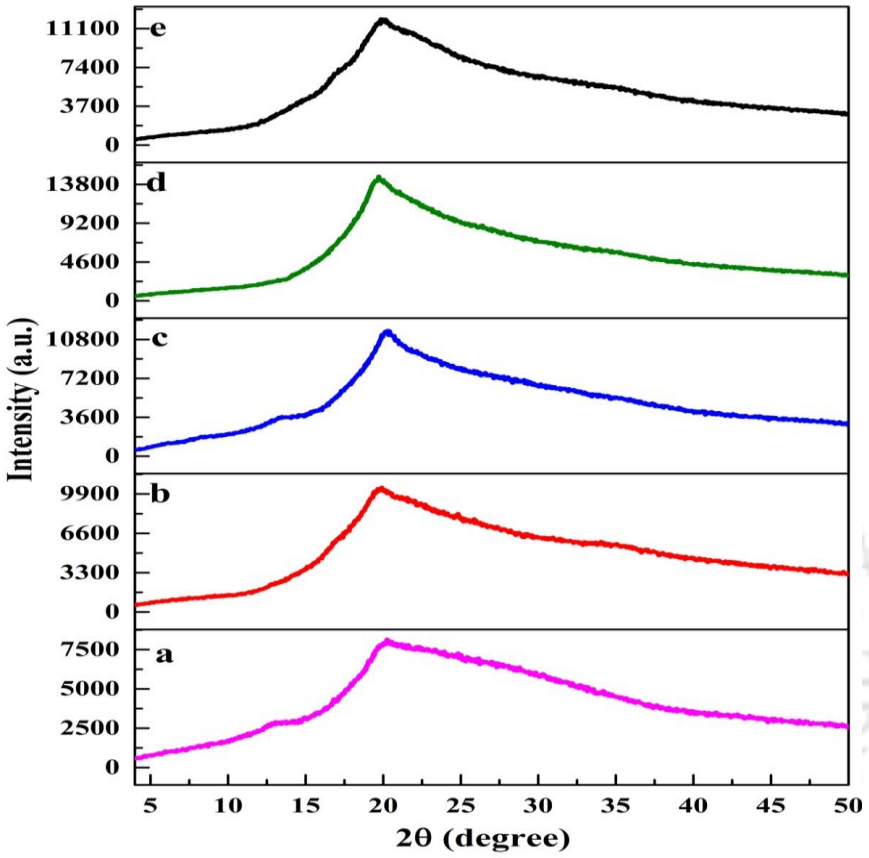

Figure 8.1. XRD patterns of starch-chitosan-nanoclay bionanocomposite films with different amounts of GFSE: (a) CS/CH/nanoclay (control), (b) CS/CH/nanoclay/0.5% GFSE, (c) CS/CH/nanoclay/1% GFSE, (d) CS/CH/nanoclay/1.5% GFSE and (e) CS/CH/nanoclay/2% GFSE.

The crystalline intensity in XRD increases with increase in GFSE from 0.5% to 1.5% (v/v) **(Figure 8.1 (b-d))** and it significantly decreases for 2% GFSE (v/v) **(Figure 8.1 (e))** due to the presence of citric acid in GFSE. It was observed that citric acid showed dual function as both crosslinking and plasticizing agent after certain an optimum concentration **(Shi et al., 2008)**. The XRD patterns exhibited no peak intensity for nanoclay in all the films due to extensive intercalation of polymer chains inside the Na-MMT galleries of

nanoclay. The crystalline structure increases mechanical as well as water barrier properties (**Aytunga et al., 2014)**.

8.3.2. Thickness and mechanical properties

The thickness and mechanical properties of CS/CH/nanoclay bionanocomposite film with varying amounts of GFSE are shown in **Figure 8.2, 8.3 and 8.4.**

The thickness of CS/CH/nanoclay bionanocomposite film was increased from 3.7 to 73.7 µm for increasing amounts of GFSE as shown in **Figure 8.2**. It is due to addition of high molecular weight GFSE. There is a significant difference observed between CS/CH/nanoclay/1.5% GFSE and CS/CH/nanoclay/2% GFSE bionanocomposite films. Similar results were observed in chitosan/GFSE, barley bran protein/GFSE and carrageenan/GFSE **(Rubilar et al., 2013; Song et al., 2012; Kanmani and Rhim, 2014b)**.

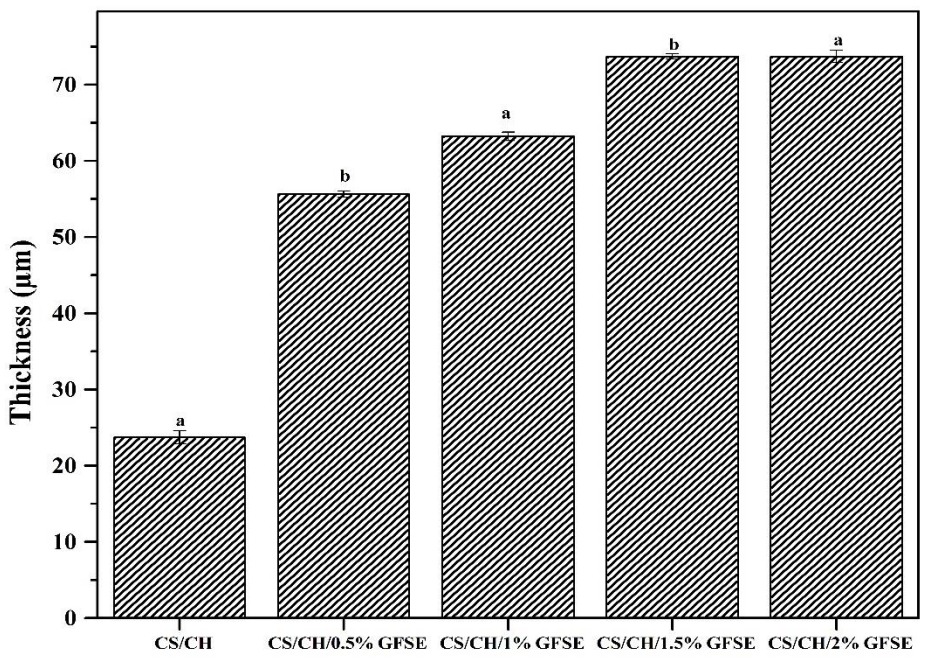

Figure 8.2. Thickness of starch-CH-nanoclay bionanocomposite films with different ratios of GFSE. [a-b]Different letters represent a significant difference using Tukey test ($p < 0.05$).

During shipping and handling, failure of the packaging materials can be avoided, if the mechanical properties (tensile strength and elongation at break) of the packaging films are above the threshold level. The tensile strength of the films was affected with varying concentrations of GFSE. The tensile strength of CS/CH/nanoclay, CS/CH/nanoclay/0.5%

GFSE, CS/CH/nanoclay/1% GFSE, CS/CH/nanoclay/1.5% GFSE and CS/CH/nanoclay/2% GFSE films were found to be 23.8, 15.5, 16.7, 19.6 and 17.4 MPa, respectively **(Figure 8.3)**.

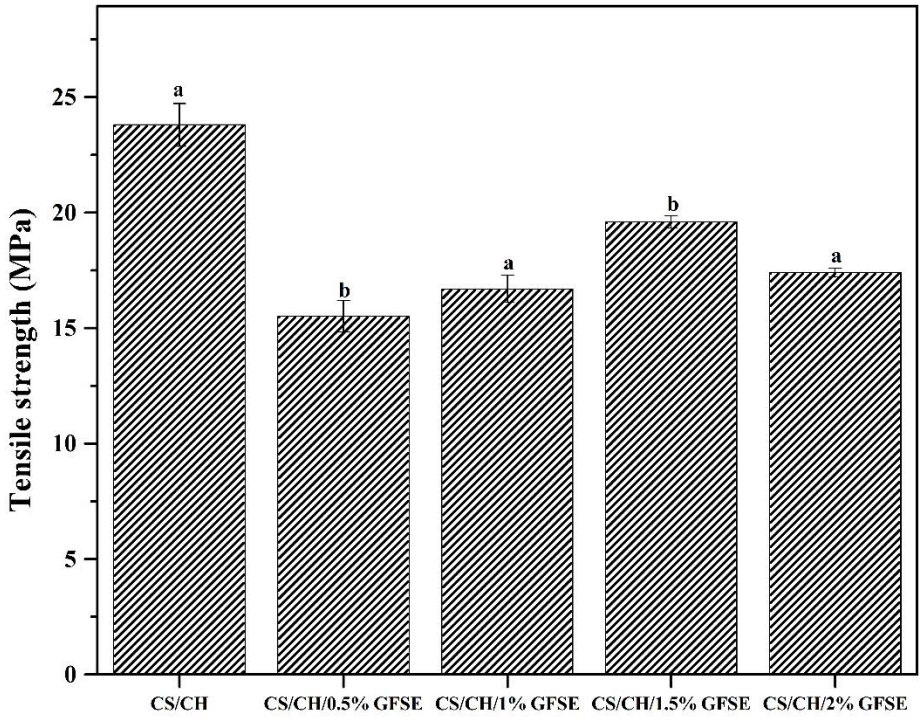

Figure 8.3. Tensile strength of starch-CH-nanoclay bionanocomposite films with different ratios of GFSE. [a-b]Different letters represent a significant difference using Tukey test ($p < 0.05$).

The highest tensile strength was observed for CS/CH/nanoclay/1.5% GFSE bionanocomposite film. It is due to citric acid (in GFSE) crosslinks between CS and CH from 0.5 to 1.5% GFSE (v/v). Hence, tensile strength increases up to 1.5% GFSE (v/v). Afterwards, citric acid acts as a plasticizer which decreases the tensile strength in CS/CH/nanoclay/2% GFSE bionanocomposite film. According to XRD results, the degree of crystallinity was higher in CS/CH/nanoclay/1.5% GFSE bionanocomposite film compared to other films. The tensile strength results are in accordance with XRD results **(Figure 8.1)**.

Elongation at break (EB) describes the films flexibility and stretchability. The lower EB was found for CS/CH/nanoclay control films (18.3%) due to the absence of GFSE **(Figure 8.3)**.

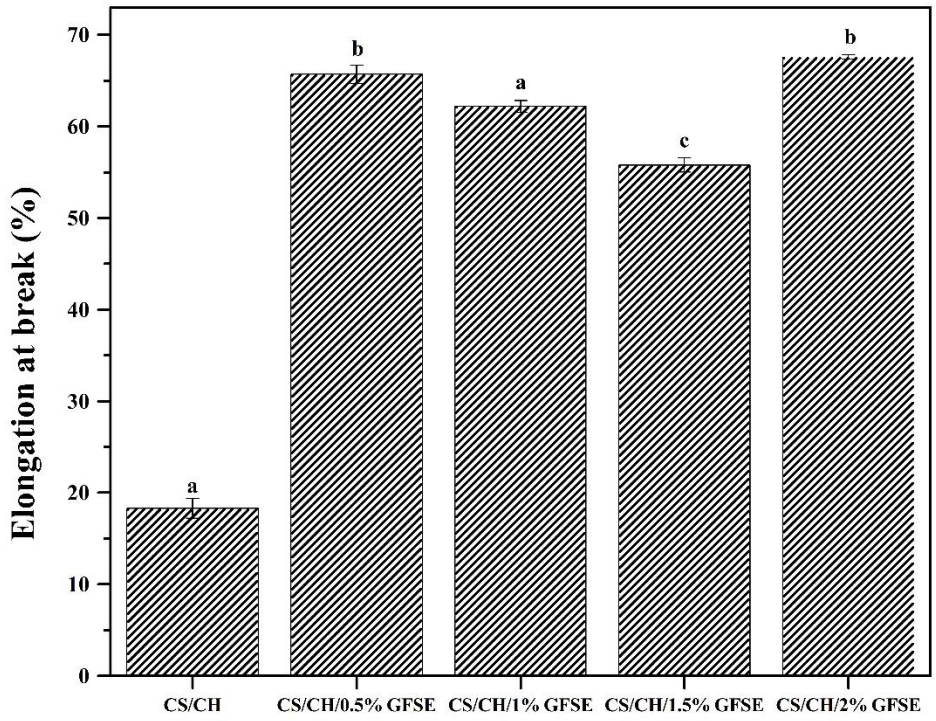

Figure 8.4. Elongation at break of starch-CH-nanoclay bionanocomposite films with different ratios of GFSE. [a-c]Different letters represent a significant difference using Tukey test ($p < 0.05$).

The CS/CH/nanoclay/2% GFSE bionanocomposite film showed highest EB of 67.6% among all the films. It could be attributed to high moisture content (**Figure 8.5)**, low crystallinity (**Figure 8.1)** and high tensile strength (**Figure 8.3)** of CS/CH/nanoclay/2% GFSE film. Also, chain mobility of polymers was enhanced due to plasticizing effect of water, citric acid (in GFSE) and sorbitol in CS/CH/nanoclay/2% GFSE film. The lowest value of EB is observed in the case of CS/CH/nanoclay/1.5% GFSE among the GFSE added bionanocomposite films which is in accordance with higher crystallinity and higher tensile strength.

8.3.3. Physical and barrier properties of films

8.3.3.1 Physical properties of films

The physical properties of the films such as moisture content and solubility are shown in **Figures 8.5 and 8.6.**

The moisture content of starch-based films depends on the relative humidity of the environment, chemical structure and size of branching point, **(Bertoft and Blennow, 2009; Mua and Jackson, 1997)**. CS/CH/nanoclay control films showed lowest moisture content due to the absence of GFSE which consists of hydrophilic constituents. The highest moisture content was observed for CS/CH/nanoclay/2% GFSE films. Though, moisture content of bionanocomposite films was found to be increased with increase in amounts of GFSE, it is not significant ($p > 0.05$) from 0.5% to 1.5% GFSE. But, it was significant ($p < 0.05$) for addition of 2% GFSE (**Figure 8.5)**. The moisture content is in accordance with crystallinity (**Figure 8.1)** and mechanical properties (**Figures 8.3 and 8.4)**.

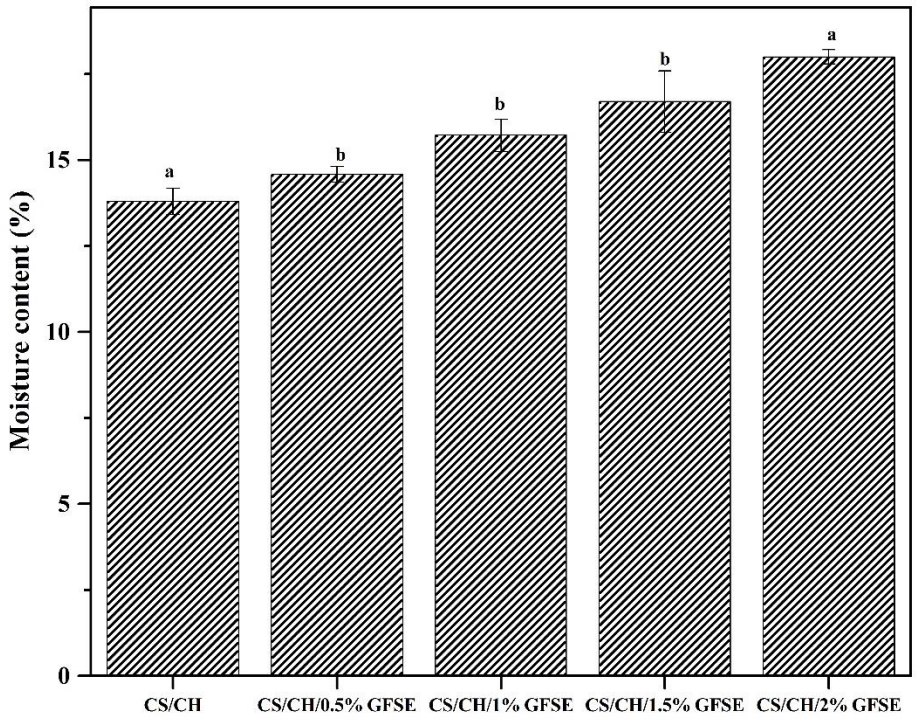

Figure 8.5. Effect of different amounts of GFSE on moisture content of starch-chitosan-nanoclay bionanocomposite films. [a-b]Different letters represent a significant difference using Tukey test ($p < 0.05$).

The solubility of biodegradable films plays a vital role in food preservation. A lower solubility of films is required in food packaging applications in order to improve the food quality. As shown in **Figure 8.6**, the solubility of CS/CH/nanoclay/2% GFSE was found to be 25.6% which was higher than 0.5-1.5% GFSE films. It could be attributed to low crystallinity and low tensile strength.

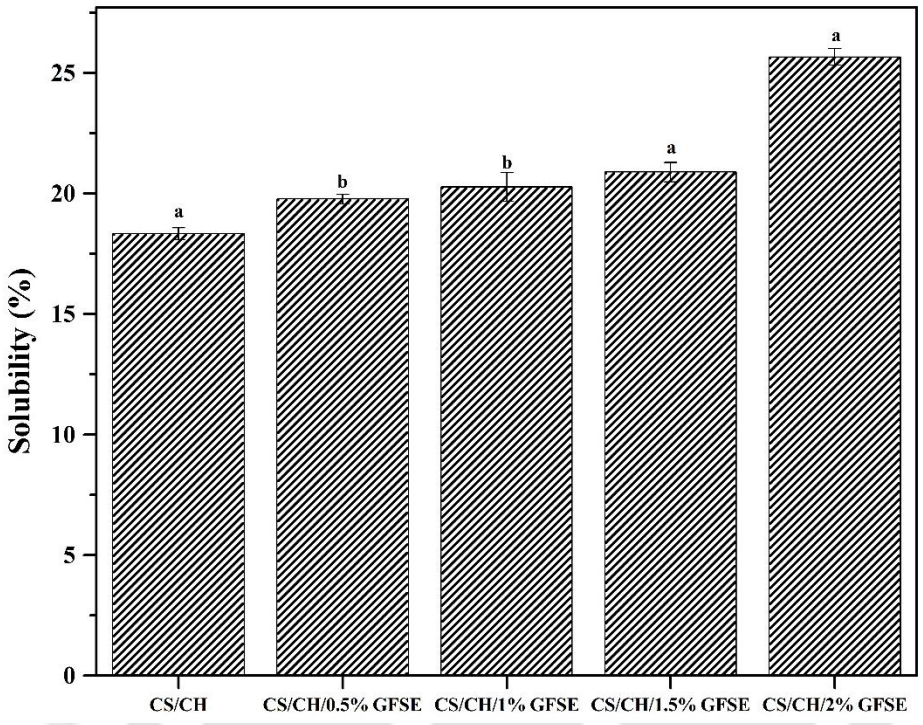

Figure 8.6. Effect of different amounts of GFSE on solubility of starch-chitosan-nanoclay bionanocomposite films. [a-b]Different letters represent a significant difference using Tukey test ($p < 0.05$).

The films were prepared from 0.5-1.5% GFSE showed higher water resistance because of strong intermolecular interaction between polymers, resulted in enhanced cohesiveness and lower swelling of the films.

8.3.3.2 Barrier properties of films

The water vapor permeability (WVP) of films is an essential property for food packaging applications. Food spoilage occurs due to low water barrier properties of packaging materials. The WVP property mainly depends on the film structure, amount of plasticizer in the film, relative humidity and temperature. The WVP of prepared films were

shown in **Figure 8.7.** It was observed that WVP was in the order of CS/CH/nanoclay > CS/CH/nanoclay/0.5% GFSE > CS/CH/nanoclay/1% GFSE > CS/CH/nanoclay/2% GFSE > CS/CH/nanoclay/1.5% GFSE.

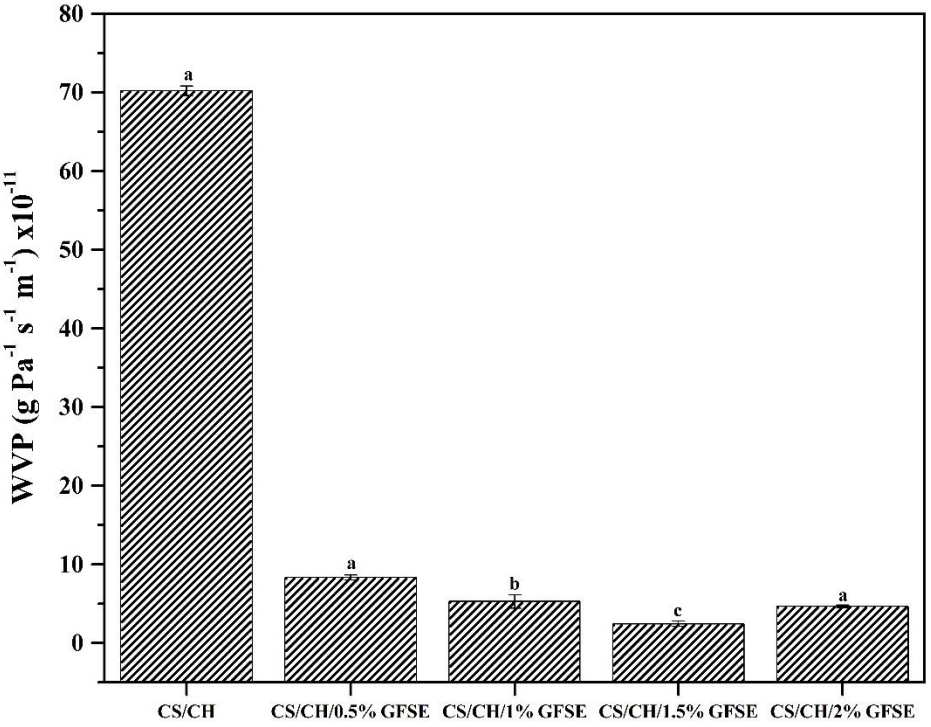

Figure 8.7. Effect of different amounts of GFSE on water vapour permeability of starch-chitosan-nanoclay bionanocomposite films. [a-c]Different letters represent a significant difference using Tukey test ($p < 0.05$).

As it is known, water enters through amorphous zones present in the film. The control film showed high WVP of 70.2×10^{-11}g Pa^{-1} s^{-1} m^{-1} because of higher amorphous content in the film compared to other films **(Figure 8.1a)**. The WVP of CS/CH/nanoclay/0.5% GFSE and CS/CH/nanoclay/1% GFSE film samples was found to be 8.34 and 5.29×10^{-11} g Pa^{-1} s^{-1} m^{-1}, respectively. The CS/CH/nanoclay/1.5% GFSE film exhibited lowest WVP of 2.45×10^{-11} g Pa^{-1} s^{-1} m^{-1} among all films. The high degree of crystallinity of the film makes it to be more compact structure and thus reducing molecular space for water to enter into the networks.

The WVP results of CS/CH/nanoclay/1.5% GFSE film are in accordance with higher crystallinity and lower moisture content as shown in **Figure 8.1** and **Figure 8.5**,

respectively. Therefore, the addition of CH and GFSE could be promising reinforcing materials to improve water vapor resistance in starch films for food packaging applications.

8.3.4. Thermal stability of bionanocomposite films (TGA)

Thermal property of the starch-CH-nanoclay bionanocomposite films with different ratios of GFSE was studied (**Figures 8.8)**.

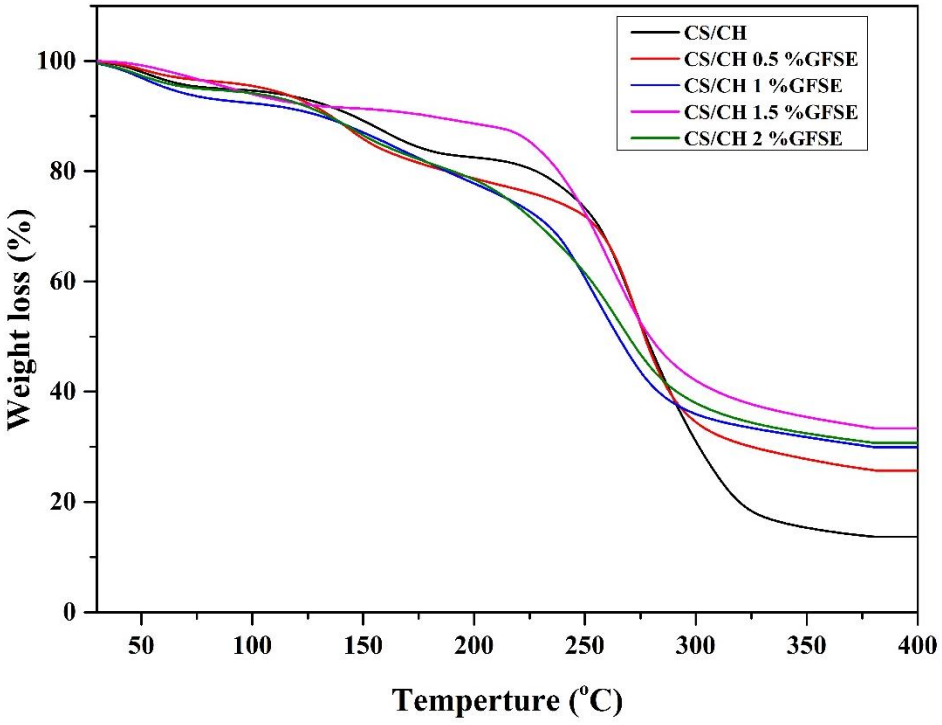

Figure 8.8. TGA curve of starch-CH-nanoclay bionanocomposite films with different ratios of GFSE.

Three stages of weight loss were observed in all the films. In the first stage, desorption of water was observed at 90°C. Bound moisture from GFSE and sorbitol was evaporated in the second stage between 150°C and 200°C. In the third weight loss stage, polymers decomposed in between 300°C and 400°C. The residual mass of CS/CH/nanoclay, CS/CH/nanoclay/0.5% GFSE, CS/CH/nanoclay/1% GFSE, CS/CH/nanoclay/1.5% GFSE and CS/CH/2% GFSE was found to be 14%, 25%, 30%, 34% and 31%, respectively. TGA study reveals that CS/CH/nanoclay/1.5% GFSE bionanocomposite film is more thermally stable than other films. The higher thermal

stability could be attributed to the strong intermolecular hydrogen bond and higher crystallinity of the film.

8.3.5. Fourier transform infrared (FTIR) analysis of bionanocomposite films

Fourier transform infrared spectroscopy (FT-IR) spectra of starch-chitosan-nanoclay bionanocomposite films with different ratios of GFSE were shown in **Figure 8.9.**

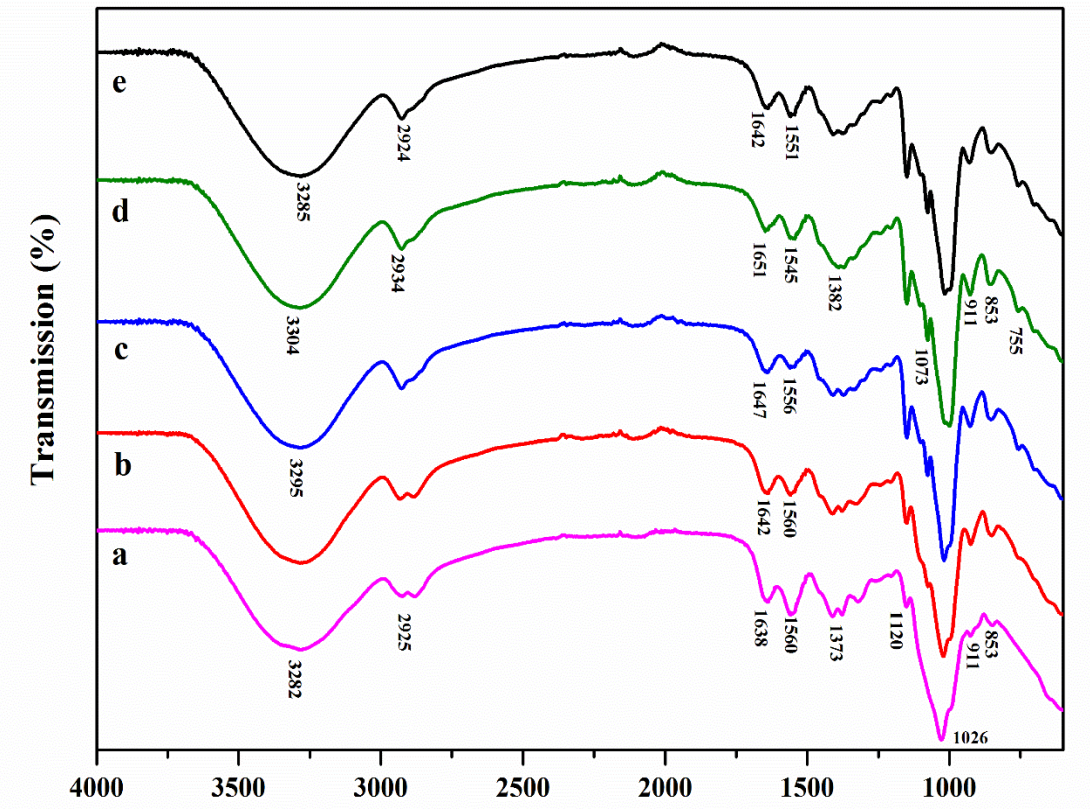

Figure 8.9. FTIR patterns of starch-chitosan-nanoclay bionanocomposite films with different ratios of GFSE: (a) CS/CH/nanoclay (b) CS/CH/nanoclay/0.5% GFSE (c) CS/CH/1% GFSE (d) CS/CH/1.5% GFSE and (e) CS/CH/2% GFSE.

Two broad characteristic peaks are observed at 1630 cm^{-1} and 1550 cm^{-1} in pure chitosan film (CH) due to C=O stretching vibrations (amide I) and NH bending (amide II), respectively. The band at 1026 cm^{-1} is due to stretching vibration of C–O–C of polysaccharide skeleton (**Ren et al., 2017**). The broad band at 3282 cm^{-1} is attributed to O–H stretching from CS/CH. The small peak at 2925 cm^{-1} is corresponded to C–H stretching from polymers **(Figure 7.9 (a))**. The stretching vibrations of Si-O and Al-OH

are observed at 1120 cm^{-1} and 911 cm^{-1}, respectively, due to nanoclay from CS/CH/nanoclay films. The stretching of the CH_2 group is shown as shoulder peak at 1310–1330 cm^{-1} **(Figure 8.9 (a)).**

The presence of peaks at 755 cm^{-1} and 1073 cm^{-1} is due to methylene group (-CH_2) and ester group in GFSE containing films **(Figure 8.9 (b-e)) (Mohansrinivasan et al., 2015).** The strong peak intensity is observed at 755 cm^{-1} and 1073 cm^{-1} for CS/CH/nanoclay/1.5% GFSE compared to other bionanocomposite films **(Figure 8.9 (d))**. Moreover, the band of –OH (3282 cm^{-1}), C-H (2925 cm^{-1}), -CH_2 (1373 cm^{-1}) and C=O (1638 cm^{-1}) vibrations are shifted to higher wavenumber 3304 cm^{-1}, 2934 cm^{-1}, 1382 cm^{-1} and 1651 cm^{-1}, respectively, for CS/CH/nanoclay/1.5% GFSE compared to other bionanocomposite films **(Figure 8.9 (d)).** It is due to strong intermolecular hydrogen bonding among the compounds of GFSE and CH (—NH_2, C=O group) and CS (–OH group). The strong molecular interaction in CS/CH/nanoclay/1.5% GFSE is accordance with its high degree of crystallinity **(Figure 8.1)**, high tensile strength **(Figure 8.3)**, high water barrier properties **(Figure 8.7)** and high thermal stability **(Figure 8.8)**.

8.3.6. Microbial degradation of bionanocomposite films

Microorganisms convert long chains of a polymer into smaller ones and then subsequently into small molecules that are easily absorbed and metabolized inside the microorganism by intracellular enzymes. In a recent study, microbial degradation have been analyzed for several blends **(Pathak and Kumar, 2017).** The prepared starch-CH-nanoclay bionanocomposite films with different ratios of GFSE were incubated in a mineral salt medium containing *Rhodococcus ocupus* for 3 days of microbial degradation.

The microbial growth was appeared due to degradation of the films and all the mineral salt medium was observed as turbid as shown in **Figure 8.10.** Percentage of weight loss was calculated before and after the degradation of films by *Rhodococcus ocupus* (**Table 8.1**). CS/CH/nanoclay (control) film showed higher percentage of microbial biodegradation because of the absence of the antimicrobial agent (GFSE). As it is known, enzymes mainly attack the amorphous domains of a film and make it more susceptible to degradation. CS/CH/nanoclay/0.5% GFSE film showed higher biodegradability than CS/CH/nanoclay/1% GFSE, CS/CH/nanoclay/1.5% GFSE and

CS/CH/nanoclay/2% GFSE due to low concentration of GFSE, low degree of crystallinity and weak molecular interactions.

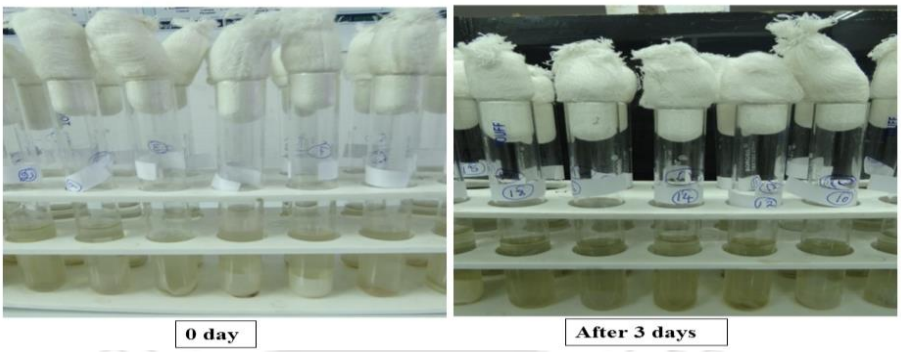

Figure 8.10. Microbial degradation of starch-CH-nanoclay bionanocomposite films with different ratios of GFSE and synthetic plastic films.

The rate of microbial degradation of decreases with an increase in crystallinity of the polymer (**Tokiwa et al., 2009**).

Table 8.1. Weight loss in different CS/CH/nanoclay/GFSE films and synthetic plastic films after 3 days of microbial degradation.

S.No.	Films	Weight loss (%)
1.	CS-CH/nanoclay (positive control)	63.1±0.95
2.	CS/CH/nanoclay /0.5 % GFSE	58.7±1.07
3.	CS/CH/nanoclay/1% GFSE	55.9±0.23
4.	CS/CH/nanoclay/1.5% GFSE	48.8±0.66
5.	CS/CH/ nanoclay/2% GFSE	52.4±0.81
6.	CS/CH/naoclay (negative control)	10.4±0.80
7.	LDPE	0.1±0.77

The lowest percentage of microbial degradation was found to be 48.8±0.66% for CS/CH/nanoclay/1.5% GFSE among the prepared films. It could be attributed to strong molecular interactions and high degree of crystallinity. In the case of negative control (CS/CH/nanoclay), the weight loss was found to be 10.4±0.80% because of the absence

Rhodococcus ocupus. No significant weight loss was found out for LDPE in the presence of *Rhodococcus ocupus*.

FESEM images of *Rhodococcus opacus* degraded CS/CH/nanoclay bionanocomposite films on 0^{th} and after 3 days are shown in **Figure 8.11 (a-k).**

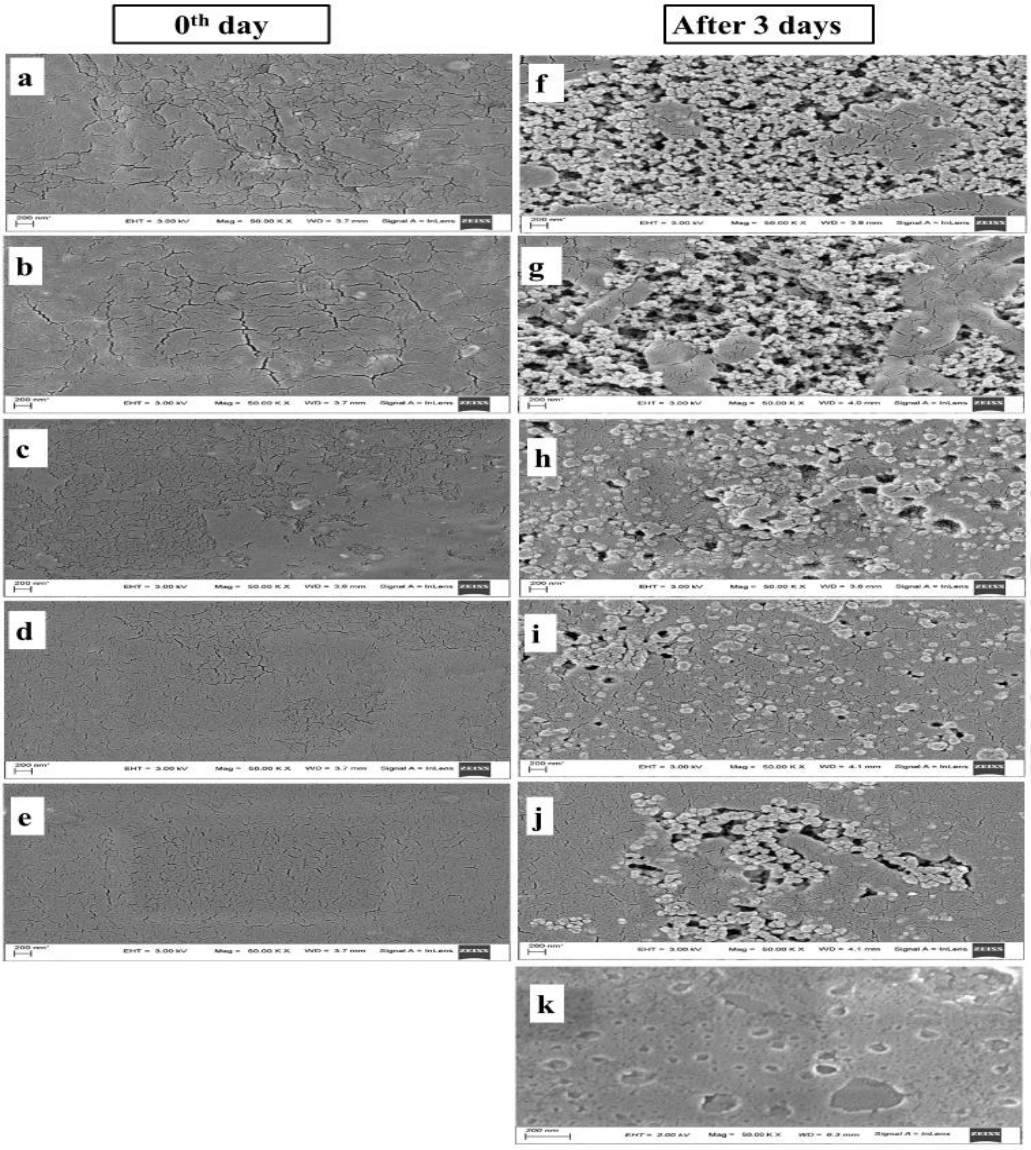

Figure 8.11. FESEM images of *Rhodococcus opacus* degraded CS/CH/nanoclay bionanocomposite films on 0^{th} and after 3 days. Films of CS/CH/nanoclay (a and f), CS/CH/nanoclay/0.5% GFSE (b and g), CS/CH/nanoclay/1% GFSE (c and h), CS/CH/nanoclay/1.5% GFSE (d and i), CS/CH/nanoclay/2% GFSE (e and j) and (k) CS/CH/nanoclay (negative control).

Before microbial degradation (on 0^{th} day), all the films showed rough surface without any phase separation (**Figure 8.11 (a-e))**. The control film (CS/CH/nanoclay) showed lengthier cracks compared with GFSE added films (**Figure 8.11 (a)).** As increase in GFSE concentration, the film became smoother and less no of cracks compared with control films (**Figure 8.11 (b-e))**. The CS/CH/nanoclay/1.5% GFSE film showed smoother surface with minimum no of cracks because of strong molecular interaction **(Figure 8.9 (d))** and high degree of crystallinity **(Figure 8.1 (d)).**

After 3 days of microbial degradation, the morphology of bionanocomposite films is shown in **Figure 8.11 (f-j)**. Because of the absence of GFSE and low degree of crystallinity, the control film (CS/CH/nanoclay) became more porous with more microbial population **(Figure 8.11 (f)).** Among the GFSE added films, the CS/CH/nanoclay/1.5% GFSE film was more compact in structure with few microbial populations **(Figure 8.11 (i)).** Similar observation was found in previous literatures for chitosan/GFSE and agar/GFSE composite films **(Rubilar et al., 2013; Kanmani and Rhim, 2014a).** In the case of negative control, no significant microbial population was found **(Figure 8.11 (k)).**

8.3.7. Soil burial degradation test

Soil degradability of packaging materials is important factor in food industry and among the consumers. The soil degradability of all prepared films was studied by evaluating the weight loss of the films for 60 days (**Figure 8.12).**

The degradation of control film (CS/CH/nanoclay) was faster by 60 days compared to GFSE added films. The degradation was rapid in the initial period for 15 days and it was followed by a slow degradation for GFSE added films. The order of soil degradation was found to be CS/CH/nanoclay/1.5% GFSE < CS/CH/nanoclay/2% GFSE < CS/CH/nanoclay/1% GFSE < CS/CH/nanoclay/0.5% GFSE < CS/CH/nanoclay which is in agreement with decrease in crystallinity **(Figure 8.1)** and tensile strength **(Figure 8.3)**. The less crystalline film is prone to microbial attack through diffusion of water, resulting in swelling and degradation of the film. The films containing GFSE exhibit a higher resistance against the soil microbes because of the antimicrobial agent.

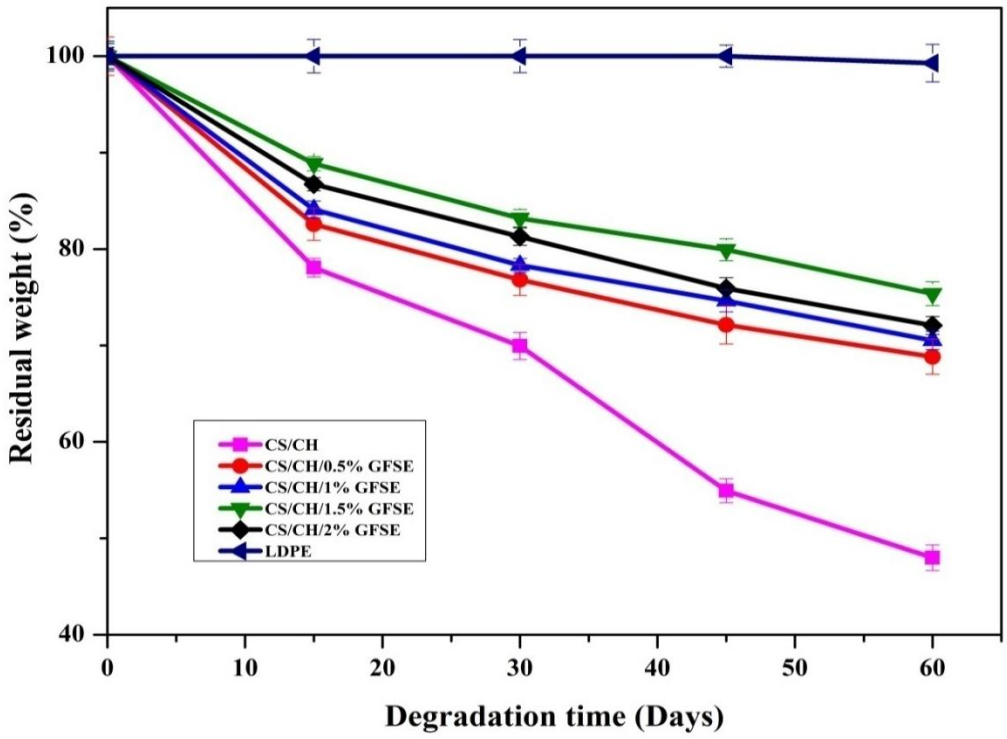

Figure 8.12. Weight loss (%) of starch-CH-nanoclay bionanocomposite films with different ratios of GFSE and LDPE against degradation time (Days).

There was about 1% weight loss in LDPE film compared to prepared films. The photographic images of soil biodegradability of prepared bionanocomposite films and LDPE for 0, 30 and 60 days are shown in **Figure 8.13.**

Figure 8.13. Images of soil biodegradability of starch-chitosan-nanoclay bionanocomposite films with different ratios of GFSE and LDPE for (a) 0 day, (b) 30 and (c) 60 days.

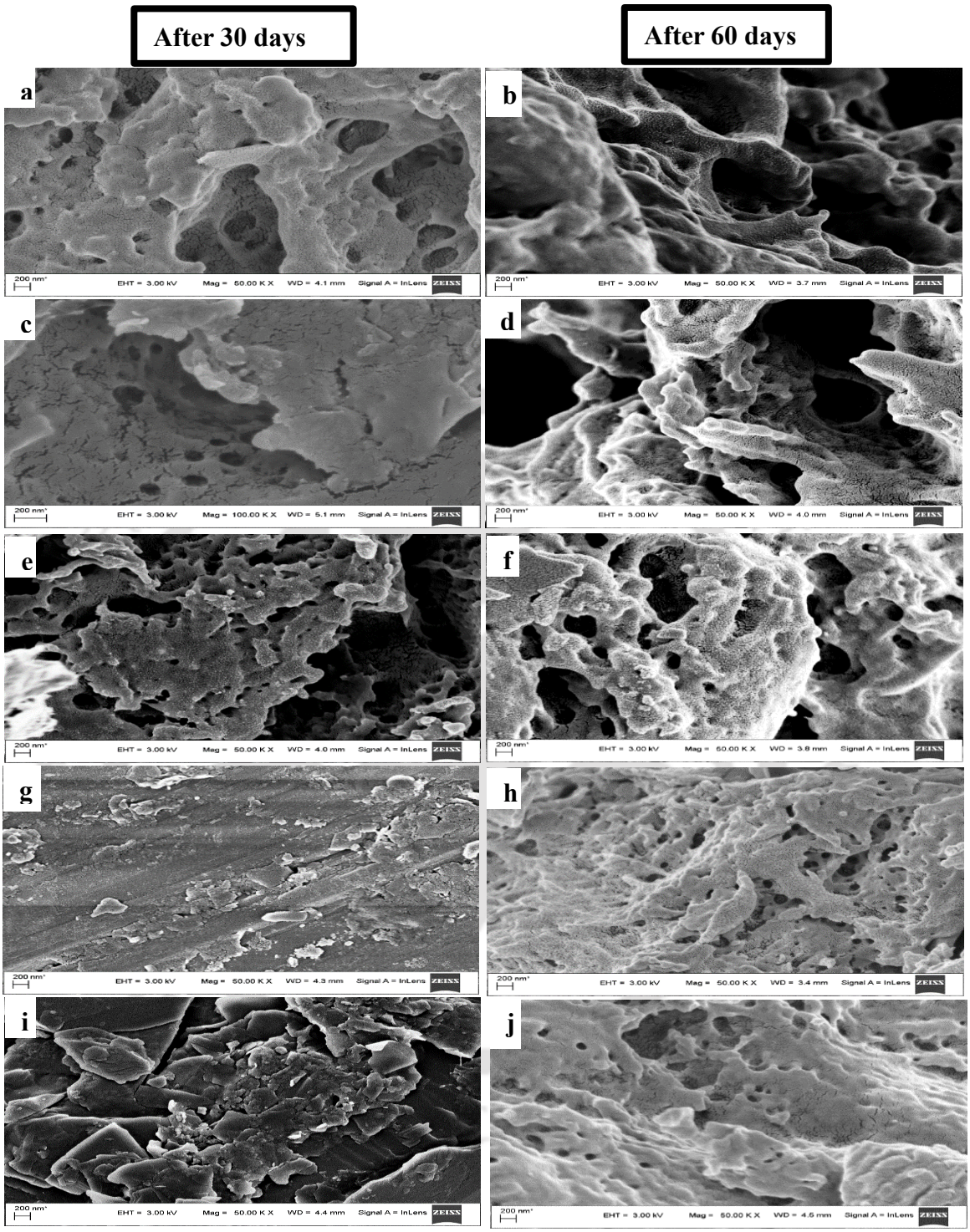

Figure 8.14. FESEM images after 30 and 60 days of soil burial test: (a and b) CS/CH/nanoclay, (c and d) CS/CH/nanoclay/0.5% GFSE (e and f) CS/CH/nanoclay/1% GFSE (g and h) CS/CH/nanoclay/1.5% GFSE (i and j) CS/CH/nanoclay/2% GFSE.

FESEM morphology of bionanocomposite films after 30 and 60 days of soil degradation is shown in **Figure 8.14 (a-j).** The control film (CS/CH/nanoclay) showed large number of big holes after 30 and 60 days of soil degradation (**Figure 8.14 (a,b)**). The size of holes was decreased as increase in GFSE concentration because of antibacterial activity of GFSE against soil microbes. The CS/CH/nanoclay/1.5% GFSE film ((**Figure 8.14 (i,j)**) was not significantly degraded compared to CS/CH/nanoclay/2% GFSE, CS/CH/nanoclay/1% GFSE and CS/CH/nanoclay/0.5% GFSE. It could be attributed to high antibacterial activity **(Figure 8.15 d)** and high crystallinity **(Figure 8.1 d).** This results are in accordance with weight loss of films due to microbial degradation **(Table 8.1)**

8.3.8. Agar diffusion test for antifungal activity

Antifungal activity of bionanocomposite films incorporated with different ratios of GFSE is shown in **Figure 8.15 (a-g)**. The inhibitory zone (mm) of bionanocomposite films against *A. niger* was observed after 72 h of incubation at 37°C.

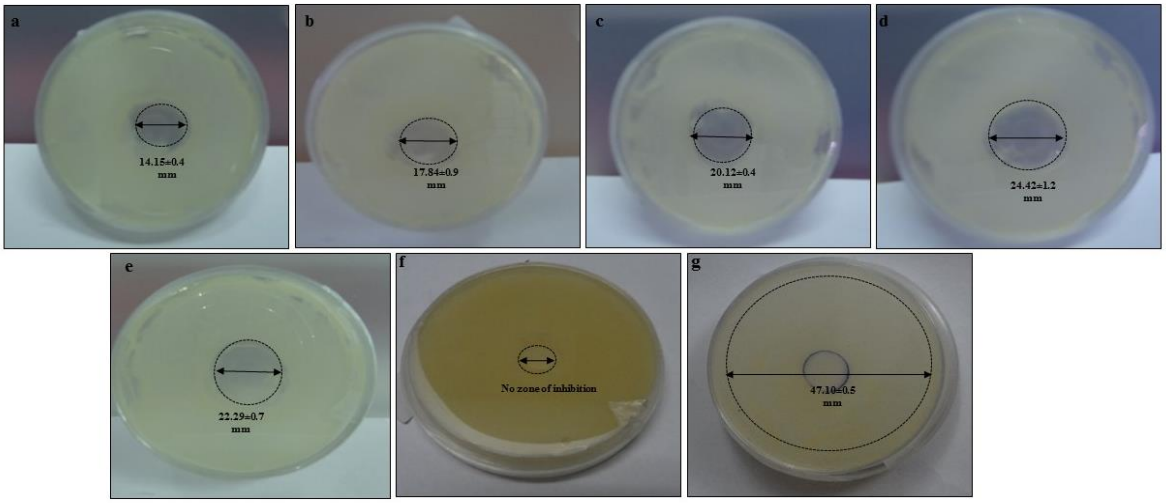

Figure 8.15. Antifungal activity of bionanocomposite films against *A. niger*: (a) CS/CH/nanoclay, (b) CS/CH/nanoclay/0.5% GFSE, (c) CS/CH/nanoclay/1% GFSE, (d) CS/CH/nanoclay/1.5% GFSE, (e) CS/CH/nanoclay/2% GFSE, (f) LDPE and (g) Ampicillin B.

The CS/CH/nanoclay (control) film showed a zone of inhibition of 14.15±0.4 mm because of the presence of chitosan (CH) **(Figure 8.15 (a))**. The antifungal activity of

CS/CH bionanocomposite film was notably increased with an increasing content of GFSE from 0.5% to 2% **(Figure 8.15 (b-e))**. Though, GFSE concentration was high in CS/CH/nanoclay/2% GFSE film, the zone of inhibition was not significant compared to CS/CH/nanoclay/1.5% GFSE film. No zone of inhibition was observed against *A. niger* for LDPE **(Figure 8.15 (f)).** The positive control of ampicillin showed a zone of inhibition of 47.10±0.50 mm **(Figure 7.16 (g))**. The present reveals that 1.5% GFSE (v/v) incorporated bionanocomposite films can be used for food packaging applications.

8.3.9. Antifungal activity of bionanocomposite film

Comparative study of bread sample packed by CS/CH/1.5% GFSE biocomposite films and low-density polyethylene (LDPE) films is shown in **Figure 8.16**. CS/CH/nanoclay/1.5% GFSE biocomposite film was chosen for bread packaging because of low moisture content, low water vapor permeability, low solubility, high tensile strength and high thermal stability. The LDPE film served as control.

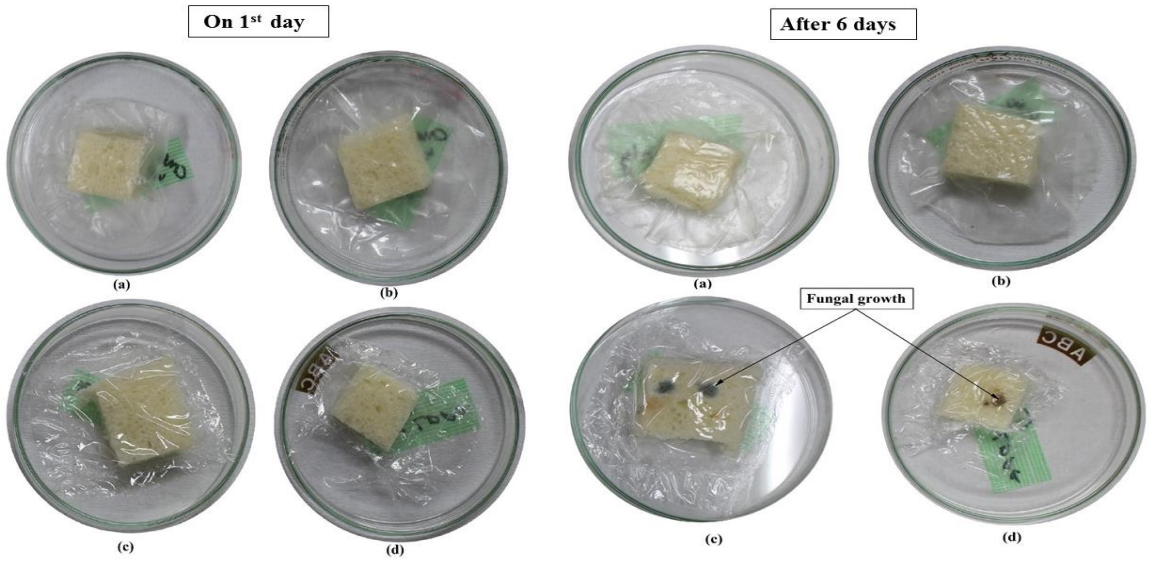

Figure 8.16. Comparative study on bread sample packed with (a and b) CS/CH/nanoclay/1.5% GFSE films (c and d) low density polyethylene films.

The fungal growth was observed on 6th day in control samples, which were packed by LDPE films **(Figure 7.16 (c,d))**. But, in the case of bread samples packed by CS/CH/nanoclay/1.5% GFSE nanoclay films, the fungal growth was not observed until 20 days. It could be attributed to the presence of CH and GFSE in the films. Also, metal ions

were released from nanoclay during its interactions with fungi (**Malachova et al., 2011).** Hence, the prepared bionanocomposite film can be a potential candidate for food packaging applications to extend the shelf life of products and food safety.

8.3.10. Comparative study of corn starch with CH and GFSE selected natural and synthetic polymeric films

The tensile strength, elongation at break and WVP of CS/CH/nanoclay films were compared with selected natural and synthetic polymeric films **(Table 8.2).**

Table 8.2. Tensile strength, elongation at break and water vapour permeability of various films**.**

Film type	Test condition	TS (MPa)	EB (%)	WVP (g/m s Pa)	Reference
CS/CH/nanoclay CS/CH/nanoclay/0.5% GFSE CS/CH/nanoclay/1% GFSE CS/CH/nanoclay/1.5% GFSE CS/CH/nanoclay/2% GFSE	25°C, 75% RH	23.8 15.5 16.7 19.6 17.4	18.3 65.7 62.2 55.8 67.6	7.2×10^{-10} 8.34×10^{-11} 5.29×10^{-11} 2.45×10^{-11} 4.67×10^{-11}	**Present study**
CS	25°C, 75% RH	3.8-4.3	4.0-10.0	-	**Mali et al. (2006)**
CS/CH	25°C,75 % RH 25°C,95 % RH	3.2-6.3 1.0-3.5	58.0-122 25.0-100	$1.5\text{-}7.8\times 10^{-10}$ $1.8\text{-}9.2\times 10^{-10}$	**Ren et al. (2017)**
CS/CH/$CaCO_3$	25°C,75 % RH	2.04-10.7	78.7-134.3	$1.58\text{-}7.47\times 10^{-10}$	**Ji et al. (2017)**
CH/0-1.5(% v/v) GFSE	23°C,50 % RH	54.9-8.93	4.72-96.8	-	**Tan et al. (2016)**
CS/CH/0-3% GFSE	23°C,50 % RH	18.3-14.4	57-67	$2.08\text{- }2.08\times 10^{-9}$	**Bofet al. (2016)**
Low density polyethylene (LDPE)	38°C,90 % RH	7.6-17.3	500.0	$9.25\ x10^{-13}$	**Bourtoo and Chinnan (2008)**
High density polyethylene (HDPE)	38°C, 90% RH	17.3-34.6	300.0	2.31×10^{-13}	
Polyester	38°C, 90% RH	178.0	70.0-100.0	-	
Cellophane	38°C, 90% RH	-	-	8.41×10^{-11}	

In the present study, CS/CH/nanoclay/1.5% v/v GFSE film showed lower WVP (2.45×10^{-11} g/m s Pa) and higher tensile strength (19.5 MPa) compared with other films (**Ji et al., 2017; Mali et al., 2006; Ren et al., 2017 and Tan et al., 2016).** The WVP of CS/CH/1.5% GFSE nanoclay film was lower than synthetic polymer cellophane film **(Bourtoom and Chinnan, 2008)** and CS/CH/0-3% v/v GFSE film **(Bof et al., 2016)**. The low water barrier property of CS/CH/nanoclay/1.5% v/v GFSE film compared with LDPE and HDPE can be explained that the inherent hydrophilicity of the components such as CS, CH and GFSE.

8.4. Summary

Corn starch-chitosan-nanoclay bionanocomposite films with different ratios of GFSE (0- 2% v/v) were prepared. The prepared films were studied for their physical, mechanical and thermal properties. Among the prepared films, CS/CH/nanoclay/1.5% GFSE showed better physical, mechanical and thermal properties than CS/CH/nanoclay, CS/CH/nanoclay/0.5% GFSE, CS/CH/nanoclay/1% GFSE and CS/CH/nanoclay/2% GFSE. A broad characterization showed that CS/CH/nanoclay/1.5% GFSE bionanocomposite films possess high crystallinity, low hydrophilicity, high water barrier and high mechanical properties. The FESEM study showed that CS/CH/nanoclay/1.5% GFSE film was found to be smoother and homogeneous than other films because of strong molecular interactions among CS, CH and GFSE. The prepared CS/CH/nanoclay/1.5% GFSE bionanocomposite film showed high antifungal activity of stored bread sample at 25°C, 59% RH for 20 days. These results strongly encourage that the prepared film can be used to enhance the shelf life of perishable food products.

Chapter 9

Conclusions and future directions

In this chapter, the remarkable accomplishments of the present work and significant conclusions of the entire doctoral work are summarized. The directions for further extension of the present work are also mentioned.

9.1. Overall conclusions

The major conclusions drawn on the basis of overall observations and major findings of the research work are as follows:

- The microwave-assisted dry heating treatment (MADH) is quick, uniform as well as energy-efficient and showed better starch functionalities compared to conventional heating.
- The detailed study exhibited that modified potato starch with xanthan, microwave heated at 8 min (PSX-8 min) via MADH showed a higher peak viscosity, apparent viscosity and water holding capacity than other modified potato starches with different heating times. The modified starches showed significantly superior properties of gelatinization temperature and low crystalline intensity compared to native potato starch. Modified potato starch with xanthan microwave heated at 8 min (PSX-8 min) showed a sharp absorption peak inferring to an ester bond between starch and xanthan according to FTIR analysis. X-ray diffraction pattern revealed that the peak intensity of PSX-8 min slightly decreased compared to crystalline intensity of PSX-0 min as a result of stronger interaction between starch and xanthan. The modified starch can be used in different applications of food and pharmaceutical industries.
- Carboxylmethyl cellulose and chitosan revealed their potential for improvement in starch properties on blending with starch. Amylose and amylopectin ratio regulated the orientation of molecular structure in the starch-based films.

- Corn starch (CS) (28:72) based films were found to show higher tensile strength, lower WVP, higher T_g and higher thermal stability. XRD study revealed that the crystallinity was higher for CS/CMC/nanoclay bionanocomposite films due to the formation of strong intermolecular hydrogen bond among CS/CMC/nanoclay as confirmed by FTIR results. The SEM study exhibited that the bionanocomposite films containing CS showed more uniform surfaces than other films. The prepared starch based bionanocomposite films showed heat sealing properties, which is a main criterion to develop tougher and more resistant packages. The prepared CS/CMC/nanoclay bionanocomposite films exhibited antifungal activity of stored bread sample at 25°C, 59% RH for 15 days.
- CS/CH/nanoclay bionanocomposite films showed higher tensile strength, lower film solubility, lower water vapor permeability and higher glass transition temperature. CS demonstrated a strong interaction with chitosan and nanoclay. XRD confirmed the higher crystallinity and molecular miscibility of corn starch with chitosan (-NH, -COOH) and nanoclay (Si-O-Si, Al-OH). Fourier transform infrared spectroscopy (FTIR) confirmed shifting of amine peak to higher wavenumber that indicates hydrogen bonding between starch and chitosan. Low density polyethylene (LDPE) exhibited fungal growth within 5 days when packed with bread slices whereas corn starch/CH/nanoclay bionanocomposite films exhibited no fungal growth for at least 20 days when bread samples were packed at 25°C and 59% RH.
- After optimization of amylose:amylopectin ratio, corn starch (CS) showed better results among the chosen combinations as compared to other bionanocomposite films. The corn starch blended with chitosan possessed higher tensile strength and antifungal properties.
- For further improvements, the effect of different plasticizers (GLY and SOR) and antifungal agents (KS and GFSE) on corn starch-chitosan based bionanocomposite films was studied for its crystallinity, mechanical, water barrier and thermal properties. Among the chosen combinations, SOR/GFSE and SOR/KS showed better physical properties than GLY/GFSE and GLY/KS. XRD patterns revealed that the crystallinity was increased in CS/CH/nanoclay/SOR/GFSE films due to the

formation of strong intermolecular hydrogen bond among CS, CH, SOR, GFSE and nanoclay as confirmed by FTIR results.

- CS/CH/nanoclay/SOR/GFSE film was found to have high tensile strength, low WVP, high storage modulus and enhanced thermal properties. The SEM micrograph revealed that the bionanocomposite film containing CS/CH/nanoclay/SOR/GFSE showed more uniform surfaces than other films. CS/CH/nanoclay/SOR/GFSE films showed better microbial properties, soil degradation and maximum zone of inhibition in antifungal test than CS/CH/nanoclay/SOR/KS films.
- The prepared CS/CH/nanoclay/SOR/GFSE bionanocomposite films showed antifungal activity on stored bread sample against *Aspergillus niger* at 25°C, 59% RH for 20 days. The prepared films could be a better alternative to bio-plastics for food packaging purposes.
- Bread samples were very sensitive to the proliferation of *Aspergillus niger*. The prepared CS/CH/nanoclay/SOR/GFSE bionanocomposite films effectively inhibited the growth of *Aspergillus niger.*
- Among chosen GFSE ratios (0.5-2% v/v), CS/CH/nanoclay/SOR/1.5%GFSE bionanocomposite films were found to have high tensile strength, low WVP, enhanced thermal properties and antifungal activity of stored bread samples at 25°C, 59% RH for 20 days.
- All these results confirmed that the produced eco-friendly bionanocomposite films, which is an alternative option for conventional plastic, could be used in the field of active packaging to enhance food safety and extend the shelf life of perishable food products.

9.2. Significance of the findings

- The rising concern towards environmental pollution especially due to heavy usage of plastic in food packaging has lead the researchers to find alternatives. Biodegradable packaging material is one of the possible solution at its infancy. Therefore, the application of biodegradable materials, incorporated with natural

polymers as food packaging materials becomes an area of increasing interest and relevance in the food industry.

- The current study aims to find an alternative of conventional plastic based packaging material by using starch based bionanocomposite films (carboxylmethyl cellulose, chitosan, nanoclay, potassium sorbate and grapefruit seed extract) as food packaging materials where all the ingredients were obtained from natural resources.
- The mechanical, physical and biological properties of the developed bionanocomposite films were also studied to ensure the shelf life of the food products and were found to be competent enough as an alternative of conventional plastic based packaging materials.

9.3. Scope for future work

Recommendations for future research are as follows:

- Studies on filler materials in starch blended bionanocomposite films to improve its hydrophobic properties and limitations on water barrier properties. This can be further explored in the future by comparing WVP values with typical synthetic based films such as LDPE.
- Further investigations on biodegradable packaging materials, which are to be used to enhance prolonged periods of storage, safety and quality assurance of perishable foods such as cheese, processed meat, fruits and bakery products
- Molecular dynamic behaviour of barrier, thermal and mechanical properties of starch blended bionanocomposite films and its experimental validation.
- Enhancement of the capability of packaging material to retain food product with higher moisture content (>40%).
- Reduction of the production cost by finding alternatives for raw material, especially from food wastes and simultaneously ensuring the standards of various physical properties.

Reference

Abdou, E.S., Sorour, M.A., 2014. Preparation and characterization of starch/carrageenan edible films. International Food Research Journal 21, 189–193.

Abreu, A.S., Oliveira, M., De Sa, A., Rodrigues, R.M., Cerqueira, M.A., Vicente, A.A., Machado, A. V., 2015. Antimicrobial nanostructured starch based films for packaging. Carbohydrate Polymers 129, 127–134.

Adzahan, N., 2002. Modification of Wheat, Sago and Tapioca Starches by Irradiation and Its Effect on the Physical Properties of Fish Crackers (keropok). University of Putra Malaysia. Thesis (Masters).

Aider, M., 2010. Chitosan application for active bio-based films production and potential in the food industry: Review. LWT - Food Science and Technology 43, 837–842.

Alamri, M.S., Mohamed, A.A., Hussain, S., 2012. Effect of okra gum on the pasting, thermal, and viscous properties of rice and sorghum starches. Carbohydrate Polymers 89, 199–207.

Alcazar-Alay, S.C., Meireles, M.A.A., 2015. Physicochemical properties, modifications and applications of starches from different botanical sources. Food Science and Technology (Campinas) 35, 215–236.

Alekseeva, O. V., Rodionova, A.N., Bagrovskaya, N.A., Agafonov, A. V., Noskov, A. V., 2017. Hydroxyethyl cellulose/bentonite/magnetite hybrid materials: structure, physicochemical properties, and antifungal activity. Cellulose 24, 1825–1836.

Almasi, H., Ghanbarzadeh, B., Entezami, A.A., 2010. Physicochemical properties of starch-CMC-nanoclay biodegradable films. International Journal of Biological Macromolecules 46, 1–5.

Alves, V.D., Mali, S., Beléia, A., Grossmann, M.V.E., 2007. Effect of glycerol and amylose enrichment on cassava starch film properties. Journal of Food Engineering 78, 941–946.

Amagliani, L., O'Regan, J., Kelly, A.L., O'Mahony, J.A., 2016. Chemistry, structure,

functionality and applications of rice starch. Journal of Cereal Science 70, 291–300.

Arvanitoyannis, I., Biliaderis, C.G., 1999. Physical properties of polyol-plasticized edible blends made of methyl cellulose and soluble starch. Carbohydrate Polymers 38, 47–58.

Arvanitoyannis, I., Biliaderis, C.G., Ogawa, H., Kawasaki, N., 1998. Biodegradable films made from low-density polyethylene (LDPE), rice starch and potato starch for food packaging applications: Part 1. Carbohydrate Polymers 36, 89–104.

ASTM, 1996. Standard Test Methods for Tensile Properties of Thin Plastic Sheeting, D882-91. American Society for Testing and Material, Philadelphia, PA.

Atwell, W.A., Hood, L.F., Lineback, D.R., Varriano-Marston, E., H. F. Zobel, 1988. The terminology and methodology associated with basic starch phenomenon. Cereal foods world 33, 306–311.

Aytunga, E., Arik, K., Us, F., 2014. Evaluation of structural properties of cellulose ether-corn starch based biodegradable films. International Journal of Polymeric Materials and Polymeric Biomaterials 63, 342–351.

Bai, H., Zhou, Y., Wang, X., Zhang, L., 2012. The permeability and mechanical properties of cellulose acetate membranes blended withpPolyethylene glycol 600 for treatment of municipal sewage. Procedia Environmental Sciences 16, 346–351.

Balázs, N., Sipos, P., 2007. Limitations of pH-potentiometric titration for the determination of the degree of deacetylation of chitosan. Carbohydrate Research 342, 124–130.

Bangyekan, C., Aht-Ong, D., Srikulkit, K., 2006. Preparation and properties evaluation of chitosan-coated cassava starch films. Carbohydrate Polymers 63, 61–71.

Baron, J. K., and Sumner, S.S., 1993. Antimicrobial containing edible films as an inhibitory system to control microbial growth on meat products. Journal of Food Potection 56, 916–925.

Barzegar, H., Azizi, M.H., Barzegar, M., Hamidi-Esfahani, Z., 2014. Effect of potassium sorbate on antimicrobial and physical properties of starch-clay nanocomposite films.

Carbohydrate Polymers 110, 26–31.

Basnett, P., Knowles, J.C., Pishbin, F., Smith, C., Keshavarz, T., Boccaccini, A.R., Roy, I., 2012. Novel biodegradable and biocompatible poly(3-hydroxyoctanoate)/bacterial cellulose composites. Advanced Engineering Materials 14, 330–343.

Bensadoun, F., Kchit, N., Billotte, C., Trochu, F., Ruiz, E., 2011. A comparative study of dispersion techniques for nanocomposite made with nanoclays and an unsaturated polyester resin. Journal of Nanomaterials 2011, 1–12.

Bertoft, E., Blennow, A., 2009. Structure of Potato Starch, in: Advances in Potato Chemistry and Technology: Second Edition. pp. 83–98.

Bertuzzi, M.A., Gottifredi, J.C., Armada, M., 2012. Mechanical properties of a high amylose content corn starch based film, gelatinized at low temperature. Campinas 15, 219–227.

Biomass Packaging, 2015. The pros and cons of polylactic acid (PLA) bioplastic "Corn Plastics". http://www.biomasspackaging.com/the-pros-and-cons-of-polylactic-acid-pla-bioplastic-the-corn-plastics/. Last accessed on 19-09-2018.

Biswas, A., Shogren, R.L., Selling, G., Salch, J., Willett, J.L., Buchanan, C.M., 2008. Rapid and environmentally friendly preparation of starch esters. Carbohydrate Polymers 74, 137–141.

Blanshard, J.M. V, 1987. Starch: properties and potential. John Wiley & Sons.

Bof, M.J., Jimenez, A., Locaso, D.E., Garcia, M.A., Chiralt, A., 2016. Grapefruit Seed Extract and Lemon Essential Oil as Active Agents in Corn Starch–Chitosan Blend Films. Food and Bioprocess Technology 9, 2033–2045.

Borges, J.A., Romani, V.P., Cortez-Vega, W.R., Martins, V.G., 2015. Influence of different starch sources and plasticizers on properties of biodegradable films. International Food Research Journal 22, 2346–2351.

Bourtoom, T., Chinnan, M.S., 2008. Preparation and properties of rice starch-chitosan blend biodegradable film. LWT - Food Science and Technology 41, 1633–1641.

Bratovcic, A., Odobasic, A., Catic, S., Sestan, I., 2015. Application of polymer nanocomposite materials in food packaging. Croatian Journal of Food Science and Technology 7, 86–94.

Cardenas, G., Diaz, J., Melendrez, M.F., Cruzat, C., 2008. Physicochemical properties of edible films from chitosan composites obtained by microwave heating. Polymer Bulletin 61, 737–748.

Chai, M.N., Isa, M.I.N., 2013. The oleic acid composition effect on the carboxymethyl cellulose based biopolymer electrolyte. Journal of Crystallization Process and Technology 3, 1–4.

Chandrasekaran, S., Ramanathan, S., Tanmay Basak, 2013. Microwave Food Processing-A review. Food Research International 52, 243-261.

Chang, Y.P., Abd Karim, A., Seow, C.C., 2006. Interactive plasticizing-antiplasticizing effects of water and glycerol on the tensile properties of tapioca starch films. Food Hydrocolloids 20, 1–8.

Chanvrier, H., Uthuyakumaran, S., Appelqvist, I.A.M., Gidley, M.J., Gilbert, E.P., Lopez-Rubio, A., 2007. Influence of storage conditions on the structure, thermal behaviour and formation of enyzme resistant starch in extruded starches. Journal of Agricultural and Food Chemistry 55, 9883–9890.

Cheng, H., Wintersdorff, P., 1981. Xanthan gum-modified starches. 4,298,729.

Chiu, C.W., Schiermeyer, E., Thomas, D.J., Shah, M.B., Hanchett, D.J., Jeffcoat, R., 1999. Thermally inhibited non-pregelinzed granular starches and flours and process for their production. 5,932,017.

Chiumarelli, M., Hubinger, M.D., 2014. Evaluation of edible films and coatings formulated with cassava starch, glycerol, carnauba wax and stearic acid. Food Hydrocolloids 38, 20–27.

Choi, J.S., Lee, Y.R., Ha, Y.M., Seo, H.J., Kim, Y.H., Park, S.M., Sohn, J.H., 2014. Antibacterial effect of Grapefruit Seed Extract (GSE) on makgeolli-brewing

microorganisms and its application in the preservation of fresh makgeolli. Journal of Food Science 79, 1159–1167.

Christianson, D.D., Hodge, J.E., Osborne, D., Detroy, R.W., 1981. Gelatinization of wheat starch as modified by xanthan gum, guar gum, and cellulose gum. Cereal Chemistry 58, 513–517.

Chung, H.-J., Min, D., Kim, J.-Y., Lim, S.-T., 2013. Effect of Minor Addition of Xanthan on Cross-Linking of Rice Starches by Dry Heating with Phosphate Salts Hyun-Jung. Journal of Applied Polymer Science 105, 2280–2286.

Chung, Y.L., Ansari, S., Estevez, L., Hayrapetyan, S., Giannelis, E.P., Lai, H.M., 2010. Preparation and properties of biodegradable starch-clay nanocomposites. Carbohydrate Polymers 79, 391–396.

Corrales, M., Han, J.H., Tauscher, B., 2009. Antimicrobial properties of grape seed extracts and their effectiveness after incorporation into pea starch films. International Journal of Food Science and Technology 44, 425–433.

Craig, S.A., Maningat, C.C., Seib, P.A., Hoseney, R.C., 1989. Starch paste clarity., Cereal chemistry. USA.

Da Roz, A.L., Carvalho, A.J.F., Gandini, A., Curvelo, A.A.S., 2006. The effect of plasticizers on thermoplastic starch compositions obtained by melt processing. Carbohydrate Polymers 63, 417–424.

Das, S., 2013. Greendiamz biotech bets big on biodegradable plastic. Business Standard News 1–6. https://www.business-standard.com/article/companies/greendiamz-biotech-bets-big-on-biodegradable-plastic-111022500009_1.html. Last accessed on 19-09-2018.

De Oliveira Faria, F., Vercelheze, A.E.S., Mali, S., 2012. Physical properties of biodegradable films based on cassava starch, polyvinyl alcohol and montmorillonite. Quimica Nova 35, 487–492.

Debnath, S., Habibur Rahman, S.M., Deshmukh, G., Duganath, N., Pranitha, C., Chiranjeevi, A., 2011. Antimicrobial Screening of Various Fruit Seed Extracts.

Pharmacognosy Journal 3, 83–86.

Dias, A.B., Müller, C.M.O., Larotonda, F.D.S., Laurindo, J.B., 2010. Biodegradable films based on rice starch and rice flour. Journal of Cereal Science 51, 213–219.

Durango, A.M., Soares, N.F.F., Benevides, S., Teixeira, J., Carvalho, M., Wobeto, C., Andrade, N.J., 2006. Development and evaluation of an edible antimicrobial film based on yam starch and chitosan. Packaging Technology and Science 19, 55–59.

Edhirej, A., Sapuan, S.M., Jawaid, M., Zahari, N.I., 2017. Effect of various plasticizers and concentration on the physical, thermal, mechanical, and structural properties of cassava-starch-based films. Starch/Staerke 69, 1–11.

European Bioplastics, 2017. Bioplastics—Facts and Figures. https://docs.european-bioplastics.org/2016/publications/EUBP_facts_and_figures.pdf. Last accessed on 19-09-2018.

Ezeoha, S.L., Ezenwanne, J.., 2013. Production of Biodegradable Plastic Packaging Film from Cassava Starch. IOSR Journal of Engineering 3, 14–20.

Farahnaky, A., Saberi, B., Majzoobi, M., 2013. Effect of glycerol on physical and mechanical properties of wheat starch edible films. Journal of Texture Studies 44, 176–186.

Ferrero, C., Martino, M.N., Zaritzky, N.E., 1994. Corn starch-xanthan gum interaction and its effect on the stability during storage of frozen gelatinized suspension. Starch - Stärke 46, 300–308.

FICCI, 2017. 3rd National confernce on sustainable infrastructure with plastics, New Delhi, India.

FICCI, 2014. A report on "Potential of Plastics Industry in Northern India with Special Focus on Plasticulture and Food Processing-2014".

Flores, S., Haedo, A.S., Campos, C., Gerschenson, L., 2007. Antimicrobial performance of potassium sorbate supported in tapioca starch edible films. European Food Research and Technology 225, 375–384.

García, M.A., Pinotti, A., Martino, M.N., Zaritzky, N., 2009. Characterization of Starch and Composite Edible Films and Coatings, Edible Films and Coatings for Food Applications. Edible films and coatings for food applications. New York : Springer, New York.

Gernat, C., Radosta, S., Anger, H., Damaschun, G., 1993. Crystalline Parts of Three Different Conformations Detected in Native and Enzymatically Degraded Starches. Starch - Stärke 45, 309–314.

Geyer, R., Jambeck, J.R., Law, K.L., 2017. Production, use, and fate of all plastics ever made. Science Advances 3, 1–5.

Ghanbarzadeh, B., Almasi, H., Entezami, A.A., 2011. Improving the barrier and mechanical properties of corn starch-based edible films: Effect of citric acid and carboxymethyl cellulose. Industrial Crops and Products 33, 229–235.

Ghanbarzadeh, B., Almasi, H., Entezami, A.A., 2010. Physical properties of edible modified starch/carboxymethyl cellulose films. Innovative Food Science and Emerging Technologies 11, 697–702.

Gironi, F., Piemonte, V., 2011. Bioplastics and petroleum-based plastics: Strengths and weaknesses. Energy Sources, Part A: Recovery, Utilization and Environmental Effects 33, 1949–1959.

Gul, K., Riar, C.S., Bala, A., Sibian, M.S., 2014. Effect of ionic gums and dry heating on physicochemical, morphological, thermal and pasting properties of water chestnut starch. LWT - Food Science and Technology 59, 348–355.

Guohua, Z., Ya, L., Cuilan, F., Min, Z., Caiqiong, Z., Zongdao, C., 2006. Water resistance, mechanical properties and biodegradability of methylated-corn starch/poly(vinyl alcohol) blend film. Polymer Degradation and Stability 91, 703–711.

Hadj-Hamou, A.S., Matassi, S., Abderrahmane, H., Yahiaoui, F., 2014. Effect of cloisite 30B on the thermal and tensile behavior of poly(butylene adipate-co-terephthalate)/poly(vinyl chloride) nanoblends. Polymer Bulletin 71, 1483–1503.

Hagenmaier, R.D., Shaw, P.E., 1990. Moisture permeability of edible films made with fatty

acid and (hydroxypropyl)methylcellulose. Journal of Agricultural and Food Chemistry 38, 1799–1803.

Hoidy, W.H., Ahmad, M.B., Jaffar Al Mulla, E.A., Ibrahim, N.A.B., 2009. Synthesis and characterization of organoclay from sodium montmorillonite and fatty hydroxamic acids. American Journal of Applied Sciences 6, 1567–1572.

Hoover, R., 2001. Composition, molecular structure, and physicochemical properties of tuber and root starches: a review. Carbohydrate Polymers 45, 253–267.

Ji, N., Qin, Y., Xi, T., Xiong, L., Sun, Q., 2017. Effect of chitosan on the antibacterial and physical properties of corn starch nanocomposite films. Starch - Stärke 69, 1600114–1600122.

JISZ0208, 1976. Testing Methods for Determination of the Water Vapour Transmission Rate of Moisture-proof Packaging Materials. Japanese Standards Association (in Japanese).

Kanmani, P., Rhim, J.W., 2014a. Antimicrobial and physical-mechanical properties of agar-based films incorporated with grapefruit seed extract. Carbohydrate Polymers 102, 708–716.

Kanmani, P., Rhim, J.W., 2014b. Development and characterization of carrageenan/grapefruit seed extract composite films for active packaging. International Journal of Biological Macromolecules 68, 258–266.

Kappe, C.O., Dallinger, D., 2009. Controlled microwave heating in modern organic synthesis: Highlights from the 2004-2008 literature. Molecular Diversity 13, 71–193.

Katzbauer, B., 1998. Properties and applications of xanthan gum. Polymer Degradation and Stability 59, 81–84.

Kim, J.C., Kong, B.W., Kim, M.J., Lee, S.H., 2008. Amylolytic hydrolysis of native starch granules affected by granule surface area. Journal of Food Science 73, 621–624.

Kraak, A., 1992. Industrial applications of potato starch products. Industrial Crops and Products 1, 107–112.

Kumar, P., Sandeep, K.P., Alavi S., Truong, V.D., Gorga, R.E, 2010. Effect of type and content of modified montmorillonite on the structure and properties of bio-nanocomposite films based on soy protein isolate and montmorillonite. Journal of Food Science 75, N46-N56.

Kuorwel, K.K., Cran, M.J., Orbell, J.D., Buddhadasa, S., Bigger, S.W., 2015. Review of mechanical properties, migration, and potential applications in active food packaging systems containing nanoclays and nanosilver. Comprehensive Reviews in Food Science and Food Safety 14, 411–430.

Kuorwel, K.K., Cran, M.J., Sonneveld, K., Miltz, J., Bigger, S.W., 2011. Antimicrobial activity of biodegradable polysaccharide and protein-based films containing active agents. Journal of Food Science 76, 90–102.

Kurt, A., Kahyaoglu, T., 2014. Characterization of a new biodegradable ediblefilm made from salep glucomannan. Carbohydrate Polymers 104, 50–58.

Lagos, Vicentini M, Dos Rodolfo M C, Bittante Q B, Sobral Paulo J A, 2015. Mechanical properties of cassava starch films as affected by different plasticizers and different relative humidity conditions. International Journal of Food Studies 4, 116–125.

Laycock, B.G. and, Halley, P.J., 2014. Starch Applications: State of Market and New Trends, Starch Polymers: From Genetic Engineering to Green Applications. Elsevier B.V., San Diego.

Leja, K., Lewandowicz, G., 2010. Polymer biodegradation and biodegradable polymers - A review. Polish Journal of Environmental Studies 19, 255–266.

Lewandowicz, G., Fornal, J., Walkowski, A., 1997. Effect of microwave radiation on physico-chemical properties and structure of potato and tapioca starches. Carbohydrate Polymers 34, 213–220.

Li, Y., Zhang, H., Shoemaker, C.F., Xu, Z., Zhu, S., Zhong, F., 2013. Effect of dry heat treatment with xanthan on waxy rice starch. Carbohydrate Polymers 92, 1647–1652.

Lim, G.O., Jang, S.A., Song, K. Bin, 2010. Physical and antimicrobial properties of Gelidium corneum/nano-clay composite film containing grapefruit seed extract or thymol. Journal of Food Engineering 98, 415–420.

Lim, H., Han, J.-A., N. BeMiller, J., Lim, S.-T., 2006. Physical modification of waxy maize starch by dry heating with ionic gums. Journal of Applied Glycoscience 53, 281–286.

Lim, H.S., BeMiller, J.N., Lim, S.T., 2003. Effect of dry heating with ionic gums at controlled pH on starch paste viscosity. Cereal Chemistry 80, 198–202.

Lim, S.T., Han, J.A., Lim, H.S., BeMiller, J.N., 2002. Modification of starch by dry heating with ionic gums. Cereal Chemistry 79, 601–606.

Liu, R., Peng, Y., Cao, J., Luo, S., 2014. Water absorption, dimensional stability, and mold susceptibility of organically-modified-montmorillonite modified wood flour/polypropylene composites. BioResources 9, 54–65.

Loredo RA Yaneli, Rocío Rodríguez-hernández, A.I., Morales-sánchez, E., Gómez-aldapa, C.A., Velazquez, G., 2016. Effect of equilibrium moisture content on barrier , mechanical and thermal properties of chitosan films 196, 560–566.

Lourdin, D., Valle, G. Della, Colonna, P., 1995. Influence of amylose content on starch films and foams. Carbohydrate Polymers 27, 261–270.

Maizura, M., Fazilah, A., Norziah, M.H., Karim, A.A., 2008. Antibacterial activity of modified sago starch-alginate based edible film incorporated with lemongrass (Cymbopogon citratus) oil. International Food Research Journal 15, 233-236.

Maizura, M., Fazilah, A., Norziah, M.H., Karim, A.A., 2007. Antibacterial activity and mechanical properties of partially hydrolyzed sago starch-alginate edible film containing lemongrass oil. Journal of Food Science 72, 324–330.

Malachova, K., Praus, P., Rybkova, Z., Kozak, O., 2011. Antibacterial and antifungal activities of silver, copper and zinc montmorillonites. Applied Clay Science 53, 642–645.

Mali, S., Grossmann, M.V.E., García, M.A., Martino, M.N., Zaritzky, N.E., 2006. Effects

of controlled storage on thermal, mechanical and barrier properties of plasticized films from different starch sources. Journal of Food Engineering 75, 453–460.

Mandala, I.G., Palogou, E.D., Kostaropoulos, A.E., 2002. Influence of preparation and storage conditions on texture of xanthan – starch mixtures. Journal of Food Engineering 53, 27–38.

Manek, R. V., Builders, P.F., Kolling, W.M., Emeje, M., Kunle, O.O., 2012. Physicochemical and binder properties of starch obtained from cyperus esculentus. AAPS PharmSciTech 13, 379–388.

Megazyme, 2016. Amylose : amylopectin assay kit: for the measurement of the amylose and amylopectin contents of starch. Megazyme International Ireland Ltd., Co.Wicklow, Ireland.

Mehta, V., Nishith, D., Marjadi, D., 2014. Production and evaluation of microbial plastic for its degradation capabilities. Journal of Environmental Research and Development 8, 934–940.

Mekonnen, T., Mussone, P., Khalil, H., Bressler, D., 2013. Progress in bio-based plastics and plasticizing modifications. Journal of Materials Chemistry A 1, 13379–13398.

Melo, C., Garcia, P.S., Grossmann, M.V.E., Yamashita, F., Dall'Antônia, L.H., Mali, S., 2011. Properties of extruded xanthan-starch-clay nanocomposite films. Brazilian Archives of Biology and Technology 54, 1223–1333.

Miltz, J., Rsydlo, T., Mor, A., Polyakov, V., 2006. Potency evaluation of a dermaseptin S4 derivative for antimicrobial food packaging applications. Packaging Technology and Science 19, 345–354.

Mohanty, A.K., Misra, M., Hinrichsen, G., 2000. Biofibres, biodegradable polymers and biocomposites: An overview. Macromolecular Materials and Engineering 276–277, 1–24.

Mua, J.P., Jackson, D.S., 1997. Fines structure of corn amylose and amylopectin fractions with various molecular weights. Journal of Agricultural and Food Chemistry 45, 3840–3847.

Muller, C.M.O., Laurindo, J.B., Yamashita, F., 2009. Effect of cellulose fibers addition on the mechanical properties and water vapor barrier of starch-based films. Food Hydrocolloids 23, 1328–1333.

Muller, J., González-Martínez, C., Chiralt, A., 2017. Combination Of Poly(lactic) acid and starch for biodegradable food packaging. Materials 10, 1–22.

Nair, S., Alummoottil, J., Moothandasserry, S., 2017. Chitosan-konjac glucomannan-cassava starch-nanosilver composite films with moisture resistant and antimicrobial properties for food-packaging applications. Starch/Staerke 69, 1–12.

Nam, S., Scanlon, M.G., Han, J.H., Izydorczyk, M.S., 2007. Extrusion of pea starch containing lysozyme and determination of antimicrobial activity. Journal of Food Science 72, 233–236.

Park, H., Lee, W., Park, C., Cho, W., Ha, C., 2003. Environmentally friendly polymer hybrids. Journal of Materials Science 38, 909–915.

Pathak, M.V., Kumar, N., 2017. Implications of SiO 2 nanoparticles for in vitro biodegradation of low-density polyethylene with potential isolates of Bacillus , Pseudomonas , and their synergistic effect on Vigna mungo growth. Energy, Ecology and Environment 2, 418–427.

Paunonen, S., 2013. Strength and barrier enhancements of cellophane and cellulose derivative films: A review. BioResources 8, 3098–3121.

Peelmana, N., Ragaerta, P., Meulenaer, B. De, Adons, D., Peeters, R., Cardon, L., Impe, F. Van, Devlieghere, F., 2013. Application of bioplastics for food packaging. Trends in Food Science & Technology 32, 128–141.

Pelissari, F., Grossmann, M., Yamashita, F., Pineda, E. et al, 2009. Antimicrobial, Mechanical, and Barrier Properties of Cassava Starch-Chitosan Films Incorporated with Oregano Essential Oil. Journal of Agricultural and Food Chemistry 57, 7599–7504.

Phan The, D., Debeaufort, F., Voilley, A., Luu, D., 2009. Biopolymer interactions affect the functional properties of edible films based on agar, cassava starch and

arabinoxylan blends. Journal of Food Engineering 90, 548–558.

Pinotti, A., García, M.A., Martino, M.N., Zaritzky, N.E., 2007. Study on microstructure and physical properties of composite films based on chitosan and methylcellulose. Food Hydrocolloids 21, 66–72.

Piyada, K., Waranyou, S., Thawien, W., 2013. Mechanical , thermal and structural properties of rice starch films reinforced with rice starch nanocrystals. International Food Research Journal 20, 439–449.

Pramodrao, K.S., Riar, C.S., 2014. Comparative study of effect of modification with ionic gums and dry heating on the physicochemical characteristic of potato, sweet potato and taro starches. Food Hydrocolloids 35, 613–619.

Prashanth, H.K.V., Tharanathan, R.N., 2007. Chitin/chitosan: modifications and their unlimited application potential—an overview. Trends in Food Science & Technology 18, 117–131.

Qi, Z., Ye, H., Xu, J., Chen, J., Guo, B., 2013. Improved the thermal and mechanical properties of poly(butylene succinate-co-butylene adipate) by forming nanocomposites with attapulgite. Colloids and Surfaces A: Physicochemical and Engineering Aspects 421, 109–117.

Ratnayake, W.S., Hoover, R., Warkentin, T., 2002. Pea starch: composition, structure and properties - A review. Starch/Staerke 54, 217–234.

Raucci, M.G., Giugliano, D., Alvarez-Perez, M.A., Ambrosio, L., 2015. Effects on growth and osteogenic differentiation of mesenchymal stem cells by the strontium-added sol-gel hydroxyapatite gel materials. Journal of Materials Science: Materials in Medicine 26, 90.

Ray, S.S., Bousmina, M., 2005. Biodegradable polymers and their layered silicate nanocomposites: In greening the 21st century materials world. Progress in Materials Science 50, 962–1079.

Ren, L., Yan, X., Zhou, J., Tong, J., Su, X., 2017. Influence of chitosan concentration on mechanical and barrier properties of corn starch/chitosan films. International Journal

of Biological Macromolecules 105, 1636–1643.

Rhim, J., Park, H., Ha, C., 2013. Bio-nanocomposites for food packaging applications. Progress in Polymer 38, 1629–1652.

Robertson, G., 2008. State-of-the-art biobased food packaging materials, Environmentally Compatible Food Packaging. Boca Raton , Fla. : Woodhead Publishing Ltd. and CRC Press LLC.

Rodriguez, M., Osés, J., Ziani, K., Maté, J.I., 2006. Combined effect of plasticizers and surfactants on the physical properties of starch based edible films. Food Research International 39, 840–846.

Rubilar, J.F., Cruz, R.M.S., Silva, H.D., Vicente, A.A., Khmelinskii, I., Vieira, M.C., 2013. Physico-mechanical properties of chitosan films with carvacrol and grape seed extract. Journal of Food Engineering 115, 466–474.

Saha, D., Bhattacharya, S., 2010. Hydrocolloids as thickening and gelling agents in food: A critical review. Journal of Food Science and Technology 47, 587–597.

Salleh, E., Muhamad, I., Khairuddin, N., 2007. Preparation, characterization and antimicrobial analysis of antimicrobial starch-based film incorporated with chitosan and lauric acid. Asian Chitin Journal 3, 55–68.

Santana, A., Angela, M., 2014. New starches are the trend for industry applications: A Review. Food and Public Health 4, 229–241.

Sanyang, M.L., Salit M. Sapuan, Jawaid, M., Ishak, M.R., Sahari, J., 2015. Effect of plasticizer type and concentration on tensile, thermal and barrier properties of biodegradable films based on Sugar Palm (Arenga pinnata) starch. Polymers 7, 1106–1124.

Sarka, E., Dvoracek, V., 2017. New processing and applications of waxy starch (a review). Journal of Food Engineering 206, 77–87.

Sayanjali, S., Ghanbarzadeh, B., Ghiassifar, S., 2011. Evaluation of antimicrobial and physical properties of edible film based on carboxymethyl cellulose containing

potassium sorbate on some mycotoxigenic Aspergillus species in fresh pistachios. LWT - Food Science and Technology 44, 1133–1138.

Seetharaman, G., 2017. India wants to double consumption of cheap material in 5 yrs, what about its plastic waste? The Economic Times 1–8.

Shalviri, A., Liu, Q., Abdekhodaie, M.J., Wu, X.Y., 2010. Novel modified starch-xanthan gum hydrogels for controlled drug delivery: Synthesis and characterization. Carbohydrate Polymers 79, 898–907.

Shevkani, K., Singh, N., Bajaj, R., Kaur, A., 2017. Wheat starch production, structure, functionality and applications—a review. International Journal of Food Science and Technology 52, 38–58.

Shin, Y.J., Song, H.Y., Jo, W.S., Lee, M.J., Song, K. Bin, 2013. Physical properties of a barley protein/nano-clay composite film containing grapefruit seed extract and antimicrobial benefits for packaging of Agaricus bisporus. International Journal of Food Science and Technology 48, 1736–1743.

Shogren, R.L., Biswas, A., 2006. Preparation of water-soluble and water-swellable starch acetates using microwave heating. Carbohydrate Polymers 64, 16–21.

Silva, K., 2011. Environmentally Friendly Packaging Materials from Renewable Resources as Alternatives for Oil-based Polymers. Brunel University. Thesis (Doctoral).

Singh, J., Kaur, L., McCarthy, O.J., 2007. Factors influencing the physico-chemical, morphological, thermal and rheological properties of some chemically modified starches for food applications-A review. Food Hydrocolloids 21, 1–22.

Singh, A. V., Nath, L.K., Singh, A., 2010. Pharmaceutical, food and non-food applications of modified starches: A critical review. Electronic Journal of Environmental, Agricultural and Food Chemistry 9, 1214–1221.

Song, H.Y., Shin, Y.J., Song, K. Bin, 2012. Preparation of a barley bran protein-gelatin composite film containing grapefruit seed extract and its application in salmon packaging. Journal of Food Engineering 113, 541–547.

Soroka, W., 2010. Fundamentals of Packaging Technology. DEStech Publications, Inc., UK.

Souza, A.C., Benze, R., Ferrão, E.S., Ditchfield, C., Coelho, A.C. V, Tadini, C.C., 2012. Cassava starch biodegradable films: Influence of glycerol and clay nanoparticles content on tensile and barrier properties and glass transition temperature. LWT - Food Science and Technology 46, 110–117.

Staroszczyk, H., 2009a. Microwave-assisted silication of potato starch. Carbohydrate Polymers 77, 506–515.

Staroszczyk, H., 2009b. Microwave-assisted boration of potato starch. Polimery 54, 31–41.

Staroszczyk, H., Janas, P., 2010. Microwave-assisted preparation of potato starch silicated with silicic acid. Carbohydrate Polymers 81, 599–606.

Stevens, D.J., Elton, G.A.H., 1971. Thermal properties of the starch/water system Part I. Measurement of heat of gelatinisation by differential scanning calorimetry. Starch - Starke 23, 8–11.

Sun, Q., Si, F., Xiong, L., Chu, L., 2013. Effect of dry heating with ionic gums on physicochemical properties of starch. Food Chemistry 136, 1421–1425.

Sun, Q., Xi, T., Li, Y., Xiong, L., 2014a. Characterization of corn starch films reinforced with $CaCO_3$ nanoparticles. PLOS ONE 9, 1–6.

Sun, Q., Xu, Y., Xiong, L., 2014b. Effect of microwave-assisted dry heating with xanthan on normal and waxy corn starches. International Journal of Biological Macromolecules 68, 86–91.

Sung, S.-Y., Sin, L.T., Tee, T.-T., Bee, S.-T., Rahmat, A.R., Rahman, W.A.W.A., Tan, A.-C., Vikhraman, M., 2013. Antimicrobial agents for food packaging applications. Trends in Food Science & Technology 33, 110–123.

Talja, R.A., Helén, H., Roos, Y.H., Jouppila, K., 2007. Effect of various polyols and polyol contents on physical and mechanical properties of potato starch-based films.

Carbohydrate Polymers 67, 288–295.

Tan, Y.M., Lim, S.H., Tay, B.Y., Lee, M.W., Thian, E.S., 2015. Functional chitosan-based grapefruit seed extract composite films for applications in food packaging technology. Materials Research Bulletin 69, 142–146.

Tanada-Palmu, P.S., Grosso, C.R.F., 2003. Development and characterization of edible films based on gluten from semi-hard and soft Brazilian wheat flours (development of films based on gluten from wheat flours). Ciência e Tecnologia de Alimentos 23, 264–269.

Tang, X., Alavi, S., Herald, T.J., 2008. Barrier and mechanical properties of starch-clay nanocomposite films. Cereal Chemistry 85, 433–439.

Tang, Z.X., Qian, J.Q., Shi, L.E., 2007. Preparation of chitosan nanoparticles as carrier for immobilized enzyme. Applied Biochemistry and Biotechnology 136, 77–96.

Tokiwa, Y., Calabia, B.P., Ugwu, C.U., Aiba, S., 2009. Biodegradability of plastics. International Journal of Molecular Sciences 10, 3722–3742.

Tongdeesoontorn, W., Mauer, L.J., Wongruong, S., Sriburi, P., Rachtanapun, P., 2011. Effect of carboxymethyl cellulose concentration on physical properties of biodegradable cassava starch-based films. Chemistry Central Journal 5, 6.

Toral, F.L.B., Furlan, A.C., Scapinello, C., Peralta, R.M., Figueiredo, D.F., 2002. Digestibility of two starch sources and enzymatic activity of 35 and 45 days old rabbits. Revista Brasileira de Zootecnia 31, 1434–1441.

Tummala, P., Liu, W., Drzal, L.T., Mohanty, A.K., Misra, M., 2006. Influence of plasticizers on thermal and mechanical properties and morphology of soy-based bioplastics. Industrial and Engineering Chemistry Research 45, 7491–7496.

Vania Blasques Bueno, Bentini, R., Catalani, L.H., Petri, D.F.S., 2013. Synthesis and swelling behavior of biodegradable cellulose-based hydrogels. Carbohydrate Polymers 92, 1091–1099.

Varsha, C., Bajpai, S.K., Navin, C., 2010. Investigation of water vapour permeation and

antibacterial properties of nano silver loaded cellulose acetate film. International Food Research Journal 17, 623–639.

Vashishta, D., Pandeya, A., Anca Hermeneanb, M.J.Y., Nez-Gasconc, Perez-Sanchezd, H., Kumar, K.J., 2017. Effect of dry heating and ionic gum on the physicochemical and release properties of starch from Dioscorea 95, 557–563.

Vivaldo-Lima, and Saldivar-Guerra, 2013. Handbook of polymer synthesis, characterization, and processing. John Wiley & Sons.

Vroman, I., Tighzert, L., 2009. Biodegradable polymers. Materials 2, 307–344.

Wang, C., He, X.W., Huang, Q., Fu, X., Liu, S., 2013. Physicochemical properties and application of micronized corn starch in low fat cream. Journal of Food Engineering 116, 881–888.

Wongsagonsup, R., Pujchakarn, T., Jitrakbumrung, S., Chaiwat, W., Fuongfuchat, A., Varavinit, S., Dangtip, S., Suphantharika, M., 2014. Effect of cross-linking on physicochemical properties of tapioca starch and its application in soup product. Carbohydrate Polymers 101, 656–665.

Xie, Y., Yan, M., Yuan, S., Sun, S., Huo, Q., 2013. Effect of microwave treatment on the physicochemical properties of potato starch granules. Chemistry Central Journal 113, 1–7.

Yoon, S.J., Lee, Y., Yoo, B., 2016. Rheological and pasting properties of naked barley flour as modified by guar, Xanthan, and locust bean gums. Preventive Nutrition and Food Science 21, 367–372.

Yoon, S. Do, Park, M.H., Byun, H.S., 2012. Mechanical and water barrier properties of starch/PVA composite films by adding nano-sized poly(methyl methacrylate-co-acrylamide) particles. Carbohydrate Polymers 87, 676–686.

YR Ottarsdottir, E.V.A., 2015. Preparation and properties of starch – lignosulfonate blends for food packaging applications. KTH Royal Institute Of Technology School. Thesis (Masters).

Yu, K., Wang, Y., Xu, Y., Guo, L., Du, X., 2016. Correlation between wheat starch annealing conditions and retrogradation during storage. Czech Journal of Food Sciences 34, 79–86.

Zavareze, E.D.R., Dias, A.R.G., 2011. Impact of heat-moisture treatment and annealing in starches: A review. Carbohydrate Polymers 83, 317–328.

Zhang, Q.X., Yu, Z.Z., Xie, X.L., Naito, K., Kagawa, Y., 2007. Preparation and crystalline morphology of biodegradable starch/clay nanocomposites. Polymer 48, 7193–7200.

Zhang, Y., Han, J.H., 2006. Mechanical and thermal characteristics of pea starch films plasticized with monosaccharides and polyols. Journal of Food Science 71, 109–118.

Zhao, K., Li, B., Xu, M., Jing, L., Gou, M., Yu, Z., Zheng, J., Li, W., 2018. Microwave pretreated esterification improved the substitution degree, structural and physicochemical properties of potato starch esters. LWT - Food Science and Technology 90, 116–123.

Zhao, Q., Xiong, H., Selomulya, C., Chen, X.D., Huang, S., Ruan, X., Zhou, Q., Sun, W., 2013. Effects of Spray Drying and Freeze Drying on the Properties of Protein Isolate from Rice Dreg Protein. Food and Bioprocess Technology 6, 1759–1769.

Zia-ud-Din, Xiong, H., Fei, P., 2017. Physical and chemical modification of starches: A review. Critical Reviews in Food Science and Nutrition 57, 2691–2705.

Zou, Y., Wang, L., Zhang, H., Qian, Z., Mou, L., Wang, J., Liu, X., 2004. Stabilization and mechanical properties of biodegradable aliphatic polyesteramide and its filled composites. Polymer Degradation and Stability 83, 87–92.

भारतीय प्रौद्योगिकी संस्थान गुवाहाटी
Indian Institute of Technology Guwahati

Research output from the thesis

Journal Publications

1. Pankaj Jha, Dharmalingam K, Takahisa Nishizu, Nakako Katsuno and R. Anandalakshmi, Effect of amylose-amylopectin ratios on physical, mechanical and thermal properties of starch based bionanocomposite films incorporated with CMC and nanoclay *Starch-Stärke* (2019): 1900121.

2. Pankaj Jha, Takahisa Nishizu and R. Anandalakshmi, Influence of amylose-amylopectin ratios on barrier, mechanical and thermal properties of starch based bionanocomposite films *(Under review).*

3. Pankaj Jha, and R. Anandalakshmi, Comparison of microwave and conventional heating methods for modification of starch with xanthan gum *(Under review).*

4. Pankaj Jha, Takahisa Nishizu and R. Anandalakshmi, Effect of plasticizers and antifungal agents on corn starch based bionanocomposite films (*Under review).*

5. Pankaj Jha and R. Anandalakshmi, Effect of antifungal agent on physical properties of corn starch-chitosan-nanoclay bionanocomposite films (*Under preparation*).

Conferences

1. Pankaj Jha, and R. Anandalakshmi, Microwave-assisted modification of potato starch with xanthan gum, *REFLUX-2019*, September 28-29, Indian Institute of Technology Guwahati, Guwahati, Assam,India.
2. Pankaj Jha, and R.Anandalakshmi, Effect of Microwave assisted dry-heating on corn starch with xanthan, *CHEMCON-2015*, December 27-30, Indian Institute of Technology Guwahati, Guwahati, Assam, India.

Program/Fellowship

1. Selected for a six-month sandwich program offered by The United School of Agriculture Science, GIFU University (UGSAS-GU), from October 2016 to March 2017.

2. Scholarship recipient of Japan Student Services Organization (JASSO) during sandwich program for 6 months.